



Router-based Network Traffic Observation by Terminal Sliding Mode Control Theory

A thesis submitted in fulfilment of the requirements for the degree of Doctor of Philosophy

Long Xu

MEng Elec, RMIT University

BEng Elec, Nanjing University of Information Science and Technology

School of Engineering

College of Science, Engineering and Health

RMIT University

March 2018



*This thesis is dedicated to my parents  
and to my wife.*

*Thank you all for helping to give me  
the life I love today.*





## **Declaration**

I certify that except where due acknowledgement has been made, the work is that of the author alone; the work has not been submitted previously, in whole or in part, to qualify for any other academic award; the content of the thesis is the result of work which has been carried out since the official commencement date of the approved research program; any editorial work, paid or unpaid, carried out by a third party is acknowledged; and, ethics procedures and guidelines have been followed.

Long Xu

March 2018



## **Acknowledgements**

This thesis would not be possible without the support and encouragement of many people. I would like to express my sincere gratitude to my senior supervisor Professor Xinghuo Yu, associate supervisor Doctor Fengling Han and Professor Liuping Wang, thank you for all of your support throughout the past four years.

First and foremost, I am grateful to Prof. Xinghuo Yu who gave me the initial opportunity to pursue Ph.D. candidature at RMIT University. It has been both a pleasure and an honour to be his Ph.D. student and learn from him. He is expertise in providing constructive comments on my research, creating unbridled vigour and invaluable motivation. To be one of his students, I received his excellent guidance, unlimited patience, tremendous encouragement and endless positive which cultivate my critical thinking and logical reasoning throughout my doctoral studies. Without his advice and support, the research presented in this thesis would not have been possible.

I would like to thank Prof. Yong Feng for the continuous support of my Ph.D. study and research, for his patience, motivation, enthusiasm and immense knowledge. His guidance helped me all the time of research and writing of this thesis. I would like to thank my associate supervisor, Dr. Fengling Han, for every suggestion shared with me on my research. Also, I would like to thank my associate supervisor Prof. Liuping Wang for her support of my Ph.D study. Furthermore, I would like to thank Prof. Jiankun Hu and Prof. Zahir Tari for their suggestion and support on my Ph.D. research.

I would like to thank all my colleagues of the research group for making studying and

working at RMIT University such an enjoyable experience. In particular, I appreciate the assistance by Mr. Jingjian Wang, Mr. Jiangxia Zhong, Dr. Chaojie Li, Mrs. Ragini Patel, Dr. Qingmai Wang, Dr. Peter Sokolowski, Dr. Miguel Combariza, Dr. Mitchell Lennard, Mr. Lei Chen, Mr. Minhao Zhou, Dr. Zhiwei Liu, Dr. Wenjun Xiong, Dr. Guanghui Wen, Dr. Wenwu Yu, Dr. Xinghua Liu, Dr. Bochao Zheng, Dr. Jun Yang and Dr. Haibo Du who spent a memorable period with me.

I owe my deepest gratitude to my parents and my wife, who have provided me with unconditional love, support, and understanding throughout my life and especially through my Ph.D. study. Last but not least, I would like to thank all those whose names I may have missed out but who have joined me in some way on my research journey.

# Abstract

Since the Internet emerges, network traffic monitoring (NTM) has always played a strategic role in understanding and characterising users' activities. Nowadays, with the increased complexity of Internet infrastructure, applications, and services, this role has become more crucial than ever. The aims of NTM mainly focus on the three improvements, which are the quality of service (QoS) of the networks, optimization of resource usage, and enhancement of security in computer networks. Specifically speaking, first, network conditions can be recognized by the network manager with NTM scheme. It provides the complete details about the QoS of the network, such as bandwidth, throughput, propagation delay, jitter, link availability, server memory, database space and etc. Second, with NTM being implemented at network nodes, i.e., network gateways, such as routers, or network links, the network traffic that is traversing the network is under online observation. Thereby, the network utilization can be improved by optimizing the resource usage to avoid the network congestion. Third, unauthenticated services or approaches to the server will be identified by regularly monitoring the traffic. The network conventions and statistics about the traffic will be obtained easily and then help troubleshoot the network. Security events will also be investigated and the entry of the user will be maintained for responsibility.

The work in this thesis focuses on the development of an intelligent real-time dynamic router-based network traffic observation (RNTO) by using the terminal sliding-mode (TSM) theory. The RNTO mechanisms are applied at network gateways, i.e., routers, to estimate the status of the traffic flows at the router level. The aims of the proposed RNTO tech-

nique is to estimate the traffic states, such as queue length (QL) in router buffer, the average congestion window size (ACwnd), and the queuing dynamics of the additional traffic flow (ATF). Furthermore, the main contributions of the work can be broadly categorised into four parts that are described as follows.

First, the problem of router-based network traffic monitoring is formulated as an observer design by using TSM theory for RNTD applications. The proposed TSM observer in the research is a network-based monitoring, which is implemented into the network gateways, i.e., network routers. Different from the static network traffic monitoring methods, the TSM observer is designed by using control methods based on the fluid-flow mathematical model, which represents the traffic dynamics of the interactions in a set of TCP traffic flows through network routers. By considering the time delay and stochastic properties in data transmission network, the sliding-mode observation strategy is proposed with its high robustness with system parameter uncertainties as well as the external disturbance rejection. Given the natural weakness of chattering in sliding mode control signal, which can affect the system state, the chattering avoiding technique of the proposed TSM observation was utilized by using a smooth control signal for estimating the abnormal dynamics. It does not need any low-pass filter, which will lead to a phase lag. In addition, for the stochastic dynamics of the network traffics, fast transient convergence at a distance from and within a close range of the equilibrium of the traffic dynamics is essential to quickly capture traffic dynamics in network systems. Thus, a fractional term has been considered in the TSM for faster convergence in system states to efficiently estimate the traffic behaviours.

Second, the issue of internal dynamics in network observation system is studied by proposing a novel full-order TSM strategy to speed up convergence rate of the estimation error. In the RNTD scheme, the precise estimation for ACwnd is needed to estimate the queuing dynamics of ATF. However, the estimation error for ACwnd is not available and it converges to origin asymptotically, which results in a long response time in estimation. The

proposed novel TSM observer has been designed to drive the estimation error for ACwnd to a defined area in a finite-time, which can be calculated. Thereby, the estimation error of ACwnd can converge to origin asymptotically within the defined area. This strategy has shortened the response time and improved the estimation accuracy. This further improves the estimation accuracy for ATF. The comparative studies are conducted to evaluate the performance.

Third, the issue of algorithm-efficient RNTD is investigated by considering an event triggered sliding mode observer to reduce the computational load and the communication burden. Instead of the time-driven observation scheme, the control of the sliding mode observer is formulated under the event triggered scheme. The control of the observer is designed to be smooth and is directly applied to estimate the dynamics of the additional traffic flows. The event triggered observation algorithms is developed to reduce the computational load of the network router and the communication resource of output link in the network.

Fourth, the problem of global RNTD is addressed by developing a fuzzy TSM observer by using fuzzy theory to achieve global operation under network uncertainties. The existing RNTD schemes are based on the linearisation of certain network conditions, i.e., a fixed number of TCP connections, which is a constant value  $N$ . Given the network suffers from time-varying fading, shadowing and interference and the data rate changes over time, the current methods proposed so far might not effectively and accurately monitor and estimate the traffic dynamics under network uncertainties. The T-S fuzzy models are used to model the traffic dynamics of the time-varying data changes in network link resources, i.e. the time-varying number of TCP sections,  $N(t)$  in the mathematical model. Based on the T-S fuzzy models, the fuzzy terminal sliding mode observer is established by using fuzzy logic theory to estimate the states of the network traffic to achieve the global observation performance under the network uncertainties. In the fuzzy terminal sliding mode observer, the control signal is designed to be continuous for application in estimating the additional

traffic flows without the low-pass filter.

To evaluate the proposed RNTD technique, the networking simulator tool Network Simulator II (NS-II) has been used. The proposed RNTD algorithms are coded and implemented into network routers in NS-II. Numerous simulation scenarios are considered and performed. The comparative studies are also conducted by analysing the NS-2 results. The results have demonstrated the effectiveness and efficiency of the proposed RNTD algorithms.



# Contents

|  |              |
|--|--------------|
| <b>Abstract</b>  | <b>ix</b>    |
| <b>Contents</b>  | <b>xiii</b>  |
| <b>List of Figures</b>                                       | <b>xvii</b>  |
| <b>List of Tables</b>  | <b>xxi</b>   |
| <b>Nomenclature</b>  | <b>xxiii</b> |
| <b>List of Publications</b>                                  | <b>xxix</b>  |
| <b>1 Introduction</b>  | <b>1</b>     |
| 1.1 Intrusion Detection . . . . .                            | 4            |
| 1.2 Network Traffic Monitoring . . . . .                     | 6            |
| 1.2.1 Router-based Network Traffic Observation . . . . .     | 8            |
| 1.3 Motivation . . . . .                                     | 9            |
| 1.4 Research Scope . . . . .                                 | 11           |
| 1.5 Research Questions, Objective and Contribution . . . . . | 13           |
| 1.5.1 Research Questions and Objectives . . . . .            | 14           |
| 1.5.2 Contributions . . . . .                                | 15           |
| 1.6 Structure of Thesis . . . . .                            | 16           |

|          |   |           |
|----------|---|-----------|
| 1.7      | Summary . . . . .   | 18        |
| <b>2</b> | <b>Literature Review: Router-based Network Traffic Observation Problems</b> | <b>19</b> |
| 2.1      | Introduction . . . . .  | 19        |
| 2.2      | Some Issues of RNT0 . . . . .   | 20        |
| 2.2.1    | Source Information Analysis . . . . .                                       | 20        |
| 2.2.1.1  | Probabilistic Sampling . . . . .  | 20        |
| 2.2.1.2  | Real-time Series . . . . .  | 21        |
| 2.2.2    | Flow-based Observation . . . . .  | 22        |
| 2.2.2.1  | NRNT0 . . . . .   | 23        |
| 2.2.2.2  | RNT0 . . . . .  | 25        |
| 2.2.3    | Network Management . . . . .  | 28        |
| 2.2.3.1  | Optimization Approach . . . . .   | 29        |
| 2.2.3.2  | Control Theory . . . . .  | 30        |
| 2.3      | Main Methodologies in RNT0 . . . . .  | 32        |
| 2.3.1    | Neuron Network Approach . . . . .   | 32        |
| 2.3.2    | Fuzzy Approach . . . . .  | 34        |
| 2.3.3    | SMC Approach . . . . .  | 36        |
| 2.4      | Some Key Challenging Problems in RNT0 . . . . .                             | 39        |
| 2.5      | Sliding Mode Control Theory . . . . .                                       | 42        |
| 2.5.1    | State-of-the-Art SMC . . . . .  | 42        |
| 2.5.1.1  | LSM . . . . .   | 43        |
| 2.5.1.2  | TSM . . . . .   | 44        |
| 2.5.2    | Fundamentals of SMC Theory . . . . .  | 45        |
| 2.5.3    | SMC Methodologies . . . . .   | 50        |
| 2.5.3.1  | High-order SMC . . . . .  | 50        |
| 2.5.3.2  | Terminal SMC . . . . .  | 56        |

---

|          |  |           |
|----------|--|-----------|
| 2.6      | Summary . . . . .  | 61        |
| <b>3</b> | <b>Real-time Terminal Sliding Mode Observation Strategy</b>  | <b>63</b> |
| 3.1      | Introduction . . . . .                                       | 63        |
| 3.2      | Fluid-flow Model of a Router-based Network . . . . .         | 64        |
| 3.2.1    | Router-based TCP/IP Networks . . . . .                       | 64        |
| 3.2.2    | Fluid-flow Model of a Router-based Network . . . . .         | 66        |
| 3.2.3    | Linearisation . . . . .                                      | 71        |
| 3.3      | Real-time Router-based Network Traffic Observation . . . . . | 74        |
| 3.3.1    | Conventional Sliding Mode Based RNT0 . . . . .               | 74        |
| 3.3.2    | Super-twisting Based RNT0 . . . . .                          | 78        |
| 3.3.3    | Terminal Sliding Mode Based RNT0 . . . . .                   | 82        |
| 3.4      | Simulations . . . . .  | 87        |
| 3.4.1    | Model Description . . . . .                                  | 87        |
| 3.4.2    | Simulation Results and Discussion . . . . .                  | 89        |
| 3.5      | Summary . . . . .  | 92        |
| <b>4</b> | <b>Full-order Terminal Sliding Mode Observation Strategy</b> | <b>93</b> |
| 4.1      | Introduction . . . . .                                       | 93        |
| 4.2      | Problem Formulation . . . . .                                | 94        |
| 4.3      | Full-order Terminal Sliding Mode Based RNT0 . . . . .        | 97        |
| 4.3.1    | Controller Design of the Second Error Subsystem . . . . .    | 98        |
| 4.3.2    | Controller Design of the First Error Subsystem . . . . .     | 100       |
| 4.4      | Simulation . . . . .   | 108       |
| 4.4.1    | Model Description . . . . .                                  | 108       |
| 4.4.2    | Simulation Results and Discussion . . . . .                  | 110       |
| 4.5      | Summary . . . . .  | 114       |

|          |   |            |
|----------|---|------------|
| <b>5</b> | <b>Event-triggered Sliding Mode Observation Strategy</b>      | <b>117</b> |
| 5.1      | Introduction . . . . .  | 117        |
| 5.2      | Problem Formulation . . . . .                                 | 118        |
| 5.3      | Event-triggered Full-order Sliding Mode Based RNT0 . . . . .  | 120        |
| 5.4      | Simulation . . . . .  | 130        |
| 5.4.1    | Model Description . . . . .                                   | 130        |
| 5.4.2    | Simulation Results and Discussion . . . . .                   | 131        |
| 5.5      | Summary . . . . .   | 135        |
| <b>6</b> | <b>Fuzzy Terminal Sliding-mode Observation Strategy</b>       | <b>137</b> |
| 6.1      | Introduction . . . . .  | 137        |
| 6.2      | Takagi-Sugeno Fuzzy Model of a Router-based Network . . . . . | 138        |
| 6.3      | Fuzzy Terminal Sliding Mode Based RNT0 . . . . .              | 143        |
| 6.4      | Simulation . . . . .  | 149        |
| 6.4.1    | Model Description . . . . .                                   | 149        |
| 6.4.2    | Simulation Results and Discussion . . . . .                   | 150        |
| 6.4.3    | Experimental Results . . . . .                                | 155        |
| 6.5      | Summary . . . . .   | 157        |
| <b>7</b> | <b>Conclusions</b>  | <b>159</b> |
| 7.1      | Research Findings Summary . . . . .                           | 159        |
| 7.2      | Future Research Directions . . . . .                          | 164        |
| 7.2.1    | Prototype Implementation and Analysis for RNT0 . . . . .      | 164        |
| 7.2.2    | Global Analysis for Multi-router based RNT0 . . . . .         | 164        |
| 7.2.3    | RNT0 in Software-defined Network . . . . .                    | 165        |
|          | <b>Bibliography</b>   | <b>167</b> |

# List of Figures

|     |   |    |
|-----|---|----|
| 1.1 | Number of Internet users worldwide (in millions) from 2000 to 2017 (source: International Telecommunications Union) [1]. . . . .  | 2  |
| 1.2 | Global IP traffic by 2021 [2]. . . . .  | 3  |
| 1.3 | Router-based Network Traffic Observation (RNTO). . . . .  | 9  |
| 1.4 | A typical router-based TCP/IP network topology. . . . .   | 12 |
| 3.1 | A typical router-based network topology . . . . .   | 64 |
| 3.2 | Fluid-flow analysis of a router-based network traffic . . . . .   | 66 |
| 3.3 | Block diagram of RNTO in a router . . . . .   | 71 |
| 3.4 | State and control of the proposed TSMO in Scenario 1.: (a) The number of QL $q(t)$ in router buffer. (b) Estimated ACwnd $w(t)$ in <i>packets</i> at the router. (c) Estimated dynamics of ATF $d(t)$ and the true DDoS flooding rate. (d) The value of the sliding variable $s_{tsm}(t)$ in <i>packets</i> . . . . . | 89 |
| 3.5 | State and control of the proposed TSMO in Scenario 2.: (a) The number of QL $q(t)$ in router buffer. (b) Estimated ACwnd $w(t)$ in <i>packets</i> at the router. (c) Estimated dynamics of ATF $d(t)$ and the true DDoS flooding rate. (d) The value of the sliding variable $s_{tsm}(t)$ in <i>packets</i> . . . . . | 90 |

|     |   |     |
|-----|---|-----|
| 4.1 | State and control of the proposed FTSMO in Scenario 1. : (a) The number of QL $q(t)$ in router buffer. (b) Estimated ACwnd $w(t)$ in <i>packets</i> at the router. (c) Estimated dynamics of ATF $d(t)$ and the true DDoS flooding rate. (d) The value of the sliding variable $s_{ftsm}(t)$ in <i>packets</i> . (e) Estimation error $e_{2ftsm}(t)$ in <i>packets</i> . (f) Control signal of $v_{1ftsm}(t)$ . . . . . | 111 |
| 4.2 | State and control of the proposed FTSMO in Scenario 2.: (a) The number of QL $q(t)$ in router buffer. (b) Estimated ACwnd $w(t)$ in <i>packets</i> at the router. (c) Estimated dynamics of ATF $d(t)$ and the true DDoS flooding rate. (d) The value of the sliding variable $s_{ftsm}(t)$ in <i>packets</i> . (e) Estimation error $e_{2ftsm}(t)$ in <i>packets</i> . (f) Control signal of $v_{1ftsm}(t)$ . . . . .  | 112 |
| 4.3 | The estimated ACwnd by the proposed FTSMO algorithm in Scenario 3. . . . .  | 113 |
| 4.4 | The estimated dynamics of ATF by the proposed FTSMO algorithm in Scenario 3. . . . .  | 113 |
| 5.1 | Event-triggering framework. (a) System model with event-triggered sampling of error system states $e_{sm}^2(t)$ ; (b) the model where the event-triggering induced error is represented as an external input $e(t)$ . . . . .   | 119 |
| 5.2 | State and control of the proposed FTSMO in Scenario 1. : (a) The number of QL $q(t)$ in router buffer. (b) Estimated ACwnd $w(t)$ in <i>packets</i> at the router. (c) Estimated dynamics of ATF $d(t)$ and the true DDoS flooding rate. (d) The value of the sliding variable $s_{et}(t)$ in <i>packets</i> . (e) Estimation error $e_{et}^2(t)$ in <i>packets</i> . (f) The triggered events. . . . .                 | 132 |
| 5.3 | State and control of the proposed FTSMO in Scenario 2.: (a) The number of QL $q(t)$ in router buffer. (b) Estimated ACwnd $w(t)$ in <i>packets</i> at the router. (c) Estimated dynamics of ATF $d(t)$ and the true DDoS flooding rate. (d) The value of the sliding variable $s_{et}(t)$ in <i>packets</i> . (e) Estimation error $e_{et}^2(t)$ in <i>packets</i> . (f) The triggered events. . . . .                  | 133 |

|     |  |     |
|-----|--|-----|
| 5.4 | The estimated ACwnd by the proposed FTSMO algorithm in Scenario 3. . .   | 134 |
| 5.5 | The estimated ACwnd by the proposed FTSMO algorithm in Scenario 3. . .   | 134 |
| 5.6 | The estimated ACwnd by the proposed FTSMO algorithm in Scenario 3. . .   | 135 |
| 6.1 | Fuzzy inference system . . . . .   | 138 |
| 6.2 | State and control of the proposed FTSMO in Scenario 2.: (a) The number of QL $q(t)$ in router buffer. (b) Estimated ACwnd $w(t)$ in <i>packets</i> at the router. (b) The number of TCP sections. (d) Estimated dynamics of ATF $d(t)$ and the true DDoS flooding rate. (e) Estimation error $e_f^2(t)$ in <i>packets</i> . (f) The value of the sliding variable $s_f(t)$ in <i>packets</i> . . . . . | 151 |
| 6.3 | State and control of the proposed FTSMO in Scenario 2.: (a) The number of QL $q(t)$ in router buffer. (b) Estimated ACwnd $w(t)$ in <i>packets</i> at the router. (b) The number of TCP sections. (d) Estimated dynamics of ATF $d(t)$ and the true DDoS flooding rate. (e) Estimation error $e_f^2(t)$ in <i>packets</i> . (f) The value of the sliding variable $s_f(t)$ in <i>packets</i> . . . . . | 152 |
| 6.4 | The estimated ACwnd by the proposed Fuzzy TSMO algorithm in Scenario 3.  | 153 |
| 6.5 | The estimated ACwnd by the proposed Fuzzy TSMO algorithm in Scenario 3.  | 153 |
| 6.6 | The estimated ACwnd by the proposed Fuzzy TSMO algorithm in Scenario 3.  | 154 |
| 6.7 | The estimated ACwnd by the proposed Fuzzy TSMO algorithm in "CAIDA DDoS 2007 attack dataset". . . . .  | 156 |
| 6.8 | The estimated ACwnd by the proposed Fuzzy TSMO algorithm in "CAIDA DDoS 2007 attack dataset". . . . .  | 156 |





# List of Tables

|     |  |     |
|-----|--|-----|
| 3.1 | Comparative studies of LO, SMO, STO and TSMO in Scenario 1. . . . .  | 90  |
| 3.2 | Comparative studies of LO, SMO, STO and TSMO in Scenario 2. . . . .  | 91  |
| 4.1 | Comparative studies of LO, SMO, STO and FTSMO in Scenario 1. . . . . | 110 |
| 4.2 | Comparative studies of LO, SMO, STO and FTSMO in Scenario 2. . . . . | 110 |



# Nomenclature

## Symbols/Acronyms

|                           |   |
|---------------------------|---|
| $\mathbb{N}$              | the natural numbers   |
| $\mathbb{R}$              | the field of real numbers   |
| $\mathbb{C}$              | the field of complex numbers  |
| $\text{Re}[z]$            | the real part of the complex number $z$                             |
| $\text{Im}[z]$            | the imaginary part of the complex number $z$                        |
| $\mathbb{R}_+$            | the set of strictly positive real numbers                           |
| $\mathbb{R}^{n \times m}$ | the set of real matrices with $n$ rows and $m$ columns              |
| $ a $                     | the absolute value of the real number $a$                           |
| $\text{sgn}(\cdot)$       | the signum function   |
| $a_{ij}$                  | the entry in the $i$ -th row and $j$ -th column of a matrix $A$     |
| $\text{rank}(A)$          | the rank of the matrix $A$  |
| $\lambda(A)$              | the spectrum of the square matrix $A$ , i.e. the set of eigenvalues |
| $\lambda_{\max}(A)$       | the largest eigenvalue of the square matrix $A$                     |

---

|                        |   |
|------------------------|---|
| $\lambda_{min}(A)$     | the smallest eigenvalue of the square matrix $A$  |
| $I_n$                  | the $n \times n$ identity matrix  |
| $A > 0$                | implies the square matrix $A$ is asymmetric positive definite   |
| $A > B$                | implies the square matrix $A - B$ is asymmetric positive definite   |
| $\ \cdot\ $            | the Euclidean norm for vectors and the spectral norm for matrices   |
| $\dot{y}$              | the derivative of $y$ with respect to time  |
| $\ddot{y}$             | the second derivative of $y$ with respect to time   |
| $\nabla f(\mathbf{x})$ | The gradient of a function $f(\mathbf{x})$ , that is $\nabla f(\mathbf{x}) = (\frac{\partial f(\mathbf{x})}{\partial x_1} \dots \frac{\partial f(\mathbf{x})}{\partial x_N})$ |
| $\equiv$               | equivalent to   |
| $\triangleq$           | equal to by definition  |

## Abbreviations

|        |   |
|--------|---|
| ACK    | Acknowledges                              |
| AM     | Active monitoring                         |
| AQM    | Active queue management                   |
| AFRED  | Adaptive fuzzy based random early drop    |
| AFREM  | Adaptive fuzzy random exponential marking |
| ANN    | Adaptive neural network                   |
| AN-AQM | Adaptive neuron active queue management   |

|          |   |
|----------|---|
| AVQ      | Adaptive virtual queue                        |
| ATF      | Additional traffic flow                       |
| ACwnd    | Average congestion window                     |
| BDP      | Bandwidth-delay product                       |
| BEB      | Binary exponential back-off                   |
| CABEB    | Capture avoidance binary exponential back-off |
| CoA      | Centre of area                                |
| CoM      | Centre of maximum                             |
| CBR      | Constant bit rate                             |
| CSMC     | Conventional sliding mode control             |
| DDoS     | Distributed denial of service                 |
| DiffServ | Differentiated services                       |
| DoS      | Denial of service                             |
| BDN      | Dynamic bayesian network                      |
| DRED     | Dynamic random early drop                     |
| ETSMO    | Event triggered sliding-mode observer         |
| EB       | Exabytes                                      |
| EWMA     | Exponentially weighted moving average         |
| EXPAND   | Extended passive monitoring server            |

|         |   |
|---------|---|
| FTSMO   | Full-order terminal sliding mode observer               |
| FAPIDNN | Fuzzy assisted PID controller based on neuron network   |
| FCRED   | Fuzzy control based random early drop                   |
| FLCD    | Fuzzy logic congestion detection                        |
| FUZREM  | Fuzzy logic controller based random exponential marking |
| HOSM    | High-order sliding mode                                 |
| HM      | Hybrid monitoring                                       |
| ITU     | International Telecommunication Union                   |
| IDSs    | Intrusion detection systems                             |
| LMI     | Linear matrix inequality                                |
| LSM     | Linear sliding mode                                     |
| LTI     | Linear time invariant                                   |
| LO      | Luenberger observer                                     |
| MID     | Management information databased                        |
| Pmax    | Maximum drop probability parameter                      |
| MoM     | Mean of maximum   |
| NIDS    | Network intrusion detection systems                     |
| NTM     | Network traffic monitoring                              |
| NRNTO   | Non-router based network traffic observation            |

|        |  |
|--------|--|
| NN     | Neuron network                                 |
| NN-RED | Neural network based random early drop         |
| NN-MPC | Neural network model predictive control        |
| NRL    | Neuron reinforcement learning                  |
| NNTM   | Non-router based network traffic monitoring    |
| NFTSMC | Nonsingular fast terminal sliding-mode control |
| OS     | Operating system                               |
| PM     | Passive monitoring                             |
| P      | Proportional                                   |
| PI     | Proportional integral                          |
| PID    | Proportional integral derivative               |
| QoS    | Quality of service                             |
| QL     | Queue length                                   |
| REM    | Random exponential marking                     |
| RMON   | Remote monitoring                              |
| RTT    | Round-trip time                                |
| RNTM   | Router-based network traffic monitoring        |
| RNTO   | Router-based network traffic observation       |
| SOSM   | Second order sliding modes                     |

---

|       |   |
|-------|---|
| SCNM  | Self-configuring network monitor                |
| STREM | Self-tuning random exponential marking          |
| SPAND | Shared passive network performance discovery    |
| SNMP  | Simple network monitoring protocol              |
| SMC   | Sliding mode control                            |
| SMO   | Sliding mode observer (SMO)                     |
| SDN   | Software-defined networking                     |
| SAVQ  | Stabilized adaptive virtual queue               |
| SVB   | Stabilized virtual buffer                       |
| STO   | Super-twisting observer                         |
| STSMC | Super-twisting sliding mode control             |
| T-S   | Takagi-Sugeno                                   |
| TSM   | Terminal sliding mode                           |
| TSMC  | Terminal sliding mode control                   |
| TSMO  | Terminal sliding mode observer                  |
| TSMs  | Terminal sliding modes                          |
| TCP   | Transmission Control Protocol                   |
| VBR   | Variable bit rate                               |
| VSS   | Variable structure systems                      |
| WREN  | Watching resources from the edge of the network |



# List of Publications

## Resulting Papers in Journal

1. **Long Xu**, Yong Feng, Xinghuo Yu, Fengling Han, Jiankun Hu and Zahir Tari, "A terminal sliding-mode observer for the traffic flow monitoring in a TCP/IP network," *IEEE Transactions on Cybernetics*. (Submitted)
2. Wenjun Xiong, **Long Xu**, Tingwen Huang, Xinghuo Yu, and Yuehao Liu, "Finite-iteration Tracking of Singular Coupled Networks Based on Learning Control with Packet Losses," *IEEE Transactions on Systems, Man and Cybernetics: Systems*, DOI: 10.1109/TSMC.2017.2770160., December 2017.
3. Wenjun Xiong, **Long Xu**, Daniel Ho, Jinde Cao, and Tingwen Huang, "Synchronous and Asynchronous Iterative Learning Strategies of T-S Fuzzy Systems with Measurable and Unmeasurable State Information," *IEEE Transactions on Fuzzy Systems*, DOI: 10.1109/TFUZZ.2017.2787156, December 2017.
4. Xinghua Liu, Alessandro N. Vargas, Xinghuo Yu, and **Long Xu**, "Stabilizing two-dimensional stochastic systems through sliding mode control," *Journal of the Franklin Institute*, vol. 354, no. 14, pp. 5813–5824, 2017.
5. Alessandro N. Vargas, Marcio A. F. Montezuma, Xinghua Liu, **Long Xu**, and Xinghuo Yu, "Sliding-mode control for stabilizing high-order stochastic systems: application

to one-degree-of-freedom aerial device," *IEEE Transactions on Systems, Man and Cybernetics: Systems*, DOI: 10.1109/TSMC.2018.2849846, July 2018.

## Published Papers in Conference

1. **Long Xu**, Xinghuo Yu, Yong Feng, Fengling Han, Jiankun Hu and Zahir Tari, "A Fast Terminal Sliding Mode Observer for TCP/IP Network Anomaly Traffic Detection," In *Proceedings of the IEEE International Conference on Industrial Technology*, March 2015, Seville, Spain.
2. **Long Xu**, Xinghuo Yu, Yong Feng, Fengling Han, Jiankun Hu and Zahir Tari, "Comparative Studies of Router-based Observation Schemes for Anomaly Detection in TCP/UDP Networks," In *Proceedings of the IEEE International Conference on Industrial Technology*, March 2016, Taipei, Taiwan.
3. **Long Xu**, Xinghuo Yu, Yong Feng, Fengling Han, Jiankun Hu and Zahir Tari, "State estimation for a TCP/IP network using terminal sliding-mode methodology," In *Proceedings of the 43rd Annual Conference of the IEEE Industrial Electronics Society*, October 2017, Beijing, China.
4. **Long Xu**, Lei Chen, and Guanghui Wen, "Characteristic Modelling Approach based Sliding-mode Control," In *Proceedings of the 14th International Workshop on Complex Systems and Networks*, December 2017, Doha, Qatar.
5. Fengling Han, **Long Xu**, Xinghuo Yu, Zahir Tari, Yong Feng and Jiankun Hu, "Sliding-mode observers for real-time DDoS detection," In *Proceedings of the IEEE International Conference on Industrial Electronics and Applications*, June 2016, Hefei, China.

# Chapter 1

## Introduction

As the world has become increasingly interconnected through Internet, there has been a globally dramatic increase in the numbers of Internet users. According to the latest data released by the International Telecommunication Union (ITU), as shown in Fig. 1.1, the number of Internet users has come online hit more than 3.5 billion in 2017 [1]. The Internet consumers are pervasive, especially in the developed countries. As an example, nearly 90 percent of Australia's population are online and spend more than five hours a day on the Internet [3, 4]. Considering that 90 percent of Australia's population is between 5 and 80 years old, it could be generalized that everybody in a suitable age is online using the Internet. The Internet is a virtual space which is used by people nowadays to manage work both at home and office. Moreover, the Internet is a ubiquitous technology that has offered almost every company, university, governmental organization and critical infrastructure a way to become globally connected.

In the last decade, technological investments push forward the infrastructure level of network equipment. The optical fiber infrastructure support access speeds of Gbps connectivity nowadays, while it was a privilege reserved for large Internet service providers and research institutes in the past. Thus, the bandwidth of wired connections is not an obstacle anymore, and higher bandwidth services are available to the Internet costumers.

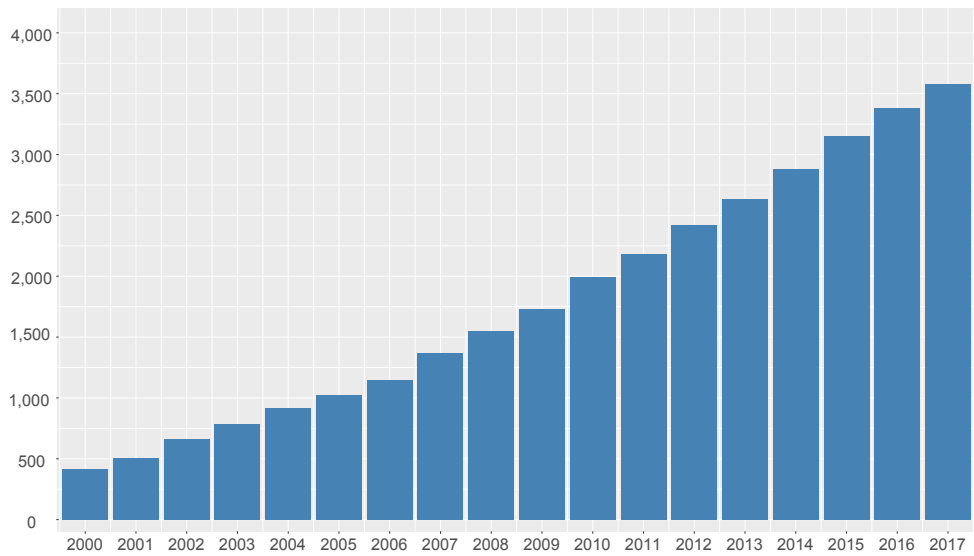


Fig. 1.1 Number of Internet users worldwide (in millions) from 2000 to 2017 (source: International Telecommunications Union) [1].

However, technological improvements on Internet and computer networks have brought new challenges to network management. First, the amount of Internet traffic has been steadily rising. According to the latest statistics by Cisco [2], the annual global IP traffic was 96 exabytes (EB) in 2016 and expected to reach 278 EB by 2021. The rapid growth of traffic volume has imposed great challenges on traditional Internet platforms in monitoring and managing the network.

Second, cyber attacks are increasing and being evolving. An attack could be launched by individuals, groups, or organizations aiming at computer information, computer networks, infrastructure or personal details by means of malicious activities destroying or hacking into a susceptible system. A few of researchers have attempted to evaluate and quantify impacts of the attacks on physical processes in critical infrastructures [5]. Besides damages to infrastructure, some attackers attempt to collect business information or personal details through the Internet in order to make a profit. For example, some attacks, such as SPAM, represent as a form of pervasive advertisement to gather personal information, bank details etc. It is estimated that nearly 90 percent of sent mails around the world are SPAM, and this

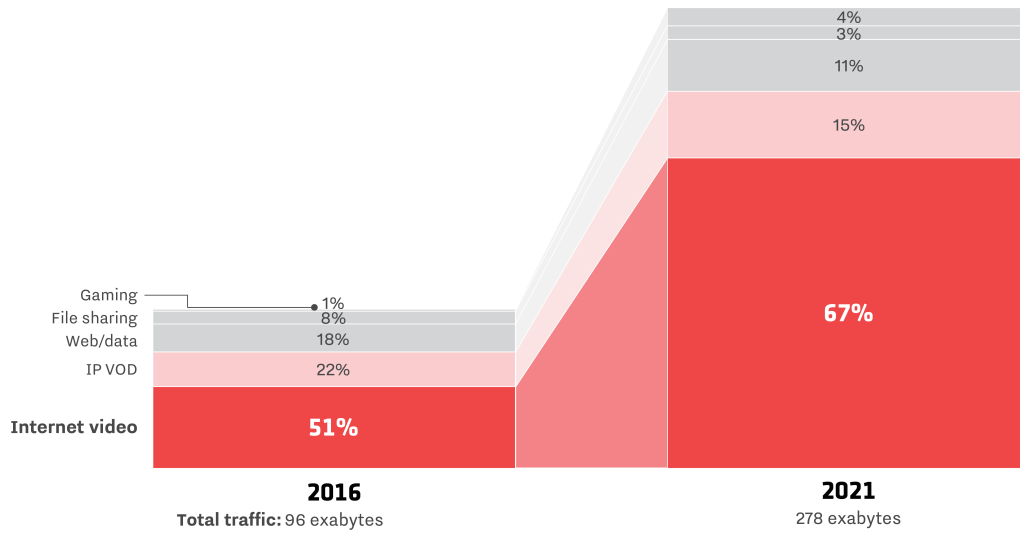


Fig. 1.2 Global IP traffic by 2021 [2].

does not have a sign to decrease [6].

Considering the growth in network load and attack frequency, it is challenging to effectively detect intruders. The network monitoring community faces the ever-growing amount of network data by concentrating on network flows, rather than individual network packets [7, 8]. A flow is a sequence of packets that are sent from a particular source to a destination that the source desires to label as a flow [9]. The means of monitoring on traffic flows offer an aggregated view of network traffic information and drastically improve the efficiency of the analysis on the amount of data. Therefore, the flow-based monitoring scheme is a possible solution to deal with the issues of scalability in network monitoring. However, analysis tools of intrusion detection that can deal with higher throughput are unable to maintain state between different steps of an attack or they are limited to the analysis of packet headers [10]. From the perspective of cybersecurity, the issue of intrusion detection under the environment of high-speed networks is a big challenge for the traditional packet-based solutions that may no longer be feasible. Moreover, the network traffic is traversing the Internet or computer networks through the network gateways, such as network routers [11]. Thus, the router-based real-time traffic flow monitoring is a promising approach that may lead to im-

proved results in the field of intrusion detection in computer networks with the high-speed environment.

In the following, we first introduce the topics of intrusion detection in **Section 1.1**, and then the network traffic monitoring and the router-based network traffic observation are reviewed in the field in **Section 1.2**. In addition, the motivation and research scope of this thesis is presented in **Section 1.3** and **1.4** respectively. Furthermore, the analysis of the issues leads us to present the research questions to be addressed, the objectives and the contributions of this thesis in **Section 1.5**. Finally, we present the outline of this thesis in **Section 1.6** and summarize the introduction in **Section 1.7**.

## 1.1 Intrusion Detection

Intrusion detection is a security tool to capture and monitor the events occurring in computer networks or systems, and analyse them to detect intrusions [12]. *Intrusion* is an attempt to compromise the confidentiality, integrity, and availability, or to bypass the security mechanisms of a computer or network [13]. Intrusions are launched by means of a sequence of actions to access the systems via Internet, then obtain the authorization of the systems to gain additional privileges, or to misuse the privileges. Intrusion Detection Systems (IDSs) are security tools that aim to strengthen the security of information and computer networks by automatically monitoring and detecting intrusion attempts [14].

In the last decades, the research on intrusion detection have developed many taxonomies of IDSs. The main taxonomies of IDS are proposed according to the characteristics, such as detection methodology, behaviour on detection, source of audit data, detection paradigm and usage frequency [15, 16]. However, the most widely used classification features are source of audit data, i.e., *host-based* or *network-based* IDS, and detection methodology, i.e., *misuse-based* or *anomaly-based* IDS.

The source of audit data is mainly classified as *host* (or *application logs*) and *network*

*data*. Depending on the types of information source, IDS can be categorized as host-based IDS and network-based IDS. A host-based IDS monitors the characteristics of a host based logs and analyses events, such as system calls and process identifiers which are related to operating system (OS) information, for suspicious activities [17]. The host based logs include OS kernel logs, application program logs, network equipment logs, etc. Besides, a network-based IDS monitors the behaviours of network traffic events and analyses network activities to identify malicious activity [18]. The network traffic data are directly captured on a multicast network such as Ethernet in terms of traffic volume, protocol usage, IP address etc.

Depending on the types of analysis, the IDSs can be classified as signature-based (or misuse-based) and anomaly-based schemes [19]. Signature-based scheme analyses the data by comparing the pre-defined patterns or signatures which have been stored. Thus, they are unable to detect the new attacks or unknown malicious activities. However, the anomaly-based detection techniques are intended to capture deviations from the established normal behaviours, and they are capable to detect unfamiliar intrusions. A lot of security tools have been designed and developed based on anomaly-based network intrusion detection systems (NIDS). In general, these NIDS detection techniques are classified into three main categories statistical-based techniques, machine learning-based, and knowledge-based [20–22]. This research aims to develop the time series analysis on network traffic for intrusion detection. The aim is to investigate how it is possible to describe anomalous events, by mathematically considering the evolution over time of flows in dynamic methods. Here, it should be noted that the network flow based intrusion detection is supposed to complement the packet-based approach by allowing early detection.

## 1.2 Network Traffic Monitoring

With the increased complexity of the Internet infrastructure, applications, and services, IDSs are required to be able to deal with the increasing number of malicious activities, the rise in the amount of traffic as well as the growth in bandwidth speed [23]. However, the processing capability of the payload-based IDSs is assessed at a low level, such as at between 100 *Mbps* and 200 *Mbps* with commodity hardware being employed, and approximated at 1 *Gbps* with dedicated hardware being used [24]. Moreover, payload-based IDSs are processed in the way of per-packet inspection that relies only on header information in order to identify misuses in encrypted protocols [25]. Given these issues, *network-based* (or flow-based) approaches seem to be promising candidates for intrusion detection research. *Flows* are monitored by built-in specialized accounting modules in network routers. After exporting the reports of flow events to external collectors by the modules, network-based monitoring system will analyse these flows to suspect on malicious activities. Compared to the conventional host-based approach, network traffic based monitoring approach can be used as a complement of packet inspection, which are capable to manage a considerable amount of network traffic data. The question remains in network-based monitoring whether only the flow information is enough to be useful for intrusion detection, compared with the payload-based inspection approach. Flow measurements are the information of aggregated network traffic. So, it does not deliver the detection precision. However, flow measurements give an aggregated viewpoint of the traffic data transferred between hosts over the network.

*Network traffic monitoring* (NTM) has been playing an important role in understanding and characterizing users' activities only though the flow-based information in computer networks and systems. The aims of NTM are mainly focused on the three improvements, which include the quality of service (QoS) of the network, optimization of resource usage, and enhancement of security in computer networks [26]. Specifically, first, network conditions can be recognized by the network manager with NTM scheme. It provides the



complete details about the QoS of network, such as bandwidth, throughput, propagation delay, link availability, jitter, server memory, database space and etc [27]. Second, with NTM being implemented at network nodes, i.e., network gateways, such as network routers, the network traffic that is traversing the network is under online observation [28]. Thereby, the network utilization can be improved by optimizing the resource usage to avoid the network congestions. Third, malicious activities, unauthenticated service or approaches to the server will be identified by regularly monitoring the traffic flow [29]. The network convention and statistics about the traffic will be known easily which helps to troubleshoot the network. Security events will also be investigated and the entry of the user will be maintained for responsibility. Over the years, a number of methodologies have been proposed in NTMs to understand network performance and users' behaviour to monitor and analyse network traffic behaviours [30]. Depending on the locations where it applied in computer networks, the NTM techniques can be categorised into two main classes, that is, *router-based network traffic monitoring* (RNTM) techniques and *non-router based network traffic monitoring* (NNTM) techniques. Some RNTM methods proposed in [31–33] are hard-coded into network routers. RNTM is responsible for collecting information which is located on managed devices, and also execute applications that monitor and control the managed devices. On the other hand, some NNTM methods [26, 34, 35] transmit probes into the network to collect measurements between at least two endpoints in the network. It deals with metrics, such as availability, routes, packet delay, packet loss, packet inter-arrival jitter, and bandwidth measurements (capacity, achievable throughputs). In this research, the techniques of RNTM that built in network gateway, i.e., network routers, will be developed to monitor the network traffic characteristics against malicious activities.

### 1.2.1 Router-based Network Traffic Observation

Router-based Network Traffic Observation (RNTO) is network flow based monitoring mechanism that built in network routers to capture the IP traffic information, analysing traffic characteristics and monitoring network traffic for malicious activities.

Some network traffic monitoring schemes are developed for traffic observations to improve the network performance. Simple network monitoring protocol (SNMP) is an application layer protocol that is part of the TCP/IP protocol suite [36]. SNMP collects the statistic information of network traffic by passive sensors at network router and destination side. By collecting and organizing information on IP networks, administrative computers have the task to monitor and manage a group of hosts in the computer networks [37]. Remote Monitoring (RMON) enables various network monitors to exchange data of network monitoring [38, 39]. Unlike SNMP that need to send out a request for information, RMON is capable to set alarms that pre-set based on a certain criteria for network monitoring. In addition, it is allowed to manage local networks and remote sites as well. NetFlow is introduced by Cisco that provides the capability to collect IP network traffic on network routers [40, 41]. By analysing the data provided by NetFlow, the network traffic information such as the source and destination, class of service, and the causes of congestion can be determined.

However, the existing RNTO techniques in the aforementioned references analyse the traffic behaviour and characteristics in a static and statistical way. With the increased complexity of the network usage, the static analytical approach is incapable to online monitor the network traffic in real-time to deal with the growth in network load and attack frequency.

The dynamics of network traffic in the router-based network can be represented by a fluid-flow model [42]. Moreover, the fluid-flow model can be further formulated by stochastic nonlinear equations to describe the traffic dynamics. With the simplified flow model describing the network traffic on routers, the control theory methods have been applied to analyse the dynamical behaviours of traffic flows on the router. These control theories-based

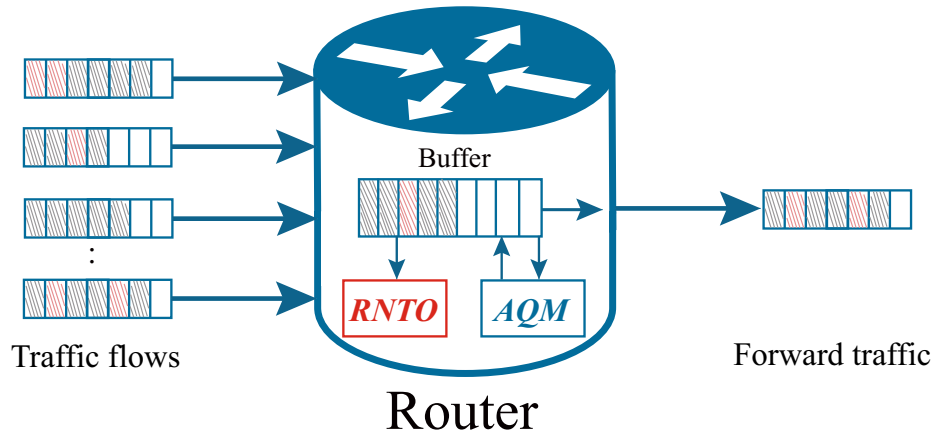


Fig. 1.3 Router-based Network Traffic Observation (RNTO).

methods have demonstrated great effectiveness in monitoring and managing network traffic on the routers. As shown in Fig. 1.3, some active queue management (AQM) algorithms are developed to be applied into network routers to stabilize the queue length in router buffer at a desired value for congestion avoidance to manage the network [43, 44]. Besides AQM algorithms, RNTO is embedded into network routers. They have two main applications. First, it is applied in the advanced AQM algorithms for network congestion control [45–47]. Second, it monitors the traffic flow in TCP networks [48–50]. Considering network anomaly in the router-based network as a perturbation into the network, RNTO is responsible to estimate and detect the network anomalies. Some methods has demonstrated great effectiveness in monitoring network traffic.

## 1.3 Motivation

Some of the issues in the existing methods in network traffic monitoring motivated this research to investigate new RNTO techniques, which are presented in the following aspects.

The growing complexity of Internet infrastructure, applications and services has brought challenges to router-based network monitoring in dealing with the increase of malicious activities, traffic amount as well as bandwidth speed. As known, it is problematic to efficiently

and accurately monitor states of the network traffic in real-time in the manner of static methods under stochastic uncertainties of the network. There are a large amount of technical and economic issues existing in the traffic observation scheme [43, 45–53].

First, the existed operating schemes of the network traffic monitoring periodically collect traffic information of a network at the router, and then convert the traffic information into a set of statistical parameters to reflect the network status. It provides periodical analysis and monitoring on network traffic characteristics [31–33]. However, with the increased complexity and the growing amount network usages, the static analytical approach is incapable of monitoring the network traffic in real-time to meet the criteria in accuracy and efficiency. In addition, the network traffic inherently features the stochastic and time delay properties in data communication. However, the static analysing method and the high stochastic uncertainties are two main limitation factors for deployment of router-based network traffic observation to meet the real-time requirements [34, 35, 40, 54, 55].

Second, in the router-based network system, it is a problem that some information of network traffic is unmeasurable and cannot be used to manage the network, such as stabilizing the queue length in router buffer in active queue management. The issue will result in low accuracy in regulating and a long response time for the targeted traffic state, and thereby cause oscillation and instability in network [45–52]. The internal system dynamics characterize the behaviour of the unmeasurable state, i.e., average Cwnd at the router. Cwnd is a state of the TCP at each host, which affects the sending rate of the TCP traffic, and it is known at the host end, while the average Cwnd that is an average value of all the connected TCP sections is unmeasurable at the router. However, the existing observation methods fail to deliver any control strategy for the internal dynamics of the system to estimate the unmeasurable state of the network traffic, which is a main limiting factor of state estimation in low accuracy and a long response time [43, 45–52, 56–59].

Third, the status of the network traffic and the traffic observation are required to be

examined in the real-time. The existing observation methods estimate the state of the traffic dynamics by the algorithms built in network routers for the time-driven computation [43, 45–53]. In the time-driven operating scheme, the information of the network traffic is sampled equidistantly in a periodic manner. However, the periodic calculation for large amount traffic data causes high consumptions on the calculation capacity and the memory space. Moreover, the resource of the communication channel and the bandwidth of the link output of the router are highly occupied. Therefore, the computational efficiency in the real-time network traffic observation will be another challenging issue [60–67].

Fourth, in the router-based network, the active TCP traffic features time-varying and stochastic network conditions [42, 43, 45–50]. Furthermore, the round-trip time is the length of time it takes for a signal to be sent from the host side plus the length of time it takes for an acknowledgement of that signal to be received. This time delay consists of the propagation time between the two points of a signal and the queuing time delay in network routers. In addition, the required queue length in router buffers varies on different performance of the network, such as the throughput, bandwidth and the congestion level. However, the existing methods of network traffic observation are developed based on the linearised model, which is linearised around a certain network condition, such as the number of TCP sections, the targeted queue length, and the round-trip time. Therefore, the global observation performance under the high stochastic uncertain network condition would be a big challenging issue [68, 69].

This research mainly focuses on investigating the techniques of RNTD which aims to solve the above mentioned challenging issues.

## 1.4 Research Scope

As an industry-standard suite of protocols, the TCP/IP suite is a descriptive framework for the Internet Protocol Suite of computer network and Internet [70]. It provides data commu-

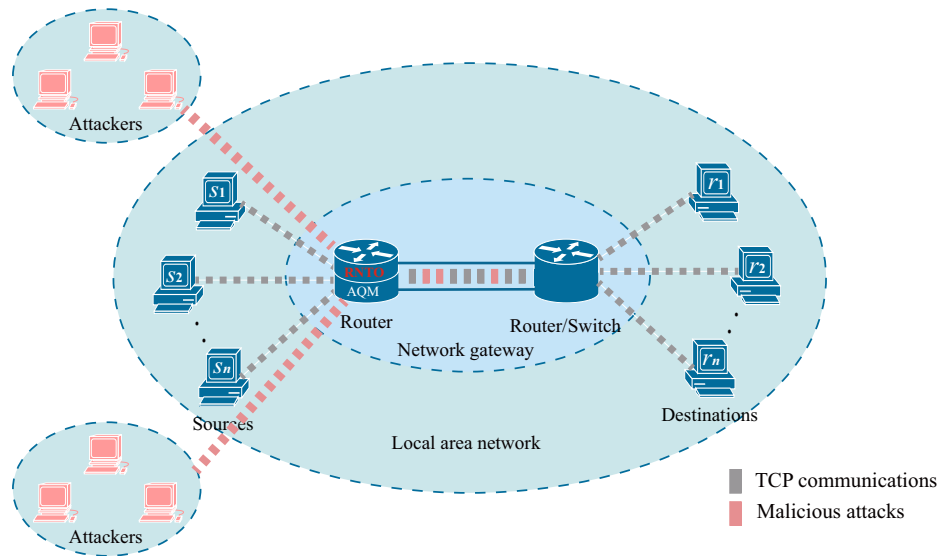


Fig. 1.4 A typical router-based TCP/IP network topology.

communications in a heterogeneous environment which is composed of dissimilar elements (hosts or clients). According to the functionality in data communications serving, the TCP/IP suite has a network model consisting of five layers: physical network, data link, network, transport, and application layers. In this model, the TCP and IP protocols are operated in transport and network layers respectively. The higher layer, TCP, is in charge of assembling of a message or file from upper layer (data link layer) into smaller packets that are transmitted over computer networks or the Internet. Once the packets are received at their destination, a TCP layer reassembles them into the original message. The lower layer, IP, is responsible for packing each packet known as IP datagrams, which contain source and destination address information (IP address) that is used to forward the datagrams between hosts or clients across computer networks or Internet. Computer network topology is a physical communication scheme used by connected devices. It is the layout pattern of interconnections of various elements (nodes, links, peripherals, etc.) of a computer network. There are five basic types of network topologies and hybrid topologies, the former include bus, ring, star, mesh, and tree, the latter are a combination of two or more of the five basic topologies.

This research takes into account a typical TCP/IP network topology, as shown in Fig.

1.4. The star is the most common used topology with its advantages of compatibility with applications, ease of implementation, cost effective, and reliability in enterprise network, in-home network, campus network, department network and public network [71]. All of the nodes, including computer workstations or any other peripherals, are essentially connected to the network gateway, i.e., a router. It can be seen in Fig. 1.4 that  $N$  homogeneous sources connect to one destination through a router. The router operates in the IP layer, which not only forwards data packets, but also plays an important role in two mechanisms: an AQM and a RNTD. AQM scheme regulates the queue length in router buffer with a randomization of choosing connections to notify the congestion, so that the TCP network utilization and QoS can be improved. The RNTD is utilized to monitor the traffic flows through the router for anomaly detection.

The proposed research aims to investigate the new RNTD for network traffic monitoring in computer networks. The RNTD is embedded into network routers to observe the network traffics states traversing the targeted routers. Thereby, the real-time traffic states are accurately estimated, which reflect the network QoS, i.e., bandwidth, jitters, delays, and congestions, etc. The estimated traffic states can be utilized by AQM scheme in order to stabilize the router-based network for congestion avoidance and QoS enhancement. For this purpose, RNTD scheme is intended to estimate the following traffic states at a network router: (a). queue length of the router buffer; (b). average congestion window (ACwnd) at the router; (c). the dynamics of the additional traffic flows (ATF). Motivated by the key issues existed in the current network traffic monitoring methods, the main contributions of this research are captured in the following formulated research questions.

## 1.5 Research Questions, Objective and Contribution

In order to overcome the aforementioned issues, we have outlined four research questions and objectives which mainly cover the techniques to develop a real-time dynamic RNTD.

### 1.5.1 Research Questions and Objectives

- **Research Question 1:** How to develop an effective real-time (dynamic) observer based on terminal sliding mode (TSM) for estimating traffic dynamics in a router-based network?

**Objective 1:** Develop a real-time dynamic observation scheme that is built in network router to monitor the network traffic flows in the router-based networks by using the sliding mode control theory.

- **Research Question 2:** How to improve the speed of internal dynamics for traffic observation in a router-based network?

**Objective 2:** Investigate a framework of real-time full-order terminal sliding mode observer for RNTTO to accelerate the convergence of the internal dynamics for solving the problem of estimating the unmeasurable state of the internal dynamics, i.e., the average Cwnd, by a novel control strategy using the finite-time stability theory.

- **Research Question 3:** How to reduce computational load to improve the resource efficiency when addressing large amount traffic in a router-based network?

**Objective 3:** Build an event triggered sliding mode observation scheme for RNTTO to solve the issue of a waste of computational capacity, router memory and the communication resource in time-driven observation methods by estimating the states of the traffic dynamics under event triggered scheme.

- **Research Question 4:** How to achieve global observations to avoid input-output linearization in a router-based network?

**Objective 4:** Establish an fuzzy terminal sliding mode observation framework for RNTTO based on the T-S fuzzy models by using fuzzy logic theory to achieve a global performance in traffic monitoring for solving the issue of the input-output linearisation



of a router-based network under a certain network conditions.

### 1.5.2 Contributions

The contributions of the research in the thesis are summarized as following:

1. The real-time dynamic router-based network traffic observers are investigated by using terminal sliding mode control theory, where the problem of network traffic dynamics of the interactions in a set of TCP flows can be modelled as mathematical differential equations. The proposed novel TSM observation algorithm has the properties of real-time dynamic estimation, finite-time convergence of the error of QL, a smooth control strategy used for ATF estimation.
2. The real-time full-order terminal sliding observer is developed for traffic monitoring in a router-based network. In the proposed full-order TSM observation scheme, the internal dynamics of the system, i.e., the average Cwnd, is accelerated by using finite-time theory, thereafter, its estimation is obtained. Moreover, the novel continuous control strategy of the TSM is used for ATF estimation.
3. An event-triggered SMC based observation scheme is proposed to solve the issue of the waste of computational capacity, router memory and the communication resource in a router-based network. In the novel algorithm, the computational load and the communication burden is reduced. Furthermore, the event-triggered control strategy is designed to be smooth for the state estimation.
4. The real-time fuzzy terminal sliding observer is developed to overcome the issue of the input-output linearisation design approach that only features local stability. In the proposed novel fuzzy TSM observation algorithm, the global observation performance is obtained by using fuzzy logic theory. Based on the fuzzy rules, the smooth

fuzzy control strategy is developed for the ATF dynamic estimations. Moreover, the error of QL converges to the origin in a finite-time.

## 1.6 Structure of Thesis

The thesis is organized as follows:

- **Chapter 1** provides an overview of the router-based network traffic observation. Then, the motivation and the scope of research are proposed. Afterwards, the research questions, objectives and contributions of this research are emphasised.
- **Chapter 2** presents a literature review on router-based network traffic observation problem. In addition, the main control methodologies developed in RNT0 are reviewed. Furthermore, the existing key challenging issues to be solved out are discussed and identified. Finally, the brief introduction to the sliding mode control theory and the two main SMC methods, which are used in the following chapters, are given.
- **Chapter 3** studies the problem of router-based network traffic monitoring. A real-time dynamic RNT0 scheme is developed by using sliding mode control theory for overcoming the drawbacks of static methods. The dynamics of the router-based network can be modelled by a fluid-flow model using mathematical equations. Based on the fluid-flow model, the real-time sliding mode observers, such as the conventional sliding mode observer, the super-twisting observer and the novel terminal sliding mode observer, are investigated for RNT0 to estimate the states of the network traffic. In the novel terminal sliding mode observer, a smooth control signal is obtained and directly used to estimate the dynamics of the additional traffic flows. The effectiveness and capability of the proposed sliding mode observers have been eval-

- uated in network simulator 2. In addition, the comparative studies of the proposed sliding mode observers are conducted and discussed.
- **Chapter 4** establishes a real-time dynamic full-order terminal sliding mode observer to estimate the system states for a class of systems where some system states are unmeasurable. By considering the unmeasurable state of the internal dynamics in the network system, a control strategy is developed by using the finite-time stability theory to speed up the convergence of the internal dynamics. A continuous control signal is designed and directly used for the traffic monitoring in the real-time without any low-pass filter. The stability of the proposed observer system is analysed and proofed. The comparative simulation results among the sliding mode observers in the network simulator 2 have been studied and discussed.
  - **Chapter 5** investigates an event triggered sliding mode observer for traffic monitoring to reduce the computational load and the communication burden in RNT0. Instead of the time-driven observation scheme, the control of the sliding mode observer is formulated under the event triggered scheme. The control of the observer is designed to be smooth and is directly applied to estimate the dynamics of the additional traffic flows. The event triggered observation algorithms is developed to reduce the computational load of the network router and the communication resource of output link in the network. The simulation is studied via the network simulator 2 to demonstrate the efficient monitoring.
  - **Chapter 6** develops a real-time fuzzy terminal sliding observer to overcome the input-output linearisation of a router-based network for RNT0. The T-S fuzzy models for the dynamics of router-based network traffic are constructed by using fuzzy logic theory. Based on the T-S fuzzy models, the fuzzy terminal sliding mode observer is established by using fuzzy logic theory to estimate the states of the network traffic

to achieve the global observation performance under network uncertainties. In the fuzzy terminal sliding mode observer, the control signal is designed to be continuous for applications in estimating the additional traffic flows without the low-pass filter. The stability of the fuzzy observer system is studied and proofed. The capacity of the proposed global RNTD scheme is validated via the network simulator 2 with the simulation results presented.

- **Chapter 7** concludes the significance of each state of the investigations in earlier chapters of this thesis.

Apart from the main text, the bibliography of this thesis is presented, and the cited articles and sources information are provided. In addition, publications during Ph.D. studies are listed which include journal and conference papers.

## 1.7 Summary

This chapter has introduced the background of the router-based network traffic observation. The motivation and research scope of this thesis have also been presented. In addition, the research questions, the objective and contributions are presented. Finally, the organization and the main content of each chapter have been briefly summarised.

## Chapter 2

# Literature Review: Router-based Network Traffic Observation Problems

### 2.1 Introduction

This chapter provides a review the existing literature of typical network traffic observation issues in router-based networks. First, some challenging issues of router-based network traffic observation are discussed in **Section 2.2**. Second, the main control methodologies developed in RNTTO are reviewed in **Section 2.3**. Third, some challenging problems to be solved out are discussed and identified in **Section 2.4**. Fourth, the brief introduction to the sliding mode control theory and the other two main SMC methods, which are used in the following chapters, are given in **Section 2.5**. Finally, a brief summary is given in **Section 2.6**.

## **2.2 Some Issues of RNTO**

### **2.2.1 Source Information Analysis**

In this section, the problems of router-based network traffic monitoring (RNTM) are discussed. Since Internet is a complex dynamic system connected with billions of hosts or clients, RNTM is pivotal for effective network management in measuring the network traffic behaviours of Internet. RNTM collects the information of traffic flow to analyse the behaviours and execute applications that monitor and control the network.

Traffic flow is one of the most critical information sources in RNTM. The traffic packet headers include the information of IP address, packet size, number of packets, number of flows and etc [30]. Some approaches are proposed to analyse the characteristics of traffic packets to inspect behaviours of traffic information for detecting the malicious activities. Depending on the characteristics of the packet data, there are two main types of the methods, such as probabilistic sampling and real-time series [72].

#### **2.2.1.1 Probabilistic Sampling**

A number of researchers have proposed the monitoring methods by probabilistic sampling analysis using the machine learning and signal processing to analyse the characteristics of the traffic packet headers to discover abnormal activities due to the changes in traffic pattern [19, 73–75]. The significant changes of network traffic patterns are investigated in the probabilistic distribution viewpoint. In fact, the philosophical attackers tend to launch the malicious attacks with gradual rate change to avoid sudden changes in traffic patterns [76]. However, it is difficult to detect the anomalies that do not cause significant changes in the probabilistic distribution of a single traffic feature.

Traffic packets are projected to four matrices according to different bits of the IP address. Many methods have proposed to analyse the IP address attributes to monitor the abnormal

behaviours [77]. Internet Protocol (IP) is a set of rules that defines how a computer sends data to another computer. Computers and devices have a unique IP address. The usage of this is to route a packet via a network from source to destination. IP assigns unique addresses to devices across networks, encapsulates the data into datagrams and sends the datagram to its destination [78]. There are various types of IP versions however IPv4 (Internet Protocol version 4) and IPv6 (Internet Protocol version 6) are currently coexist in the global Internet [79]. In [54], the structure of the addresses included in IPv4 traffic with different lengths of prefixes is analysed for traffic measurement and monitoring. Besides analysing the characteristics of IP addresses, the statistical characteristics of users' behaviours are studied by analysing the protocol, the client, the server port, and the total number of packets transferred in the network. Some approaches are proposed to analyse the statistical characteristics of users' behaviours to perform abnormal behaviour monitoring [80–82]. However, the information capturing for each packet to get the detailed address is necessary for these methods, which may degrade the efficiency of the real-time RNTM monitoring system.

#### 2.2.1.2 Real-time Series

To overcome the issue of probabilistic sampling methods, the NetFlow is developed by Cisco of analysing the characteristics of the packet data in time series[40]. The idea of traffic flow in NetFlow is to create logic links between hosts and provide a way to analyse the characteristics of packet data that transferred between hosts. Some methods developed to analyse the traffic data with time series, which include wavelets [83], time-series forecast by exponentially weighted moving average (EWMA) [84], and some signal processing techniques [85]. They are mainly focusing on the detection of deviations from the expected values. Besides these methods, the entropy in information theory is proposed as a critical method of measurement for the distributed traffic characteristics [86]. It is used for anomaly detection at the network ingress point for malicious activities that cannot be purely identi-

fied by adopting flow volume based methods, i.e., worm attacks, etc. [87, 88]. By setting the baseline of normal values in the flow based model, the abnormal behaviour such as worms and port scan can be identified and detected [89, 90].

There are two main methods used to reduce the amount of flow records and develop real-time detection systems. One is the method in sampling analysis, which is capable to analyse massive traffic data. It is used to significantly reduce the computational complexity in data storing and processing. Some sampling methods are studied for high speed traffic monitoring, such as the random sampling method, the sample and hold sampling method, and the smart sampling method [91–93]. However, the limitation of the sampling rate by the size of space usage can cause missing information of network flow data especially for large amount data flows that combined with some small volume data packets that launched by DoS or DDoS flooding attacks [94]. The sketch method is proposed to analyse network data in massive streams, which is similar to the bloom filter and widely applied in data stream computations [55, 95]. By using a probabilistic dimension reduction method, a large amount data of traffic states is sketched into a probabilistic summary for massive data streams. This method is used to deal with the heavy hitters, changes and flow size distribution, which are the key factors for network traffic monitoring, accounting, and anomaly detection [55, 96–99]. In order to satisfy the small storage and low computational requirements, the accuracy of the sketch method is sacrificed and many heavy hitters or changes may be missed.

### **2.2.2 Flow-based Observation**

In recent years, a great number of methods have been proposed in flow-based observation to manage the network and analyse network traffic behaviours [30]. Based on the locations where it implemented in the network, it can be categorised into two main methods, such as non-router based network traffic observation (NRNTO) and router-based network traffic observation (RNTO).



### 2.2.2.1 NRNT0

A NRNT0 technique is responsible to measure network information include network delay, jitter, packet loss, bandwidth utilization and throughputs. The NRNT0 methodologies can be categorized into active monitoring (AM) methods, passive monitoring (PM) methods and hybrid monitoring (HM) methods (include both active and passive monitoring) [100].

AM schemes are to transmit probes into the network for the measurement collection between network nodes (at least two endpoints) [101]. A technique called packet-pair probing is proposed to measure the bandwidth of the network bottleneck [102]. This method deals with system startup, retransmission and timeout strategy, and dynamic set-point probing in a single source, the interactions of multiple sources, and the behavior of packet-pair sources in a variety of benchmark scenarios. Furthermore, many AM schemes are developed based on this scheme and available in the literature [102–104]. For example, an AM scheme called Pathchar combines the packet-pair probing traceroute to derive per-hop network information [103]. The ping is a common AM approach that measures network delay and the packet loss, and trace route to construct the network topology. It sends probes such as Internet Control Message Protocol (ICMP) packets to the target nodes and then receives the response information that is sent back from the target nodes [105]. The problem in existing AM methods is introducing probes into the network, which can be an interference to the normal network. As a result, AM methods are rarely implemented as stand-alone methods for network monitoring due to a number of overhead is introduced into the network. However, PM approaches do not introduce much if any overhead into the network.

PM methods overcome the issues of AM methods associated with overheads and delay by monitoring streams in progress. PM techniques do not inject traffic into the network [106, 107]. Different from AM techniques, PM schemes are to collect information of only one network node in the network. A PM method is to monitor the network flow that travel on a single link between two network nodes. It can deal with network information, such

as traffic and protocol mixes accurate bit, packet rates and packet timing and inter-arrival timing. A PM method called shared passive network performance discovery (SPAND) is proposed to determine network characteristics by making shared, passive measurements from a collection of hosts [108]. It extends the basic passive monitoring by providing facilities for sharing of measurement results among hosts in order to increase the accuracy. Although PM methods do not have the problem of overhead that is existing in AM schemes, it has its own set of issues. With PM techniques, measurements of network information can only be analysed off-line. Thus, it is a challenging issue of processing the large amount of network data that are collected. Considering the advantages of PM methods of overhead data that is not injected into the network but post-processing time can take a large amount of time, a combination of the two monitoring methods is the route to overcome the existing problems.

A HM scheme combines a PM method where possible and resorts to an AM method when passive information is unavailable. The HM approach provides a universal monitoring tool for the emerging wireless Internet environment [100]. An extended passive monitoring server (EXPAND) method as a HM scheme is proposed to provide both AM and PM techniques in the wireless access networks [100]. The EXPAND server is to respond with the requested information about the fixed network segment. Moreover, the request-response packets are used by the requesting mobile host as active probes to determine the characteristics of the wireless access network. However, there exist highly varying characteristics in a wireless link. So, the reliable estimation of the network characteristics is not possible by using raw data from the active probes. In addition, the capture effects can result in false estimates over CSMA links such as 802.11. To overcome the issue of capture effects, a capture avoidance binary exponential back-off (CABEB) algorithm is proposed by applying the standard binary exponential back-off (BEB) with enhancements for collision resolution in the special case when a station attempts to capture the channel subsequent to

an uninterrupted consecutive transmit [109]. Due to the active probing only takes place on demand, and only when passive information is unavailable, in the above scheme, the probing traffic overhead is minimized. Moreover, a scheme for watching resources from the edge of the network (WREN) is investigated by combining both AM and PM techniques to actively monitor network traffic when at a low volume and passively monitor network traffic high volume [110]. This method is to monitor network traffic at both the source and destination end by using packet traces to measure the available bandwidth. Furthermore, self-configuring network monitor (SCNM) is an HM method that applies both active and passive monitoring techniques to collect information at network routers and significant network nodes [111]. The SCNM provides critical functionality needed to diagnose network problems by allowing end users to monitor their own traffic. It improves the efficiency of the software to allow capture of higher rate streams and deployment of the monitor to additional sites.

#### 2.2.2.2 RNTD

Various RNTM approaches are proposed in to be implemented into network routers to collect information of network traffic that is located at managed devices, and also execute applications that monitor and control the managed devices. A brief explanation of the most commonly used RNTD techniques is given below.

A simple network monitoring protocol (SNMP) scheme is proposed as an application layer protocol that is part of the TCP/IP protocol suite [37]. In the short-term, the SNMP is used to manage network nodes in the Internet community. In addition, in the long-term, the application of the OSI network management framework was to be examined [36]. It is responsible to manage network performance, detect and solve out network issues. This approach is to statistically collect traffic information by passive sensors that are implemented at network routers and host ends. Furthermore, SNMPv1 and SNMPv2 are developed to

deliver enhancements on monitoring performance, such as additional protocol operations [112]. Moreover, SNMPv3 is studied to provide secure access to devices by authenticating and encrypting data packets over the network [113]. This method deals with the issue of security features and the configuration of the security mechanism to handle SNMP packets [114]. However, the SNMP scheme is an application layer protocol that uses passive sensors to monitor network traffic and performance. It has an issue of the vulnerability to security threats due to the lack of any authentication capabilities [115–117].

To overcome the issue of vulnerability to security in SNMP approaches, a remote monitoring (RMON) method is proposed to monitor the network layer and below, rather than at the application layer in SNMP methods [118]. RMON is to monitor devices for the purpose of managing a network. Normally, these remote probes are stand-alone devices and devote significant internal resources for the sole purpose of network management. The RMON extends the management information databased (MIB) of that in SNMP. Different of SNMP that need to send out a request for information, RMON is capable to set alarms which monitor the network based on certain criteria. In this method, the administrators are allowed to manage the local networks and the remote sites. In addition, RMON version 2 is developed to monitor the network packets on network layers [119]. This technique is used for monitoring the IP traffic flows and the application level traffic flows as well. However, the RMON scheme is established on the SNMP protocol, the analysis of the traffic monitoring by the SNMP and RMON methods are limited the monitoring features.

To consider the limitation in the existing SNMP and RMON methods, Netflow is proposed to deliver many analysis software packages to monitor the network traffics [33]. Netflow scheme is to collect IP network traffic as the traffic enters its interface. By analysing the traffic data provided by Netflow, the traffic information such as the source and destination of the traffic, class of service, and the cause of congestion can be determined. This scheme has the feature of creating the numerous different graphs in network activity details. How-

ever, sampled NetFlow has shortcomings that hinder the collection and analysis of traffic data. Thus, it is impossible to estimate without bias the number of active flows for aggregates with non-TCP traffic. To overcome this issue, an adaptive NetFlow is developed by an update to router software, which addresses many shortcomings of NetFlow by dynamically adapting the sampling rate to achieve robustness without sacrificing accuracy [120]. Various flow monitoring methods are studied by using NetFlow data to monitor the network traffic and manage the network flow [121–123].

Some methods of RNT0 are proposed to be implemented in routers. It features two main applications. Firstly, they can be applied in the advanced AQM algorithms for network congestion control [45–47]. Secondly, they can monitor the traffic flow in TCP networks [48–50]. Since a network anomaly can be considered as a perturbation in the traffic flow of the router level, an observer can be designed to estimate the network anomaly. It can collaborate with AQM in the router to detect and estimate anomalies [49, 51]. This method has demonstrated great effectiveness in monitoring network traffic [124, 125]

The observers in the aforementioned references include mainly the Luenberger observer, fuzzy observer, and sliding-mode observer. A Luenberger observer was embedded in a router to monitor the TCP traffic flows [45]. In [46, 47], a Luenberger observer was synthesized to estimate the state of the network for the optimal queue length control and the congestion avoidance. A Luenberger observer was applied to reconstruct the unmeasurable ACwnd for avoiding congestion in [46]. A fuzzy observer was designed to build an observer-based fuzzy controller to implement a T-S fuzzy control algorithm for the congestion control [68]. Another fuzzy observer was applied to constitute an AQM controller for a TCP/IP network to track the desired queue length accurately and avoid network congestion [69]. A sliding-mode observer was used to detect anomalies [51]. A higher-order sliding-mode observer was applied for anomaly detection [52]. Its robustness and fast response enhance the efficiency of the traffic monitoring.

In three observers aforementioned, the Luenberger observer is a classic widely-used observer. However, in the presence of unknown signals or uncertainty, it is usually unable to accurately observe the system states [45–47]. To overcome its drawbacks, the Fuzzy observer was presented by using Takagi-Sugeno fuzzy system which is consisted of a number of linear time-invariant models to approximate the nonlinear plant. But local linear observers are still hardly to force the estimation errors to zero [68, 69]. A sliding-mode observer is a class of robust observer. It is designed using Sliding-mode control (SMC) theory. The SMC has attractive advantages, such as low sensitivity to parameter variations and strong robustness to external disturbances [126–130]. Main applications of sliding mode observers include the congestion control and the traffic monitoring in the TCP/IP networks.

### 2.2.3 Network Management

Network congestion is a challenging issue that affecting network quality of service (QoS) [131, 132]. It occurs when a network node or link, e.g., the network router and the link bandwidth, is carrying more data that exceeds the capacity of the resource [133]. The congestion of a network results in a high delay, packet loss, jitter, wasted resources, and even global synchronization, i.e., the throughput drops to zero, the response time tends to infinity and QoS is extremely poor [134]. In order to deal with the issue of network congestion, the aim of research is to control network congestion or even avoid congestion. As one of the most effective congestion control mechanism, active queue management (AQM) algorithm has been widely implemented on the Internet due to simplicity and scalability [135]. As the AQM being implemented in routers, the traffic flow through the routers can be analysed and controlled. The AQM mechanism is implemented in network routers to control and analyse the traffic flow through the routers and then achieve the following goals: managing queue lengths, providing a lower interactive delay, and avoiding global synchronization [136].

Over the past few years, many research on AQM schemes have been proposed for net-

work management. Based on the approach, these schemes can be classified into two main categories: optimization approach and control theory.

### 2.2.3.1 Optimization Approach

The optimization approach formulates the problem of congestion control as that of the maximization of an aggregate source utility via an approximate gradient algorithm according to constraints of network capacity [137]. A random exponential marking (REM) approach is first proposed in [138] as an optimization approach to control congestion, which is derived from earlier work on the optimization flow control. In this approach, the optimal controller is able to deal with the congestion by optimizing source rates or the congestion measure. Many improved REM algorithms have been proposed. In [139], an adaptive REM algorithm is studied to enhance the performance of REM algorithm. Moreover, another strategy of adaptive fuzzy REM scheme is proposed by adjusting the dropping probability subject to the network load [140]. However, both of them optimize the local problem without theoretical tools to design comprehensively and systematically. Furthermore, a self-tuning REM (STREM) is proposed to change the control parameter automatically according to the changes of round trip time, link capacity and number of TCP loads [141].

In addition, an adaptive virtual queue (AVQ) algorithm is proposed in [142] to maintain the arrival rate at a desired utilization by optimizing a source rate in AQM mechanism to achieve a low-loss, low-delay and high utilization operation at the link. The AVQ method is to find the fastest rate at which the marking probability adaptation can take place by considering the certain system parameters such as the maximum delay and the number of users to remain the system stable. However, the desired utilization parameter in AVQ algorithm has an influence on the dynamics of queue and link utilization, which is difficult to achieve a fast system response and high link utilization. In this condition, an stabilized AVQ (SAVQ) is proposed by adaptive setting on utilization parameter subject to the QL to obtain a high

link utilization [143]. In order to achieve stability condition, a scalable parameter tuning approach for AVQ is proposed to decouple the control parameter from the parameters related to network conditions such that the control parameter is tuned to maintain stability as capacity scales up [144].

Furthermore, a stabilized virtual buffer (SVB) is developed to optimize both the packet arrival rate and the QL as its congestion indicator to control the packet arrival rate and the QL at their desired values using a virtual queue based approach [145]. Same as REM, the SVB scheme considers both the packet arrival rate and queue size to stabilize them around the target values. However unlike REM, SVB maintains a virtual queue and responds to the traffic dynamics faster for better stability, especially in the presence of short flows. In the SVB scheme, the packets are marked with a probability based on the virtual queue dynamics that is adaptively adjusted according to the packet arrival rate. To support multiple traffic classes, while focusing on the stability, fairness, and QoS predictability issues, a class-based stabilized virtual buffer is developed to improve the queue stability, fairness and bandwidth assurance for various classes of Internet connection [146].

### 2.2.3.2 Control Theory

The control theoretic approach is used to model the dynamics of TCP flows with RED dynamics with the properties of the stability and fast time respond in network communication system [42]. A great number of research are proposed on the analysis of RED using control theory. In the conventional RED mechanism, it is a challenging issue of parameterising RED to stabilize the QL with good performance under the different congestion scenarios. It fails to achieve the goal of QL stabilization in router buffer, due to the equilibrium QL strongly depends on the number of TCP loads. To overcome the drawback, a dynamic random early drop (DRED) is proposed by using the control theoretic approach to stabilize the QL at a desired level independent of the number of active TCP connections when a router buffer



gets congested [147]. This can achieve the properties of high resource utilization, bounded delays, more certain buffer provisioning and traffic-load independent network performance.

Furthermore, proportional (P) controller is developed in AQM scheme to achieve good transient response [148]. However, it suffered steady-state errors in QL regulation. To solve out this problem, proportional integral (PI) control strategy is proposed to show a better performance under different network scenarios considered in [148]. Moreover, a proportional integral derivative (PID) controller is investigated to detect the incipient congestion and control the congestion proactively [149]. Various control strategies such as PID AQM schemes by a linear quadratic regulator method [150], PD controller for AQM [151], adaptive PI AQM [152], robust nonlinear PI AQM [153], self-tuning PI algorithm [154], Switching resilient PI controllers [155] are developed to stabilize the QL to ensure the QoS of the network. However, the majority of those schemes have the problems of oscillations, overshoots and the characteristic limitation of throttling the controller dynamics to maintain stability when applied to feedback systems with delay [156].

A number of methods focus on effective control by considering the time-varying delays in the networks. A stable controller strategy is investigated to regulate the traffic in multiple connections with uncertain time-varying propagation delays [43]. The controller, which is obtained by the minimization of appropriate  $H^\infty$  norm, satisfies a weighted fairness condition and guarantees asymptotic stability of the QL. However, the time varying forward delay induces steady-state oscillations, which cannot be avoided unless some information of the forward delay uncertainty is known. To improve the performance, a  $H^\infty$  norm-based controller is proposed in [157]. An adaptive controller is proposed to effectively combine the benefits of control theoretic and fuzzy-logic approach was also proposed to address the issue of uncertain and time-varying delays [158]. The QL can be stabilized at a reference value, while the fuzzy element adjusts the adaptive multiplicative gain to compensate for the transmitter saturation. In the work [159], the developed regulator showed an improved per-

formance when compared with the  $H^\infty$  scheme. Fuzzy logic method is applied in [160] to address the flow regulation problem in the network with multiple uncertain time delays. The fuzzy immune-PID controller is proved to handle different network scenarios, such as the saturation nonlinearities. The improved strategy is studied by providing the sufficient condition for the stability of the closed-loop system [161]. To achieve better performance in network stability, a sliding mode control based strategy is developed to maintain the weighted fairness [162]. The results demonstrate better dynamical performance and improved stability compared with the work in [160].

## 2.3 Main Methodologies in RNTTO

Over the last decade, a large number of results focus on network management of AQMs and RNTTOs by taking one, two, or more issues mentioned in previous section. A review on the main control methodologies is given in the following sections. Components of the main control methods are classical control approach, adaptive control approach, neuron network approach, fuzzy approach and sliding mode control approach.

### 2.3.1 Neuron Network Approach

The neuron network (NN) approach is applied as an efficient predictor of traffic in computer networks by learning the complex patterns in computer networks, which features high ability of self-learning and versatility. Normally, AQM schemes cannot achieve optimal performance due to unpredictable traffic variability. By adopting the concept of the NN strategies, it is potential to improve efficiency of parameter tuning and system performance.

Over the last few years, various research focus on the neural network based AQM schemes development. For example, a neural network model predictive control (NN-MPC) is investigated to control the traffic flows in [163]. The proposed NN-MPC demonstrates

the better transient and steady behaviors compared with the classical PI controller. In [164], a neural network based RED (NN-RED) is studied to improve RED by applying a neural network as a prediction method to determine the future values of QL and the dropping probability in router buffer. It features the property of less parameter to be set when compared with the conventional RED algorithms. Moreover, an adaptive neural network (ANN) based strategy is developed for traffic flow management [165]. The ANN scheme classifies the network traffic condition into three different traffic scenarios: light traffic, medium traffic and heavy traffic. Based on these conditions, it determines the control value of the dropping probability by using a Dynamic Bayesian Network (DBN) stochastic process. A neuron PID is developed to adaptively tune the parameters of a PID controller by applying the errors of QL as the neuron input [166, 167]. This strategy implements an associative learning based on both supervised and unsupervised learning, i.e., Hebbian Learning, to achieve the network management. In addition, an adaptive neuron AQM (AN-AQM) is developed by considering the errors of link capacity, QL, and the sending rate as the neuron input [168]. The proposed method improves the performance in the network environment with the long delay networks and the dynamics of the additional traffic flows. Furthermore, a neuron reinforcement learning (NRL) based AQM scheme is studied in [169]. It considers both the error of QL and the sending rate as the neuron input to apply in the reinforcement learning rule to generate the dropping probability as the output value. Moreover, a fuzzy assisted PID controller based on neuron network (FAPIDNN) is proposed in [170]. In this scheme, a neural network based PID controller is used to derive the dropping probability of AQM by a fuzzy logic controller to calculate the learning rate of NN.

Even though the NN approach can achieve a good performance in parameter turning of the network management by self-learning capability under the network uncertainties, there are still some challenging issues existed in the methods. For example, the large black box in NN makes them difficult to train, where the training outcome can be non-deterministic

and depend crucially on the choice of initial parameters, which cannot meet the real-time requirement under the large amount of traffic flows in the network.

### 2.3.2 Fuzzy Approach

In the past few decades, the Takagi-Sugeno (T-S) fuzzy model has been proven to be an effective model to describe many nonlinear complicated real systems such as multiple nonlinear systems, switched nonlinear hybrid systems, and second-order non-holonomic systems [171–174]. In [175], a discrete-time switching fuzzy system is developed, which inherently contains the features of switched hybrid systems and T-S fuzzy systems. Therefore, fuzzy logic theory has been widely applied in the control area [176–179].

An fuzzy congestion control mechanism is proposed to control the network flow based on a variable length virtual output QL [180]. In this scheme, the fuzzy logic control is used to provide the properties of controlling of the nonlinear time-varying systems due to its capability of dynamically adapting its parameters. In contrast, the other control strategies would have to be held a constant value even under the network environment with time-varying traffic load, round trip times, etc. The existing methods are developed based on the linearised model, which is linearised around a certain network condition, such as the number of TCP sections, the targeted QL, and the round-trip time. Fuzzy control avoids this to achieve a global nonlinear performance. In [181], fuzzy-logic control is developed without a precise model. Some research on fuzzy logic in telecommunications networks are presented in the literature [182].

A fuzzy control based RED (FCRED) is investigated to adjust the parameter of the RED algorithm [183]. This work presents a brief summary of fuzzy logic control theory in communication network. There are three main parts in the fuzzy controller design: the fuzzification unit, fuzzy-inference engine with fuzzy-rule base and defuzzification unit. The fuzzification unit is to map the input values to be controlled to a fuzzy set, such as the mem-

bership functions. In addition, the fuzzy-rule base is to provide the connection between the input data and the appropriate output values. It is constructed according to a combination of trial and error [184]. The fuzzy model consists of a set of IF-THEN rules. Furthermore, the defuzzification unit maps this fuzzy output variable to a crisp controller output. According to the results in [185], defuzzification methods include: centre of area (CoA), centre of maximum (CoM) and mean of maximum (MoM) that the plant understands.

A fuzzy based RED is proposed to generate the control of the packet dropping probability subject to the average QL and the packet loss rate based on a fuzzy logic method [184]. Moreover, another improved fuzzy RED algorithm is investigated to dynamically tune the maximum drop probability parameter (Pmax) of the RED. It use the Pmax and the error signal as the input data in the controller, then the output value of the controller is the change of Pmax in RED. An adaptive fuzzy based RED (AFRED) AQM control is developed to adapt the fuzzy rule and parameters in membership functions for improving the stability [181]. Thus, AFRED features an adaptive adjust module with the input variable of the instantaneous QL to produce the control of packet drop probability. The fuzzy rules of AFRED are changed based on the real packet drop ratio measured in AQM. A fuzzy logic controller based REM (FUZREM) is designed in [186]. In addition, an adaptive fuzzy REM (AFREM) is developed to adapt its fuzzy rules for the REM mechanism [69]. Furthermore, a fuzzy GREEN is proposed in [185]. Moreover, a DEEP BLUE [187] is designed by combining the BLUE AQM algorithm with the fuzzy extension of Q-learning, a reinforcement learning technique, to achieve the online model-free optimization. Also, a fuzzy logic congestion detection (FLCD) algorithm is investigated in [188].

A fuzzy-based PID AQM strategy is developed by to operate in conjunction with a conventional PID controller via a fuzzy switching mechanism [189]. The fuzzy PID controller consists of two inputs, such as the error QL and the error of its change rate. In order to consider the error of the link input rate, a enhanced fuzzy controller is studied to generate

the output variable of dropping probability in [190]. In the fuzzy-logic control strategy, the maximum QL of virtual output queues that is adjusted by the controller can induce packet drops in the real queue [191]. Thus, a self-adaptive fuzzy controller [192] is developed to calculate the learning rate for a neural-network-based PID controller [193]. The further work on fuzzy control for network traffic management can be found in the literature [194–197].

Some observation strategies are proposed to be implemented in routers to improve the performance in AQM schemes and to monitor the traffic flow in TCP networks [48–50]. A fuzzy observer was designed to build an observer-based fuzzy controller to implement a T-S fuzzy control algorithm for the congestion control [68]. Another fuzzy observer was applied to constitute an AQM controller for a TCP/IP network to track the desired QL accurately and avoid network congestion [69]. To achieve the performance in the presence of unknown signals or uncertainties in the networks, the fuzzy observer was presented by using T-S fuzzy system which is consisted of a number of linear time-invariant models to approximate the nonlinear plant. However, the issues of the local linear observation in the subsystem of the fuzzy system are still hardly to force the estimation errors to zero [68, 69].

### 2.3.3 SMC Approach

In a router-based network traffic system, the main concern is robustness to handle network traffic to meet the requirement of network QoS. There are a great number of results on efficient congestion control methods to overcome this critical issue for achieving this desirable property. In the aforementioned literature, it has been demonstrated the advantages of using systematic control theoretical approach in the AQM algorithms design. Among the existing methodologies, the sliding mode control (SMC) theory is the one with particularly appealing robustness properties and efficiency in stabilizing complex nonlinear systems [126]. Some approaches have appeared in the literature regarding the application of SMC to manage the

network traffic and estimate the traffic dynamics. Then, several examples are discussed in the following.

Various SMC based AQM schemes are proposed to manage network traffic flows of the router-based network system in the literature. Some SMC methods are developed for AQM flow control in the continuous-time domain, where can be obtained without explicit consideration of the network delay in the feedback [198, 199]. Moreover, a fuzzy logic based SMC algorithm is investigated to improve the error convergence for a simplified router-based fluid-flow network model ignoring delay effectiveness by combining the advantages of linear and terminal sliding manifold designs [200]. In addition, a fuzzy-based integral SMC is studied for differentiated services (DiffServ) networks [201]. In DiffServ networks, a fuzzy SMC scheme is used to regulate the premium traffic flow, while an integral SMC is implemented for the ordinary service. Furthermore, an adaptive SMC approach is developed for a fluid-flow model of DiffServ networks neglecting the feedback latency by using the backstepping strategy [202]. To consider network delay in the model of DiffServ networks, a second-order SMC algorithm is investigated [203]. In this method, the three second-order SMC schemes are used for chattering reduction, ordinary traffic regulation, and the premium traffic control.

In the router-based network system, the SMC theory is applied to control the TCP traffic dynamics to ensure the network QoS. An SMC based AQM algorithm is studied by considering the time delay of the dropping probability, which is the input signal of the network system [204]. Moreover, the stability of the network system is analysed by only considering the matched uncertainties. To consider the input delay and the unmatched uncertainties in the system, an improved SMC AQM scheme is developed [205]. Furthermore, both the input delay and the state delay are taken into account to develop an SMC based flow control mechanism [206]. In this method, the maximum allowable bound of the time delay for the network system is given to guarantee the system stability. Moreover, a discrete-time SMC

method is developed as an AQM scheme to control the network flow [207]. However, the method is studied the router-based fluid-flow model with neglecting the input and state delay. In this approach, the linear matrix inequality (LMI) method is applied to obtain the asymptotic stability of the system with parameter uncertainties. In addition, an observer-based SMC strategy is investigated by using LMI method to consider the uncertainties, input delay and the saturated input signal in the system [208]. In this approach, the observer is applied to estimate the ACwnd and the QL in the router-based network system, and the controller is used to regulate the target QL at a desired value. The results of the method are demonstrated a faster response time and less oscillatory transient behaviour when compared with the AQM schemes that are designed in [204].

In the observation strategy, the fuzzy approach based observer is designed to estimate the system states in the presence of unknown signals or uncertainty by using a T-S fuzzy systems based on fuzzy logic rules. However, the control strategy in each subsystem of the T-S systems is still hardly to force the estimation errors to zero due to its linear feed back control strategy [68, 69]. To address the problems, a sliding-mode observer is a possible strategy that is a class of robust observer. It is designed using SMC theory. The SMC has attractive advantages, such as low sensitivity to parameter variations and strong robustness to external disturbances [126–130]. Main applications of slidingmode observers include the congestion control and the traffic monitoring in the TCP/IP networks. A sliding-mode observer was used to estimate the system states under the network uncertainties [51]. Furthermore, a higher-order sliding-mode observer was applied for anomaly detection [52]. Its robustness and fast response enhance the efficiency of the traffic monitoring.

Clearly, the application of SMC in the problems of traffic flow in communication networks received lots of attention over the last few years. However, the important issues related to the asymptotic stability in systems, which fails to meet the real-time cafeterias such as the time response and the accurate finite-time estimation [51, 52]. In this thesis, we



intend to fill some of the gaps in the RNT0 applications of SMC to the problem of traffic dynamic estimation in the router-based networks.

## 2.4 Some Key Challenging Problems in RNT0

Although a great number of results on RNT0s are presented in the literature, there are still a number of challenging problems to be solved out. The following presents four key challenging issues.

1. **Real-time dynamic RNT0:** It is challenging to develop a real-time dynamic RNT0 scheme due to the static analysis, network induced delays, packet dropouts and stochastic uncertainties in the networks.
  - (i) *Static analysis:* the existing NTM methods periodically collect the traffic information, and then convert it into a set of statistical parameters to reflect the network status [31–33]. In this way, it only provides a periodical analysis and monitoring on traffic characteristics [34, 35, 40, 54, 55].
  - (ii) *Non-robustness:* network traffic inherently features the stochastic and time delay properties in data communication networks. The existing methods are incapable to deal with the network uncertainties to precisely estimate the state of network traffic [46–48, 50].
  - (iii) *Asymptotic stability:* the errors of state estimations are forced to converge to the origin asymptotically by the control strategies proposed in the existing RNT0 schemes. However, the asymptotic stability cannot guarantee the real-time criteria of traffic monitoring in terms of estimation time response [45, 49, 51, 52].
2. **Fast dynamic RNT0:** It is challenging to investigate a real-time RNT0 scheme to accelerate convergence rate of the internal dynamics due to unmeasurable state, i.e., the ACwnd, in the system.

- (i) *Low accuracy and long response time:* some information of network traffic is unmeasurable and cannot be used to manage the network. This will result in low accuracy in regulating and a long response time for the targeted traffic state, and thereby cause oscillation and instability in network [45–52].
- (ii) *No control for internal dynamics:* the internal system dynamics characterize the behaviour of the unmeasurable state, i.e., ACwnd of TCP at the router. The absence of ACwnd brings a big challenge for observer designing for the internal dynamics to accurately estimate ACwnd and further precisely estimate the ATF. The existing methods have not proposed any control strategies for the ACwnd estimation [43, 45–52, 56–59].
- (iii) *High frequency signal:* the SM based RNTD schemes are developed to estimate ATF for anomaly detection [49, 51, 52]. However, the control signal of a SMO is applied for the estimation, which includes the high frequency signal caused by the sign function of the control. So, the low pass filter is used to attenuate the signals with frequencies higher than the cut-off frequency, which can lead to a phase lag, a long response time for state estimations and decrease the estimation accuracy.

3. **Algorithm-efficient RNTD:** Considering a waste of computational capacity, router memory and the communication resource over a router-based network, it is challenging to develop an algorithm-efficient RNTD to reduce the computational load and the communication burden.

- (i) *High computational load:* the microprocessors is embedded into the network router that forming computational core to process a variety of tasks. As the limited computational resource in microprocessors, the existing real-time scheduling algorithms of RNTD is calculated periodically, which cause high consump-

tions on the computational capacity [43, 45–53].

- (ii) *Low efficiency of communication resource*: the resource of the network router is a small network device with constraints of memory space and the communication resource. The existing methods analyse the information of network traffic in a periodic sampling manner in real time. The real-time monitoring for large amount traffic data might cause high occupations on the memory space. In addition, the resource of the communication channel and the bandwidth of the link output of the router are highly occupied [60–67].
  - (iii) *Non-smooth control*: the event trigger based SMO is developed to estimate ATF for anomaly detection. However, the control signal that is used for state estimation is a non-smooth signal due to the signum function of the control based on the event triggered schemes [209–211]. So, the low pass filter is used to attenuate the signals, which can lead to a phase lag, a long response time for state estimations and decrease the estimation accuracy.
4. **Global RNTO**: The current studies on the input-output linearisation of a router-based network only have the property of local stability in observation performance. It is challenging to establish a real-time global RNTO strategy to achieve a global stability in the presence of the network uncertainties.
- (i) *Local observation*: the existing methods are developed based on the linearised model, which is linearised around a certain network condition [42, 43, 45–50]. However, they are incapable to achieve globally stability in state estimation of the traffic dynamics under the network conditions featuring time-varying characteristics in the mathematical model.
  - (ii) *Asymptotic stability*: the existed fuzzy sliding mode based methods in the router-based network system are developed by designing a linear sliding manifold, on

which the system features asymptotic stability once reached and maintained [68, 69]. The asymptotic property of RNTD in real-time observation can decrease the estimation accuracy and increase the response time.

- (iii) *Non-continuous control*: the fuzzy sliding mode observers are developed to estimate ATF by directly using the control signal of the observer is used to state estimation. However, the control strategy of the existed fuzzy sliding mode based methods is non-continuous as the sign function applied [178, 179]. Therefore, the low-pass filter is used to attenuate this control signal, which results in a phase lag. The real-time requirements in estimation accuracy and response time will not be met.

## 2.5 Sliding Mode Control Theory

This thesis focuses on solving the four key problems in real-time dynamic RNTD as aforementioned in the previous **Section 2.4**. The sliding mode control methods are considered to investigate the algorithms due to the inherent properties such as strong robustness and the insensitivity to the uncertainties and the external disturbance. In this section, we will give some brief introduction to the sliding mode control theory. **Section 2.5.1** surveys the state of the art of SMC. **Section 2.5.2** presents the fundamentals of SMC theory. The preliminary studies of the SMC methodologies, which are used in the following chapters, are given in **Section 2.5.3**.

### 2.5.1 State-of-the-Art SMC

Sliding mode control (SMC) is discovered as a special class in variable structure systems (VSS) [212–215]. It inherently features the properties such as low sensitivity to external disturbances and model uncertainties as well as strong robustness to parasitic dynamics

[126, 216]. Because of its simplicity and the properties, SMC has been extensively studied over the past 50 years and widely applied in practical applications [126, 217–222]. The idea of SMC is to seek a controller with the form of switching control strategies to drive the system trajectories to reach, and subsequently maintain on a prescribed switching manifold. The dynamical behaviour of the system when confined to the manifold is described as ideal sliding motion. Generally, this requires an infinite switching to ensure the sliding motion.

In the last decade, there have been extensive research focus on SMC by taking the key issues of chattering, the removal of the effects by unmodeled dynamics, disturbances and uncertainties, adaptive learning, and improvement of robustness. Depending on the methods of sliding manifold design, SMC can be categorized as two main types, such as conventional linear sliding mode (LSM) control and terminal sliding mode (TSM) control.

#### 2.5.1.1 LSM

The classical theory of SMC was established by Prof. V. I. Utkin by involving the discontinuous control actions to provide finite-time convergence to the sliding manifold [126]. However, the conventional SMC has key issues including chattering and asymptotic convergence of the state variables [216]. The twisting algorithm that is the second order sliding modes (SOSM) is proposed to realize a finite-time stabilizing control for a system of dimension two [217], where the control of SOSM is discontinuous as well. A continuous second-order sliding mode super-twisting sliding mode control (STSMC) is proposed in [223], where the state of a one-dimensional system can be stabilized along with its first derivative. The STSMC features the robustness to unbounded disturbances that are satisfying a Lipschitz condition. Various research focus on twisting and super-twisting algorithms in terms of the robust control and observer design [220–222]. However, the typical issue of STSMC is that for systems with relative degree  $r = 2$ , the sliding manifold can be reached in a finite-time, but the convergence of the system state to the origin is asymptotic. Some efforts to

attenuate chattering can be found in the works of boundary layer method [126], high-order sliding-mode method [218, 219, 223], and disturbance estimation method [224]. However, the high-order sliding mode (HOSM) control in particular has attracted an increasing attention due to its effectiveness of reducing chattering magnitude [128, 225]. The HOSM is to hide the discontinuity of control in its higher derivatives.

### 2.5.1.2 TSM

TSM has the property of finite-time stability, when the dynamical behaviour of the system confined to the terminal sliding mode manifold. Compared to LSM control, TSM control exhibits various superior properties, such as fast and finite-time convergence and high accuracy in smaller steady-state tracking errors [127, 226, 227]. A number of efforts have been made on research on TSM. First, in order to obtain a finite-time convergence, the conventional TSMC has been investigated [228–230]. However, the conventional TSMC has the key issues such as a slow convergence speed and singular problem. To overcome the issues of slow convergence speed, fast TSMC have been proposed [231–233]. Moreover, for the problem of singularity, some strategies of nonsingular TSMC have been developed [234–236]. Unfortunately, the individual methods based on fast TSMC or nonsingular TSMC have only considered the problem of its one aspect, which ignored the common issues of SMC. In order to obtain both fast finite-time convergence and singular elimination, nonsingular fast terminal sliding-mode control (NFTSMC) has been proposed [233, 237, 238]. Second, to solve the issue of the slow transient response in conventional SMC, the integral SMC is proposed in [239–242]. It has the properties of compensations in the slower and more oscillatory transient, and prediction of the system behaviour from the initial time. In order to obtain both fast transient response and finite-time convergence, integral TSMC is developed in [243, 244]. However, the conventional integral TSMC adopted the strategy of the conventional TSMC in the design, and therefore, the aforementioned problems of

the SMC are still existed. Third, in order to overcome the issue of chattering, many methods are investigated by using boundary methods [245, 246], disturbance observer based methods [247, 248] and HOSM methods [218, 219, 223, 224, 249]. Among these methodologies, HOSM in particular has attracted an increasing attention due to its effectiveness of high tracking accuracy and chattering elimination.

The issues of the conventional SMC has been tackled by a corresponding suitable approach. However, in the literature the existed methods fail to consider all the drawbacks of SMC together and solves these issues simultaneously. In short, the aim is to design the SMC to feature the properties such as fast transient response, finite-time convergence, and chattering elimination.

### 2.5.2 Fundamentals of SMC Theory

Consider the uncertain system represented by

$$\dot{x}(t) = Ax(t) + Bu(t) + f(t, x, u) \quad (2.1)$$

where  $x(t) \in \mathbb{R}^n$  and  $u(t) \in \mathbb{R}^m$  are the system states and the control input with  $1 \leq m \leq n$ .  $A \in \mathbb{R}^{n \times n}$  and  $B \in \mathbb{R}^{n \times m}$ . Without loss of generality it can be assumed that the input distribution matrix  $B$  has full rank. The function  $f(t, x, u) \in \mathbb{R}^n$  represents the system uncertainties, which include internal parameter variations and external disturbances, with known upper bounds.

The design procedure of SMC consists of two main steps:

- (i) *Reaching phase*: when the trajectory of the closed-loop dynamical behaviours are being driven towards the switching manifolds from any initial state in a finite-time;
- (ii) *Sliding-mode phase*: when the system states reach the switching manifolds and the sliding motion takes place.

The design procedure of SMC comprises two main steps that correspond to the aforementioned two main phases of SMC.

- (i) *Switching manifold selection*: design a sliding manifolds in the state space so that the sliding motion satisfies the design specifications;
- (ii) *Discontinuous control design*: develop a control law combined with discontinuous function about the sliding manifolds, such that the trajectory of the closed-loop motion are directed towards the manifolds.

Consider the switching manifolds in the state space given by

$$S = \{x \in \mathbb{R}^n : s(x) = 0\} \quad (2.2)$$

where  $S \in \mathbb{R}^{m \times n}$  is of full rank and let  $S$  be the hyperplane as defined in (2.2). The switching manifolds can be denoted  $s(x) \in \mathbb{R}^m$ , where  $s = (s_1, \dots, s_m)^T$  a  $m$ -dimensional vector underpinned by the desired dynamical properties.

**Definition 1.** [216] Suppose there exists a finite time  $t^s$  such that the solution to (2.1) represented by  $x(t)$  satisfies

$$s(t) = 0, \quad \forall t \geq t^s \quad (2.3)$$

then an ideal sliding motion is said to be taking place for all  $t \geq t^s$ .



### Filippov Solution

If the control  $u(t)$  in (2.1) is discontinuous and designed by the following structure defined by

$$u = \begin{cases} u^+(t), & \text{for } s(x) > 0 \\ u^-(t), & \text{for } s(x) < 0 \end{cases} \quad (2.4)$$

Then, the differential equation describing the resulting closed-loop system can be written as

$$\dot{x}(t) = F(t, x) \quad (2.5)$$

is such that the function  $F : \mathbb{R} \times \mathbb{R}^n \mapsto \mathbb{R}^n$  is discontinuous with respect to the state vector. From a rigorous mathematical viewpoint, the classical theory of differential equations is not applicable due to Lipschitz conditions are usually applied to guarantee the existence of unique solution. For example, it is assumed that there exists a scalar constant  $L$  that such that

$$\|F(t, x_1) - F(t, x_2)\| \leq L \|x_1 - x_2\| \quad (2.6)$$

Since any function which satisfies Lipschitz conditions is necessarily continuous, an alternative approach must be adopted. In practice, an ideal sliding motion is not attainable – imperfections such as delays, hysteresis and unmodelled dynamics will result in a chattering motion in the neighbourhood of the sliding-mode manifold. Utkin discusses that the ideal sliding motion can therefore be thought of as the ideal solution obtained as the imperfections diminish [126].

Filippov proposed the solution concept for differential equations with discontinuous right-hand sides, constructs a solution which is the "average" of the solution obtained from

approaching the point of discontinuity from different directions [250].

Suppose  $x_0$  is a point of discontinuity on the surface  $S$  and  $F_-(t, x_0)$  and  $F_+(t, x_0)$  denote the limits of  $F(t, x)$  as the point  $x_0$  is approached from opposite sides of the tangent to  $S$  at  $x_0$ . The solution proposed by Filippov is given by

$$\dot{x}(t) = (1 - \alpha)F_-(t, x) + \alpha F_+(t, x) \quad (2.7)$$

where the scalar  $0 < \alpha < 1$ .

The scalar  $\alpha$  is chosen so that

$$F_a := (1 - \alpha)F_- + \alpha F_+ \quad (2.8)$$

is tangential to  $S$ .

**Definition 2.** [126] *A differential inclusion  $\dot{x} \in F(x), x \in \mathbb{R}^n$ , is called a Filippov differential inclusion if the vector set  $F(x)$  is non-empty, closed, convex, locally bounded, and upper-semi-continuous. The latter condition means that the maximal distance of the points of  $F(x)$  from the set  $F(y)$  vanishes when  $x \rightarrow y$ . Solutions are defined as absolutely continuous functions of time satisfying the inclusion almost everywhere.*

Recall in this context that a function is absolutely continuous if and only if it can be represented as a Lebesgue integral of some integrable function. Thus, such a function is almost everywhere differentiable. Solutions of Filippov differential inclusions always exist and have most of the well-known standard properties except the uniqueness.

### Equivalent Control

One way to undertake this analysis is by the so-called *equivalent control* method attributed to Utkin [126]. This defines the equivalent control as the control action necessary to maintain an ideal sliding motion on  $S$ .

In describing the method of equivalent control it will initially be assumed that the uncertain function in (2.1) is identically zero, i.e.

$$\dot{x}(t) = Ax(t) + Bu(t) \quad (2.9)$$

Suppose that at time  $t^s$  the system states maintain on the surface  $S$  defined in (2.2) and an ideal sliding motion occurs, i.e.  $s(t) = Cx(t) = 0$  and  $\dot{s}(t) = C\dot{x}(t) = 0$  for all  $t \geq t^s$ .

The constraint on the derivative of  $s$  can be written as

$$\dot{s} = CAx(t) + CBu(t) = 0, \quad \forall t \geq t^s \quad (2.10)$$

Note that the matrix  $C$  is designed to satisfy the square matrix  $CB$  is nonsingular.

**Definition 3.** *The control  $u$  in (2.1) can be described as*

$$u(t) = u_{eq}(t) + u_n(t) \quad (2.11)$$

*The equivalent control associated with the nominal system (2.2), written as  $u_{eq}$ , is defined to be the unique solution to the equation (2.10), namely*

$$u_{eq}(t) = -(CB)^{-1}CAx(t) \quad (2.12)$$

*and*

$$u_n(t) = -(CB)^{-1}k \operatorname{sgn}(s(t)) \quad (2.13)$$

where  $k > 0$  is a constant control gain and  $\text{sgn}(\cdot)$  is a sign function and defined as

$$\text{sgn}(x) = \begin{cases} 1, & \text{for } x > 0 \\ -1, & \text{for } x < 0 \end{cases}$$

Under this control law, one has  $s(t)\dot{s}(t) < -k|s(t)|$ . Therefore, the ideal sliding mode is guaranteed to be reached in finite time.

### 2.5.3 SMC Methodologies

Three main SMC methods will be used in the following chapters to develop the RNTD algorithms. Components of the SMC methodologies are conventional sliding mode control (CSMC), super-twisting sliding mode control (STSMC) and terminal sliding mode control (TSMC). Besides the CSMC method that is already introduced in **Section 2.5.2**, basic concepts and definitions of high-order SMC method that includes second-order STSMC and high-order SMC, and TSMC method which consists of second-order TSMC and high-order TSMC, are studied in this section respectively.

#### 2.5.3.1 High-order SMC

##### Super-Twisting SMC

Consider a smooth dynamic system of the form

$$\dot{x} = a(t, x) + b(t, x)u, \quad \sigma = \sigma(t, x) \quad (2.14)$$

where  $x \in \mathbb{R}^n$  is the system state and  $u(t) \in \mathbb{R}$  is the scalar control, and  $a(x)$  and  $b(x)$  are smooth functions.  $\sigma$  is the only measured output, and the smooth functions  $a, b, \sigma$  are unknown. The aim is to make the output  $\sigma$  vanish in a finite-time.

Consider the dynamical system (2.22) of relative degree 1 and suppose that

$$\dot{\sigma} = h(t, x) + g(t, x)u, \quad \sigma = \sigma(t, x) \quad (2.15)$$

Moreover, it can be assumed that for some positive constants  $C, K_M, K_m, U_M, q$  satisfy the following

$$|\dot{h}| + U_M|\dot{g}| \leq C, \quad 0 \leq K_m \leq g(t, x) \leq K_M, \quad |h/g| < qU_M, \quad 0 < q < 1 \quad (2.16)$$

By defining that

$$u = -\lambda |\sigma|^{1/2} \text{sgn}(\sigma) + u_1 \quad (2.17)$$

$$\dot{u}_1 = \begin{cases} -u, & |u| > U_M \\ -\alpha \text{sgn}(\sigma), & |u| \leq U_M \end{cases} \quad (2.18)$$

Then, it can be obtained the following results.

**Theorem 1.** [217] With  $K_m \alpha > C$  and  $\lambda$  sufficiently large, the controller (2.17) and (2.18) guarantees the appearance of a 2-sliding mode  $\sigma = \dot{\sigma} = 0$  in system (2.15), which attracts the trajectories in finite time. The control  $u$  enters in finite time the segment  $[-U_M, U_M]$  and stays there. It never leaves the segment, if the initial value is inside at the beginning.

**Remark 1.** Note that the controller does not need measurements of  $\dot{\sigma}$ . The controller given in Eqs. (2.17) and (2.18) are called the super-twisting controller [217].

### High-Order SMC

**Definition 4.** [129, 217] Consider a discontinuous differential equation  $\dot{x} = f(x)$  (Filippov differential inclusion  $\dot{x} \in F(x)$ ) with a smooth output function  $\sigma = \sigma(x)$ , and let it be understood in the Filippov sense. Then, if

(a) the total time derivatives  $\sigma, \dot{\sigma}, \ddot{\sigma}, \dots, \sigma^{(r-1)}$  are continuous functions of  $x$

(b) The set

$$\sigma = \dot{\sigma} = \ddot{\sigma} = \sigma^{(r-1)} = \dots = 0 \quad (2.19)$$

is a non-empty integral set (i.e., consists of Filippov trajectories)

(c) The Filippov set of admissible velocities at the  $r$ -sliding points equation (2.19) contains more than one vector

Hence,  $r$ -sliding modes are determined by equalities (2.19) which impose an  $r$ -dimensional condition on the state of the dynamic system. The sliding order characterizes the dynamics smoothness degree in some vicinity of the sliding mode.

Suppose that  $\sigma, \dot{\sigma}, \ddot{\sigma}, \dots, \sigma^{(r-1)}$  are differentiable functions of  $x$  and that

$$\text{rank} \left[ \nabla \sigma, \nabla \dot{\sigma}, \dots, \nabla \sigma^{(r-1)} \right] = r \quad (2.20)$$

Equality (2.20) together with the requirement for the corresponding derivatives of  $\sigma$  to be differentiable functions of  $x$  is referred to as  $r$ -sliding regularity condition. If regularity condition (2.20) holds, then the  $r$ -sliding set is a differentiable manifold and  $\sigma, \dot{\sigma}, \ddot{\sigma}, \dots, \sigma^{(r-1)}$  may be supplemented up to new local coordinates.

**Proposition 1.** [251] *Let regularity condition (2.20) be fulfilled and  $r$ -sliding manifold (2.19) be non-empty. Then an  $r$ -sliding mode with respect to the constraint function  $\sigma$  exists if and only if the intersection of the Filippov vector-set field with the tangential space to manifold (2.19) is not empty for any  $r$ -sliding point.*

Let  $\sigma(x)$  be a differentiable function, where  $x \in \mathbb{R}^n$  and  $f(x)$  is a vector field, i.e., an  $n$ -dimensional vector function. Then the *Lie derivative* of  $\sigma$  with respect to  $f$  at the point  $x_0$  is defined as

$$L_f \sigma(x_0) = \nabla \sigma(x_0) \cdot f(x_0) = \sum_{i=1}^n \frac{\partial}{\partial x_i} \sigma(x_0) f_i(x_0) \quad (2.21)$$

Consider a smooth dynamic system

$$\dot{x} = a(x) + b(x)u \quad (2.22)$$

where  $x \in \mathbb{R}^n$  is the system state and  $u(t) \in \mathbb{R}$  is the scalar control, and  $a(x)$  and  $b(x)$  are smooth functions.

The total derivative of the output  $\sigma$  is defined as the time derivative of  $\sigma$  along the trajectory of the system

$$\dot{\sigma} = \frac{d}{dt} \sigma(x(t)) = \nabla \sigma(x) (a(x) + b(x)u) = L_a \sigma(x) + L_b \sigma(x)u \quad (2.23)$$

The relative degree of the output  $\sigma$  with respect to the input  $u$  at the point  $x$  is defined as the order of the total derivative of  $\sigma$ , at which the control appears with a non-zero coefficient for the first time, provided the control coefficients are identically zero in all the lower-order derivatives. In particular, the relative degree equals 1 at the given point  $x_0$ , if  $L_b \sigma(x_0) \neq 0$ . Suppose that  $L_b \sigma(x) \equiv 0$  in a vicinity of  $x_0$  then differentiating (2.23) yields

$$\ddot{\sigma} = L_a^2 \sigma(x) + L_b L_a \sigma(x)u \quad (2.24)$$

Continuing the calculation in this way we obtain the following formal definition by Isidori.

**Definition 5.** [129] *The number  $r$  is called the relative degree of the output  $\sigma$  of the system*

(2.22) with respect to the input  $u$  at the point  $x_0$ , if the conditions

$$L_b \sigma(x) = L_b L_a \sigma(x) = \cdots = L_b L_a^{r-2} \sigma(x) = 0, \quad L_b L_a^{r-1} \sigma(x) \neq 0 \quad (2.25)$$

hold in some vicinity of the point  $x_0$ .

The case when the system depends on time so that

$$\dot{x}(t) = a(t, x) + b(t, x)u \quad (2.26)$$

where  $x \in \mathbb{R}^n$ ,  $u \in \mathbb{R}$  and  $\sigma = \sigma(t, x) \in \mathbb{R}$ . The above equation can be governed by introducing the fictitious equation  $\dot{i} = 1$  so that one obtains the system

$$\begin{pmatrix} \dot{x} \\ \dot{i} \end{pmatrix} = \begin{pmatrix} a(t, x) \\ 1 \end{pmatrix} + \begin{pmatrix} b(t, x) \\ 0 \end{pmatrix} u = \tilde{a}(t, x) + \tilde{b}(t, x)u \quad (2.27)$$

and the definition above then can be applied.

**Definition 6.** [129] The number  $r$  is called the relative degree of the output  $\sigma$  of the system (2.26) with respect to the input  $u$  at the point  $(t_0, x_0)$ , if the conditions

$$L_{\tilde{b}} \sigma(x) = L_{\tilde{b}} L_{\tilde{a}} \sigma(x) = \cdots = L_{\tilde{b}} L_{\tilde{a}}^{r-2} \sigma(x) = 0, \quad L_{\tilde{b}} L_{\tilde{a}}^{r-1} \sigma(x) \neq 0 \quad (2.28)$$

hold in some vicinity of the point  $(t_0, x_0)$ .

Thus, if the relative degree equals  $r$ , the output of (2.26) satisfies the equations

$$\sigma^{(i)} = L_{\tilde{a}}^i \sigma, \quad i = 1, 2, \dots, r-1, \quad \sigma^{(r)} = L_{\tilde{a}}^r \sigma + (L_{\tilde{b}} L_{\tilde{a}}^{r-1} \sigma)u \quad (2.29)$$

Therefore,  $\sigma^{(i)}$ , for  $i = 1, 2, \dots, r-1$ , are continuous functions of  $t, x$ , and keeping  $\sigma \equiv 0$  by means of a permanently switching control is only possible in the  $r$ -sliding mode.



The relative degree of the system (2.26) is assumed to be constant and known and given by  $r$  so that

$$\sigma^r = h(t, x) + g(t, x)u \quad (2.30)$$

where  $h(t, x) = L_{\tilde{a}}^r \sigma$  and  $g(t, x) = L_{\tilde{b}} L_{\tilde{a}}^{r-1} \sigma \neq 0$ . It is assumed that  $g(t, x)$  is positive and for some  $K_m, K_M, C > 0$  satisfy the following inequalities

$$0 < K_m \leq g(t, x) \leq K_M, \quad |h(t, x)| \leq C \quad (2.31)$$

If  $g(t, x)$  is negative one just needs to change the sign of the controller which will be developed. The trajectories of (2.26) are assumed infinitely extendible in time for any Lebesgue-measurable bounded control  $u(t, x)$ .

Introducing the differentiator of order  $r - 1$  given above in the feedback loop, one obtains an output-feedback  $r$ -sliding controller

$$u = -\alpha \varphi(z_0, z_1, \dots, z_{r-1}) \quad (2.32)$$

where

$$\begin{aligned} \dot{z}_0 &= v_0, & v_0 &= -\lambda_{r-1} L^{1/r} |z_0 - \sigma|^{(r-1)/r} \operatorname{sgn}(z_0 - \sigma) + z_1 \\ \dot{z}_1 &= v_1, & v_1 &= -\lambda_{r-2} L^{1/(r-1)} |z_1 - v_0|^{(r-2)/(r-1)} \operatorname{sgn}(z_1 - v_0) + z_2 \\ &\vdots \\ \dot{z}_{r-2} &= v_{r-2}, & v_{r-2} &= -\lambda_1 L^{1/2} |z_{r-2} - v_{r-3}|^{1/2} \operatorname{sgn}(z_{r-2} - v_{r-3}) + z_{r-1} \\ \dot{z}_{r-1} &= -\lambda_0 L \operatorname{sgn}(z_{r-1} - v_{r-2}) \end{aligned} \quad (2.33)$$

with  $L \geq C + \sup |\varphi| K_M$  and the parameters  $\lambda_i$  of differentiator (2.33) are properly chosen.

**Proposition 2.** [252] *For any given  $\lambda_0 > 1$  there exists an infinite positive sequence  $\{\lambda_n\}$ , such that for each natural  $r$  the parameters  $\lambda_0, \lambda_1, \dots, \lambda_r$  provide finite-time convergence of the  $r$ th-order differentiator (2.33).*

**Theorem 2.** *Let controller (2.32) be  $r$ -sliding homogeneous and finite-time stable, and the parameters of the differentiator in (2.33) be properly chosen with respect to the upper bound of  $|\phi|$ . Then the output-feedback control laws (2.32) and (2.33) provides the finite-time convergence of each trajectory to the  $r$ -sliding mode  $\sigma \equiv 0$ .*

### 2.5.3.2 Terminal SMC

In sliding-mode control systems, a set of prescribed switching manifolds which are commonly selected as asymptotically stable linear switching hyperplanes. However, for high-precision control, the asymptotic stability may not deliver a fast convergence without imposing strong control force. Nonlinear switching manifolds such as the terminal sliding modes (TSMs), can improve the transient performance substantially. TSM has been developed in [253–255] to achieve finite time convergence of the system dynamics in the terminal sliding mode. In [253, 254], the first-order terminal sliding mode control technique is developed for the control of a simple second-order nonlinear system and an  $n$ th-order nonlinear rigid robotic manipulator system with the result that the output tracking error can converge to zero in finite time. The terminal sliding mode technique is further investigated for high-order single-input and single-output linear systems in [255] where a hierarchical terminal sliding mode structure is proposed and the sliding variables can converge to zero sequentially with the result that the system origin can be reached in finite time.

In this section, the issues of terminal sliding mode control theory are reviewed. Furthermore, the notations, definitions and results on TSM for second-order and  $n$ th-order system are provided, the details of which can be found in [226, 227, 234, 253–257].

### Second-order TSM

Consider the second-order linear or nonlinear system

$$\dot{x}_1 = x_2 \quad (2.34)$$

$$\dot{x}_2 = f(x_1, x_2) + b(x_1, x_2)u(t) \quad (2.35)$$

where  $x_1$  and  $x_2$  are the system states,  $f(\cdot)$  and  $b(\cdot)$  are linear or nonlinear functions of  $x_1$  and  $x_2$ , and  $u$  is the control input.

In order to obtain the terminal convergence of the state variables, the following first-order terminal sliding variable is defined [255]:

$$s = x_2 + \beta x_1^{q/p} \quad (2.36)$$

where  $\beta > 0$ , and  $p$  and  $q$  both are positive integers, which satisfy the following condition:  $p > q$ . Note that the parameter  $p$  must be an odd integer and only real solution is considered so that for any real number  $x_1$ ,  $x_1^{q/p}$  is always a real number.

Using a sliding mode controller of the form [257]

$$u(x) = \begin{cases} u^+(x), & \text{if } s > 0 \\ u^-(x), & \text{if } s < 0 \end{cases} \quad (2.37)$$

the terminal sliding variable  $s$  can be driven to the terminal sliding mode  $s = 0$  in finite time. In the terminal sliding mode, the system dynamics are determined by the following nonlinear differential equation:

$$\dot{x}_1 = -\beta x_1^{q/p} \quad (2.38)$$

It has been shown in [258] that  $x_1 = 0$  is the terminal attractor of the system (2.38). Given

an initial state  $x_1$  at  $t = 0$  is  $x_1(0) \neq 0$  and the two two odd integers and are selected, the dynamics (2.38) will reach  $x_1 = 0$  in a finite-time. The time taken from the initial state  $x_1(0)$  to 0,  $t^s$ , is determined by

$$t^s = -\beta^{-1} \int_{x_1(0)}^0 \frac{dx_1}{x_1^{q/p}} = \frac{p}{\beta(p-q)} |x_1(0)|^{(p-q)/p} \quad (2.39)$$

Note that from (2.39), in the terminal sliding mode (2.38), the system state  $x_1$  converges to zero in finite time and also  $x_2$  converges to zero in finite time identically. The first-order terminal sliding mode technique discussed in the above has been successfully used for the control of nonlinear rigid robotic manipulators with the result that the output tracking error converges to zero in finite time [254].

### High-order Terminal Sliding Mode

Now, consider the following high-order SISO linear system [255]:

$$\begin{aligned} \dot{x}_i &= x_{i+1}, \quad i = 1, \dots, n-1 \\ \dot{x}_n &= \sum_{j=1}^n a_j x_j + u(t) \end{aligned} \quad (2.40)$$

where  $x_1, x_2, \dots, x_n$  are the system state,  $a_1, a_2, \dots, a_n$  are the system parameters, and  $u(t)$  is the scalar control.

To achieve the finite time convergence property of the system states, the following hier-

archical terminal sliding mode structure is defined:

$$\begin{aligned}
 s_1 &= \dot{s}_0 + \beta_1 s_0^{q_1/p_1} \\
 s_2 &= \dot{s}_1 + \beta_2 s_1^{q_2/p_2} \\
 s_3 &= \dot{s}_2 + \beta_3 s_2^{q_3/p_3} \\
 &\vdots \\
 s_{n-1} &= \dot{s}_{n-2} + \beta_{n-1} s_{n-2}^{q_{n-1}/p_{n-1}}
 \end{aligned} \tag{2.41}$$

where  $s_0 = x_1, \beta_i > 0, p_i > q_i$  and  $p_i, q_i$  are positive odd integers.

If a terminal sliding mode controller is designed such that  $s_{n-1}\dot{s}_{n-1} < -k|s_{n-1}|$ , then,  $s_{n-l} = 0$  can be reached in finite time. One can easily see that (using the same mechanism for the first order TSM), when  $s_{n-l} = 0$  is reached,  $s_{n-2}$  will reach zero in a finite-time, so will  $s_{n-3}, \dots, s_0$ , and then the system states can reach the system origin in finite time.

The time reaching  $x_1 = 0$  is the summation of the reaching time for each TSM and can be obtained by

$$t^s = \sum_{i=1}^{n-1} \frac{p_{n-i}}{\beta_{n-i}(p_{n-i} - q_{n-i})} |s_{n-i+1}(t_i^s)|^{(p_{n-i}-q_{n-i})/p_{n-i}} \tag{2.42}$$

Note that the structure (2.41) actually defines a path for the state  $x_1$  to converge to the equilibrium. Indeed, if  $s_{n-l} = 0$  is considered as  $n - 1$  dimensional flow in the state space,  $s_{n-2}$  can be considered as a subspace with dimension shrunk by one. So  $s_0 = 0$  will be the result of the  $n - 1$  dimensional space shrunk  $n - 1$  times.

**Theorem 3.** [255] For the system (2.40), if the control  $u$  is designed as

$$u = u_{eq} + u_n \tag{2.43}$$

where

$$u_{eq} = a_1 x_1 + a_2 x_2 + \cdots + a_n x_n - \beta_1 \frac{d^{n-1}}{dt^{n-1}} s_0^{q_1/p_1} - \beta_2 \frac{d^{n-2}}{dt^{n-2}} s_1^{q_2/p_2} - \cdots - \beta_{n-1} \frac{d}{dt} s_{n-2}^{q_{n-1}/p_{n-1}} \quad (2.44)$$

$$u_n = -k \operatorname{sgn}(s_{n-1}) \quad (2.45)$$

and  $\operatorname{sgn}$  is a sign function and defined as

$$\operatorname{sgn}(s_{n-1}) = \begin{cases} 1, & \text{for } s_{n-1} > 0 \\ -1, & \text{for } s_{n-1} < 0 \end{cases} \quad (2.46)$$

then the system will reach the sliding mode  $s_{n-1} = 0$  in finite time.

The control (2.43) involve calculation of the terms

$$\frac{d^{n-j-1}}{dt^{n-j-1}} s_j^{q_{j+1}/p_{j+1}}, \quad \text{for } j = 0, 1, \dots, n-2 \quad (2.47)$$

Here we present a qualitative result for calculation of these terms.

**Proposition 3.** [255] For any  $j \in \{0, 1, \dots, n\}$

$$\frac{d^{n-j-1}}{dt^{n-j-1}} s_j^{q_{j+1}/p_{j+1}} = f_k(s_0, \dot{s}_0, \dots, s_0^{n-1}) \quad (2.48)$$

where  $f_k$  is a nonlinear function, and  $s_0 = x_1$ .

The parameters  $p_i, q_i$  must be chosen carefully in order to avoid the singularity that while  $s_{i-1} \rightarrow 0, u \rightarrow \infty$  because of the terms

$$\frac{d^{n-j-1}}{dt^{n-j-1}} s_j^{q_{j+1}/p_{j+1}}, \quad \text{for } j = 0, 1, \dots, n-2$$

**Proposition 4.** [255] If  $(n-j-1)p_{j+1} < (n-j)q_{j+1}$ , then when  $s_j \rightarrow 0$  sequentially from

$j = n - 2$  to  $j = 0$ ,  $u$  is bounded.

## 2.6 Summary

In this chapter, a review of the challenging issues in router-based network traffic observation has been discussed. Furthermore, the existed main methodologies that are investigated to deal with these issues in RNTTO algorithms have been summarized. Although a large number of results have been developed in the literature, there are still four key challenging problems to be solved out. To solve the four key challenging problems, the sliding mode control methods have been introduced, which will be applied to develop the real-time dynamic RNTTO algorithms in the following chapters, because of its inherent properties of strong robustness and the insensitivity to the system uncertainties and the external disturbance, such as the delays, packet drop, jitter, stochastic uncertainties and external abnormal traffic dynamics that are existed in network environment as discussed in the literature.





# Chapter 3

## Real-time Terminal Sliding Mode Observation Strategy

### 3.1 Introduction

As a preliminary step toward solving the problems presented in **Section 2.2**, this chapter introduces a real-time dynamic observation algorithm for a router-based network system by using sliding mode control theory with a focus on estimation problem of RNTD appliances. This work is established on concepts from the sliding mode control theory to investigate the dynamic sliding mode observers for estimating the system states, i.e., dynamic states of the network traffic, in the presence of uncertainties for RNTD applications.

In **Section 3.3**, a conventional sliding mode observer (SMO), a super-twisting observer (STO) and a novel terminal sliding mode observer (TSMO) are investigated for real-time state estimation as the RNTD schemes. Detailed results from illustrative case studies in Network Simulator II are presented and discussed, which shows the proposed novel TSMO featuring the best performance of state estimation in effectiveness and accuracy in **Section 3.4**. Finally, some summaries are drawn in **Section 3.5**.

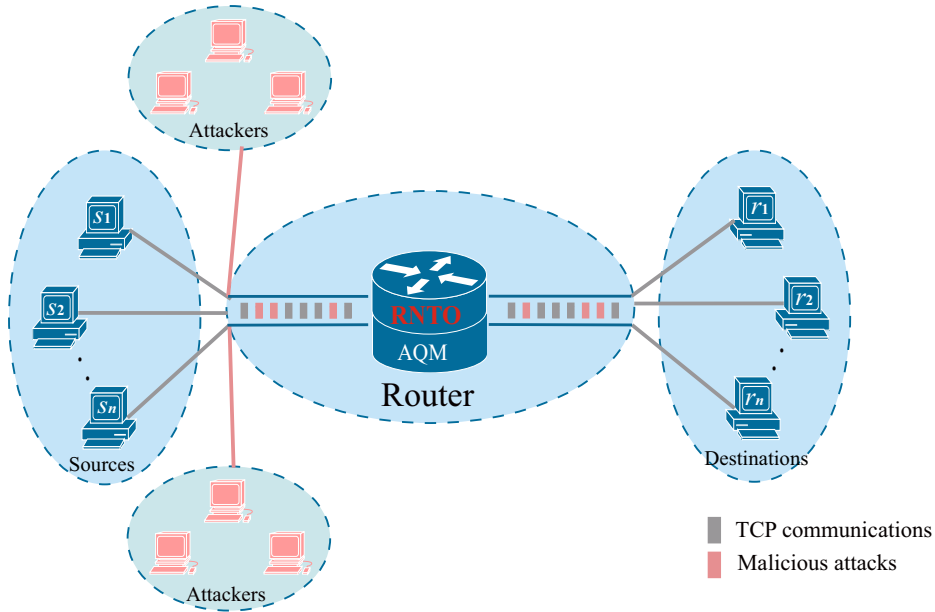


Fig. 3.1 A typical router-based network topology

## 3.2 Fluid-flow Model of a Router-based Network

### 3.2.1 Router-based TCP/IP Networks

Since the introduction of the Transmission Control Protocol (TCP) in the early 1980s, the Internet has been in constant evolution [259–261]. TCP has been the primary method for transferring data between computers and across networks [262]. It is a reliable, connection-oriented, full-duplex, byte-stream transport-layer protocol with inherent characteristic of supporting congestion control and flow control [70, 259, 263]. Due to the reliability of the TCP, it has become the de facto standard used in computer networks and the Internet.

A TCP/IP network consists of multiple computers which are physically connected by the five basic network topologies as ring, star, bus, mesh, and tree. The star is the most commonly-used topology with its compatibility with applications, ease of implementation, cost effective, and reliability in enterprise network, in-home network, campus network, department network and public network [71]. The central device of the star topology is the network router, which is a network gateway at the edge of a network, related capabilities

like firewalls and proxy servers tend to be integrated with it. Thus, the network router is a critical vantage point to control and monitor the traffic flow in computer networks and the Internet.

A basic router-based network topology is a star type and is illustrated in Fig. 3.1. The network router is a network device connected to multiple networks through which it forwards network flow. Network flow is defined as a set of packets that have common properties, i.e., the same source and the same destination. A router processes and forwards data packets between computer networks. It performs the function of network traffic directions on the Internet. Data packets are forwarded by the router via the networks until they arrived the destination node.

In a router-based network, as shown in Fig. 3.1, all of the nodes are represented by hosts, clients or any other peripherals. Each connected host (or client) has a dedicated, point-to-point connection between the host and the router. There are  $N$  sources (hosts) being connected to  $N$  destinations (clients) through a central device, i.e., a router. In the thesis, it is assumed that  $N$  sources (hosts) and  $N$  destinations (clients) are homogeneous. It means that all the sources (or destinations) are the same in structure, nature, parameters, and software implementations. Moreover, the homogeneous TCP protocol is used in each host and client over the network. A set of TCP traffic is launched by the sources to the destinations via a router. To provide a reliable and ordered data flow, the sources of TCP receive the acknowledges (ACK) packets from the destinations to create the connections [70, 263]. However, a number of attackers are trying to generate malicious data flows into the network. This will result in the degradation in QoS, network resource usage and security threats. A router, thereby, is a central viewpoint to control and monitor the traffic flow that include the TCP traffic flow and the malicious traffic flow.

In the network, TCP adjusts the sending rate at the source end via its Cwnd, which is included in the ACK file as a feedback signal. A Cwnd is one of the factors that determines

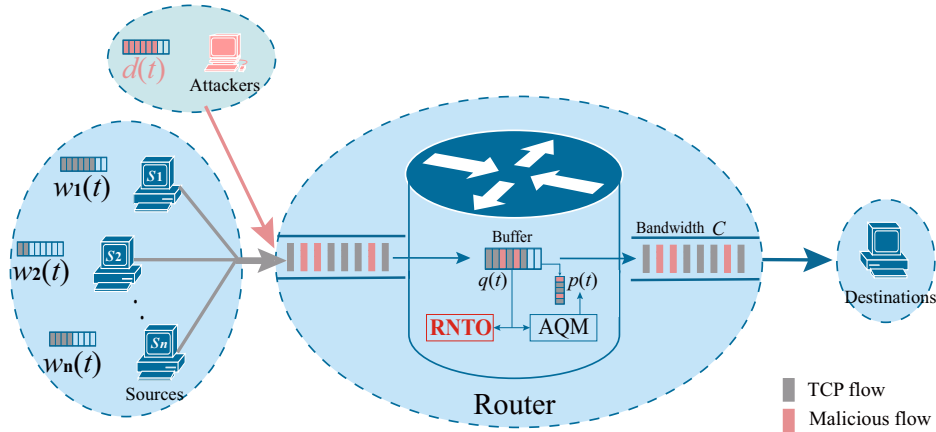


Fig. 3.2 Fluid-flow analysis of a router-based network traffic

the number of bytes that can be out sending. The  $Cwnd$ , which is maintained by the source end, is a means of avoiding a link being overloaded with too much traffic. It is calculated by estimating how much congestion occurred on the link. To guarantee the QoS in network, there are two modules embedded in a router, such as AQM scheme and RNT0, as shown in Fig. 3.2. First, the AQM is embedded at a router to regulate the network traffic for congestions avoidance. Specifically, it regulates the queue length of router buffer at a desired level to stabilize the network traffic [57], and achieve a high utilization of links, and ensure certain QoS properties of the network. Second, the RNT0 is built into a router to monitor the network dynamics and detect the malicious traffics in real-time. Furthermore, the estimated states of the network traffic dynamics are delivered to AQM and the source end to regulate the traffic flow. The dynamics of the malicious traffics are detected and further analysed by the IDSs.

### 3.2.2 Fluid-flow Model of a Router-based Network

The mathematical description of the TCP dynamics (with the timeout effects neglected) in the router-based network, as the topology shown in Fig. 3.2, can be represented by the following coupled nonlinear differential equations [42]:

$$\dot{w}(t) = \frac{1}{\tau(t)} - \frac{w(t)}{2} \frac{w(t - \tau(t))}{\tau(t - \tau(t))} p(t - \tau(t)) \quad (3.1)$$

$$\dot{q}(t) = N \frac{w(t)}{\tau(t)} - C + d(t) \quad (3.2)$$

$$\tau(t) = \frac{q(t)}{C} + T_p \quad (3.3)$$

where

- $w(t) \in \mathbb{R}$  is the average congestion window size (ACwnd) in *packets* in a router.
- $q(t) \in \mathbb{R}$  is the queue length (QL) of the router buffer in *packets*.
- $p(t) \in \mathbb{R}$  is the probability of the dropping/marking packet.
- $\tau(t) \in \mathbb{R}$  is the round-trip time (RTT) in *seconds* which induce time varying delay in communication channel.
- $d(t) \in \mathbb{R}$  is the additional traffic dynamics representing additional traffic flow (ATF).
- $N \in \mathbb{R}$  is the number of TCP sections contributing to the queue buildup in router buffer (the load factor).
- $C \in \mathbb{R}$  is the link capacity (bandwidth) in *packets/second*.
- $T_p \in \mathbb{R}$  is the propagation delay in *seconds*.

All the terms,  $w(t)$ ,  $q(t)$ ,  $p(t)$ ,  $\tau(t)$  and  $d(t)$  in equations (3.1) to (3.3) are time varying functions. Furthermore, the window size of a TCP source is limited to the interval  $w(t) \in [0, \bar{w}]$ , where  $\bar{w}$  is constant and denotes the maximum window size. The queue length in router buffer is constrained to the interval  $q(t) \in [0, \bar{q}]$ , where  $\bar{q}$  is a constant and represents the buffer capacity (buffer size) set in router. The packet marking probability is subject to the fundamental constraint  $p(t) \in [0, 1]$ .

Note that the queue length of the router buffer  $q(t)$  is available in a router. Moreover, the probability of the dropping/marking packet  $p(t)$  is available and can be measured in a router as well. Some software programs, such as Net-flow, PacketScope, Loss Measurement Management, have been developed and installed in routers. These tools can monitor and measure the queue length  $q(t)$  and the probability of dropping/marking packet  $p(t)$  in the router [264]. However, The ACwnd, i.e.,  $w(t)$ , is unmeasurable at a router, thus the value of which cannot be used in a router system.

The time-delay  $\tau(t)$  in equations (3.1) to (3.3) satisfies the following in-equality:

$$T_p \leq \tau(t) \leq \bar{q}/C + T_p \quad (3.4)$$

where  $\bar{q}$ ,  $C$  and  $T_p$  are defined in system (3.1) to (3.3). It should be noted that the lower bound of  $\tau(t)$  in the inequality (3.4),  $T_p$ , is actually the propagation delay at the circumstance of neither congestions nor queuing delay in a router, i.e.  $\tau(t)$  cannot be less than  $T_p$ . In addition, the upper bound of  $\tau(t)$  in the inequality (3.4) is the combination of the propagation delay and the maximum queuing delay under the worst case of congestion in the router buffer, i.e.  $\tau(t)$  cannot exceed the term  $(\bar{q}/C + T_p)$ .

The derivative of time delay  $\tau(t)$  can be assumed to satisfy

$$\dot{\tau}(t) \leq \mu \quad (3.5)$$

where  $\mu$  is a known positive constant.

The proof of inequality equation (3.5) is given below. Differentiating the Eq.(3.3) with the time  $t$  gives

$$\dot{\tau}(t) = \frac{1}{C} \dot{q}(t) = \frac{1}{C} \left( N \frac{w(t)}{\tau(t)} - C + d(t) \right)$$

or

$$\dot{\tau}(t) = \frac{1}{C} \left( \frac{Nw(t) + d(t)\tau(t)}{\tau(t)} - C \right) \quad (3.6)$$

The term  $Nw(t) + d(t)\tau(t)$  in Eq.(3.6) is actually the amount of data being transmitted in the TCP/IP network, which is physically constrained to the TCP/IP network capacities, namely

$$Nw(t) + d(t)\tau(t) \leq BDP + \bar{q} \quad (3.7)$$

where  $\bar{q}$  is the buffer capacity defined in system (3.1)–(3.3).  $BDP$  is the Bandwidth-Delay Product, which represents the amount of data that can be in transit [131].  $BDP$  refers to the product of a data link's capacity  $C$  and its round-trip delay time  $\tau(t)$ , i.e.  $BDP = C\tau(t)$ , where  $C$  and  $\tau(t)$  are defined in system (3.1) to (3.3). Normally, the buffer capacity of a router in (3.1) to (3.3)  $\bar{q}$  is dependent on the  $BDP$ , i.e.  $\bar{q} = \mu C\tau(t)$ , where  $\mu = 1/\sqrt{N}$  is a constant [265]. From (3.7) we thus get

$$Nw(t) + d(t)\tau(t) \leq C\tau(t) + \mu C\tau(t) \quad (3.8)$$

and furthermore, from Eqs. (3.6) and (3.8), we have

$$\dot{\tau}(t) \leq \frac{1}{C} \left( \frac{C\tau(t) + \mu C\tau(t)}{\tau(t)} - C \right) = \mu \quad (3.9)$$

which means that the condition (3.5) is true.

The aforementioned amount of data being transmitted in the TCP/IP network,  $Nw(t) + d(t)\tau(t)$ , in Eq. (3.6) includes traffic flow of all  $N$  TCP sections  $Nw(t)$ , and additional traffic flow  $d(t)\tau(t)$ . It can be seen from (3.8) that it is physically constrained to the network

capacities, namely

$$\frac{Nw(t)}{\tau(t)} + d(t) \leq C + \mu C \quad (3.10)$$

which means that  $|d(t)| \leq (1 + \mu)C$  holds because of  $w(t) > 0$ ,  $\tau(t) > 0$ , i.e.  $|d(t)| \leq d_0$ , where  $d_0 \leq (1 + \mu)C$  is a known positive constant which can be determined in the experiments.

As  $d(t)$  is physically limited to router communication capacity, its change rate is always constrained to  $|\dot{d}(t)| \leq d_0/T$ , where  $T$  is the sampling period and kept as a constant  $T = 1/C$  [42]. Hence we have  $|\dot{d}(t)| \leq d_0/T \leq (1 + \mu)C^2$  i.e.  $|\dot{d}(t)| \leq d_1$ , where  $d_1 \leq (1 + \mu)C^2$  is a known positive constant. Summarizing the analysis above gives

$$|d(t)| \leq d_0 \text{ and } |\dot{d}(t)| \leq d_1 \quad (3.11)$$

where both  $d_0$  and  $d_1$  are known positive constants.

In the next section, we investigate the distinct choice of small-signal linearisation of the set of nonlinear equations (3.1) to (3.3) with the information about the delay retained. For the case, we linearise the system dynamics to derive a real-time RNT0 algorithm. The block diagram of the router built-in RNT0 is described in Fig. 3.3. The AQM is utilized to control the queue length  $q(t)$  to a required value by regulating the probability of the dropping/marking packet  $p(t)$ . The inputs of the RNT0 are  $q(t)$  and  $p(t)$ . They are all measurable and can be used for the observer. The outputs of the RNT0 are the estimate of  $d(t)$  and  $w(t)$ . The aims of RNT0 are to estimate the dynamics of ATF for further detecting anomalies and the states of the ACwnd in the router-based TCP/IP networks in real-time .



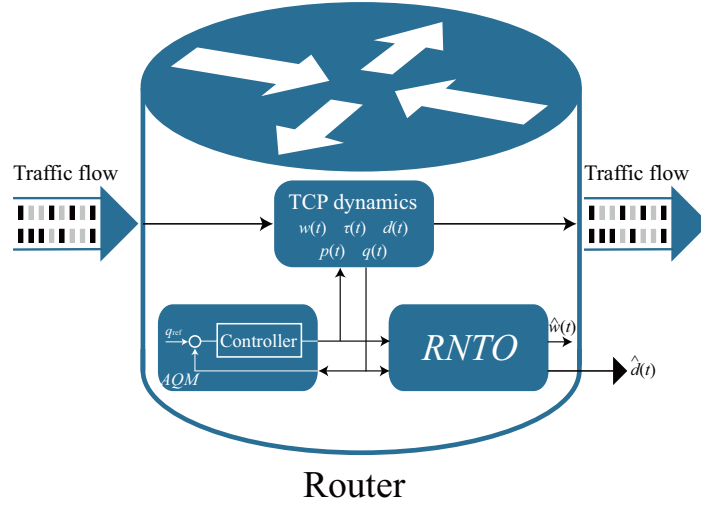


Fig. 3.3 Block diagram of RNTO in a router

### 3.2.3 Linearisation

In this section, the linearisation procedure of the nonlinear system equations (3.1) to (3.3) is performed. The linearised model, which is a Linear Time Invariant (LTI) model, represents the TCP traffic behaviour in the neighbourhood of an equilibrium point. The design of the RNTO in Chapter 3 and Chapter 4 are proposed based on the linearised LTI model.

In system (3.1) to (3.3),  $w(t)$  and  $q(t)$  are considered as the system state variables. The system is driven by the input,  $p(t)$ , which is the controller command of the AQM. The function  $q(t)$  is considered as the system output. For a given router-based network with triplet parameters of  $(N, C, T_p)$ , any triplet  $(w_0, q_0, p_0)$  is in the set:

$$\Xi = \{(w_0, q_0, p_0) : w_0 \in [0, \bar{w}], q_0 \in [0, \bar{q}], p_0 \in [0, 1]\}$$

where  $(w_0, q_0, p_0)$  is a possible operating point, which is the equilibrium point of the nonlinear system (3.1) to (3.3).  $\bar{w}$  and  $\bar{q}$  are known constant and defined in (3.1) to (3.3). In the equilibrium point triplet  $(w_0, q_0, p_0)$ ,  $q_0$  is the required queue length, which is set by in

AQM.  $w_0$  and  $p_0$  can be determined as follows by

$$\dot{w}(t) = 0 \text{ and } \dot{q}(t) = 0|_{(w_0, q_0, p_0)}$$

Hence, set the left-hand sides of (3.1) and (3.2) equal to zero, then the operating point  $(w_0, q_0, p_0)$  is obtained as the following set of relations:

$$w_0 = \tau_0 C / N, \quad \tau_0 = q_0 / C + T_p, \text{ and } p_0 = 2 / w_0^2$$

where  $\tau_0$  is the equivalent RTT. Thus, for any given network with the triplet parameters of  $(N, C, T_p)$ , the set of feasible operating point is as

$$\Xi_{(N, C, T_p)} = \left\{ \begin{array}{l} (w_0, q_0, p_0) : w_0 \in [0, \bar{w}], q_0 \in [0, \bar{q}], p_0 \in [0, 1], \\ w_0 = \tau_0 C / N, \tau_0 = q_0 / C + T_p, \text{ and } p_0 = 2 / w_0^2 \end{array} \right\} \quad (3.12)$$

By substituting the equation (3.3) into the equations (3.1) and (3.2), the simplified system dynamics can be obtained as

$$\dot{w}(t) = \frac{1}{T_p + q(t)/C} - \frac{w(t)w(t - \tau(t))}{T_p + q(t - \tau(t))/C} p(t - \tau(t)) \quad (3.13)$$

$$\dot{q}(t) = N \frac{w(t)}{T_p + q(t)/C} - C + d(t) \quad (3.14)$$

Let us analyse the small-signal deviations of the system states and the input variable from the operating point  $(w_0, q_0, p_0)$  in (3.12). Define the perturbation of the equilibrium point as

$$\delta w(t) = w(t) - w_0, \quad \delta q(t) = q(t) - q_0, \text{ and } \delta p(t) = p(t) - p_0$$

Thus, the deviation dynamics of a router-based network (3.13) and (3.14) can be linearised

around the operating point  $(w_0, q_0, p_0)$  and be expressed as

$$\delta \dot{w}(t) = -\frac{N}{\tau_0^2 C}(\delta w(t) + \delta w(t - \tau(t))) - \frac{1}{\tau_0^2 C}(\delta q(t) - \delta q(t - \tau(t))) \quad (3.15)$$

$$\begin{aligned} & -\frac{\tau_0 C^2}{2N^2} \delta p(t - \tau(t)) \\ \delta \dot{q}(t) = & \frac{N}{\tau_0} \delta w(t) - \frac{1}{\tau_0} \delta q(t) + d(t) \end{aligned} \quad (3.16)$$

To simplify the design of a RNTD for the linearised model of the router-based network, a transformation can be made to the system (3.15) and (3.16) firstly.

Define a new state variable

$$x(t) = \delta w(t) \in \mathbb{R}, y(t) = \delta q(t) \in \mathbb{R}, \text{ and } y(t) = \delta q(t) \in \mathbb{R}$$

Then, the linearised model (3.15) and (3.16) can be rewritten as

$$\dot{x}(t) = -a_{11}x(t) - a_{11}x(t - \tau(t)) - a_{12}y(t) + a_{12}y(t - \tau(t)) - b_d u(t - \tau(t)) \quad (3.17)$$

$$\dot{y}(t) = a_{21}x(t) - a_{22}y(t) + d(t) \quad (3.18)$$

where

$$a_{11} = \frac{N}{\tau_0^2 C}, a_{12} = \frac{1}{\tau_0^2 C}, b_d = \frac{\tau_0 C^2}{2N^2}, a_{21} = \frac{N}{\tau_0}, \text{ and } a_{22} = \frac{1}{\tau_0}.$$

$N$  and  $C$  are defined in (3.1) to (3.2). The operating point  $(w_0, q_0, p_0)$  are defined in (3.12).

The state variable  $x(t)$  in the linearised model (3.17) to (3.18) satisfies the following inequality:

$$|x(t)| \leq \bar{w} \quad (3.19)$$

where the known positive constant  $\bar{w}$  is the maximum window size defined in system (3.1) to (3.3).

Note that the window size refers to the amount of data that the host is currently willing to send. Normally, the maximum window size  $\bar{w}$  at the host is configured as a constant, i.e.,  $\bar{w}$  is set as 65,535 (*0xFFFF*) bytes [266]. As seen in equations (3.15) to (3.16) and (3.1) to (3.3),  $x(t)$  is the perturbation  $\delta w(t)$  around the equilibrium point of the average window size  $w(t)$  that is limited to the known constant maximum window size  $\bar{w}$ . As  $x(t) = \delta w(t)$ , so  $|x(t)|$  cannot exceed the maximum value of  $w(t)$ , i.e. the inequality (3.19) is true.

### 3.3 Real-time Router-based Network Traffic Observation

Consider the characteristics of the delays, packet drop, jittering and stochastic uncertainties in network environment as discussed in the literature, the sliding mode control methods are used to develop a real-time dynamic RNTD algorithms due to the properties of strong robustness and the insensitivity to the system uncertainties and the external disturbance. The objective is to design the real-time dynamic RNTD algorithms built in routers to estimate ACwnd and the dynamics of ATF for further detecting anomalies. In this section, three sliding mode control methods such as conventional SMO, super-twisting SMO and terminal SMO are developed for RNTDs.

#### 3.3.1 Conventional Sliding Mode Based RNTD

A conventional SMO is used to develop a real-time RNTD in this section. In the presence of unknown signals or uncertainty in the router-based network, sliding-mode based RNTD can be applied to obtain the real-time observation. First, a sliding mode observer provides an attractive solution to the issues of unknown signals or uncertainty in the network by feeding back the estimation error via a nonlinear switching term. Second, a sliding mode

observer can force the output estimation error to converge to zero in a finite-time, and while the estimated states converge to the system states asymptotically. In addition, the additional traffic dynamics are treated as the disturbance within the router-based network system can be reconstructed.

Considering the linearised system in (3.17) and (3.18), a sliding mode observer can be designed as:

$$\dot{\hat{x}}_{sm}(t) = -a_{11}\hat{x}_{sm}(t) - a_{11}\hat{x}_{sm}(t - \tau(t)) - a_{12}y(t) + a_{12}y(t - \tau(t)) - b_d u(t - \tau(t)) \quad (3.20)$$

$$\dot{\hat{y}}_{sm}(t) = a_{21}\hat{x}_{sm}(t) - a_{22}y(t) + v_{sm}(t) \quad (3.21)$$

where  $\hat{x}_{sm}(t)$  and  $\hat{y}_{sm}(t)$  represent the estimates of the system state  $x(t)$  and output  $y(t)$  respectively,  $v_{sm}(t)$  is the control signal for the SMO and is designed later.

By defining the new variables

$$e_{1sm}(t) = \hat{x}_{sm}(t) - x(t) \quad (3.22)$$

$$e_{2sm}(t) = \hat{y}_{sm}(t) - y(t) \quad (3.23)$$

as the errors between the system states and their estimates, hence the error system can be obtained from equations (3.17) to (3.18) and equations (3.20) to (3.21) as follows:

$$\dot{e}_{1sm}(t) = -a_{11}e_{1sm}(t) - a_{11}e_{1sm}(t - \tau(t)) \quad (3.24)$$

$$\dot{e}_{2sm}(t) = a_{21}e_{1sm}(t) - d(t) + v_{sm}(t) \quad (3.25)$$

A sliding mode manifold is chosen as the following form:

$$s_{sm}(t) = c_{sm}e_{2sm}(t) \quad (3.26)$$

where  $c_{sm} > 0$  is a constant.

**Theorem 4.** *The error systems (3.24) and (3.25) will reach  $s_{sm}(t) = 0$  from any initial condition  $s_{sm}(0) \neq 0$  in a finite-time  $t_{sm}^r \leq |s_{sm}(0)| / (c_{sm}\eta_{sm})$ , then converge to zero along  $s_{sm}(t) = 0$  asymptotically, if a sliding mode manifold  $s_{sm}(t)$  is selected as (3.26) and the control law is given by*

$$v_{sm}(t) = -k_{sm}\text{sgn}(s_{sm}(t)) \quad (3.27)$$

where  $k_{sm} = a_{21}\bar{w} + d_0 + \eta_{sm}$ ,  $\eta_{sm} > 0$  is a constant,  $\bar{w}$  and  $d_0$  both are known constants defined in system (3.1) to (3.3).

*Proof.* Differentiating  $s_{sm}(t)$  in (3.26) with respect to time  $t$  along the error system (3.25) yields

$$\dot{s}_{sm}(t) = c_{sm}(a_{21}e_{1sm}(t) - d(t) + v_{sm}(t))$$

Substituting the control (3.27) into the above equation gives

$$\dot{s}_{sm}(t) = c_{sm}(a_{21}e_{1sm}(t) - d(t) - k_{sm}\text{sgn}(s_{sm}(t)))$$

For the output error  $e_2$ , a candidate Lyapunov function is considered and given by

$$V_{sm}(t) = \frac{1}{2}s_{sm}^2(t) \quad (3.28)$$

Taking the derivative of  $V_{sm}(t)$  along the trajectories of (3.25), and from the above equation, we have the following

$$\begin{aligned}
s_{sm}(t)\dot{s}_{sm}(t) &= s_{sm}(t)c_{sm}(a_{21}e_{1sm}(t) - d(t)) - c_{sm}k_{sm}|s_{sm}(t)| \\
&\leq c_{sm}a_{21}|e_{1sm}(t)||s_{sm}(t)| + c_{sm}|d(t)||s_{sm}(t)| - c_{sm}k_{sm}|s_{sm}(t)| \\
&\leq c_{sm}(a_{21}|e_{1sm}(t)| - a_{21}\bar{w})|s_{sm}(t)| + c_{sm}(|d(t)| - d_0)|s_{sm}(t)| - c_{sm}\eta_{sm}|s_{sm}(t)|
\end{aligned}$$

From the conditions (3.19) and (3.11) and the above inequality, we have

$$\dot{V}_{sm}(t) = s_{sm}(t)\dot{s}_{sm}(t) \leq -c_{sm}\eta_{sm}\sqrt{2V_{sm}^{1/2}}(t) < 0, \text{ for } s_{sm}(t) \neq 0$$

which means that error system (3.25) will reach to  $s_{sm}(t) = 0$  within the finite-time  $s_{sm}(0) \neq 0$  in a finite-time  $t_{sm}^r \leq |s_{sm}(0)|/(c_{sm}\eta_{sm})$ , in other words,  $s_{sm}(t) = 0, \forall t \geq t_{sm}^r$ . Once the ideal sliding-mode  $s_{sm}(t) = 0$  is established, the error system (3.25) will maintain on  $s_{sm}(t) = 0$  thereafter and the error  $e_{2sm}(t)$  will converge to zero along  $s_{sm}(t) = 0$  asymptotically. This completes the proof.  $\square$

The asymptotic stability of the state error  $e_1$  is verified as follows. To ensure the asymptotic convergence of the error system (3.24) to zero, a linear system with time-varying delay can be considered. The time delay,  $\tau(t)$ , is a time-varying continuous function that satisfies  $\tau_1 < \tau(t) < \tau_2$  and  $\dot{\tau}(t) \leq \mu$ , where  $\tau_1 = T_p$  and  $\tau_2 = \bar{q}/C + T_p$  and  $\mu$  are all known constants and defined in (3.4) and (3.5). The system (3.17) is asymptotically stable, refers to the proof in [267]. Therefore, the error systems (3.24) and (3.25) converge to zero asymptotically. From the error system (3.25), then, we can obtain that

$$\dot{e}_{2sm}(t) = -d(t) + v_{sm}(t) = 0 \quad (3.29)$$

The observation of the additional traffic dynamics,  $d(t)$ , can be obtained by

$$\hat{d}_{sm}(t) = v_{sm}(t) \quad (3.30)$$

where  $v_{sm}(t)$  is defined in (3.27), which has highly frequent switching phenomenon. So, a low-pass filter is needed for estimating the state.

A sliding-mode based algorithm is used to develop a real-time RNT0 in this section. First, a nonlinear switching term in the control signal in (3.27) is used to feed back the estimation error  $e_{2sm}$  in the presence of the additional traffic dynamics, which is seen as the external unknown disturbance in the system. Second, a sliding-mode manifold strategy in (3.26) is used to force the estimation error towards to zero in a finite-time  $t_{sm}^*$ , which is defined in Theorem 4, while the state of estimation error will maintain on the sliding surface and converge towards zero asymptotically. Third, the additional traffic dynamics can be reconstructed by the control signal in (3.30), which is which is a high frequent switching signal. So, a low-pass filter is required to obtain the estimation.

### 3.3.2 Super-twisting Based RNT0

To overcome the a high frequent switching in the estimation of the additional traffic dynamics that is reconstructed by the control signal in CSMO, a super-twisting algorithm is used to develop a real-time RNT0 in this section, which avoids the chattering phenomenon in ATF estimation with a smooth signal.

A STO as a second-order sliding mode algorithm is considered to develop a real-time RNT0 in this section. First, a super-twisting algorithm is used to avoid the chattering phenomenon [217], which is a high frequent switching phenomenon as in the conventional sliding mode strategy. By the benefit of STO used for RNT0, it is not required to filter the estimation of the additional traffic dynamics by a low-pass filter, which is necessary in



the conventional SMO. Second, a super-twisting algorithm offers a finite reaching time and which can be used for sliding mode based observation.

Considering the linearised system in (3.17) and (3.18), the following super-twisting observer is designed:

$$\dot{\hat{x}}_{st}(t) = -a_{11}\hat{x}_{st}(t) - a_{11}\hat{x}_{st}(t - \tau(t)) - a_{12}y(t) + a_{12}y(t - \tau(t)) - b_d u(t - \tau(t)) \quad (3.31)$$

$$\dot{\hat{y}}_{st}(t) = a_{21}\hat{x}_{st}(t) - a_{22}y(t) + v_{st}(t) \quad (3.32)$$

where  $\hat{x}_{st}(t)$  and  $\hat{y}_{st}(t)$  represent the estimates of the system state  $x(t)$  and output  $y(t)$  respectively,  $v_{st}(t)$  is the control signal of the STO and will be given later.

Define the new variables  $e_{st}^1(t) = \hat{x}_{st}(t) - x(t)$  and  $e_{st}^2(t) = \hat{y}_{st}(t) - y(t)$  as the errors between the system states and their estimates. Then, combining the system (3.17) to (3.18) and the observer (3.31) to (3.32), we can obtain the error system by

$$\dot{e}_{st}^1(t) = -a_{11}e_{st}^1(t) - a_{11}e_{st}^1(t - \tau(t)) \quad (3.33)$$

$$\dot{e}_{st}^2(t) = a_{21}e_{st}^1(t) - d(t) + v_{st}(t) \quad (3.34)$$

A sliding-mode manifold is selected as the following form:

$$s_{st}(t) = e_{st}^2(t) \quad (3.35)$$

**Theorem 5.** *The error systems (3.33) and (3.34) will reach  $s_{st}(t) = 0$  from any initial condition  $s_{st}(0) \neq 0$  in a finite-time, then converge to zero along  $s_{st}(t) = 0$  asymptotically, if a sliding mode manifold  $s_{st}(t)$  is selected as (3.35) and the control laws are given by*

$$v_{st}(t) = -k_{st}^1 |s_{st}(t)|^{\frac{1}{2}} \text{sgn}(s_{st}(t)) + v_{st}^n(t) \quad (3.36)$$

$$\dot{v}_{st}^n(t) = -k_{st}^2 \text{sgn}(s_{st}(t)) \quad (3.37)$$

where  $k_{st}^1 > 0$  and  $k_{st}^2 > 0$  both are constant. The error system (3.33) and (3.34) is asymptotically stable if there exists a positive definite matrix

$$\mathbf{P}_{st} = \begin{bmatrix} p_{st}^1 & p_{st}^3 \\ p_{st}^3 & p_{st}^2 \end{bmatrix}$$

and  $\mathbf{T}_{st} \in \mathbb{R}^{2 \times 1}$  such that the following two linear matrix inequalities are verified:

$$\frac{1}{2}\mathbf{I}_{st}^T \mathbf{P}_{st} + \frac{1}{2}\mathbf{P}_{st} \mathbf{I}_{st} - \mathbf{B}_{st}^T \mathbf{T}_{st}^T - \mathbf{T}_{st} \mathbf{B}_{st} \pm 2\Gamma_{st} \begin{bmatrix} p_{st}^3 & \frac{1}{2}p_{st}^2 \\ \frac{1}{2}p_{st}^2 & 0 \end{bmatrix} < 0 \quad (3.38)$$

where  $\mathbf{B}_{st} = [1 \ 0]$ ,  $\Gamma_{st} = \sup_t (|a_{21}(a_{11}e_{st}^1(t) + a_{11}e_{st}^1(t - \tau(t)))| + d_1)$ , and

$$\mathbf{I}_{st} = \begin{bmatrix} 0 & 1 \\ 0 & 0 \end{bmatrix}.$$

where  $d_1$  is a known constant and defined in (3.1) to (3.3).

*Proof.* Define a variable  $e_{st}^3(t) = a_{21}e_{st}^1(t) + v_{st}^n(t) - d(t)$  as the observation error. Differentiating the error  $e_{st}^3(t)$  along with time  $t$ , it can be obtained by

$$\dot{e}_{st}^3(t) = a_{21}\dot{e}_{st}^1(t) + \dot{v}_{st}^n(t) - \dot{d}(t)$$

Substituting the control laws in (3.36) and (3.37) into the above equation, and combining with the error system (3.33) and (3.34), the error dynamics can be rewritten by

$$\dot{e}_{st}^1(t) = -a_{11}e_{st}^1(t) - a_{11}e_{st}^1(t - \tau(t)) \quad (3.39)$$

$$\dot{e}_{st}^2(t) = e_{st}^3(t) - k_{st}^1 |s_{st}(t)|^{\frac{1}{2}} \text{sgn}(s_{st}(t)) \quad (3.40)$$

$$\dot{e}_{st}^3(t) = a_{21}(-a_{11}e_{st}^1(t) - a_{11}e_{st}^1(t - \tau(t))) - k_{st}^2 \text{sgn}(s_{st}(t)) - \dot{d}(t) \quad (3.41)$$

Define a new vector variable as

$$\theta_{st}(t) = \begin{bmatrix} \theta_{1st}(t) & \theta_{2st}(t) \end{bmatrix}^T = \begin{bmatrix} |s_{st}(t)|^{\frac{1}{2}} \text{sgn}(s_{st}(t)) & e_{st}^3(t) \end{bmatrix}^T$$

The dynamics of the system in the  $\theta_{st}$  coordinates is given by:

$$\dot{\theta}_{st}(t) = |\theta_{1st}(t)|^{-1} \left( K_{et} \theta_{st}(t) + \begin{bmatrix} 0 & |\theta_{1st}(t)| r(t) \end{bmatrix}^T \right) \quad (3.42)$$

where  $r(t) = a_{21} (a_{11} e_{st}^1(t) + a_{11} e_{st}^1(t - \tau(t))) - \dot{d}(t)$  is a bounded function, i.e., for all  $t$ ,  $|r(t)| \leq \Pi_{st}$ ,  $K_{et} = \begin{pmatrix} -\frac{k_{st}^1}{2} & \frac{1}{2} \\ -k_{st}^2 & 0 \end{pmatrix}$  is Hurwitz.

To prove the state  $\theta_{st}(t)$  converging to zero in a finite-time, a candidate Lyapunov function is chosen as

$$V_{st}(t) = \theta_{st}^T(t) P_{st} \theta_{st}(t)$$

For a positive-definite matrix  $P_{st}$ , the LMI holds in (3.38), there exists a positive definite matrix  $Q$  such that:

$$\dot{V}_{st}(t) = -|\theta_{1st}(t)|^{-1} \theta_{st}^T(t) Q \theta_{st}(t)$$

This implies the states  $s_{st}$  and  $e_{st}^3(t)$  converge towards to zero in a finite-time. Once the ideal sliding-mode  $s_{st}(t) = 0$  is established, the error system (3.34) will maintain on  $s_{st}(t) = 0$  thereafter and the error  $e_{st}^2(t)$  will converge to zero along  $s_{st}(t) = 0$  asymptotically. This completes the proof.  $\square$

The asymptotic stability of the state error  $e_1$  is verified as follows. To ensure the asymptotic convergence of the error system (3.33) to zero, a linear system with time-varying delay can be considered. The time delay,  $\tau(t)$ , is a time-varying continuous function that satisfies

$\tau_1 < \tau(t) < \tau_2$  and  $\dot{\tau}(t) \leq \mu$ , where  $\tau_1 = T_p$  and  $\tau_2 = \bar{q}/C + T_p$  and  $\mu$  are all known constants and defined in (3.4) and (3.5). The system (3.17) is asymptotically stable, refers to the proof in [267].

From the error system (3.41), then, we can obtain that

$$e_{st}^3(t) = v_{st}^n(t) - d(t) = 0 \quad (3.43)$$

Then, the additional traffic dynamics,  $d(t)$ , can be estimated by

$$\hat{d}_{st}(t) = v_{st}^n(t) \quad (3.44)$$

where  $v_{st}^n(t)$  is defined in (3.37), which is a smooth control signal. So, a low-pass filter is not required for estimating this state.

A super-twisting algorithm is used to develop a real-time RNTTO in this section. It is used to avoid the chattering phenomenon in (3.36) and (3.37). So, a high frequent switching control signal is replaced with a smooth signal, which is used for estimation. In this way, a low-pass filter is not required, which can cause the phase legs in estimation.

### 3.3.3 Terminal Sliding Mode Based RNTTO

In the super-twisting based RNTTO algorithm, the dynamics of the estimation error of ACwnd is designed as a LTM, which features asymptotic convergence. As the real-time criteria in RNTTOs, a finite-time convergence of the error state is required to achieve the estimation timing performance. Thus, the TSMO is adopted by designing a fast terminal sliding-mode manifold that has the characteristic of finite-time convergence.

A TSMO is used to develop a real-time RNTTO in this section. In this novel terminal sliding-mode algorithm, a smooth control signal for the observer is proposed and directly used to estimate the additional traffic dynamic in a router-based network. Moreover, a fast

terminal sliding-mode manifold strategy is proposed to force the estimation error towards to zero in a finite-time. In the real-time RNTD by using TSMO algorithm, first, a smooth control signal is directly applied for estimation to avoid the usage of any low-pass filter, which is needed for a higher speed digital circuit in a router and cause the phase legs as well; second, a novel terminal sliding-mode manifold is developed to fasten the convergence of estimation error to zero in a finite-time to achieve the real-time requirements.

Considering the linearised system in (3.17) and (3.18), a terminal sliding mode observer is designed as:

$$\dot{\hat{x}}_{tsm}(t) = -a_{11}\hat{x}_{tsm}(t) - a_{11}\hat{x}_{tsm}(t - \tau(t)) + \rho(t) \quad (3.45)$$

$$\dot{\hat{y}}_{tsm}(t) = a_{21}\hat{x}_{tsm}(t) - a_{22}y(t) + v_{tsm}(t) \quad (3.46)$$

where  $\hat{x}_{tsm}(t)$  and  $\hat{y}_{tsm}(t)$  represent the estimates in TSMO for the system state  $x(t)$  and output  $y(t)$  respectively.  $\rho(t) = -a_{12}y(t) + a_{12}y(t - \tau(t)) - b_d u(t - \tau(t))$  is a known function, and  $v_{tsm}(t)$  is the control signal for the TSMO, which will be designed later.

It is assumed that the control signal of the observer  $v_{tsm}(t)$  in system (3.45) and (3.46) cannot be infinite and is bounded by satisfying the following condition:

$$T_{tsm}v_{tsm}(t) \leq \chi_{tsm} \quad (3.47)$$

where  $T_{tsm}$  and  $\chi_{tsm}$  are both positive constant.

By defining the variables  $e_{tsm}^1(t) = \hat{x}_{tsm}(t) - x(t)$  and  $e_{tsm}^2(t) = \hat{y}_{tsm}(t) - y(t)$  as the errors between the system states and their estimates, hence the error system can be obtained from equations (3.17) to (3.18) and equations (3.45) to (3.46) as follows:

$$\dot{e}_{tsm}^1(t) = -a_{11}e_{tsm}^1(t) - a_{11}e_{tsm}^1(t - \tau(t)) \quad (3.48)$$

$$\dot{e}_{tsm}^2(t) = a_{21}e_{tsm}^1(t) - d(t) + v_{tsm}(t) \quad (3.49)$$

A terminal sliding mode manifold is designed as

$$s_{t_{sm}}(t) = \dot{e}_{t_{sm}}^2(t) + \beta_{t_{sm}}(e_{t_{sm}}^2)^{q_{t_{sm}}/p_{t_{sm}}}(t) + \alpha_{t_{sm}}e_{t_{sm}}^2(t) \quad (3.50)$$

where  $c_{sm} > 0$  is a constant. where  $\alpha_{t_{sm}} > 0$  and  $\beta_{t_{sm}} > 0$  both are constants.  $p_{t_{sm}}$  and  $q_{t_{sm}}$  are positive odd integers which satisfy  $1 < p_{t_{sm}}/q_{t_{sm}} < 2$ .

**Theorem 6.** *The error system (3.48) and (3.49) will reach  $s_{t_{sm}}(t) = 0$  from any initial condition  $s_{t_{sm}}(0) \neq 0$  in a finite-time  $t_{t_{sm}}^r \leq |s_{t_{sm}}(0)|/(\eta_{t_{sm}})$ , then converge to zero along  $s_{t_{sm}}(t) = 0$  in a finite-time  $t_{t_{sm}}^s = p_{t_{sm}}/(\alpha_{t_{sm}}(p_{t_{sm}} - q_{t_{sm}}))(\ln(\alpha(e_{t_{sm}}^2)^{(p_{t_{sm}}-q_{t_{sm}})/p_{t_{sm}}}(t_{t_{sm}}^r) + \beta_{t_{sm}}) - \ln \beta_{t_{sm}})$ , if a terminal sliding mode manifold  $s_{t_{sm}}(t)$  is designed as (3.50) and the control law is designed as*

$$v_{t_{sm}}(t) = v_{t_{sm}}^{eq}(t) + v_{t_{sm}}^n(t) \quad (3.51)$$

$$v_{t_{sm}}^{eq}(t) = \beta_{t_{sm}}(e_{t_{sm}}^2)^{q_{t_{sm}}/p_{t_{sm}}}(t) + \alpha_{t_{sm}}e_{t_{sm}}^2(t) \quad (3.52)$$

$$\dot{v}_{t_{sm}}^n(t) + T_{t_{sm}}v_{t_{sm}}^n(t) = \omega_{t_{sm}}(t) \quad (3.53)$$

$$\omega_{t_{sm}}(t) = (\chi_{t_{sm}} + d_1 + \eta_{t_{sm}})\text{sgn}(s_{t_{sm}}(t)) \quad (3.54)$$

where  $\chi_{t_{sm}}$  and  $d_1$  are defined in (3.47) and (3.1) to (3.3).  $\eta_{t_{sm}} > 0$  is a constant

*Proof.* From system (3.49), the terminal sliding mode manifold (3.50) can be reformed as follows

$$\begin{aligned} s_{t_{sm}}(t) &= \dot{e}_{t_{sm}}^2(t) + \beta_{t_{sm}}(e_{t_{sm}}^2)^{q_{t_{sm}}/p_{t_{sm}}}(t) + \alpha_{t_{sm}}e_{t_{sm}}^2(t) \\ &= a_{21}e_{t_{sm}}^1(t) + d(t) - v_{t_{sm}}(t) + \beta_{t_{sm}}(e_{t_{sm}}^2)^{q_{t_{sm}}/p_{t_{sm}}}(t) + \alpha_{t_{sm}}e_{t_{sm}}^2(t) \end{aligned}$$

Substituting the control (3.51) into the above equation gives

$$s_{t_{sm}}(t) = a_{21}e_{t_{sm}}^1(t) + d(t) - v_{t_{sm}}^{eq}(t) - v_{t_{sm}}^n(t) + \beta_{t_{sm}}(e_{t_{sm}}^2)^{q_{t_{sm}}/p_{t_{sm}}}(t) + \alpha_{t_{sm}}e_{t_{sm}}^2(t)$$

which can be rewritten by further substituting (3.52) as

$$\begin{aligned} s_{t_{sm}}(t) &= a_{21}e_{t_{sm}}^1(t) + d(t) - (\beta_{t_{sm}}e_{t_{sm}}^{q_{t_{sm}}/p_{t_{sm}}}(t) + \alpha_{t_{sm}}e_{t_{sm}}^2(t)) - v_{t_{sm}}^n(t) \\ &\quad + \beta_{t_{sm}}(e_{t_{sm}}^2)^{q_{t_{sm}}/p_{t_{sm}}}(t) + \alpha_{t_{sm}}e_{t_{sm}}^2(t) \\ &= a_{21}e_{t_{sm}}^1(t) + d(t) - v_{t_{sm}}^n(t) \end{aligned} \quad (3.55)$$

The following Lyapunov function  $V_{t_{sm}}(t) = \frac{1}{2}s_{t_{sm}}^2(t)$  is considered. For the TSM manifold (3.50), its derivative with respect to time  $t$  along error system (3.49) can be achieved from (3.55) as follows:

$$\begin{aligned} \dot{s}_{t_{sm}}(t) &= \dot{d}(t) - \dot{v}_{t_{sm}}^n(t) = \dot{d}(t) - \dot{v}_{t_{sm}}^n(t) + T_{t_{sm}}v_{t_{sm}}^n(t) - T_{t_{sm}}v_{t_{sm}}^n(t) \\ &= \dot{d}(t) - \omega_{t_{sm}}(t) + T_{t_{sm}}v_{t_{sm}}^n(t) \end{aligned}$$

hence,

$$\begin{aligned} s_{t_{sm}}(t)\dot{s}_{t_{sm}}(t) &= \dot{d}(t)s_{t_{sm}}(t) - (\chi_{t_{sm}} + d_1 + \eta_{t_{sm}})|s_{t_{sm}}(t)| + T_{t_{sm}}v_{t_{sm}}^n(t)s_{t_{sm}}(t) \\ &\leq (|\dot{d}(t)| - d_1)|s_{t_{sm}}(t)| - \eta_{t_{sm}}|s_{t_{sm}}(t)| + |T_{t_{sm}}v_{t_{sm}}^n(t) - \chi_{t_{sm}}||s_{t_{sm}}(t)| \end{aligned}$$

From the conditions (3.47) and (3.11) and the above inequality, we have

$$\dot{V}_{t_{sm}} = s_{t_{sm}}(t)\dot{s}_{t_{sm}}(t) \leq -\eta_{t_{sm}}\sqrt{2}V_{sm}^{1/2} < 0, \text{ for } s_{t_{sm}}(t) \neq 0$$

which means that error system (3.49) will reach to  $s_{t_{sm}}(t) = 0$  within the finite-time  $s_{t_{sm}}(0) \neq 0$  in a finite-time  $t_{T_{sm}}^r \leq |s_{t_{sm}}(0)|/(\eta_{t_{sm}})$ , in other words,  $s_{t_{sm}}(t) = 0, \forall t \geq t_{T_{sm}}^r$ . Once the

error system (3.49) reaches the TSM manifold, it then stays on this switching surface and converges to the equivalent point along  $s_{t_{sm}}(t) = 0$  in a finite-time  $t_{t_{sm}}^s$ . This completes the proof.  $\square$

The asymptotic stability of the state error  $e_{t_{sm}}^1$  can be proofed by considering a linear system with time-varying delay with the known bounded values of the time delay,  $\tau(t)$ , and its derivative bounded value in [267].

As the error systems (3.48) and (3.49) converge to zero, then, it can be obtained from (3.55)

$$s_{t_{sm}}(t) = d(t) - v_{t_{sm}}^n(t) = 0 \quad (3.56)$$

The estimate of the additional traffic dynamics,  $d(t)$ , can be achieved by

$$\hat{d}_{t_{sm}}(t) = v_{t_{sm}}^n(t) \quad (3.57)$$

Note that

$$\frac{v_{t_{sm}}^n(s)}{\omega_{t_{sm}}(s)} = \frac{1}{s + T_{t_{sm}}} \quad (3.58)$$

where  $\omega_{t_{sm}} = T_{t_{sm}}$  is the bandwidth of the equivalent first-order low-pass filter. Therefore, the control signal  $v_{t_{sm}}^n(t)$  is the smooth signal which can be directly applied to estimate the external disturbance by (3.58).

A terminal sliding-mode based RNTTO is developed to achieve the real-time performance in this section. First, a smooth control signal in (3.53) and (3.53) for the observer is directly used to estimate the additional traffic dynamic as in (3.58). Second, a fast terminal sliding-mode manifold strategy in (3.50) is proposed to force the estimation error towards to zero in a finite-time  $t_{t_{sm}}^s$ , which is defined in Theorem 6. In the real-time RNTTO by using TSMO



algorithm, the usage of any low-pass filter is avoided, which will cause the phase legs for the real-time estimation, and the finite-time convergence of estimation error to zero can be set to achieve the real-time requirements.

## 3.4 Simulations

To validate the proposed sliding mode based observation algorithms for RNT0, the simulations are conducted via Network Simulator II. Moreover, the comparative results among the sliding mode observer, super-twisting observer and the novel terminal sliding mode observer are presented. Particularly, the simulation results of the proposed TSMO is illustrated and discussed.

### 3.4.1 Model Description

A typical star type TCP/IP network model, as shown in Fig. 3.2, is considered in the simulation. It consists of a number of hosts and clients with one network router. The parameters of the TCP/IP network model and the designed observer are given below.

*Simulation model of router-based network:* To study the network traffic behaviours, the network simulator NS-II [268] is used. It is a discrete event-based simulator for networking research. First, the network traffic scenario in Fig. 3.2 is constructed by using the network simulator NS-II. It includes  $N$  hosts (source nodes) and  $N$  clients (destination nodes), where  $N = 60$ . The link capacity  $C$  is set to be 15 Mb. The connections between each host/client and the router use full-duplex that construct bidirectional links at propagation delay  $T_p = 200$  ms. The maximum window size is set to be 0.12 Mb. The packet size is set to be 500 bytes. The AQM mechanism is adopted in the router by using the proportional integral (PI) algorithm [125] to regulate the queue length of router buffer at desired value  $q_0 = 175$  packets. The buffer capacity (buffer size)  $\bar{q}$  is set to be 800 packets.

According to the aforementioned network configurations, the parameters in the linearised TCP/IP network model (3.17) and (3.18) can be determined as follows:  $a_{11} = 0.2630$ ,  $a_{12} = 0.0044$ ,  $b_d = 481.7708$ ,  $a_{21} = 243.2432$ , and  $a_{22} = 4.0541$ .

*Observer design:* To show the effectiveness of the proposed method, the well-known Luenberger observer (LO) [45] is applied for performance comparative studies. The parameters of LO are set as:  $L_1 = -5$  and  $L_2 = -32$ . Moreover, the parameters of SMO are designed using Theorems 4 are:  $c_{sm} = 20$ , and  $k_{sm} = 1600$ . In addition, the parameters of STO are designed using Theorems 5 are:  $k_{st}^1 = 100$ , and  $k_{st}^2 = 1600$ . Furthermore, the parameters of the proposed TSMO are designed using Theorems 6 are:  $p_{tsm} = 5$ ,  $q_{tsm} = 3$ ,  $\alpha_{tsm} = 15$ ,  $\beta_{tsm} = 5$ , and  $k_{tsm} = 1600$ .

For the fair comparison, a standardized tuning for each of the algorithms is established. The parameters of LO are determined by the trial and error method. The parameters of both SMO and STO are selected based on the principle that all the gains of the switching functions in these observers are the same with those in the proposed observer. In other words, all the variations of control signals used for the estimation are kept approximately equal. In this condition, the convergence speed and steady-state performances are compared for these observers.

To evaluate the performances of the proposed observer, the external traffic served by both constant bit rate (CBR) and variable bit rate (VBR) are considered. In reality, these two types of services, CBR and VBR, are used mainly for voice, video, other real-time constrained services and even the malicious attacks, such as DoS (or DDoS) flooding attack. The following two different scenarios are considered.

- **Scenario 1 (constant rate traffics):** three source nodes generate constant rate traffics. The “cbr” applications are invoked and attached to the “udp” agents. The sending rate of each agent is set as 500 *packets/s* between the period 50 – 150s. The simulation time is 200 *seconds*.

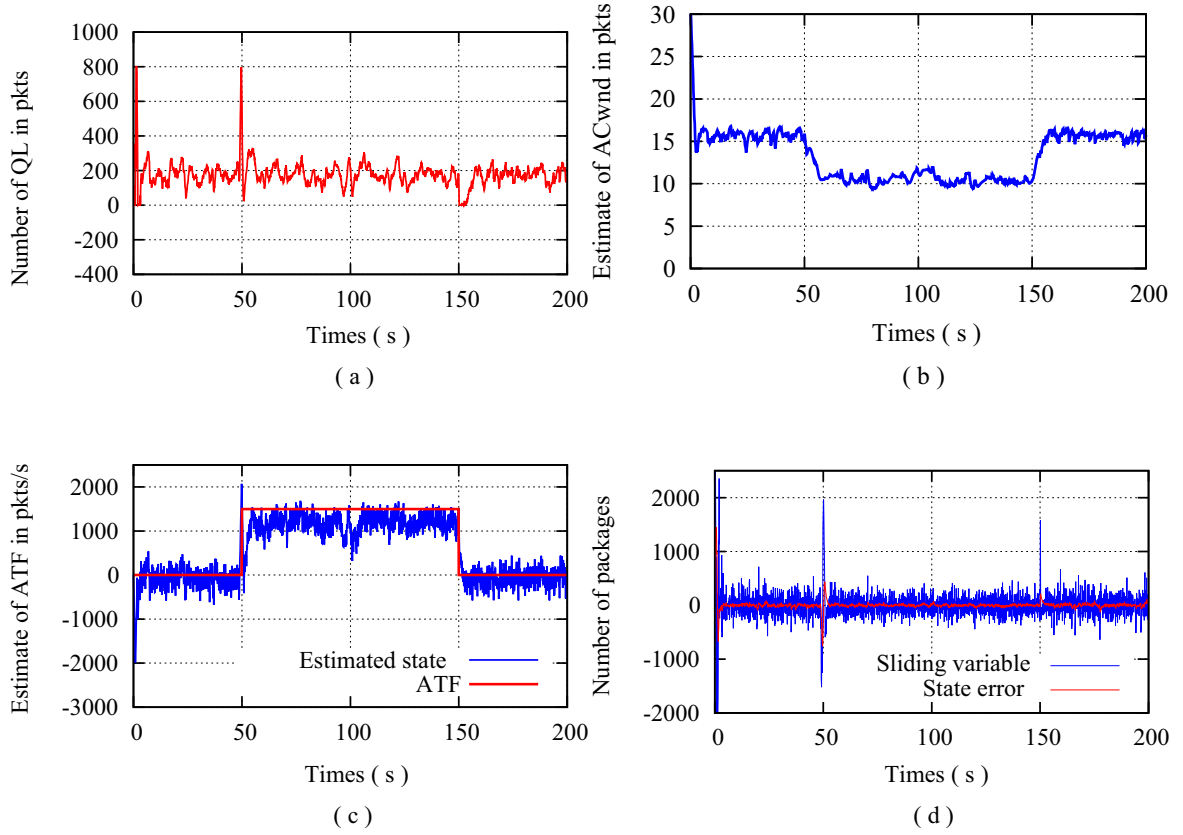


Fig. 3.4 State and control of the proposed TSMO in Scenario 1.: (a) The number of QL  $q(t)$  in router buffer. (b) Estimated ACwnd  $w(t)$  in *packets* at the router. (c) Estimated dynamics of ATF  $d(t)$  and the true DDoS flooding rate. (d) The value of the sliding variable  $s_{tsm}(t)$  in *packets*.

- **Scenario 2 (variable rate traffics):** three source nodes generate variable rate traffics.

The “vbr” applications are designed as ramp traffic and attached to the “udp” agents.

The sending rate of each agent is set as rising slope up to 500 *packets/s* between the period 50 – 150s. The simulation time is 200 *seconds*.

### 3.4.2 Simulation Results and Discussion

Figs. 3.4 and 3.5 depict the states of the proposed TSMO corresponding to the Scenarios 1 and 2. It can be seen from Figs. 3.4a and 3.5a, the queue lengths are stabilized at the desired

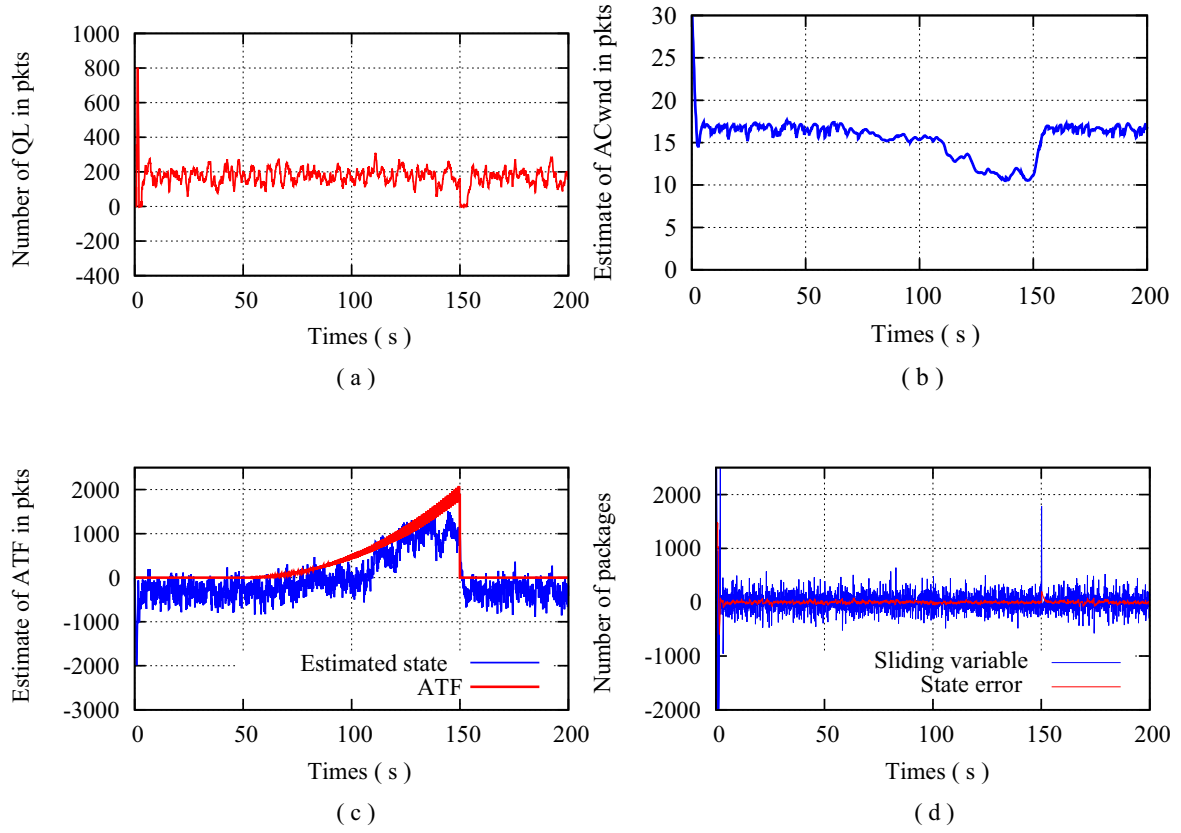


Fig. 3.5 State and control of the proposed TSMO in Scenario 2.: (a) The number of QL  $q(t)$  in router buffer. (b) Estimated ACwnd  $w(t)$  in *packets* at the router. (c) Estimated dynamics of ATF  $d(t)$  and the true DDoS flooding rate. (d) The value of the sliding variable  $s_{tsm}(t)$  in *packets*.

Table 3.1 Comparative studies of LO, SMO, STO and TSMO in Scenario 1.

|                  | LO     | SMO        | STO        | TSMO    |
|------------------|--------|------------|------------|---------|
| $t^r$            | /      | 5.2        | 3.1        | 3.2     |
| $t^s$            | /      | Asymptotic | Asymptotic | 10.5    |
| Mean of $e^1(t)$ | 1.05   | 1.05       | 1.05       | 1.05    |
| STD of $e^1(t)$  | 2.45   | 2.45       | 2.45       | 2.45    |
| Mean of $e^2(t)$ | -12.62 | 11.07      | 2.65       | 1.66    |
| STD of $e^2(t)$  | 33.21  | 53.32      | 53.60      | 18.13   |
| Mean of $e_d$    | 749.63 | -326.46    | -341.88    | -234.39 |
| STD of $e_d$     | 750.19 | 343.28     | 358.02     | 249.48  |

Table 3.2 Comparative studies of LO, SMO, STO and TSMO in Scenario 2.

|                  | LO      | SMO        | STO        | TSMO    |
|------------------|---------|------------|------------|---------|
| $t^r$            | /       | 5.1        | 4.2        | 3.8     |
| $t^s$            | /       | Asymptotic | Asymptotic | 4.5     |
| Mean of $e^1(t)$ | 1.97    | 1.97       | 1.97       | 1.97    |
| STD of $e^1(t)$  | 2.15    | 2.15       | 2.15       | 2.15    |
| Mean of $e^2(t)$ | 6.36    | 35.36      | 3.26       | 2.20    |
| STD of $e^2(t)$  | 21.68   | 48.03      | 50.56      | 21.44   |
| Mean of $e_d$    | -314.59 | -496.67    | -518.86    | -203.67 |
| STD of $e_d$     | 509.30  | 280.03     | 265.94     | 260.71  |

set points in both scenarios. With the simple observations of the queuing dynamics, it cannot identify the differences. While by the proposed observer, the unknown traffic behaviour i.e., the average Cwnd size and the additional traffic dynamics are accurately estimated. It can be seen from Figs. 3.4d and 3.5d that the estimation error  $e_{tsm}^2(t)$  in error system (3.49) converges to zero. The control signals  $v_{tsm}(t)$  in (3.51) are directly used to estimate the dynamics of ATF, as shown in Fig. 3.4c and 3.5c. The ACwnd state  $w(t)$  is estimated as presented in Figs. 3.4b and 3.5b respectively. The estimation of the average Cwnd size illustrates that there exists a degradation of throughputs in hosts and link's availability in the TCP/IP network.

From the comparative results in Tables 3.1 and 3.2 corresponding to the Scenarios 1 and 2, the proposed TSMO has the fastest dynamical response and the best steady-state accuracies of estimating  $w(t)$  and  $d(t)$  among the aforementioned observers. The proposed TSMO has been demonstrated the finite-time reaching to the sliding surface and then converge to zero in a finite time. However, the conventional SMO and the STO only feature the finite-time reachability and asymptotic convergence. Thus, the proposed TSMO features the most accuracy in estimation error  $e^2(t)$ .

### 3.5 Summary

In this chapter, the router-based network traffic monitoring problem has been reformulated by using the sliding mode control based theory, which helps develop the sliding mode observers for RNTO applications. With the sliding mode observers for the real-time dynamic solution, the robustness of the RNTO under the network uncertainties can be guaranteed, which addresses the problem widely neglected in existing literature.

By analysing the fluid-flow model which represents the traffic dynamics in the router-based TCP/IP networks, the RNTO algorithms of a conventional sliding mode observer, a super-twisting observer and a novel terminal sliding mode observer have been developed for real-time state estimation. Although the SMO features the high robustness under the network disturbance, it still has the problem of a linear convergence rate of estimation error and the high frequency signals of the ATF estimation. To overcome the issues of SMO, the STO as a high-order sliding mode method can provide a continuous control signal that is directly used to estimate the dynamics of ATF without the low-pass filter, but it has the issue of asymptotic convergence of estimation error. However, the novel TSMO has been proposed to address the previous two key issues. First, the proposed TSMO can generate a smooth control signal that is directly used to estimate ATF without any low-pass filter. Second, the estimation error of the queue length can be forced to converge to zero in a finite-time, which improves the estimation accuracy and meets the time criteria of the real-time estimation. Therefore, the proposed TSMO presents a promising performance which has a good potential for real RNTO applications.

# Chapter 4

## Full-order Terminal Sliding Mode Observation Strategy

### 4.1 Introduction

The methodology proposed in **Chapter 3** presents an acceptable real-time dynamic observation algorithms by using the sliding mode control theory for RNTD applications. However, the response time for the estimation of ACwnd is too long under the real-time environment. New technique is required to handle the internal dynamics of the system, which represents the dynamics of ACwnd. Especially for the problems of no control strategy for the internal dynamics, which brings the low accuracy, long response time in ACwnd estimation.

In this chapter, a real-time full-order terminal sliding mode observer (FTSMO) is investigated to monitor the traffic flow for RNTD applications. The challenge of the state estimation for a class of systems where some system states are unmeasurable is presented in **Section 4.2**. The novel control strategy for speeding up the convergence of internal dynamics by using the finite-time stability theory is proposed and proven in **Section 4.3**. The simulation case study in Network Simulator II are presented and discussed, which demonstrate the effectiveness and efficiency of the proposed FTSMO algorithm in **Section 4.4**.

Finally, the conclusions are made in **Section 4.5**.

## 4.2 Problem Formulation

The challenge of state estimation for a class of systems where some system states are unmeasurable is proposed in this section.

First, consider a linear time-delay system represented by

$$\dot{x}(t) = Ax(t) + A_d x(t - \tau) + Bu(t) + Dd(t) \quad (4.1)$$

where  $x(t) = [x_1(t), x_2(t)]^T \in \mathbb{R}^2$  is the system states,  $u(t) \in \mathbb{R}$  the control,  $\tau = \tau(t)$  the time delay,  $d(t) \in \mathbb{R}$  the disturbance, and

$$A = \begin{bmatrix} a_{11} & a_{12} \\ a_{21} & a_{22} \end{bmatrix}, A_d = \begin{bmatrix} a_{11d} & a_{12d} \\ 0 & a_{22d} \end{bmatrix}, B = \begin{bmatrix} 1 \\ 0 \end{bmatrix}, D = \begin{bmatrix} 0 \\ 1 \end{bmatrix}.$$

Without loss of generality it can be assumed that (4.1) is already in regular form and so

$$\dot{x}_1(t) = a_{11}x_1(t) + a_{11d}x_1(t - \tau) + a_{12}x_2(t) + a_{12d}x_2(t - \tau) + bu(t) \quad (4.2)$$

$$\dot{x}_2(t) = a_{21}x_1(t) + a_{22}x_2(t) + a_{22d}x_2(t - \tau) + d(t) \quad (4.3)$$

Some assumptions are made as

- 1). The system (4.1) is stable;
- 2). The system state  $x_2$  is measurable;
- 3). The system state  $x_1$  is unmeasurable.

The aim is to design an observer for estimating the disturbance  $d(t)$  in (4.1). Now an



observer is proposed for the system (4.1) in the following form as

$$\dot{\hat{x}}_1(t) = a_{11}\hat{x}_1(t) + a_{11d}\hat{x}_1(t - \tau) + a_{12}x_2(t) + a_{12d}x_2(t - \tau) + bu(t) + v_1(t) \quad (4.4)$$

$$\dot{\hat{x}}_2(t) = a_{21}\hat{x}_1(t) + a_{22}x_2(t) + a_{22d}x_2(t - \tau) + v_2(t) \quad (4.5)$$

$$\hat{d}(t) = \lim_{\substack{\hat{x}_1(t) \rightarrow x_1(t) \\ \hat{x}_2(t) \rightarrow x_2(t)}} v_2(t) \quad (4.6)$$

If the errors between the estimates and the true states are written as  $e_1(t) := \hat{x}(t) - x(t)$  and  $e_2(t) := \hat{y}(t) - y(t)$ , then from Eqs. (4.2) and (4.3) to Eqs. (4.4) and (4.5) the following error system is obtained

$$\dot{e}_1(t) = a_{11}e_1(t) + a_{11d}e_1(t - \tau) + v_1(t) \quad (4.7)$$

$$\dot{e}_2(t) = a_{21}e_1(t) - d(t) + v_2(t) \quad (4.8)$$

and the estimate of the disturbance follows that

$$\hat{d}(t) = \lim_{\substack{e_1(t) \rightarrow 0 \\ e_2(t) \rightarrow 0}} v_2(t) \quad (4.9)$$

The estimation of the disturbance  $d(t)$  in (4.1) includes two steps:

- i). The error system converges to zero asymptotically or in finite-time by using the control of the observer.
- ii). Once the errors converge zero, the disturbance can be estimated using (4.9).

Two control strategies  $v_1$  and  $v_2$  in system (4.7) and (4.8) can only utilize the measurable error  $e_2$ , i.e.  $v_1 = v_1(e_2)$ ,  $v_2 = v_2(e_2)$ . The control  $v_2 = v_2(e_2)$  can be designed to force  $e_2$  converging to zero although there exists unmeasurable  $e_1$  and disturbance  $d(t)$  in the error system (4.8). For the error system (4.7), there is no control in conventional observer, i.e.  $v_1 = 0$  as in references [43, 45–52, 56–59]. In this condition, the error system (4.7) can be

rewritten as

$$\dot{e}_1(t) = a_{11}e_1(t) + a_{11d}e_1(t - \tau) \quad (4.10)$$

which is the internal dynamics of the error system. The error state  $e_1$  will converge to zero asymptotically due to the assumption 1. The convergence time of  $e_1$  cannot be affected by the control of the observer  $v_2$ , and may be very long. Different to the conventional methods, in the paper, a control  $v_1$  is added in the error system (4.7), and the control strategy is proposed to speed up the convergence of the internal dynamics of the error system (4.7).

When the error system in (4.7) and (4.8) converges to zero, the estimate of the disturbance can be obtained using (4.9). Hence the control of the observer  $v_2(t)$  is required to be smooth, which is a challenge to the sliding-mode observer.

Two Lemmas are stated below. They will be used in the proof of the Theorems later.

**Lemma 1.** [269] *Given a nonlinear system  $\dot{\mathbf{x}} = \mathbf{f}(\mathbf{x})$ , where  $x \in \mathbb{R}^n$ ,  $f(0) = 0$ , and  $f(\cdot) : \mathbb{R}^n \mapsto \mathbb{R}^n$ . If there exists a positive definite continuous function  $V(x)$  such that  $\dot{V}(\mathbf{x}) + cV^\alpha(\mathbf{x}) \leq 0$ , where  $c > 0$  and  $\alpha \in (0, 1)$  are two constants. Then,  $V(x)$ ,  $\forall V(\mathbf{x}_0) \neq 0$ , approaches to zero in a finite-time  $T$ , where  $T \leq V^{1-\alpha}(\mathbf{x}_0)/(c(1-\alpha))$ ,  $\mathbf{x}_0 = \mathbf{x}(0)$ .*

**Lemma 2.** [267] *Consider a linear system with time-varying delay expressed by*

$$\begin{cases} \dot{x}(t) = Ax(t) + A_d x(t - \tau(t)), & t > 0, \\ x(t) = \varphi(t), & t \in [-\tau_2, 0] \end{cases} \quad (4.11)$$

where  $x \in \mathbb{R}^n$  is the state,  $\mathbf{A}$  and  $\mathbf{A}_d$  are constant matrices with appropriate dimensions, the time delay,  $\tau(t)$ , is a time-varying continuous function that satisfies  $\tau_1 < \tau(t) < \tau_2$  and  $\dot{\tau}(t) \leq \mu$ , where  $\tau_1$ ,  $\tau_2$  and  $\mu$  are all known constants. The system (4.11) is asymptotically stable if there exist matrices  $P > 0$ ;  $Q_i > 0$ ,  $Z_j > 0$ , for  $i = 1, 2, 3$ , and  $j = 1, 2$ ;  $N_i$ ,  $M_i$  and

$S_i$ ,  $i = 1, 2$  such that the following LMI holds:

$$\begin{bmatrix} \phi_{11} & \phi_{12} & M_1 & -S_1 & \tau_2 N_1 & \tau_{12} S_1 & \tau_{12} M_1 & A_{11} v \\ * & \phi_{22} & M_2 & -S_2 & \tau_2 N_2 & \tau_{12} S_2 & \tau_{12} M_2 & A_{11d} v \\ * & * & -Q_1 & 0 & 0 & 0 & 0 & 0 \\ * & * & * & -Q_2 & 0 & 0 & 0 & 0 \\ * & * & * & * & -\tau_2 Z_1 & 0 & 0 & 0 \\ * & * & * & * & * & -\tau_{12}(Z_1 + Z_2) & 0 & 0 \\ * & * & * & * & * & * & -\tau_{12} Z_2 & 0 \\ * & * & * & * & * & * & * & -v \end{bmatrix} < 0$$

where  $\phi_{11} = 2PA + Q_1 + Q_2 + Q_3 + 2N_1$ ,  $\phi_{12} = PA_d + N_2 - N_1 + S_1 - M_1$ ,  $\phi_{22} = -(1 - \mu)Q_3 + 2S_2 - 2N_2 - 2M_2$ ,  $v = \tau_2 Z_1 + \tau_{12} Z_2$ ,  $\tau_{12} = \tau_2 - \tau_1$ , and  $*$  denotes the symmetric terms in the symmetric matrix.

### 4.3 Full-order Terminal Sliding Mode Based RNTO

In the fluid-flow model of the TCP/IP networks in Eqs.(3.17) and (3.18), the dynamics of ATF, i.e.,  $d(t)$ , can be considered as the disturbance in Eq. (4.1). The estimate of  $d(t)$  can be used for anomaly detection. To estimate  $d(t)$ , an observer is proposed according to Eqs.(4.4) and (4.5), and can be presented as

$$\dot{\hat{x}}_{ftsm}(t) = -a_{11}\hat{x}_{ftsm}(t) - a_{11}\hat{x}_{ftsm}(t - \tau(t)) - a_{12}y(t) + a_{12}y(t - \tau(t)) \quad (4.12)$$

$$-b_d u(t - \tau(t)) + v_{1ftsm}(t)$$

$$\dot{\hat{y}}_{ftsm}(t) = a_{21}\hat{x}_{ftsm}(t) - a_{22}y(t) + v_{2ftsm}(t) \quad (4.13)$$

where  $\hat{x}_{ftsm}(t)$  and  $\hat{y}_{ftsm}(t)$  represent the estimates of the system state  $x(t)$  and output  $y(t)$  respectively,  $v_{1ftsm}(t)$  and  $v_{2ftsm}(t)$  are control signals for the observer.

Defining  $e_{1ftsm}(t) := \hat{x}_{ftsm}(t) - x(t)$  and  $e_{2ftsm}(t) := \hat{y}_{ftsm}(t) - y(t)$  as the errors between the system states and their estimates, hence the error system can be obtained from Eqs.(3.17)–(3.18) and (4.12)–(4.13) as follows:

$$\dot{e}_{1ftsm}(t) = -a_{11}e_{1ftsm}(t) - a_{11}e_{1ftsm}(t - \tau(t)) + v_{1ftsm}(t) \quad (4.14)$$

$$\dot{e}_{2ftsm}(t) = a_{21}e_{1ftsm}(t) + v_{2ftsm}(t) - d(t) \quad (4.15)$$

It should be noted that the state  $e_{2ftsm}$  in error system (4.14)–(4.15) is measurable and can be used in the controller. But the state  $e_{1ftsm}$  is unmeasurable and cannot be used in the controller, i.e. the control  $v_{1ftsm}$  and  $v_{2ftsm}$  in error system (4.14)–(4.15) can include only  $e_{2ftsm}$ .

### 4.3.1 Controller Design of the Second Error Subsystem

The second error subsystem (4.15) is firstly considered, namely

$$\dot{e}_{2ftsm}(t) = a_{21}e_{1ftsm}(t) + v_{2ftsm}(t) - d(t) \quad (4.16)$$

For the subsystem system (4.15), a TSM manifold is chosen as the following form:

$$s_{ftsm}(t) = \dot{e}_{2ftsm}(t) + \alpha_{ftsm}e_{2ftsm}(t) + \beta_{ftsm}(e_{2ftsm})^{q_{ftsm}/p_{ftsm}}(t) \quad (4.17)$$

where  $\alpha_{ftsm}, \beta_{ftsm} > 0$  are constants,  $p_{ftsm}$  and  $q_{ftsm}$  are positive odd integers which satisfy  $1 < q_{ftsm}/p_{ftsm} < 2$ .

**Theorem 7.** *The error system (4.15) will reach  $s_{ftsm}(t) = 0$  from any initial condition  $s_{ftsm}(0) \neq 0$  in a finite-time  $t_{ftsm}^r \leq |s(0)|/\eta_2$ , then converge to zero along  $s_{ftsm}(t) = 0$  in a finite-time  $t_{ftsm}^s = p_{ftsm}/(\alpha_{ftsm}(p_{ftsm} - q_{ftsm}))(\ln(\alpha_{ftsm}(e_{ftsm}^2)^{(p_{ftsm}-q_{ftsm})/p_{ftsm}}(t_r) + \beta_{ftsm}) - \ln \beta_{ftsm})$ , if a TSM manifold  $s_{ftsm}(t)$  is selected as (4.17) and the control is given*

by

$$v_{2ftsm}(t) = v_{ftsm}^{2eq}(t) + v_{ftsm}^{2n}(t) \quad (4.18)$$

$$v_{ftsm}^{2eq}(t) = -a_{21}\hat{x}_{ftsm}(t) - \alpha_{ftsm}e_{2ftsm}(t) - \beta_{ftsm}e_{2ftsm}(t)^{q_{ftsm}/p_{ftsm}} \quad (4.19)$$

$$\dot{v}_{ftsm}^{2n}(t) = -a_{12}a_{21}y(t) + a_{12}a_{21}y(t - \tau(t)) - a_{21}b_d u(t - \tau(t)) - k_2 \text{sgn}(s_{ftsm}(t)) \quad (4.20)$$

where  $k_{2ftsm} = 2a_{11}a_{21}\bar{w} + d_1 + \eta_{2ftsm}$ ,  $\eta_{2ftsm} > 0$  is a constant,  $\bar{w}$  and  $d_1$  are defined in (3.1)–(3.3) and (3.11) respectively.

*Proof.* From the error system (4.15), the TSM manifold (4.17) can be rewritten as

$$s_{ftsm}(t) = a_{21}e_{1ftsm}(t) + v_{2ftsm}(t) - d(t) + \alpha_{ftsm}e_{2ftsm}(t) + \beta_{ftsm}e_{2ftsm}^{q_{ftsm}/p_{ftsm}}(t)$$

Substituting Eqs. (4.18) and (4.19) into the above gives

$$s_{ftsm}(t) = -a_{21}x(t) + v_{ftsm}^{2n}(t) - d(t) \quad (4.21)$$

Differentiating  $s_{ftsm}(t)$  in (4.21) with respect to time  $t$  along the error system (4.15) yields

$$\begin{aligned} \dot{s}_{ftsm}(t) &= -a_{21}\dot{x}(t) + \dot{v}_{ftsm}^{2n}(t) - \dot{d}(t) \\ &= -a_{21}(-a_{11}x(t) - a_{11}x(t - \tau(t)) - a_{12}y(t) \\ &\quad + a_{12}y(t - \tau(t)) - b_d u(t - \tau(t))) + \dot{v}_{ftsm}^{2n}(t) - \dot{d}(t) \end{aligned}$$

Further substituting the control (4.20) into the above equation gives

$$\dot{s}_{ftsm}(t) = -a_{21}(-a_{11}x(t) - a_{11}x(t - \tau(t))) - (2a_{11}a_{21}\bar{w} + d_1 + \eta_{2ftsm})\text{sgn}(s_{ftsm}(t)) - \dot{d}(t)$$

Introduce a candidate Lyapunov function given by  $V_{1ftsm}(t) = 0.5s_{2ftsm}^2(t)$ . Taking the

derivative of  $v_{1ftsm}(t)$  along the trajectories of (4.14), and using the above expression, it follows that

$$\begin{aligned}
s_{ftsm}(t)\dot{s}_{ftsm}(t) &= -a_{21}(-a_{11}x(t) - a_{11}x(t - \tau(t)))s_{ftsm}(t) - (2a_{11}a_{21}2\bar{w} \\
&\quad + d_1 + \eta_{2ftsm})|s_{ftsm}(t)| - \dot{d}(t)s_{ftsm}(t) \\
&\leq |a_{21}(a_{11}x(t) + a_{11}x(t - \tau(t)))||s_{ftsm}(t)| - (2a_{11}a_{21}\bar{w} \\
&\quad + d_1 + \eta_{2ftsm})|s_{ftsm}(t)| + |\dot{d}(t)||s_{ftsm}(t)| \\
&\leq a_{21}(a_{11}|x(t)| + a_{11}|x(t - \tau(t))| - 2a_{11}\bar{w})|s_{ftsm}(t)| \\
&\quad + (|\dot{d}(t)| - d_1)|s_{ftsm}(t)| - \eta_{2ftsm}|s_{ftsm}(t)|
\end{aligned}$$

From the condition (3.19), (3.11) and the above inequality, we have

$$\dot{V}_{1ftsm}(t) = s_{ftsm}(t)\dot{s}_{ftsm}(t) \leq -\eta_{2ftsm}\sqrt{2}(V_{1ftsm})^{1/2}(t) < 0, \quad \text{for } s_{ftsm}(t) \neq 0$$

which means that second error system (4.15) will reach to  $s_{ftsm}(t) = 0$  within the finite-time  $t_{ftsm}^r \leq |s_{ftsm}(0)|/\eta_{2ftsm}$ , in other words,  $s_{ftsm}(t) = 0, \forall t \geq t_{ftsm}^r$ . Once the ideal sliding-mode  $s_{ftsm}(t) = 0$  is established, the error subsystem (4.15) will maintain on  $s_{ftsm}(t) = 0$  thereafter and behaves in an identical fashion as  $\dot{e}_{2ftsm}(t) = -\alpha_{ftsm}e_{2ftsm}(t) - \beta_{ftsm}(e_{2ftsm})^{q_{ftsm}/p_{ftsm}}(t)$ , which will converge to zero along  $s_{ftsm}(t) = 0$  in the finite-time  $t_{ftsm}^s$ . This completes the proof.  $\square$

### 4.3.2 Controller Design of the First Error Subsystem

Now consider the first error system in (4.14), namely

$$\dot{e}_{1ftsm}(t) = -a_{11}e_{1ftsm}(t) - a_{11}e_{1ftsm}(t - \tau(t)) + v_{1ftsm}(t)$$

Define an area  $\Gamma$  for  $e_{1ftsm}$  near zero as

$$\Gamma = \{e_{1ftsm} : |e_{1ftsm} - a_{21}^{-1}d| \leq a_{21}^{-1}d_0 + \varepsilon_{ftsm}\} \quad (4.22)$$

where  $d_0$  is defined in (3.11),  $\varepsilon_{ftsm}$  is a positive constant, which can be chosen by  $0 < \varepsilon_{ftsm} < a_{21}^{-1}d_0/2$ . The purpose of inducing the area  $\Gamma$  is to design a control strategy in the following Theorem to increase the convergence speed of the error  $e_{1ftsm}$ , when it is outside  $\Gamma$ .

**Theorem 8.** *The error subsystem (4.14) will converge to zero asymptotically, if the control is given by*

$$v_{1ftsm}(t) = \Pi_{-\sigma, \sigma}(s_{ftsm}(t)) \left( 1 - \Pi_{-(a_{21}^{-1}d_0 + \varepsilon_{ftsm}), a_{21}^{-1}d_0 + \varepsilon_{ftsm}}(\hat{x}_{ftsm}(t) - a_{21}^{-1}v_{ftsm}^{2n}(t)) \right) v_{ftsm}^{1a}(t) \quad (4.23)$$

$$v_{ftsm}^{1a}(t) = -k_a \operatorname{sgn} \left( \hat{x}_{ftsm}(t) - a_{21}^{-1}v_{ftsm}^{2n}(t) \right) \quad (4.24)$$

where  $k_a = a_{11}\bar{w} + \eta_{1ftsm}$ ,  $\bar{w}$  is a constant in (3.1)–(3.3),  $\eta_{1ftsm} > 0$  is a constant,  $\sigma$  is a constant used to justify the error system (4.15) to reach  $s = 0$ ,  $\Pi_{-\Delta, \Delta}(z)$  is a boxcar function expressed by

$$\Pi_{-\Delta, \Delta}(z) = \begin{cases} 1 & |z| \leq \Delta \\ 0 & |z| > \Delta \end{cases} \quad (4.25)$$

*Proof.* The whole state space of  $e_{1ftsm}$  and  $e_{2ftsm}$  can be divided into two different areas  $\Omega_1$  and  $\Omega_2$ , defined as  $\Omega_1 = \{(e_{ftsm}^1, e_{ftsm}^2) : |s_{ftsm}| > \sigma\}$  and  $\Omega_2 = \{(e_{ftsm}^1, e_{ftsm}^2) : |s_{ftsm}| \leq \sigma\}$  where  $\sigma > 0$  is defined in (4.24).

When the system states  $(e_{1ftsm}, e_{2ftsm})$  are in  $\Omega_1$ , the boxcar function  $\Pi_{-\sigma, \sigma}(s_{ftsm}) = 0$ , and then  $v_{1ftsm}(t)$  in (4.23) is equal to zero, which means that the second error system (4.15)

has not reached to the sliding manifold  $s_{ftsm}(t) = 0$ . In this case, the control (4.23) has not been applied in the first error subsystem (4.14).

The second error subsystem (4.15) will move toward the sliding manifold  $s_{ftsm} = 0$  under the control (4.18)–(4.19), once reaches to  $s = 0$ , the system states  $(e_{1ftsm}, e_{2ftsm})$  enter into the area  $\Omega_2 = \{(e_{1ftsm}, e_{2ftsm}) : |s_{ftsm}| \leq \sigma\}$ . When  $\sigma \rightarrow 0$ , an ideal sliding-mode motion appears, i.e.  $s_{ftsm} = 0$  for all  $(e_{1ftsm}, e_{2ftsm}) \in \Omega_2$ .  $\sigma$  is selected as a small constant for practical implementation.

When the second error system reaches and stays on the sliding manifold,  $s_{ftsm}(t) = 0$ , under the control in Theorem 7, it follows from (4.21) that

$$s_{ftsm}(t) = a_{21}e_{1ftsm}(t) - a_{21}\hat{x}_{ftsm}(t) + v_{ftsm}^{2n}(t) - d(t) = 0 \quad (4.26)$$

Let

$$\tilde{e}_{1ftsm}(t) = e_{1ftsm}(t) - a_{21}^{-1}d(t) \quad (4.27)$$

Considering (4.26), it follows from the above that

$$\tilde{e}_{1ftsm}(t) = \hat{x}_{ftsm}(t) - a_{21}^{-1}v_{ftsm}^{2n}(t) \quad (4.28)$$

When the system state  $e_{1ftsm}(t)$  is outside  $\Gamma$  (4.22) the control (4.23) can be rewritten as

$$v_{1ftsm}(t) = -k_a \text{sgn} \left( \hat{x}_{ftsm}(t) - a_{21}^{-1}v_{ftsm}^{2n}(t) \right) \quad (4.29)$$

Within the area  $\Gamma$  (4.22), we have



$$\text{sgn}(\tilde{e}_{1ftsm}(t)) = \text{sgn}(e_{1ftsm}(t)) \quad (4.30)$$

substituting (4.28) and (4.22) into (4.29) gives

$$v_{1ftsm}(t) = -k_a \text{sgn}(e_{1ftsm}(t)) \quad (4.31)$$

further substituting (4.23) into (4.14) yields

$$\dot{e}_{1ftsm}(t) = -a_{11}e_{1ftsm}(t) - a_{11}e_{1ftsm}(t - \tau(t)) - k_a \text{sgn}(e_{1ftsm}(t))$$

Consider a candidate Lyapunov function  $V_{2ftsm}(t) = 0.5e_{1ftsm}(t)e_{1ftsm}(t)$ . Taking the derivative of  $V_{2ftsm}(t)$  it follows that

$$\begin{aligned} \dot{V}_{2ftsm} &= e_{1ftsm}(t)\dot{e}_{1ftsm}(t) = -a_{11}(e_{1ftsm}(t))^2 - a_{11}e_{1ftsm}(t - \tau(t))e_{1ftsm}(t) - k_a |e_{1ftsm}(t)| \\ &\leq |a_{11}| |e_{1ftsm}(t - \tau(t))| |e_{1ftsm}(t)| - k_a |e_{1ftsm}(t)| \\ &\leq -(k_a - |a_{11}| |e_{1ftsm}(t - \tau(t))|) |e_{1ftsm}(t)| \\ &\leq -\eta_{1ftsm} |e_{1ftsm}(t)| < 0, \quad \text{for } |e_{1ftsm}(t)| \neq 0 \end{aligned}$$

which means that  $e_{1ftsm}$  outside  $\Gamma$  must converge into  $\Gamma$ .

Once the system state  $e_{1ftsm}$  enters into the area  $\Gamma$ , the control (4.23) becomes  $v_{1ftsm}(t) =$

0 and the system (4.14) is rewritten as

$$\dot{e}_{1fism}(t) = -a_{11}e_{1fism}(t) - a_{11}e_{1fism}(t - \tau(t)) \quad (4.32)$$

To prove the stability of the system (4.32), consider the Lyapunov function [267] as

$$\begin{aligned} V_{fism}^3 = & g(e_{1fism})^2(t) + h_1 \int_{t-T_p}^t (e_{1fism})^2(s)ds + h_2 \int_{t-(\bar{q}/C+T_p)}^t (e_{1fism})^2(s)ds \quad (4.33) \\ & + h_3 \int_{t-\tau(t)}^t (e_{1fism})^2(s)ds + \int_{-(\bar{q}/C+T_p)}^0 \int_{t+\theta}^t z_1(\dot{e}_{1fism})^2(s)d\theta \\ & + \int_{-(\bar{q}/C+T_p)}^{-T_p} \int_{t+\theta}^t z_2(\dot{e}_{1fism})^2(s)d\theta \end{aligned}$$

where  $g, h_i$ , for  $i = 1, 2, 3$  and  $z_j$ , for  $j = 1, 2$ , are all positive constants to be determined.

Assume  $m_i, n_i, s_i \in \mathbb{R}$ ,  $i = 1, 2$ . Based on Leibniz-Newton formula, the error variable  $e_{1fism}$  satisfies the following equations:

$$2[n_1 e_{1fism}(t) + n_2 e_{1fism}(t - \tau(t))] \left[ e_{1fism}(t) - e_{1fism}(t - \tau(t)) - \int_{t-\tau(t)}^t \dot{e}_{1fism}(s)ds \right] = 0 \quad (4.34)$$

$$2[s_1 e_{1fism}(t) + s_2 e_{1fism}(t - \tau(t))] \left[ e_{1fism}(t - \tau(t)) - e_{1fism}(t - \tau_2) - \int_{t-\tau_2}^{t-\tau(t)} \dot{e}_{1fism}(s)ds \right] = 0 \quad (4.35)$$

$$2[m_1 e_{1fism}(t) + m_2 e_{1fism}(t - \tau(t))] \left[ e_{1fism}(t - \tau_1) - e_{1fism}(t - \tau(t)) - \int_{t-\tau(t)}^{t-\tau_1} \dot{e}_{1fism}(s)ds \right] = 0 \quad (4.36)$$

$$-\int_{t-\tau_2}^t z_1(\dot{e}_{1ftsm})^2(s)ds = -\int_{t-\tau(t)}^t z_1(\dot{e}_{1ftsm})^2(s)ds - \int_{t-\tau_2}^{t-\tau(t)} z_1(\dot{e}_{1ftsm})^2(s)ds \quad (4.37)$$

$$-\int_{t-\tau_2}^{t-\tau_1} z_2(\dot{e}_{1ftsm})^2(s)ds = -\int_{t-\tau_2}^{t-\tau(t)} z_2(\dot{e}_{1ftsm})^2(s)ds - \int_{t-\tau(t)}^{t-\tau_1} z_2(\dot{e}_{1ftsm})^2(s)ds \quad (4.38)$$

Differentiating  $V_{ftsm}^3(t)$  in (4.33) with respect to time  $t$  along the error subsystem (4.32) gives

$$\begin{aligned} \dot{V}_3 = & 2ge_{1ftsm}(t)\dot{e}_{1ftsm}(t) + h_1(e_{1ftsm}^2(t) - (e_{1ftsm})^2(t - T_p)) + h_2((e_{1ftsm})^2(t) \\ & - (e_{1ftsm})^2(t - (\bar{q}/C + T_p))) + h_3(e_{1ftsm})^2(t) - (1 - \dot{\tau}(t))h_3(e_{1ftsm})^2(t - \tau(t)) \\ & + (\bar{q}/C + T_p)z_1(\dot{e}_{1ftsm})^2(t) - z_1 \int_{t-(\bar{q}/C+T_p)}^t (\dot{e}_{1ftsm})^2(s)ds \\ & + \frac{\bar{q}}{C}z_2(\dot{e}_{1ftsm})^2(t) - \int_{t-(\bar{q}/C+T_p)}^{t-T_p} z_2(\dot{e}_{1ftsm})^2(s)ds \end{aligned} \quad (4.39)$$

Adding the left side of Eqs. (4.34)–(4.36) to the above yields

$$\begin{aligned} \dot{V}_3 \leq & 2ge_{1ftsm}(t)\dot{e}_{1ftsm}(t) + \sum_{i=1}^3 h_i(e_{1ftsm})^2(t) - h_1(e_{1ftsm})^2(t - T_p) - h_2(e_{1ftsm})^2(t - (\bar{q}/C + T_p)) \\ & - (1 - \mu)h_3(e_{1ftsm})^2(t - \tau(t)) + \left[ z_1(\bar{q}/C + T_p) + \frac{\bar{q}}{C}z_2 \right] (\dot{e}_{1ftsm})^2(t) \\ & - \int_{t-\tau(t)}^t z_1(\dot{e}_{1ftsm})^2(s)ds - \int_{t-(\bar{q}/C+T_p)}^{t-\tau(t)} (z_1 + z_2)(\dot{e}_{1ftsm})^2(s)ds - \int_{t-\tau(t)}^{t-T_p} z_2(\dot{e}_{1ftsm})^2(s)ds \\ & + 2(n_1e_{1ftsm}(t) + n_2e_{1ftsm}(t - \tau(t))) \left[ e_{1ftsm}(t) - e_{1ftsm}(t - \tau(t)) - \int_{t-\tau(t)}^t (\dot{e}_{1ftsm})(s)ds \right] \\ & + 2(s_1e_{1ftsm}(t) + s_2e_{1ftsm}(t - \tau(t))) \left[ e_{1ftsm}(t) - e_{1ftsm}(t - (\bar{q}/C + T_p)) \right. \\ & \left. - \int_{t-(\bar{q}/C+T_p)}^{t-\tau(t)} \dot{e}_{1ftsm}(s)ds \right] + 2(m_1e_{1ftsm}(t) + m_2e_{1ftsm}(t - \tau(t))) \left[ e_{1ftsm}(t - T_p) \right. \\ & \left. - e_{1ftsm}(t - \tau(t)) - \int_{t-\tau(t)}^{t-T_p} \dot{e}_{1ftsm}(s)ds \right] \end{aligned}$$

Substituting (4.37) and (4.38) into the above inequality yields

$$\begin{aligned}
 \dot{V}_3 \leq & \mathbf{X}^T [\Phi + A((\bar{q}/C + T_p)z_1 + \frac{\bar{q}}{C}z_2)A^T \\
 & + (\bar{q}/C + T_p)Nz_1^{-1}N^T + \frac{\bar{q}}{C}S(z_1 + z_2)^{-1}S^T + \frac{\bar{q}}{C}Mz_2^{-1}M^T] \mathbf{X} \\
 & - \int_{t-(\bar{q}/C+T_p)}^{t-\tau(t)} (z_1 + z_2)^{-1} [\mathbf{X}^T S + \dot{e}_{1ftsm}(s)(z_1 + z_2)] \\
 & \times [S^T \mathbf{X} + (z_1 + z_2)\dot{e}_{1ftsm}(s)] ds \\
 & - \int_{t-\tau(t)}^t z_1^{-1} [\mathbf{X}^T N + \dot{e}_{1ftsm}(s)z_1] [N^T \mathbf{X} + z_1\dot{e}_{1ftsm}(s)] ds \\
 & - \int_{t-\tau(t)}^{t-T_p} z_2^{-1} [\mathbf{X}^T M + \dot{e}_{1ftsm}(s)z_2] [M^T \mathbf{X} + z_2\dot{e}_{1ftsm}(s)] ds
 \end{aligned} \tag{4.40}$$

where

$$\mathbf{X} = \begin{bmatrix} e_{1ftsm}(t) \\ e_{1ftsm}(t - \tau(t)) \\ e_{1ftsm}(t - T_p) \\ e_{1ftsm}(t - (\bar{q}/C + T_p)) \end{bmatrix}, \quad \Phi = \begin{bmatrix} \phi_{11} & \phi_{12} & m_1 & -s_1 \\ * & \phi_{22} & m_2 & -s_2 \\ * & * & -q_1 & 0 \\ * & * & * & -q_2 \end{bmatrix}$$

$$N = \begin{bmatrix} n_1 \\ n_2 \\ 0 \\ 0 \end{bmatrix}, \quad S = \begin{bmatrix} s_1 \\ s_2 \\ 0 \\ 0 \end{bmatrix}, \quad M = \begin{bmatrix} m_1 \\ m_2 \\ 0 \\ 0 \end{bmatrix}, \quad \text{and } A = \begin{bmatrix} -a_{11} \\ -a_{11} \\ 0 \\ 0 \end{bmatrix}.$$

where  $\phi_{11} = -2ga_{11} + h_1 + h_2 + h_3 + 2n_1$ ,  $\phi_{12} = -2ga_{11} + n_2 - n_1 + s_1 - m_1$ ,  $\phi_{22} = -(1 - \mu)h_3 + 2s_2 - 2n_2 - 2m_2$ , and  $*$  denotes the symmetric terms in the symmetric matrix. Both  $z_1$  and  $z_2$  are positive constants, so the last three terms in (4.40) are all negative. From the LMI in Lemma 2, we have the inequality:  $\mathbf{X} + A((\bar{q}/C + T_p)Z_1 + \frac{\bar{q}}{C}Z_2)A^T + (\bar{q}/C +$

$T_p)Nz_1^{-1}N^T + (\bar{q}/C + T_p)S(z_1 + z_1)^{-1} + (\bar{q}/C + T_p)Mz_2^{-1}M^T < 0$ , then  $\dot{V}_{ftsm}^3 < \gamma|e_{1ftsm}(t)|^2$  for a sufficient small  $\gamma > 0$ , which ensures the asymptotic stability of the error system (4.32), i.e. the error state  $e_{1ftsm}(t)$  in system (4.32) will converge to zero asymptotically. This complete the proof.

**Remark 2.** In (4.23),  $\sigma$  is a constant used for the box function. In ideal condition,  $\sigma = 0$ , i.e. we can detect the ideal sliding-mode  $s = 0$ . But in practical environments, detecting ideal  $s_{ftsm} = 0$  is not possible. So we can just only detect an area near zero,  $|s_{ftsm}| < \sigma$ . In this case, from (4.21) we have  $a_{21}e_{1ftsm}(t) - d(t) = a_{21}\hat{x}_{ftsm}(t) - v_{ftsm}^{2n}(t) + s_{ftsm}$ , where  $|s_{ftsm}| < \sigma$ . Hence we can chose  $\sigma$  as  $\sigma = \kappa |a_{21}\hat{x}_{ftsm}(t) - v_{ftsm}^{2n}(t)|$ , where  $\kappa = 0.02 - 0.05$ . It should be noted that  $\sigma$  can affect only the convergence speed in dynamical process, but cannot affect the precision and effect of the final observation.

**Theorem 9.** If the two controls in the error system (4.14) and (4.15) are designed using Theorems 7 and 8 respectively, the estimation error  $e_{1ftsm}(t)$  converges to zero asymptotically, and the additional traffic dynamics  $d(t)$  in (3.17) and (3.18) can be estimated as

$$\hat{d}(t) = \lim_{\substack{e_{1ftsm}(t) \rightarrow 0 \\ e_{2ftsm}(t) \rightarrow 0}} v_{2ftsm}(t) \quad (4.41)$$

where  $v_{2ftsm}(t)$  is the control signal defined in (4.18).

From Theorem 8, the error state  $e_{1ftsm}(t)$  under the control (4.23) will converge to zero asymptotically. Then Eq.(4.41) can be obtained from the above equation. In other words, the additional traffic dynamics  $d(t)$  can be estimated directly by the smooth control signal  $v_{2ftsm}(t)$  in (4.18) when the error state  $e_{1ftsm}(t)$  converges to zero asymptotically. This completes the proof.  $\square$

A real-time full-order terminal sliding observer is developed for traffic monitoring for RNT0 applications. First, for a class of systems (4.1) where the system state  $x_2$  is unmea-

surable, the novel full-order terminal sliding mode observer (4.2) and (4.3) are investigated. Second, the estimation error of the queue length  $e_{1fism}$  is converged to zero in a finite-time  $t_{fism}^s$  in Theorem 7, which guarantees the fast time response in traffic monitoring. Third, a novel control strategy in (4.23) and (4.24) is developed to speed up the convergence of the internal dynamics in (4.14) by using the finite-time stability theory, which accelerate the convergence speed of state estimation to meet the real-time requirement in RNTTO. Fourth, a smooth control signal in (4.18) to (4.20) of the full-order terminal sliding observer is proposed to directly monitor the dynamics of ATF as in (4.41) without any low-pass filter, which can cause a phase lag, thereby result in a long response time and decreasing the accuracy in state estimations.

## 4.4 Simulation

To validate the proposed RNTTO algorithms and quantify its performances, simulations via the Network Simulator II are performed and comparative results are presented in this section.

### 4.4.1 Model Description

A typical star type TCP/IP network model, as shown in Fig. 3.2, is applied in the simulation. It consists of a number of hosts and clients with one network router. The parameters of the TCP/IP network model and the designed observer are given below.

*Simulation model of router-based networks:* The network simulator NS-II is used to study the fast dynamic performance of the proposed FTSMO for RNTTO applications. The network scenario in Fig. 3.2 is constructed via NS-II. There are 60 hosts and 60 clients connected via the network router. The output link capacity  $C$  of the router is set to be 15 Mb. The connections between each host/client and the router use full-duplex that construct

bidirectional links at propagation delay  $T_p = 200 \text{ ms}$ . The maximum Cwnd  $\bar{w}$  is set to be  $0.12 \text{ Mb}$ . The packet size is set to be  $500 \text{ bytes}$ . The PI-AQM algorithm is used [125] to regulate the QL at desired level  $q_0 = 175 \text{ packets}$ . The buffer capacity  $\bar{q}$  is set to be  $800 \text{ packets}$ .

According to the aforementioned network configurations, the parameters in the linearised TCP/IP network model (3.17) and (3.18) can be determined as follows:  $a_{11} = 0.2630$ ,  $a_{12} = 0.0044$ ,  $b_d = 481.7708$ ,  $a_{21} = 243.2432$ , and  $a_{22} = 4.0541$ .

*Observer design:* To show the effectiveness of the proposed method, the LO [45] is employed for comparative studies. The parameters of LO are set as:  $L_1 = -5$  and  $L_2 = -32$ . Moreover, the parameters of SMO are designed using Theorems 4 are:  $c_{sm} = 20$  and  $k_{sm} = 1600$ . In addition, the parameters of STO are designed using Theorems 5 are:  $k_{st}^1 = 100$  and  $k_{st}^2 = 1600$ . Furthermore, the parameters of the proposed TSMO are designed using Theorems 7 and 8 are:  $\alpha_{ftsm} = 15$ ,  $\beta_{ftsm} = 5$ ,  $p_{ftsm} = 5$ ,  $q_{ftsm} = 3$ ,  $k_{1ftsm} = 1600$  and  $k_{2ftsm} = 7.5$ .

To evaluate the performances of the proposed observer, the external traffic served by both CBR and VBR are considered. The following three different scenarios are considered.

- **Scenario 1 (constant rate traffics):** three source nodes generate constant rate traffics. The “cbr” applications are invoked and attached to the “udp” agents. The sending rate of each agent is set as  $500 \text{ packets/s}$  between the period  $50 - 150\text{s}$ . The simulation time is  $200 \text{ seconds}$ .
- **Scenario 2 (variable rate traffics):** three source nodes generate variable rate traffics. The “vbr” applications are designed as ramp traffic and attached to the “udp” agents. The sending rate of each agent is set as rising slope up to  $500 \text{ packets/s}$  between the period  $50 - 150\text{s}$ . The simulation time is  $200 \text{ seconds}$ .
- **Scenario 3 (hybrid traffic rates):** three source nodes randomly generate constant and

Table 4.1 Comparative studies of LO, SMO, STO and FTSMO in Scenario 1.

|                        | LO      | SMO        | STO        | FTSMO   |
|------------------------|---------|------------|------------|---------|
| $t^r$                  | /       | 4.2        | 2.5        | 2.1     |
| $t^s$                  | /       | Asymptotic | Asymptotic | 2.2     |
| Mean of $e_{1ftsm}(t)$ | 1.05    | 1.05       | 1.05       | 0.49    |
| STD of $e_{1ftsm}(t)$  | 2.45    | 2.45       | 2.45       | 2.12    |
| Mean of $e_{2ftsm}(t)$ | -12.62  | 11.07      | 2.65       | 0.16    |
| STD of $e_{2ftsm}(t)$  | 33.21   | 53.32      | 53.60      | 16.13   |
| Mean of $e_d$          | -749.63 | -719.04    | -331.30    | -205.61 |
| STD of $e_d$           | 750.19  | 559.68     | 370.15     | 255.66  |

Table 4.2 Comparative studies of LO, SMO, STO and FTSMO in Scenario 2.

|                        | LO      | SMO        | STO        | FTSMO   |
|------------------------|---------|------------|------------|---------|
| $t^r$                  | /       | 4.2        | 2.5        | 2.1     |
| $t^s$                  | /       | Asymptotic | Asymptotic | 2.2     |
| Mean of $e_{1ftsm}(t)$ | 1.97    | 1.97       | 1.97       | 0.73    |
| STD of $e_{1ftsm}(t)$  | 2.15    | 2.15       | 2.15       | 2.16    |
| Mean of $e_{2ftsm}(t)$ | 6.36    | 35.36      | 3.26       | 0.50    |
| STD of $e_{2ftsm}(t)$  | 21.68   | 48.03      | 50.56      | 14.44   |
| Mean of $e_d$          | -749.63 | -1092.28   | -562.18    | -267.51 |
| STD of $e_d$           | 750.19  | 616.56     | 267.61     | 273.54  |

variable rate traffics. This case is the mixture of Scenarios 1 and 2. The simulation time is 1000 *seconds*.

#### 4.4.2 Simulation Results and Discussion

Figs. 4.1 and 4.2 depict the states of the proposed TSMO corresponding to the scenarios 1 and 2. As shown in Figs. 4.1a and 4.2a, the queue lengths are regulated at the desired value by AQM in both scenarios. By the proposed FTSMO algorithms, the unknown traffic behaviour i.e., the ACwnd and the dynamics of ATF are accurately estimated. It can be seen from Figs. 4.1e and 4.2e that the estimation error  $e_{2ftsm}(t)$  in error subsystem (4.15) is demonstrated converging to zero in a finite-time. The control signals  $v_{1ftsm}(t)$  in (4.23) are shown in Figs. 4.1f and 4.2f. Due to the proposed control strategy for  $e_{1ftsm}(t)$  in system



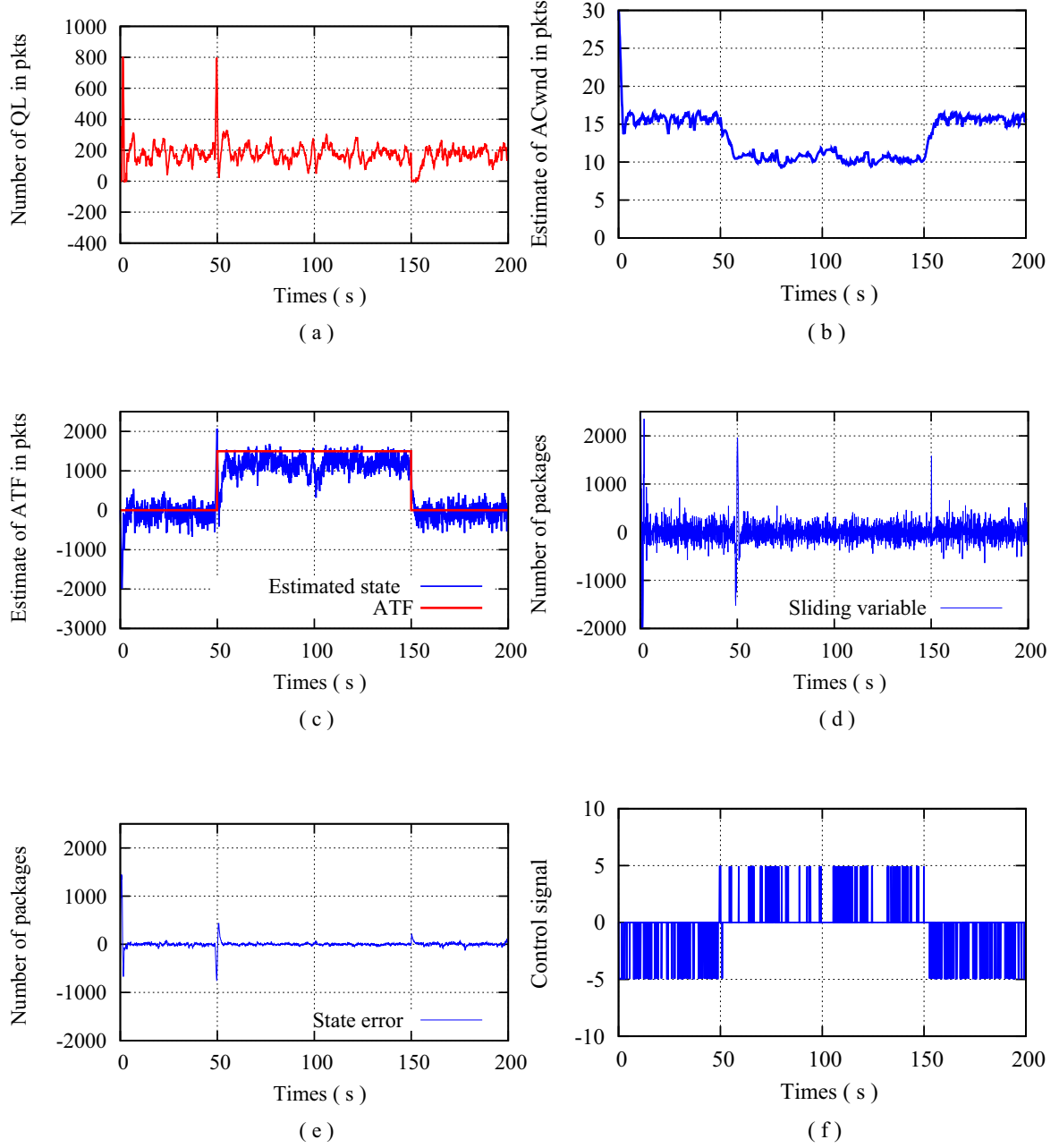


Fig. 4.1 State and control of the proposed FTSMO in Scenario 1. : (a) The number of QL  $q(t)$  in router buffer. (b) Estimated ACwnd  $w(t)$  in *packets* at the router. (c) Estimated dynamics of ATF  $d(t)$  and the true DDoS flooding rate. (d) The value of the sliding variable  $s_{ftsm}(t)$  in *packets*. (e) Estimation error  $e_{2ftsm}(t)$  in *packets*. (f) Control signal of  $v_{1ftsm}(t)$ .

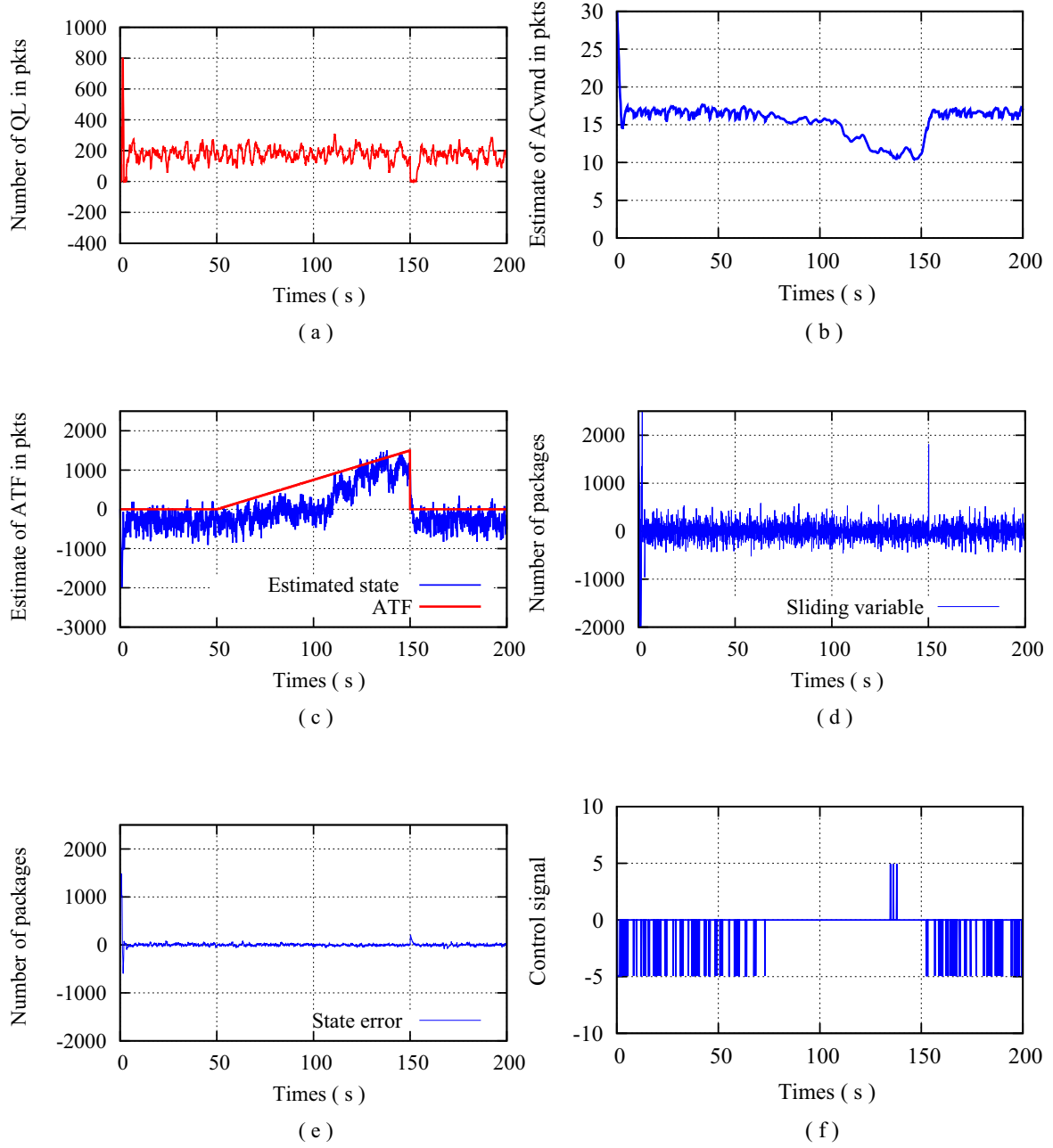


Fig. 4.2 State and control of the proposed FTSMO in Scenario 2.: (a) The number of QL  $q(t)$  in router buffer. (b) Estimated ACwnd  $w(t)$  in *packets* at the router. (c) Estimated dynamics of ATF  $d(t)$  and the true DDoS flooding rate. (d) The value of the sliding variable  $s_{ftsm}(t)$  in *packets*. (e) Estimation error  $e_{2ftsm}(t)$  in *packets*. (f) Control signal of  $v_{1ftsm}(t)$ .

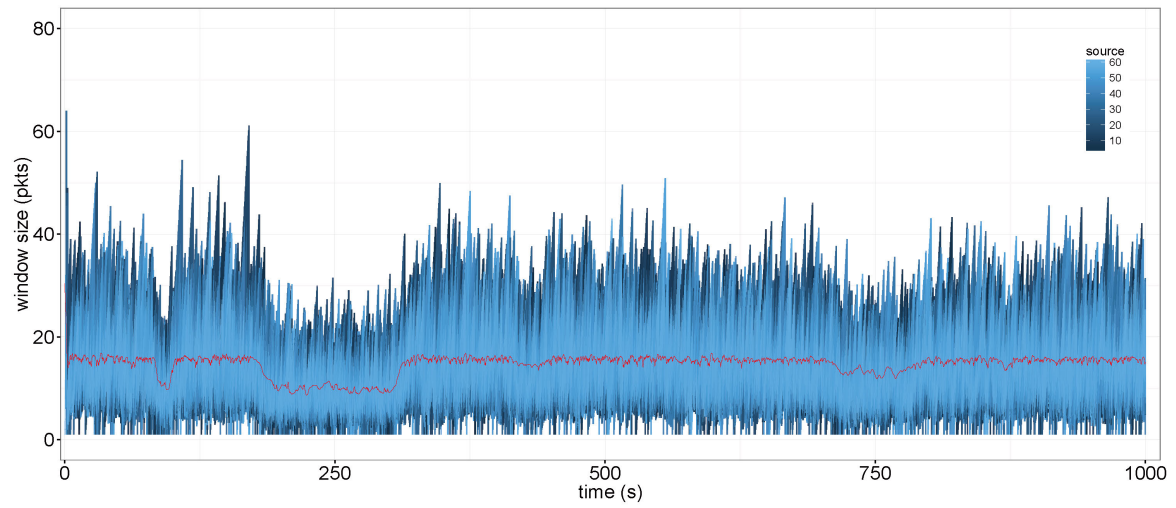


Fig. 4.3 The estimated ACwnd by the proposed FTSMO algorithm in Scenario 3.

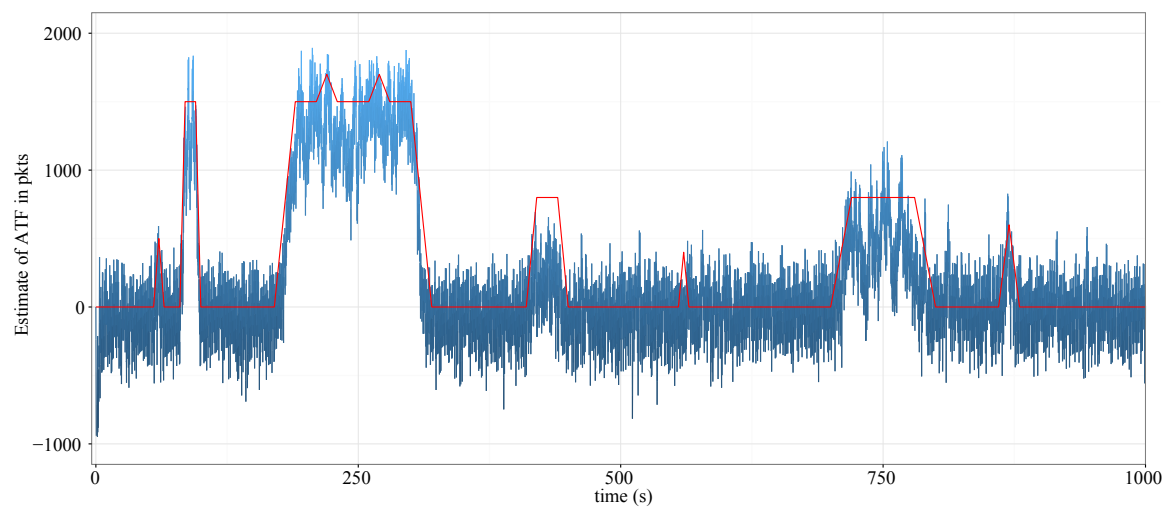


Fig. 4.4 The estimated dynamics of ATF by the proposed FTSMO algorithm in Scenario 3.

(4.14), the state  $w(t)$  and  $d(t)$  are quickly and accurately estimated as presented in Figs. 4.1b, 4.2b, 4.1c and 4.2c respectively. The estimation of the ACwnd presents a degradation of throughputs in hosts and link's availability in the TCP/IP network.

From the comparative results in Tables 4.1 and 4.2 corresponding to the scenarios 1 and 2, the proposed TSMO has the fastest dynamical response and the best steady-state accuracies of estimating  $w(t)$  and  $d(t)$  among the aforementioned observers. By the proposed novel control strategy  $v_{1ftsm}(t)$  in (4.23) in the FTSMO, the estimation error of ACwnd, i.e.,  $e_{1ftsm}(t)$ , is converged within a defined area and featuring the best performance in accuracy and convergent time as illustrated in the tables.

The simulation results of the proposed TSMO in scenario 3 are shown in Figs. 4.3 and 4.4. The instantaneous Cwnd size  $w_i(t)$ , for  $i = 1, 2, \dots, 60$ , at the host are all presented. As the  $w_i(t)$  is available at its source node but cannot be obtained at the router level, the estimated  $w(t)$  is the average value of the instantaneous Cwnd size in all the connected hosts, which accurately reflect the serious degradations in sending rate, throughput and bandwidth utilization in the TCP/IP networks. As depicted in Fig. 4.4, the dynamics of ATF  $d(t)$  generated by the random CBR and VBR traffics is quickly and accurately estimated.

## 4.5 Summary

In this chapter, a full-order terminal sliding mode observation strategy has been investigated for RNTD applications, where the estimation error is forced to maintain on the full-order terminal sliding surface and converge to zero in a finite-time. Then, the novel control strategy has been developed to accelerate the convergence rate of internal dynamics of the error system by using the finite-time stability theory to meet the real-time requirements. Furthermore, the full-order control laws of the proposed observation algorithm have been designed as a continuous signal that is adopted to estimate the dynamics of ATF for anomaly detection. The contributions have filled the gaps in present literature, which mainly proposes the

---

real-time fast dynamic router-based network traffic observation schemes.



# Chapter 5

## Event-triggered Sliding Mode Observation Strategy

### 5.1 Introduction

The algorithm efficiency is another key issue that widely exists in the RNT0. As aforementioned in the literature, the microprocessor of network routers dealing with a variety of tasks include forwarding packets in communication schemes, monitoring physical quantities, and computation of feedback control laws of RNT0 in real-time periodically scheduling algorithms, which cause high consumptions on the computational capacity. In addition, the real-time RNT0 for large amount traffic data can cause high occupations on the memory space. Moreover, the high occupation on resource of communication channel and the bandwidth of the link output is another outstanding issue that impedes the progress of RNT0.

To reduce the computation load and the resource occupations in traffic monitoring, an event-triggered based sliding mode observer is proposed for algorithm-efficient RNT0. The key issue of the event-triggered control law of the sliding mode observer is presented. Specifically, the event-driven control law is required to be smooth that is directly used for estimating the dynamics of ATF in **Section 5.2**. In this work, the control strategy under

the event-triggered environment is formulated in an event-driven scheme instead of that in time-driven process to reduce the number of computation in **Section 5.3**. The simulations based on Network Simulator II demonstrate the effectiveness and good performance of the proposed algorithms in **Section 5.4**. Finally, the conclusions are made in **Section 5.5**.

## 5.2 Problem Formulation

Considering the linearised system in (3.17) and (3.18), the conventional SMO can be designed as in (3.20) and (3.21).

The switching hyperplanes can be designed as

$$s(t) = ce_{sm}^2(t) = 0 \quad (5.1)$$

where  $c > 0$  is a constant. The control input  $v(t)$  is designed to make the manifold  $s(t) = 0$  reached in finite time and remains in it forever. This means that in sliding, the system satisfies  $s(t) = ce_{sm}^2(t) = 0$  and  $\dot{s}(t) = 0$ , and the system exhibits invariance properties, yielding motion independent of certain parameter variations and disturbances.

The control law is given by

$$v(t) = -k \operatorname{sgn}(s(t)) \quad (5.2)$$

where  $k = a_{21}\bar{w} + d_0 + \eta$ ,  $\eta > 0$  is a constant,  $\bar{w}$  and  $d_0$  both are known constants defined in system (3.1) to (3.3).

In practice, modern control systems are implemented by digital computers. Traditionally, time-triggered control method is utilized with a fixed rate, such as periodic inter-execution times. However, it is impossible to apply time-triggered control in continuous manner due to limited bandwidth, processor speed, etc.



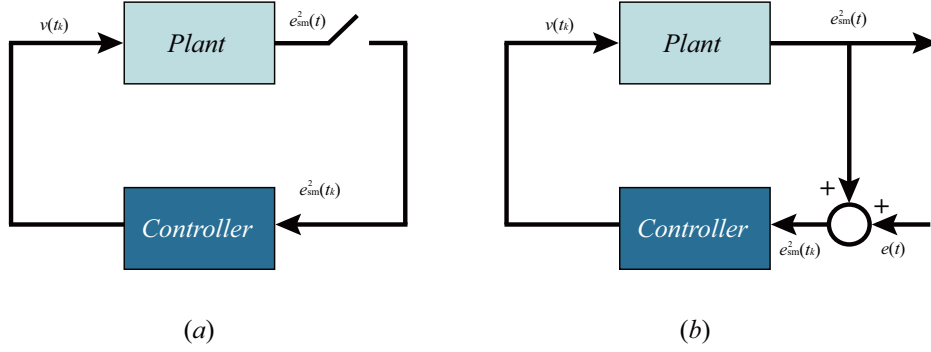


Fig. 5.1 Event-triggering framework. (a) System model with event-triggered sampling of error system states  $e_{sm}^2(t)$ ; (b) the model where the event-triggering induced error is represented as an external input  $e(t)$ .

As an alternative to periodic sampled-data control, aperiodic sampled-data control is executed after the occurrence of an event rather than after the elapse of a certain amount of time as shown in Fig. 5.1. This leads to aperiodic times of the inter-execution, which may be useful for some cases. This control strategy has been applied in many real systems where resources are scarce, such as in networked control system, wireless sensor networks and embedded systems. Under the aperiodic sampled-data environment, control law (5.2) can be rewritten as [270]

$$v(t) = -k \operatorname{sgn}(s(t_k)) |e_{sm}^2(t_k)|, \quad t \in [t_k, t_{k+1}), \quad (5.3)$$

with sliding variable  $s(t_k) = ce_{sm}^2(t_k)$  at  $t_k$ . Control law (5.3) updated again at time  $t_{k+1}$  and remains unchanged till the next trigger execution. We introduce the state error of the system as

$$e(t) = e_{sm}^2(t_k) - e_{sm}^2(t), \quad \forall t \in [t_k, t_{k+1}) \quad (5.4)$$

The state error  $e(t)$  plays an important role in the design of the sliding mode controller. Since the control is only updated at the event instant, for  $t = t_k$ ,  $e(t_k) = e_{sm}^2(t_k) - e_{sm}^2(t_k) = 0$ , the

sliding mode will occur at this moment. For  $t \in (t_k, t_{k+1})$ ,  $e(t) \neq 0$ , then the sliding variable will deviate from the sliding manifold.

The estimation of the disturbance  $d(t)$  in (3.18) can be estimated using (3.30). In this condition, the control law in (5.3) includes a sign function under the event triggered scheme, which is directly used to estimate the dynamics of ATF, i.e.,  $d(t)$ . Therefore, the low-pass filter is required to attenuates signals with frequencies, which result in a long response time and inaccuracy in traffic estimation. The issue of the smooth control law in event-triggered sliding mode observer is required to be solved for RNT0 applications.

### 5.3 Event-triggered Full-order Sliding Mode Based RNT0

The event triggered sliding-mode observer (ETSMO) for the system (3.17) and (3.18) is proposed in the following structure by

$$\dot{\hat{x}}_{et}(t) = -a_{11}\hat{x}_{et}(t) - a_{11}\hat{x}_{et}(t - \tau(t)) - a_{12}y(t) + a_{12}y(t - \tau(t)) - b_d u(t - \tau(t)) \quad (5.5)$$

$$\dot{\hat{y}}_{et}(t) = a_{21}\hat{x}_{et}(t) - a_{22}\hat{y}_{et}(t) + v_{et}(t) \quad (5.6)$$

where  $\hat{x}_{et}(t)$  and  $\hat{y}_{et}(t)$  represent the estimates in ETSMO for the system state  $x(t)$  and output  $y(t)$  respectively.  $v_{et}(t)$  is the control signal for the ETSMO, which will be designed later.

It is assumed that the control signal of the observer  $v_{et}(t)$  in system (5.5) and (5.6) cannot be infinite and is bounded by satisfying the following condition:

$$T_{et} |v_{et}(t)| \leq \chi_{et} \quad (5.7)$$

where  $T_{et}$  and  $\chi_{et}$  are both positive constant.

By defining the variables  $e_{1et}(t) = \hat{x}_{et}(t) - x(t)$  and  $e_{2et}(t) = \hat{y}_{et}(t) - y(t)$  as the errors

between the system states and their estimates, hence the error system can be obtained from equations (3.17) to (3.18) and equations (5.5) to (5.6) as follows:

$$\dot{e}_{1et}(t) = -a_{11}e_{1et}(t) - a_{11}e_{1et}(t - \tau(t)) \quad (5.8)$$

$$\dot{e}_{2et}(t) = a_{21}e_{1et}(t) - a_{22}e_{2et}(t) + v_{et}(t) - d(t) \quad (5.9)$$

The aim is to design a sliding-mode control law  $v_{et}$  for the observer system (5.5) and (5.6) to bring the trajectories of the error system (5.8) and (5.9) to a sliding manifold in a finite-time and force to maintain there for all time. In the observation scheme, a full-order sliding-mode strategy is proposed to obtain a smooth control signal, which will be directly used to estimate the additional traffic dynamics, without any low-pass filters.

A full-order sliding mode manifold is designed as

$$s_{et}(t) = \dot{e}_{2et}(t) + c_{et}e_{2et}(t) \quad (5.10)$$

where  $c_{et} = T_{et} + a_{22}$  is a positive constant,  $T_{et} > 0$  is a constant.  $v_{et}(t)$  is developed to make the sliding manifold  $s_{et}(t) = 0$  reached in a finite-time and remains on it thereafter. In practical, The control strategy are applied in the embedded kernel router where resources are scarce. The control strategies are used under the event-triggered environment with the sliding variable  $s_{et}(t_k)$  at time  $t_k$ , where  $t \in [t_k, t_k + 1)$ . The control laws  $v_{et}(t)$  are updated again at time  $t_{k+1}$  and remains the control value unchanged till the next trigger execution.

Define the state errors of the system (5.8) and (5.9) as

$$\phi_{1et}(t) = e_{1et}(t_k) - e_{1et}(t)$$

$$\phi_{2et}(t) = e_{2et}(t_k) - e_{2et}(t)$$

The state errors  $\phi_{1et}(t)$  and  $\phi_{2et}(t)$  are critical in the design of the event-triggered full-

order sliding mode observer.

The control laws are only updated at the event instant, such as the  $t = t_k$ .

(a.) at the time  $t = t_k$ , the state errors  $\phi_{et}^i(t_k) = e_{et}^i(t_k) - e_{et}^i(t_k) = 0$ , for  $i = 1, 2$ , the control laws are updated and applied, hence the sliding mode is occurring at this moment.

(b.) for the time interval  $t \in (t_k, t_{k+1})$ , the state errors  $\phi_{et}^i(t_k) \neq 0$ , for  $i = 1, 2$ , the control laws remain at the value unchanged at time  $t = t_k$ , therefore, the sliding variable will deviate from the sliding manifold.

**Theorem 10.** *If a sliding mode manifold  $s_{et}(t)$  is designed as (5.10) and the control laws are designed as the following structure*

$$\dot{v}_{et}(t) + T_{et}v_{et}(t) = \omega_{et}(t) \quad (5.11)$$

$$\omega_{et}(t) = (c_{et} - a_{22})a_{22}e_{2et}(t_k) - k_{et}\text{sgn}(s(t_k)) - \gamma_{et}\text{sgn}(s(t_k))|e_{2et}(t_k)| \quad (5.12)$$

where  $k_{et} = (c_{et} - a_{22})a_{21}\bar{w} + (c_{et} - a_{22})d_0 + d_1 + \eta_{et}$ ,  $\bar{w}$ ,  $d_0$  and  $d_1$  are constants and defined in (3.1) to (3.3),  $\eta_{et} > 0$  and  $\gamma_{et} > 0$  are constant,  $T_{et}$  is a positive constant and defined in (5.10),  $k \in \mathbb{Z}_+$ ,  $\mathbb{Z}_+$  is the set of non-negative integers, under the event-triggering condition

$$|\phi_{2et}(t)| \leq \frac{\gamma_{et}}{\zeta_{et}} |e_{2et}(t_k)| \quad (5.13)$$

with

$$\zeta_{et} = a_{22}(c_{et} - a_{22}) \quad (5.14)$$

then, the error systems (5.8) and (5.9) will reach  $s_{et}(t) = 0$  from any initial condition  $s_{et}(0) \neq 0$  in a finite-time and converge to zero along  $s_{et}(t) = 0$  asymptotically.

*Proof.* From the error system (5.9), the sliding-mode manifold (5.10) can be reformed as

follows

$$\begin{aligned} s_{et}(t) &= \dot{e}_{2et}(t) + c_{et}e_{2et}(t) \\ &= a_{21}e_{1et}(t) + (c_{et} - a_{22})e_{2et}(t) + v_{et}(t) - d(t) \end{aligned} \quad (5.15)$$

Differentiating the sliding variable  $s_{et}(t)$  in (5.15) with respect to time  $t$  along the error systems (5.8) and (5.9) yields

$$\begin{aligned} \dot{s}_{et}(t) &= a_{21}\dot{e}_{1et}(t) + (c_{et} - a_{22})\dot{e}_{2et}(t) + \dot{v}_{et}(t) - \dot{d}(t) \\ &= a_{21}(-a_{11}e_{1et}(t) - a_{11}e_{1et}(t - \tau(t))) + (c_{et} - a_{22})(a_{21}e_{1et}(t) - a_{22}e_{2et}(t) \\ &\quad + v_{et}(t) - d(t)) + \dot{v}_{et}(t) - \dot{d}(t) \\ &= a_{21}(c_{et} - a_{22} - a_{11})e_{1et}(t) - a_{21}a_{11}e_{1et}(t - \tau(t)) - a_{22}(c_{et} - a_{22})e_{2et}(t) \\ &\quad - (c_{et} - a_{22})d(t) + T_{et}v_{et}(t) + \dot{v}_{et}(t) - \dot{d}(t) \end{aligned}$$

Substituting the control laws (5.11) and (5.12) into the above equation gives

$$\begin{aligned} \dot{s}_{et}(t) &= a_{21}(c_{et} - a_{22} - a_{11})e_{1et}(t) - a_{21}a_{11}e_{1et}(t - \tau(t)) - a_{22}(c_{et} - a_{22})e_{2et}(t) - \dot{d}(t) \\ &\quad - (c_{et} - a_{22})d(t) + (c_{et} - a_{22})a_{22}e_{2et}(t_k) - k_{et}\text{sgn}(s(t_k)) - \gamma_{et}\text{sgn}(s(t_k))|e_{2et}(t_k)| \\ &= a_{21}(c_{et} - a_{22} - a_{11})e_{1et}(t) - a_{21}a_{11}e_{1et}(t - \tau(t)) + a_{22}(c_{et} - a_{22})\phi_{2et}(t) \\ &\quad - (c_{et} - a_{22})d(t) - \dot{d}(t) - k_{et}\text{sgn}(s(t_k)) - \gamma_{et}\text{sgn}(s(t_k))|e_{2et}(t_k)| \end{aligned} \quad (5.16)$$

Consider the following Lyapunov function candidate by

$$V_{et}(t) = \frac{1}{2}s_{2et}^2(t) \quad (5.17)$$

From (5.16), the time derivative of (5.17) can be obtained by

$$\begin{aligned}
\dot{V}_{et}(t) &= s_{et}(t) \dot{s}_{et}(t) = s_{et}(t) a_{21} (c_{et} - a_{22} - a_{11}) e_{1et}(t) - s_{et}(t) a_{11} a_{21} e_{1et}(t - \tau(t)) \\
&\quad + s_{et}(t) a_{22} (c_{et} - a_{22}) \phi_{2et}(t) - s_{et}(t) (c_{et} - a_{22}) d(t) - s_{et}(t) \dot{d}(t) - s_{et}(t) k_{et} \text{sgn}(s(t_k)) \\
&\quad - s_{et}(t) \gamma_{et} \text{sgn}(s(t_k)) |e_{2et}(t_k)| \\
&\leq |s_{et}(t)| |a_{21} (c_{et} - a_{22} - a_{11})| |e_{1et}(t)| + |s_{et}(t)| |a_{11} a_{21}| |e_{1et}(t - \tau(t))| + |s_{et}(t)| |\dot{d}(t)| \\
&\quad + |s_{et}(t)| |(c_{et} - a_{22}) a_{22}| |\phi_{2et}(t)| + |s_{et}(t)| |(c_{et} - a_{22}) d(t)| - s_{et}(t) k_{et} \text{sgn}(s(t_k)) \\
&\quad - s_{et}(t) \gamma_{et} \text{sgn}(s(t_k)) |e_{2et}(t_k)|
\end{aligned}$$

If the trajectories of the error systems (5.8) and (5.9) starting from a region where satisfy  $\text{sgn}(s(t_k)) = \text{sgn}(s(t))$ , then it can be further obtained from the control (5.12) and the above inequality that

$$\begin{aligned}
\dot{V}_{et}(t) &\leq |s_{et}(t)| |a_{21} (c_{et} - a_{22} - a_{11})| |e_{1et}(t)| + |s_{et}(t)| |a_{11} a_{21}| |e_{1et}(t - \tau(t))| + |s_{et}(t)| |\dot{d}(t)| \\
&\quad + |s_{et}(t)| |(c_{et} - a_{22}) a_{22}| |\phi_{2et}(t)| + |s_{et}(t)| |(c_{et} - a_{22}) d(t)| - \gamma_{et} |s_{et}(t)| |e_{2et}(t_k)| \\
&\quad - ((c_{et} - a_{22}) a_{21} \bar{w} + (c_{et} - a_{22}) d_0 + d_1 + \eta_{et}) |s_{et}(t)| \\
&\leq (|a_{21} (c_{et} - a_{22} - a_{11})| |e_{1et}(t)| - (c_{et} - a_{22} - a_{11}) a_{21} \bar{w}) |s_{et}(t)| \\
&\quad + (|a_{11} a_{21}| |e_{1et}(t - \tau(t))| - a_{11} a_{21} \bar{w}) |s_{et}(t)| + (|\dot{d}(t)| - d_1) |s_{et}(t)| \\
&\quad + |s_{et}(t)| |(c_{et} - a_{22}) a_{22}| |\phi_{2et}(t)| + (|(c_{et} - a_{22}) d(t)| - (c_{et} - a_{22}) d_0) |s_{et}(t)| \\
&\quad - \eta_{et} |s_{et}(t)| - \gamma_{et} |s_{et}(t)| |e_{2et}(t_k)|
\end{aligned}$$

From the conditions in (3.19) and (3.11), the above inequality can be further reduced to

$$\begin{aligned}\dot{V}_{et}(t) &\leq |s_{et}(t)| |a_{22}(c_{et} - a_{22})| |\phi_{2et}(t)| - \gamma_{et} |s_{et}(t)| |e_{2et}(t_k)| - \eta_{et} |s_{et}(t)| \\ &\leq (|(c_{et} - a_{22}) a_{22}| |\phi_{2et}(t)| - \gamma_{et} |e_{2et}(t_k)| - \eta_{et}) |s_{et}(t)|\end{aligned}$$

Due to the triggering conditions in (5.13) and (5.14), we have

$$\dot{V}_{et}(t) \leq -\eta_{et} |s_{et}(t)| < 0, \text{ for } s_{et}(t) \neq 0$$

which means that the error system (5.9) will reach to the sliding-mode manifold  $s_{et}(t) = 0$  in a finite-time, i.e.,  $s_{et}(t) = 0, \forall t \geq t_{et}^r$ , as long as  $\text{sgn}(s(t_k)) = \text{sgn}(s(t))$ . This holds for the triggered events at the time  $t = t_k$ , such that  $\text{sgn}(s(t_k)) = \text{sgn}(s(t))$ . Thus, the trajectories can reach within the sliding-mode manifold by the control laws in Theorem 10 and enter the region  $\Omega_{et} = \{s_{et}(t) : \text{sgn}(s_{et}(t)) \neq \text{sgn}(s_{et}(t_k)), t \in (t_k, t_{k+1})\}$ . In this region, the equation  $\text{sgn}(s(t_k)) = \text{sgn}(s(t))$  cannot be hold, while the convergence of the Lyapunov function cannot be guaranteed. Therefore, the trajectories of the error system (5.9) will deviate from the sliding manifold  $s_{et}(t) = 0$  within the region  $\Omega_{et}$ . However, the sliding trajectories are ultimately bounded within this region  $\Omega_{et}$  due to  $\dot{V}_{et}(t) \leq -\eta_{et} |s_{et}(t)| < 0$  outside this region. Therefore, the ultimate band of the deviation of the trajectories is the band of the region  $\Omega_{et}$ . The value of this band can be obtained by getting the maximum deviation of sliding trajectory.

This ultimate region can be obtained by

$$\begin{aligned}|s_{et}(t_k) - s_{et}(t)| &= |\dot{e}_{2et}(t_k) + c_{et} e_{2et}(t_k) - \dot{e}_{2et}(t) - c_{et} e_{2et}(t)| \\ &\leq |\dot{e}_{2et}(t_k) - \dot{e}_{2et}(t)| + |c_{et} e_{2et}(t_k) - c_{et} e_{2et}(t)| \\ &\leq |\dot{\phi}_{2et}(t)| + c_{et} |\phi_{2et}(t)|\end{aligned}\tag{5.18}$$

Consider the growth of the state error  $|\phi_{2et}(t)|$ , as  $\phi_{2et}(t) = e_{2et}(t_k) - e_{2et}(t)$ , it can be obtained that

$$\begin{aligned} |\dot{\phi}_{2et}(t)| &= |\dot{e}_{2et}(t)| \\ &= |a_{21}e_{1et}(t) - a_{22}e_{2et}(t) + v_{et}(t) - d(t)| \end{aligned}$$

From the condition in (5.7) and the relation  $e_{2et}(t) = e_{2et}(t_k) - \phi_{2et}(t)$ , it can be obtained that

$$\begin{aligned} |\dot{\phi}_{2et}(t)| &= |a_{21}e_{1et}(t) - a_{22}e_{2et}(t_k) + a_{22}\phi_{2et}(t) + v_{et}(t) - d(t)| \\ &\leq |a_{21}e_{1et}(t)| + |a_{22}e_{2et}(t_k)| + |a_{22}\phi_{2et}(t)| + |v_{et}(t)| + |d(t)| \\ &\leq a_{22}|e_{2et}(t_k)| + |a_{22}\phi_{2et}(t)| + \rho_{et} \\ &\leq \delta_{et}|e_{2et}(t_k)| + \rho_{et} \end{aligned} \tag{5.19}$$

where  $\delta_{et} = a_{22} + \gamma_{et}/\zeta_{et}$ , and  $\rho_{et} = a_{21}\bar{w} + \chi_{et}/T_{et} + d_0$  both are positive constants.

Thus, from the above inequality and the condition in (5.13), the bound of the region can be reformed as

$$|s(t_k) - s(t)| \leq \sigma_{et}|e_{2et}(t_k)| + \rho_{et} \tag{5.20}$$

where  $\sigma_{et} = a_{22} + (1 + c_{et})\gamma_{et}/\zeta_{et}$ , and  $\rho_{et}$  is defined in (5.19).

This gives the maximum deviation of the sliding-mode manifold (5.10) from the triggered instant at time  $t = t_k$  before the next updated event  $t = t_{k+1}$ . Thus, proof is completed.  $\square$

**Remark 3.** The control laws (5.11) and (5.12) guarantee that the sliding trajectory remains within a ultimate band as in (5.20), i.e.,  $|s(t)| \leq \sigma_{et}|e_{2et}(t_k)| + \rho_{et}$ . From the full-order



sliding-mode manifold in (5.10), it can be obtained that the system trajectories reach the origin with minimum band by

$$\begin{aligned} \dot{e}_{2et}(t) + c_{et}e_{2et}(t) &\leq \sigma_{et}|e_{2et}(t_k)| + \rho_{et} \\ a_{21}e_{1et}(t) - a_{22}e_{2et}(t) + c_{et}e_{2et}(t) + v_{et}(t) - d(t) &\leq \sigma_{et}|e_{2et}(t_k)| + \rho_{et} \\ c_{et}e_{2et}(t) - a_{22}e_{2et}(t) &\leq \sigma_{et}|e_{2et}(t_k)| + \rho_{et} - a_{21}e_{1et}(t) - v_{et}(t) + d(t) \\ e_{2et}(t) &\leq \frac{\sigma_{et}}{T_{et}}|e_{2et}(t_k)| \end{aligned}$$

Now, the trajectories of the system remain ultimately bounded in the region given below

$$\Gamma_{et} := \left\{ e_{2et}(t) \in \mathbb{R} : |e_{2et}(t)| \leq \frac{\sigma_{et}}{T_{et}}|e_{2et}(t_k)| \right\} \quad (5.21)$$

where  $\sigma_{et}$  and  $T_{et}$  are both positive constant and defined in (5.20) and (5.7) respectively.

The event-triggering sliding-mode observation scheme for (5.5) and (5.6) is discussed to ensure the sliding conditions in Theorem 10. From the state error condition (5.13), the event is triggered by

$$|\phi_{2et}(t)| \leq \frac{\gamma_{et}}{a_{22}(c_{et} - a_{22})}|e_{2et}(t_k)|, \quad t \in [t_k, t_{k+1}) \quad (5.22)$$

Then, the event is triggered to update the control laws in the observer when the following condition satisfied

$$|\phi_{2et}(t)| = \frac{\gamma_{et}}{a_{22}(c_{et} - a_{22})}|e_{2et}(t_k)|, \quad t \in [t_k, t_{k+1}) \quad (5.23)$$

The triggering time  $t_{k+1}$  can be obtained as

$$t_{k+1} = \inf \left\{ t \in (t_k, +\infty) : |\phi_{2et}(t)| \geq \frac{\gamma_{et}}{a_{22}(c_{et} - a_{22})}|e_{2et}(t_k)| \right\}, \quad \forall k \in \mathbb{Z}_+ \quad (5.24)$$

Due to the inherent limitations in the digital platform, there exists a non zero lower bound for the inter-execution time. Therefore, the inter-execution time should be bounded below by some positive lower bound in the event-triggered scheme. Consider the error system (5.8) and (5.9) by the full-order sliding-mode control laws designed in (5.11) and (5.12) under the event-triggered conditions in (5.13) for all  $t > t_k$ , and  $k \in \mathbb{Z}_+$ , where  $t_0 < t_1 < \dots$ , it can be obtained that

$$\begin{aligned} |\dot{\phi}_{2et}(t)| &= |\dot{e}_{2et}(t)| \\ &\leq |a_{21}e_{1et}(t)| + |a_{22}e_{2et}(t_k)| + |a_{22}\phi_{2et}(t)| + |v_{et}(t)| + |d(t)| \\ &\leq a_{22}|\phi_{2et}(t)| + a_{22}|e_{2et}(t_k)| + \rho_{et} \end{aligned}$$

where  $\rho_{et} = a_{21}\bar{w} + \chi_{et}/T_{et} + d_0$ .

Since the initial condition  $e_{2et}(t_k) = e_{2et}(t) + \phi_{2et}(t) = 0$ , the solution of the differential inequality can be obtained according to the comparison Lemma [271] with initial condition  $\phi_{2et}(t) = 0$  by

$$|\phi_{2et}(t)| \leq \frac{a_{22}|e_{2et}(t_k)| + \rho_{et}}{a_{22}} (\exp(a_{22}(t - t_k)) - 1) \text{ for } t \in [t_k, t_{k+1}) \quad (5.25)$$

Based on triggering conditions (5.22) and (5.23), it can be achieved that

$$\frac{\gamma_{et}}{a_{22}(c_{et} - a_{22})} |e_{2et}(t_k)| \leq \frac{a_{22}|e_{2et}(t_k)| + \rho_{et}}{a_{22}} (\exp(a_{22}(t - t_k)) - 1) \quad (5.26)$$

then, we can have

$$\begin{aligned} T_k &\geq \frac{1}{a_{22}} \ln \left( 1 + \frac{a_{22}}{a_{22}|e_{2et}(t_k)| + \rho_{et}} \frac{\gamma_{et}}{a_{22}(c_{et} - a_{22})} |e_{2et}(t_k)| \right) \\ &> 0 \end{aligned} \quad (5.27)$$

Therefore, we can derive the existence of the lower bound for inter-execution time  $T_k = t_{k+1} - t_k > 0$ .

The asymptotic stability of the state error  $e_{1et}$  can be guaranteed by considering a linear system with time-varying delay with the known bounded values of the time delay,  $\tau(t)$ , and its derivative bounded value in [267]. As the error systems (5.8) converge to zero, and (5.9) converge to the ultimately bounded region  $\Gamma_{et}$  in (5.21).

Then, the estimate of the additional traffic dynamics,  $d(t)$ , can be achieved by

$$\hat{d}(t) = v_{et}(t) \quad (5.28)$$

Note that

$$\frac{v_{et}(s)}{\omega_{et}(s)} = \frac{1}{s + T_{et}} \quad (5.29)$$

where  $\omega_{et} = T_{et}$  is the bandwidth of the equivalent first-order low-pass filter. Therefore, the control signal  $v_{et}(t)$  is the smooth signal which can be directly applied to estimate the external disturbance by (5.11) and (5.12).

A event-triggered full-order sliding-mode based RNT0 is developed to achieve the real-time performance in this section. First, a full-order sliding-mode observer (5.5) and (5.6) is used for RNT0 with event-triggered scheme. The event-triggered scheme is firstly considered in the RNT0 to reduce the number of estimation steps to be updated in (5.11) and (5.12) for energy consumption savings and communication resources efficiency. Here, the event-triggered scheme is designed depending on time  $t$ . Second, the event-triggered scheme is firstly considered in the full-order sliding-mode, the control of which is a smooth signal in (5.11) and (5.12) and is directly used to estimate the additional traffic dynamic as in (5.29). Under the event-triggered environment, the control laws are updated at time  $t_k$  and remains the control value unchanged till the next trigger execution at time  $t_{k+1}$ . Furthermore, the

estimation for the ATF is a smooth signal without any any low-pass filters in RNT0, which will cause the phase legs in the real-time RNT0.

## 5.4 Simulation

To assess the algorithm-efficient performance of the proposed even-triggered sliding mode based observation algorithms for RNT0 applications. The simulations via the NS-II are conducted and the results are discussed in this section.

### 5.4.1 Model Description

A typical star type TCP/IP network model, as shown in Fig. 3.2, is applied in the simulation. It consists of a number of hosts and clients with one network router. The parameters of the TCP/IP network model and the designed observer are given below.

*Simulation model of router-based networks:* The network simulator NS-II is used to study the global dynamic performance of the proposed fuzzy TSMO algorithms. The network scenario in Fig. 3.2 is constructed via NS-II. There are 60 hosts and 60 clients connected via the network router. The output link capacity  $C$  of the router is set to be 15 Mb. The connections between each host/client and the router use full-duplex that construct bidirectional links at propagation delay  $T_p = 200$  ms. The maximum Cwnd  $\bar{w}$  is set to be 0.12 Mb. The packet size is set to be 500 bytes. The PI-AQM algorithm is used [125] to regulate the QL at desired level  $q_0 = 175$  packets. The buffer capacity  $\bar{q}$  is set to be 800 packets.

According to the aforementioned network configurations, the parameters in the linearised TCP/IP network model (3.17) and (3.18) can be determined as follows:  $a_{11} = 0.2630$ ,  $a_{12} = 0.0044$ ,  $b_d = 481.7708$ ,  $a_{21} = 243.2432$ , and  $a_{22} = 4.0541$ . The parameters of the proposed event-triggered SMO are designed using Theorems 10 are:  $T = 10$  and  $k_{et} = 1600$ .

To evaluate the performances of the proposed observer, the external traffic served by both CBR and VBR are considered. The following three different scenarios are considered.

- **Scenario 1 (constant rate traffics):** three source nodes generate constant rate traffics. The “cbr” applications are invoked and attached to the “udp” agents. The sending rate of each agent is set as 500 *packets/s* between the period 100 – 200s. The simulation time is 300 *seconds*.
- **Scenario 2 (variable rate traffics):** three source nodes generate variable rate traffics. The “vbr” applications are designed as ramp traffic and attached to the “udp” agents. The sending rate of each agent is set as rising slope up to 500 *packets/s* between the period 100 – 200s. The simulation time is 300 *seconds*.
- **Scenario 3 (hybrid traffic rates):** three source nodes randomly generate constant and variable rate traffics. This case is the mixture of Scenarios 1 and 2. The simulation time is 2000 *seconds*.

### 5.4.2 Simulation Results and Discussion

Figs. 5.2 and 5.3 present the states of the proposed event-triggered sliding mode observer corresponding to the scenarios 1 and 2. As illustrated in Figs. 5.2a and 5.3a, the queue lengths are stabilized by AQM in both scenarios. By the proposed event-triggered schemes, the unknown traffic behaviour i.e., the ACwnd size and the dynamics of ATF are accurately estimated. From Figs. 5.2e and 5.3e that the estimation error  $e^2(t)$  is validated to converges to zero. By the control signals  $v_{et}(t)$  in 5.11 under the event-driven schemes, the state  $w(t)$  and  $d(t)$  are quickly and accurately estimated as presented in Figs. 5.2b, 5.3b, 5.2c and 5.3c respectively. The triggered events are shown in Figs. 5.2f and 5.3f with the computation rate of 26.4% and 27.3% respectively.

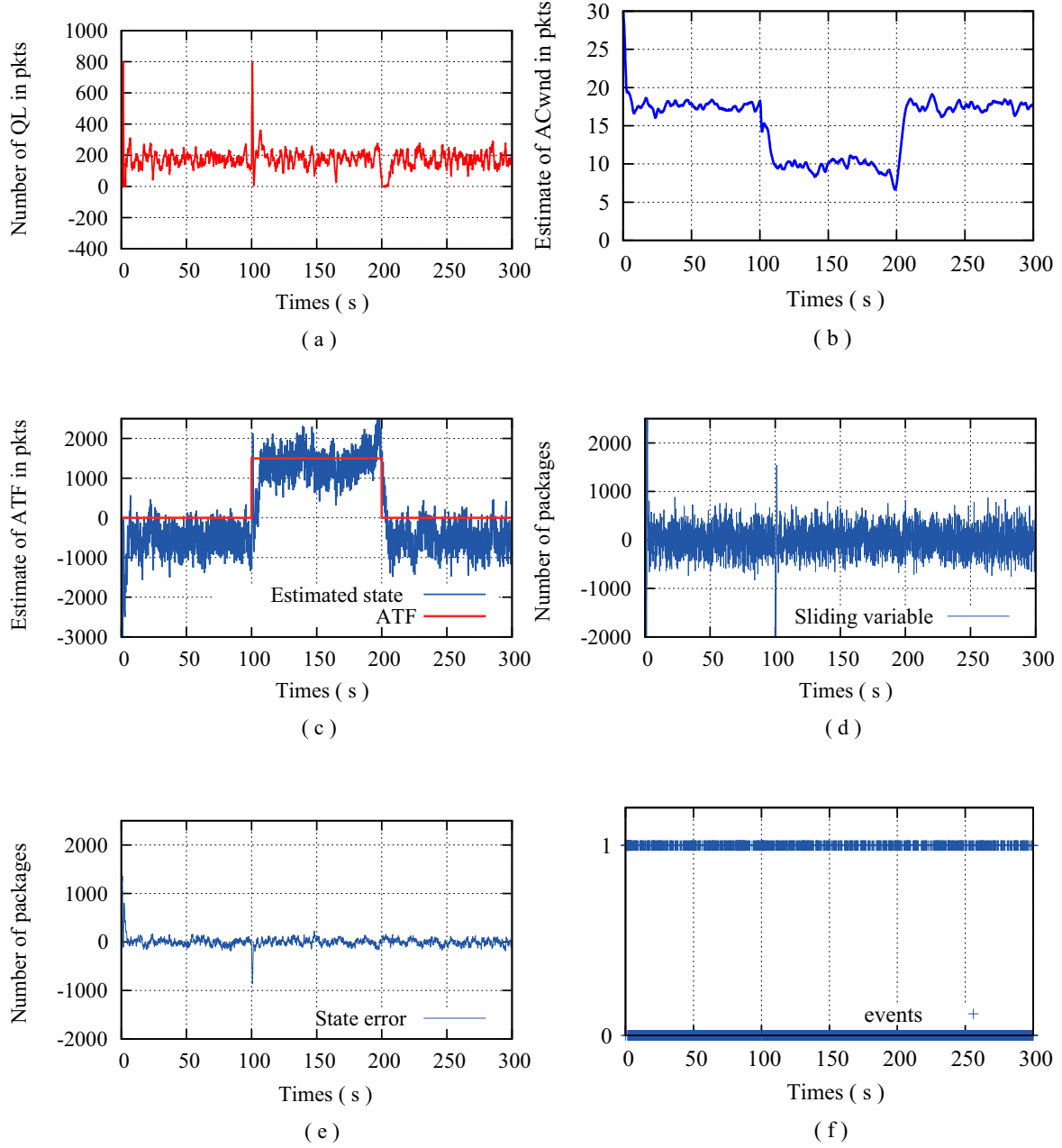


Fig. 5.2 State and control of the proposed FTSMO in Scenario 1. : (a) The number of QL  $q(t)$  in router buffer. (b) Estimated ACwnd  $w(t)$  in *packets* at the router. (c) Estimated dynamics of ATF  $d(t)$  and the true DDoS flooding rate. (d) The value of the sliding variable  $set(t)$  in *packets*. (e) Estimation error  $e_{et}^2(t)$  in *packets*. (f) The triggered events.

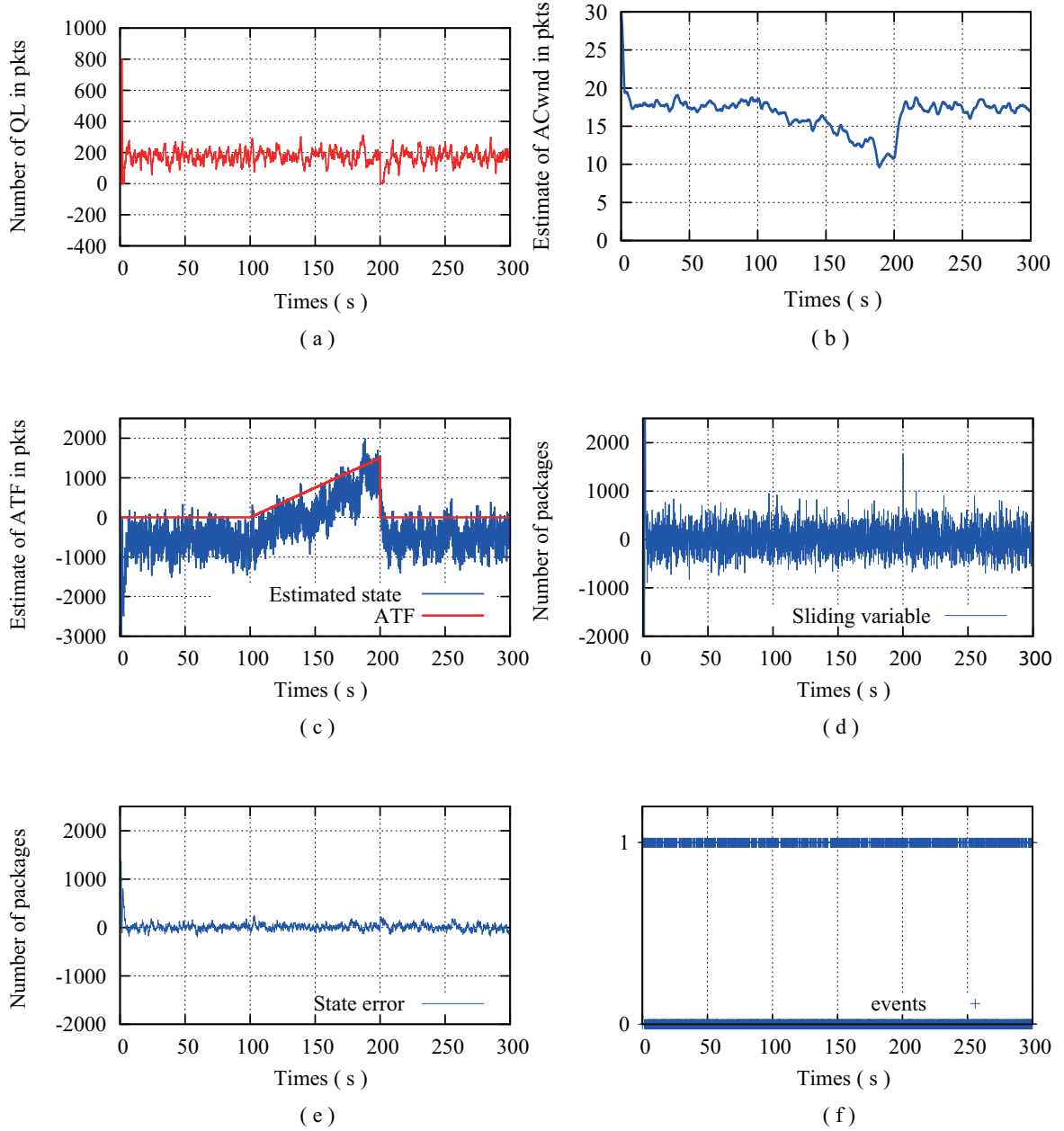


Fig. 5.3 State and control of the proposed FTSMO in Scenario 2.: (a) The number of QL  $q(t)$  in router buffer. (b) Estimated ACwnd  $w(t)$  in *packets* at the router. (c) Estimated dynamics of ATF  $d(t)$  and the true DDoS flooding rate. (d) The value of the sliding variable  $s_{et}(t)$  in *packets*. (e) Estimation error  $e_{et}^2(t)$  in *packets*. (f) The triggered events.

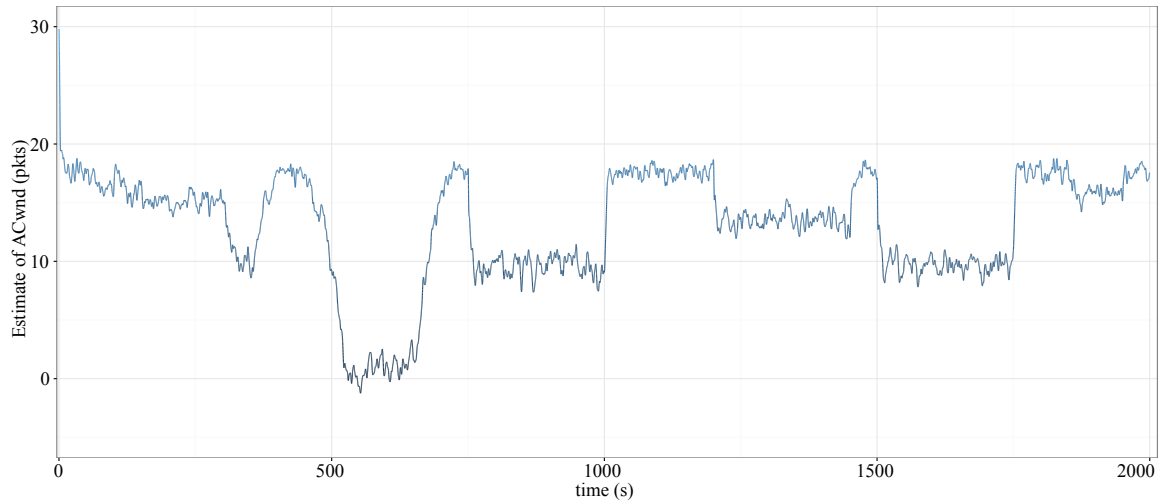


Fig. 5.4 The estimated ACwnd by the proposed FTSMO algorithm in Scenario 3.

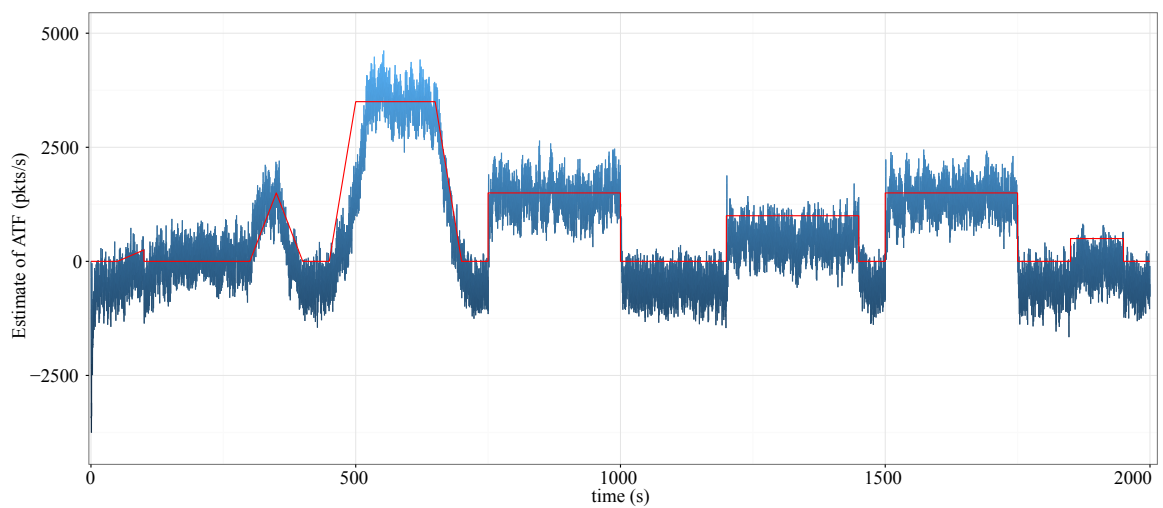


Fig. 5.5 The estimated ACwnd by the proposed FTSMO algorithm in Scenario 3.



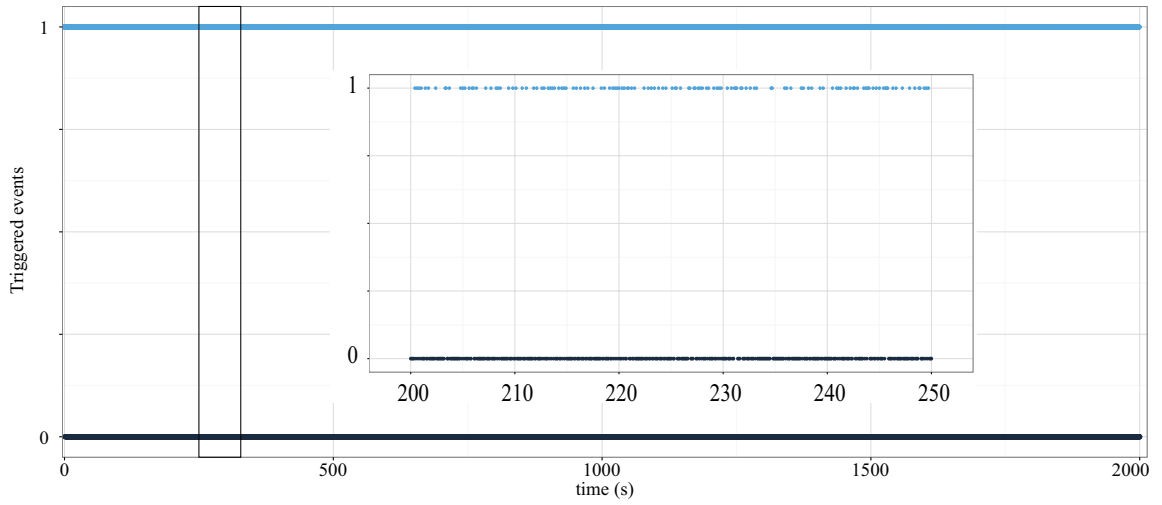


Fig. 5.6 The estimated ACwnd by the proposed FTSMO algorithm in Scenario 3.

The simulation results of the proposed event-triggered sliding mode observer in scenario 3 are shown in Figs. 5.4, 5.5 and 5.6. The estimated ACwnd  $w(t)$ , as shown in Fig. 5.4, is accurately reflect the serious degradations in sending rate, throughput and bandwidth utilization in the networks. As depicted in Fig. 5.5, the dynamics ATF  $d(t)$  generated by the mixed CBR and VBR types of traffics is quickly and accurately estimated. The triggered events are shown in Fig. 5.6 with the computation rate of 26.5%.

## 5.5 Summary

In this chapter, the event-triggered based scheme for algorithm-efficient RNT0 by using full-order sliding mode control theory has been investigated. A full-order sliding mode control law under the event-triggered environment has been designed to construct a smooth signal that is employed for ATF estimation in RNT0 applications. Moreover, the event-triggered mechanisms are developed to reduce the computational load and the communication burden in RNT0. This method provides a efficient technique that the real-time dynamic traffic observation is operating with lower computation load, memory occupation and communication bandwidth requirements.

The results fill the gap that is associated with the key issues of the computation efficiency and communication bottleneck. One remarkable feature is embedded in the event-triggered scheme which shows the trade-off between accuracy of traffic estimation and the number of computation and communications. The algorithm-efficient dynamic RNTD can balance the trade-off depending on network resource condition.

# Chapter 6

## Fuzzy Terminal Sliding-mode Observation Strategy

### 6.1 Introduction

The methodologies of the real-time dynamic, fast dynamic and algorithm-efficient observation algorithms by using sliding mode control theory are proposed for RNTTO applications in previous chapters. However, the methods are deployed based on the input-output linearisation of the router-based network system. It only features the local stability of the observation system. Due to the property of time varying in network variables such as the number of TCP sections  $N(t)$ , the round-trip time  $\tau(t)$  and the queue length of router buffer  $q(t)$ , the equivalent point of the system can be changed. Therefore, the stability of the observer cannot be guaranteed. The local stability is a key issue in the existed RNTTO algorithms need to be solved.

In this chapter, a real-time fuzzy terminal sliding mode observer is investigated to monitor the traffic flow for RNTTO applications. The T-S fuzzy model for the router-based network traffic is formulated in **Section 6.2**. The novel control strategy for the T-S fuzzy network system by using full-order terminal sliding mode control theory is proposed and proven

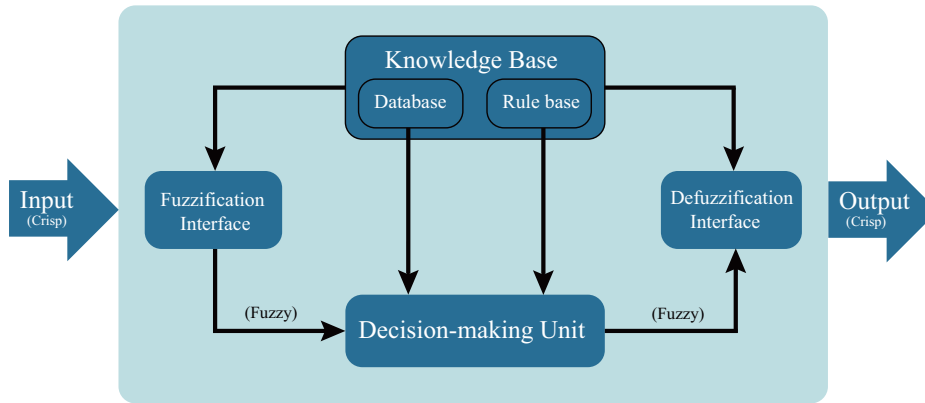


Fig. 6.1 Fuzzy inference system

in **Section 6.3**. The fuzzy control laws are required and designed to be smooth for traffic observation. The simulation case study in Network Simulator II are presented and discussed, which demonstrate the effectiveness and efficiency of the proposed fuzzy global observation algorithm in **Section 6.4**. Finally, some summaries are made in **Section 6.5**.

## 6.2 Takagi-Sugeno Fuzzy Model of a Router-based Network

A Takagi-Sugeno (T-S) fuzzy system is one kind of the most common fuzzy models [272]. The T-S fuzzy model is described by a set of *IF-THEN* rules which represents exhibit the property of local linear input–output relations of a nonlinear system. The main feature of a T-S fuzzy model is to express the local dynamics of each fuzzy rule by a linear system model. The overall fuzzy model of the system is achieved with fuzzy aggregation of the linear system models. Inspired by [272], we shall construct T-S fuzzy models to describe dynamic systems with variable structures. In this section, the router-based network traffic dynamics will be represented by T-S fuzzy models to approximate the complex nonlinear system dynamics to achieve a global observation performance at high degree of precision.

Fuzzy inference systems also known as fuzzy rule-based systems or fuzzy models are

schematically shown in Figure 6.1. They are composed of 5 blocks:

- **Rule-base** contains a number of fuzzy *IF-THEN* rules;
- **Database** defines the membership functions of the fuzzy sets used in the fuzzy rules;
- **Decision-making unit** performs the inference operations on the rules;
- **Fuzzification interface** transform the crisp inputs into degrees of match with linguistic values;
- **Defuzzification interface** transform the fuzzy results of the inference into a crisp output.

The goal is to derive a T-S fuzzy model from the fluid-flow based nonlinear system equations (3.1) to (3.3) by the sector approach as if the response of the T-S fuzzy model in the specified domain exactly match with the original system.

## Rule-base

A T-S fuzzy model uses fuzzy rules, which are linguistic *IF-THEN* statements including fuzzy sets, fuzzy logic, and fuzzy inference to represent expert modelling knowledge. The  $i$ th rules of the T-S fuzzy models are formulated as follows

**Model Rule  $i$ :**

**IF**  $f_1(\theta(t))$  is  $M_1^i$  and  $f_2(\theta(t))$  is  $M_2^i$  and  $\dots$  and  $f_s(\theta(t))$  is  $M_s^i$

**THEN**

$$\begin{cases} \dot{x}(t) = -a_{11}^i x(t) - a_{11}^i x(t - \tau(t)) - a_{12}^i y(t) + a_{12}^i y(t - \tau(t)) - b_d^i u(t - \tau(t)) \\ \dot{y}(t) = a_{21}^i x(t) - a_{22}^i y(t) + d(t) \\ \text{for } i = 1, 2, \dots, r. \end{cases} \quad (6.1)$$

where  $M_j^i$  is the fuzzy set of the  $i$ -th rule,  $f_j(\theta(t))$  is the  $j$ -th measurable premise variable,  $i = 1, 2, \dots, r$ ,  $j = 1, 2, \dots, s$ ,  $r$  is the number of the fuzzy rules, and  $s$  is the number of the fuzzy sets.  $x(t) \in \mathbb{R}$  is the system state,  $y(t) \in \mathbb{R}$  is the system output,  $u(t) \in \mathbb{R}$  is the control signal,  $d(t) \in \mathbb{R}$  denotes the external disturbance, and the time delay  $\tau(t)$  is a time-varying continuous function, which are all defined in system (3.17) and (3.18).

The  $i$ th fuzzy system (6.1), which is the equivalent operating point in (3.17) and (3.18), is in the specified domain of the original nonlinear system (3.1) to (3.3). In the  $i$ th fuzzy system, with the triplet parameters of  $(N_i, C_i, T_p^i)$ , the set of feasible operating point of  $i$ th fuzzy system is as

$$\Xi_{(N_i, C_i, T_p^i)}^i = \left\{ \begin{array}{l} (w_0^i, q_0^i, p_0^i) : w_0^i \in [0, \bar{w}], q_0^i \in [0, \bar{q}], p_0^i \in [0, 1], \\ w_0^i = \tau_0^i C_i / N_i, \tau_0^i = q_0^i / C_i + T_p^i, \text{ and } p_0^i = 2 / w_0^{i^2} \end{array} \right\} \quad (6.2)$$

where  $(w_0^i, q_0^i, p_0^i)$  is a possible operating point of the  $i$ th rule system in (6.1). Note that each linear consequent equation represented by **Model Rule  $i$**  with  $\Xi_{(N_i, C_i, T_p^i)}^i$  is called a “subsystem” of overall T-S fuzzy model.

## Database

In a T-S fuzzy model, the database determine the membership functions of the fuzzy variables and fuzzy sets used in the Rule-base. The membership function of a fuzzy set is a generalization of the indicator function in classical sets. In fuzzy logic, it is a curve that defines how each point in the input space is mapped to a membership value with a range covering the interval  $(0, 1)$ .

Set  $h_i(\theta(t))$  as the normalized fuzzy membership function of the inferred fuzzy set  $M_j^i$

and is described as the following form:

$$h_i(\theta(t)) = \frac{w_i(f(\theta(t)))}{\sum_{i=1}^r w_i(f(\theta(t)))} \quad (6.3)$$

and

$$w_i(f(\theta(t))) = \prod_{j=1}^s \mu_{M_j^i}(f_j(\theta(t))) \quad (6.4)$$

where  $\mu_{M_j^i}(f_j(\theta(t)))$  is the membership function of  $f_j(\theta(t))$  in  $M_j^i$ .

The property of  $w_i(f(\theta(t)))$  is that

$$w_i(f(\theta(t))) \geq 0, \quad \sum_{j=1}^r w_j(f(\theta(t))) > 0, \quad i = 1, 2, \dots, r, \quad (6.5)$$

and

$$h_i(\theta(t)) \geq 0, \quad \sum_{j=1}^r h_j(\theta(t)) = 1, \quad i = 1, 2, \dots, r, \quad (6.6)$$

It can be assumed that all membership functions are continuous and piecewise continuously differentiable and the defuzzification method is continuous as well.

The derivative of the membership function  $h_i(\theta(t))$  can be assumed to satisfy by:

$$\frac{dh_i(\theta(t))}{dt} \leq l, \quad (6.7)$$

## Defuzzification interface

Defuzzification interface transform the fuzzy results of the inference into a crisp output. Based on the weighted average fuzzy inference method, the defuzzified output of the T-S

fuzzy system (6.1) can be represented as follows:

$$\dot{x}(t) = \sum_{i=1}^r h_i(\theta(t)) (-a_{11}^i x(t) - a_{11}^i x(t - \tau(t)) - a_{12}^i y(t) + a_{12}^i y(t - \tau(t)) - b_d^i u(t - \tau(t))) \quad (6.8)$$

$$\dot{y}(t) = \sum_{i=1}^r h_i(\theta(t)) (a_{21}^i x(t) - a_{22}^i y(t)) + d(t) \quad (6.9)$$

where  $\sum_{i=1}^r h_i(\theta(t))$  is the normalized fuzzy membership function and defined in (6.3).

To simplify the above defuzzified output of the T-S fuzzy system, it can be reformed by

$$\dot{x}(t) = -\bar{a}_{11}x(t) - \bar{a}_{11}x(t - \tau(t)) - \bar{a}_{12}y(t) + \bar{a}_{12}y(t - \tau(t)) - \bar{b}_d u(t - \tau(t)) \quad (6.10)$$

$$\dot{y}(t) = \bar{a}_{21}x(t) - \bar{a}_{22}y(t) + d(t) \quad (6.11)$$

where

$$\begin{aligned} \bar{a}_{11} &= \sum_{i=1}^r h_i(\theta(t)) a_{11}^i, & \bar{a}_{12} &= \sum_{i=1}^r h_i(\theta(t)) a_{12}^i, & \bar{b}_d &= \sum_{i=1}^r h_i(\theta(t)) b_d^i, \\ \bar{a}_{21} &= \sum_{i=1}^r h_i(\theta(t)) a_{21}^i, & \bar{a}_{22} &= \sum_{i=1}^r h_i(\theta(t)) a_{22}^i. \end{aligned}$$

In the following, the symbols  $\bar{a}_{11}$ ,  $\bar{a}_{12}$ ,  $\bar{b}_d$ ,  $\bar{a}_{21}$ , and  $\bar{a}_{22}$  are used as the system parameters of the T-S fuzzy system (6.10) and (6.11).



### 6.3 Fuzzy Terminal Sliding Mode Based RNT0

The fuzzy observer for the T-S fuzzy system (6.10) and (6.11) is proposed in the following structure by

**Observer Rule  $i$ :**

**IF**  $f_1(\theta(t))$  is  $M_1^i$  and  $f_2(\theta(t))$  is  $M_2^i$  and  $\dots$  and  $f_s(\theta(t))$  is  $M_s^i$

**THEN**

$$\left\{ \begin{array}{l} \dot{\hat{x}}_f(t) = -a_{11}^i \hat{x}_f(t) - a_{11}^i \hat{x}_f(t - \tau(t)) - a_{12}^i y(t) + a_{12}^i y(t - \tau(t)) \\ \quad - b_d^i u(t - \tau(t)) \\ \dot{\hat{y}}_f(t) = a_{21}^i \hat{x}_f(t) - a_{22}^i y(t) + v_f(t) \\ \text{for } i=1, 2, \dots, r. \end{array} \right. \quad (6.12)$$

where  $\hat{x}_f(t)$  and  $\hat{y}_f(t)$  are the estimations of the state  $x(t)$  and the output  $y(t)$  of the system respectively,  $v_f(t)$  is the fuzzy observer control and is designed later.

The overall fuzzy observer is represented as follows:

$$\dot{\hat{x}}_f(t) = \sum_{i=1}^r h_i(\theta(t)) \left( \begin{array}{l} -a_{11}^i \hat{x}_f(t) - a_{11}^i \hat{x}_f(t - \tau(t)) - a_{12}^i y(t) \\ \quad + a_{12}^i y(t - \tau(t)) - b_d^i u(t - \tau(t)) \end{array} \right) \quad (6.13)$$

$$\dot{\hat{y}}_f(t) = \sum_{i=1}^r h_i(\theta(t)) (a_{21}^i \hat{x}_f(t) - a_{22}^i y(t) + v_f(t)) \quad (6.14)$$

where  $\sum_{i=1}^r h_i(\theta(t))$  is the normalized fuzzy membership function and defined in (6.3).

Define the estimation errors as  $e_{1f}(t) =: \hat{x}_f(t) - x(t)$  and  $e_{2f}(t) =: \hat{y}_f(t) - y(t)$  between the system states and their estimates.

By differentiating the estimation errors  $e_{1f}(t)$  and  $e_{2f}(t)$ , it can be obtained from the

system (6.10) to (6.11) and the fuzzy observer (6.13) to (6.14)

$$\dot{e}_{1f}(t) = \sum_{i=1}^r h_i(\theta(t)) a_{11}^i (-e_{1f}(t) - e_{1f}(t - \tau(t))) \quad (6.15)$$

$$\dot{e}_{2f}(t) = \sum_{i=1}^r h_i(\theta(t)) a_{21}^i e_{1f}(t) + v_f(t) - d(t) \quad (6.16)$$

For the error system (6.15) and (6.16), a TSM manifold can be chosen as the following form:

$$s_f(t) = \dot{e}_{2f}(t) + \alpha_f e_{2f}(t) + \beta_f (e_{1f})^{q_f/p_f}(t) \quad (6.17)$$

where  $\alpha_f, \beta_f > 0$  are design constants,  $p_f$  and  $q_f$  are positive odd integers which satisfy  $1 < p_f/q_f < 2$ .

**Theorem 11.** *The error system (6.16) will reach  $s_f(t) = 0$  from any initial condition  $s_f(0) \neq 0$  in a finite-time  $t_f^r \leq |s_f(0)|/(\eta_f)$ , then converge to zero along  $s_f(t) = 0$  in a finite-time, if a terminal sliding mode manifold  $s_f(t)$  is designed as (6.17) and the control laws are designed as*

$$v_f(t) = v_f^{eq}(t) + v_f^n(t) \quad (6.18)$$

$$v_f^{eq}(t) = - \sum_{i=1}^r h_i(\theta(t)) a_{21}^i \hat{x}_f(t) - \alpha_f e_{2f}(t) - \beta_f (e_{1f})^{q_f/p_f}(t) \quad (6.19)$$

$$\begin{aligned} \dot{v}_f^n(t) = & \sum_{i=1}^r \sum_{j=1}^r h_i(\theta(t)) h_j(\theta(t)) a_{21}^j (-a_{12}^i y(t) + a_{12}^i y(t - \tau(t)) \\ & - b_d^i u(t - \tau(t))) - k_f \text{sgn}(s_f(t)) \end{aligned} \quad (6.20)$$

where  $k_f = \sum_{i=1}^r \sum_{j=1}^r l a_{21}^i (1 + 2l a_{11}^j) \bar{w} + d_1 + \eta_f$ ,  $\bar{w}$ ,  $d_1$  are defined in (3.1) to (3.3),  $l$  is defined in (6.7), and  $\eta_f > 0$  is a constant.

*Proof.* From the error system (6.16), the TSM manifold (6.17) can be rewritten as

$$s_f(t) = \sum_{i=1}^r h_i(\theta(t)) a_{21}^i e_{1f}(t) + v_f(t) - d(t) + \alpha_f e_{2f}(t) + \beta_f (e_{1f})^{q_f/p_f}(t)$$

Substituting the control laws (6.18) and (6.19) into the above gives

$$\begin{aligned} s_f(t) &= \sum_{i=1}^r h_i(\theta(t)) a_{21}^i (\hat{x}_f(t) - x(t)) + v_f^{eq}(t) + v_f^n(t) - d(t) + \alpha_f e_{2f}(t) + \beta_f (e_{1f})^{q_f/p_f}(t) \\ &= \sum_{i=1}^r h_i(\theta(t)) a_{21}^i (\hat{x}_f(t) - x(t)) + v_f^{eq}(t) + \left( - \sum_{i=1}^r h_i(\theta(t)) a_{21}^i \hat{x}_f(t) - \alpha_f e_{2f}(t) \right. \\ &\quad \left. - \beta_f (e_{1f})^{q_f/p_f}(t) \right) - d(t) + \alpha_f e_{2f}(t) + \beta_f (e_{1f})^{q_f/p_f}(t) \\ &= - \sum_{i=1}^r h_i(\theta(t)) a_{21}^i x(t) + v_f^n(t) - d(t) \end{aligned} \quad (6.21)$$

Differentiating the sliding variable  $s_f(t)$  in (6.3) with respect to time  $t$  along the system (6.10) yields

$$\begin{aligned} \dot{s}_f(t) &= - \frac{d}{dt} \left( \sum_{i=1}^r h_i(\theta(t)) a_{21}^i x(t) \right) + \dot{v}_f^n(t) - \dot{d}(t) \\ &= - \sum_{i=1}^r \left( \frac{d}{dt} h_i(\theta(t)) \right) a_{21}^i x(t) - \sum_{i=1}^r \sum_{j=1}^r h_i(\theta(t)) h_j(\theta(t)) a_{21}^i (-a_{11}^j x(t) - a_{11}^j x(t - \tau(t)) \\ &\quad - a_{12}^j y(t) + a_{12}^j y(t - \tau(t)) - b_d^j u(t - \tau(t))) + \dot{v}_f^n(t) - \dot{d}(t) \end{aligned}$$

Further substituting the control law (6.20) into the above equation gives

$$\begin{aligned} \dot{s}_f(t) &= - \sum_{i=1}^r \left( \frac{d}{dt} h_i(\theta(t)) \right) a_{21}^i x(t) - \sum_{i=1}^r \sum_{j=1}^r h_i(\theta(t)) h_j(\theta(t)) a_{21}^i (-a_{11}^j x(t) - a_{11}^j x(t - \tau(t)) \\ &\quad - a_{12}^j y(t) + a_{12}^j y(t - \tau(t)) - b_d^j u(t - \tau(t))) + \sum_{i=1}^r \sum_{j=1}^r h_i(\theta(t)) h_j(\theta(t)) a_{21}^i (-a_{12}^j y(t) \\ &\quad + a_{12}^j y(t - \tau(t)) - b_d^j u(t - \tau(t))) - k_f \text{sgn}(s_f(t)) - \dot{d}(t) \end{aligned}$$

$$\begin{aligned}
&= - \sum_{i=1}^r \left( \frac{d}{dt} h_i(\theta(t)) \right) a_{21}^i x(t) - \sum_{i=1}^r \sum_{j=1}^r h_i(\theta(t)) h_j(\theta(t)) a_{21}^i (-a_{11}^j x(t) - a_{11}^j x(t - \tau(t))) \\
&\quad - k_f \text{sgn}(s_f(t)) - \dot{d}(t)
\end{aligned}$$

Consider a Lyapunov function candidate given by

$$V_f = \frac{1}{2} s_f^2(t) \quad (6.22)$$

Taking the derivative of (6.22) along the trajectories of (6.15) and (6.16), it follows that

$$\begin{aligned}
s_f(t) \dot{s}_f(t) &= - \sum_{i=1}^r \left( \frac{d}{dt} h_i(\theta(t)) \right) a_{21}^i x(t) s_f(t) - \sum_{i=1}^r \sum_{j=1}^r h_i(\theta(t)) h_j(\theta(t)) a_{21}^i (-a_{11}^j x(t) \\
&\quad - a_{11}^j x(t - \tau(t))) s_f(t) - k_f \text{sgn}(s_f(t)) s_f(t) - \dot{d}(t) s_f(t) \\
&\leq \left| \sum_{i=1}^r \left( \frac{d}{dt} h_i(\theta(t)) \right) a_{21}^i x(t) \right| |s_f(t)| + \left| \sum_{i=1}^r \sum_{j=1}^r h_i(\theta(t)) h_j(\theta(t)) a_{21}^i \right. \\
&\quad \left. \times (-a_{11}^j x(t) - a_{11}^j x(t - \tau(t))) \right| |s_f(t)| \\
&\quad - \left( \sum_{i=1}^r \sum_{j=1}^r l a_{21}^i (1 + 2l a_{11}^j) \bar{w} + d_1 + \eta_f \right) |s_f(t)| + |\dot{d}(t)| |s_f(t)| \\
&\leq \left( \left| \sum_{i=1}^r \left( \frac{d}{dt} h_i(\theta(t)) \right) a_{21}^i x(t) \right| - \sum_{i=1}^r l a_{21}^i \bar{w} \right) |s_f(t)| + (|\dot{d}(t)| - d_1) |s_f(t)| \\
&\quad + \left( \left| \sum_{i=1}^r \sum_{j=1}^r h_i(\theta(t)) h_j(\theta(t)) a_{21}^i \right. \right. \\
&\quad \left. \left. \times (-a_{11}^j x(t) - a_{11}^j x(t - \tau(t))) \right| - \sum_{i=1}^r \sum_{j=1}^r a_{21}^i a_{11}^j 2\bar{w} l^2 \right) |s_f(t)| - \eta_f |s_f(t)|
\end{aligned}$$

Therefore, we have

$$\dot{V}_f(t) = s_f(t) \dot{s}_f(t) \leq -\eta_f \sqrt{2V_1}^{1/2}(t) < 0$$

which means that error system of system (6.16) will reach to  $s_f(t) = 0$  within the finite-time  $t_f^r \leq |s_f(0)|/\eta_f$ , in other words,  $s_f(t) = 0, \forall t \geq t_f^r$ . Once the ideal sliding-mode  $s_f(t) = 0$

is established, the error system (6.16) will maintain on  $s_f(t) = 0$  thereafter and behaves in an identical fashion as  $\dot{e}_{2f}(t) = -\alpha_f e_{2f}(t) - \beta_f (e_{2f})^{q_f/p_f}(t)$ , which will converge to zero along  $s_f(t) = 0$  in a finite-time.

Next, consider the stability of the error system (6.15), such as that

$$\dot{e}_{1f}(t) = \sum_{i=1}^r h_i(\theta(t)) a_{11}^i (-e_{1f}(t) - e_{1f}(t - \tau(t))) \quad (6.23)$$

where  $h_i(\theta(t))$  is the normalized fuzzy membership function of the inferred fuzzy set  $M_j^i$  and is defined in (6.3).

**Lemma 3.** [273] *Consider the fuzzy system with time-varying delay expressed by*

$$\dot{x}(t) = \sum_{i=1}^r h_i(\theta(t)) (A_{1i}x(t) + A_{2i}x(t - \tau(t))) \quad (6.24)$$

where  $x \in \mathbb{R}^n$  is the state,  $A_{1i}$  and  $A_{2i}$  are constant matrices with appropriate dimensions of the  $i$ th plant, and  $h_i(\theta(t))$  is the normalized fuzzy membership function. The time-varying delay  $\tau(t)$  satisfies  $\tau_1 < \tau(t) < \tau_2$  and  $\dot{\tau}(t) \leq \mu$ , where  $\tau_1$ ,  $\tau_2$  and  $\mu$  are all known constants.

*If there exist two common matrices  $P > 0$ ,  $S > 0$  such that*

$$A_{1i}^T P + P A_{1i} + P A_{2i} S^{-1} A_{2i}^T + \frac{1}{1 - \mu} S < 0 \quad (6.25)$$

*The continuous-time fuzzy system with time delay in (6.24) is asymptotically stable.*

As in Lemma 3, the error system (6.23) with the time delay  $\tau(t)$ , which satisfies the conditions in (3.4) and (3.5), is asymptotically stable.

Thus, the error system (6.16) has been proved to reach to the sliding surface  $s_f(t) = 0$  in a finite-time and converge to zero along the surface in a finite-time. From (6.3), it can be obtained that

$$\hat{d}_f(t) = \lim_{\substack{e_{1f} \rightarrow 0 \\ e_{2f} \rightarrow 0}} \int_0^t \sum_{i=1}^r \sum_{j=1}^r h_i(\theta(\sigma)) h_j(\theta(\sigma)) \begin{pmatrix} a_{21}^j (-a_{12}^i y(\sigma) + a_{12}^i y(\sigma - \tau(\sigma))) \\ -b_d^i u(\sigma - \tau(\sigma)) - k_f \text{sgn}(s_f(\sigma)) \end{pmatrix} d\sigma \quad (6.26)$$

From Theorem 11, the error state  $e_{2f}(t)$  converge to zero in a finite-time, while the error state  $e_{1f}(t)$  will converge to zero asymptotically as in Lemma 3, then, the estimated value of the  $d(t)$  can be obtained by (6.26). It can be seen that the estimation of  $d(t)$  is directly estimated by a smooth signal in (6.26). This completes the proof.  $\square$

**Theorem 12.** *If the control laws in the error system (6.15) and (6.16) are designed as in Theorems 11, thus the estimation error  $e_f^1(t)$  converges to zero asymptotically, and the dynamics of ATF  $d(t)$  in (3.17) and (3.18) can be estimated as*

$$\hat{d}(t) = \lim_{\substack{e_f^1(t) \rightarrow 0 \\ e_f^2(t) \rightarrow 0}} v_f(t) \quad (6.27)$$

where  $v_f(t)$  is the control signal defined in (6.18) to (6.20).

*Proof.* From Lemma 3, the error state  $e_f^1(t)$  can converge to zero asymptotically. Then Eq.(6.27) can be obtained from the above equation. In other words, the dynamics of ATF  $d(t)$  can be estimated directly by the smooth control signal  $v_f(t)$  in (6.18) to (6.20) when the error state  $e_f^1(t)$  converges to zero asymptotically. This completes the proof.  $\square$

A fuzzy terminal sliding-mode based RNTD has been developed to achieve the real-time performance in this section. First, the T-S fuzzy models in (6.1) for the network traffic dynamics of the interactions in a set of TCP flows (3.1) to (3.3) can be constructed by using

fuzzy logic theory. Second, a fuzzy terminal sliding-mode observer (6.12) is proposed for RNTTO with fuzzy logic theory. The fuzzy scheme is firstly considered in the RNTTO to achieve the global stability for network state estimation. Moreover, the novel fuzzy control law designed in (6.18) to (6.20) is a smooth signal and is directly applied for ATF estimation without any low-pass filters.

## 6.4 Simulation

To evaluate the global performance of the proposed fuzzy terminal sliding mode based observation algorithms for RNTTO applications. The simulations via the NS-II are performed and the results are presented in this section.

### 6.4.1 Model Description

A typical star type TCP/IP network model, as shown in Fig. 3.2, is applied in the simulation. It consists of a number of hosts and clients with one network router. The parameters of the TCP/IP network model and the designed observer are given below.

*Simulation model of router-based networks:* The network simulator NS-II is used to study the global dynamic performance of the proposed fuzzy TSMO algorithms. The network scenario in Fig. 3.2 is constructed via NS-II. There are  $N$  hosts and  $N$  clients connected via the network router, where the number of TCP sections  $N$  varies between 40 – 60. The output link capacity  $C$  of the router is set to be 15 Mb. The connections between each host/client and the router use full-duplex that construct bidirectional links at propagation delay  $T_p = 200$  ms. The maximum Cwnd  $\bar{w}$  is set to be 0.12 Mb. The packet size is set to be 500 bytes. The PI-AQM algorithm is used [125] to regulate the QL at desired level  $q_0 = 175$  packets. The buffer capacity  $\bar{q}$  is set to be 800 packets.

According to the aforementioned network configurations, the parameters in the lin-

earised TCP/IP network model (3.17) and (3.18) can be determined as follows:  $a_{11} = 0.2630$ ,  $a_{12} = 0.0044$ ,  $b_d = 481.7708$ ,  $a_{21} = 243.2432$ , and  $a_{22} = 4.0541$ . The parameters of the proposed TSMO are designed using Theorems 11 are:  $\alpha = 15$ ,  $\beta = 5$ ,  $\rho = 5$ ,  $\phi = 3$ ,  $k_{fsm}^1 = 1600$ , and  $k_{fsm}^2 = 7.5$ .

To evaluate the performances of the proposed observer, the external traffic served by both CBR and VBR are considered. The following three different scenarios are considered.

- **Scenario 1 (constant rate traffics):** The number of TCP sources  $N$  varies between 40 – 60. Three source nodes generate constant rate traffics. The “cbr” applications are invoked and attached to the “udp” agents. The sending rate of each agent is set as 500 *packets/s* between the period 100 – 200s. The simulation time is 300 *seconds*.
- **Scenario 2 (variable rate traffics):** The number of TCP sources  $N$  varies between 40 – 60. Three source nodes generate variable rate traffics. The “vbr” applications are designed as ramp traffic and attached to the “udp” agents. The sending rate of each agent is set as rising slope up to 500 *packets/s* between the period 150 – 200s. The simulation time is 300 *seconds*.
- **Scenario 3 (hybrid traffic rates):** The number of hosts are time-varying between 40 – 70s to launch TCP traffic flows. Three source nodes randomly generate constant and variable rate traffics. This case is the mixture of Scenarios 1 and 2. The simulation time is 2000 *seconds*.

### 6.4.2 Simulation Results and Discussion

Figs. 6.2 and 6.3 presents the results of the proposed fuzzy terminal sliding mode observer algorithm corresponding to the scenarios 1 and 2. It can be seen from Figs. 6.2a and 6.3a, the queue lengths are regulated, and the network are stabilized by AQM in both scenarios. As shown in Figs. 6.2c and 6.3c, the number of TCP sections are time-varying between



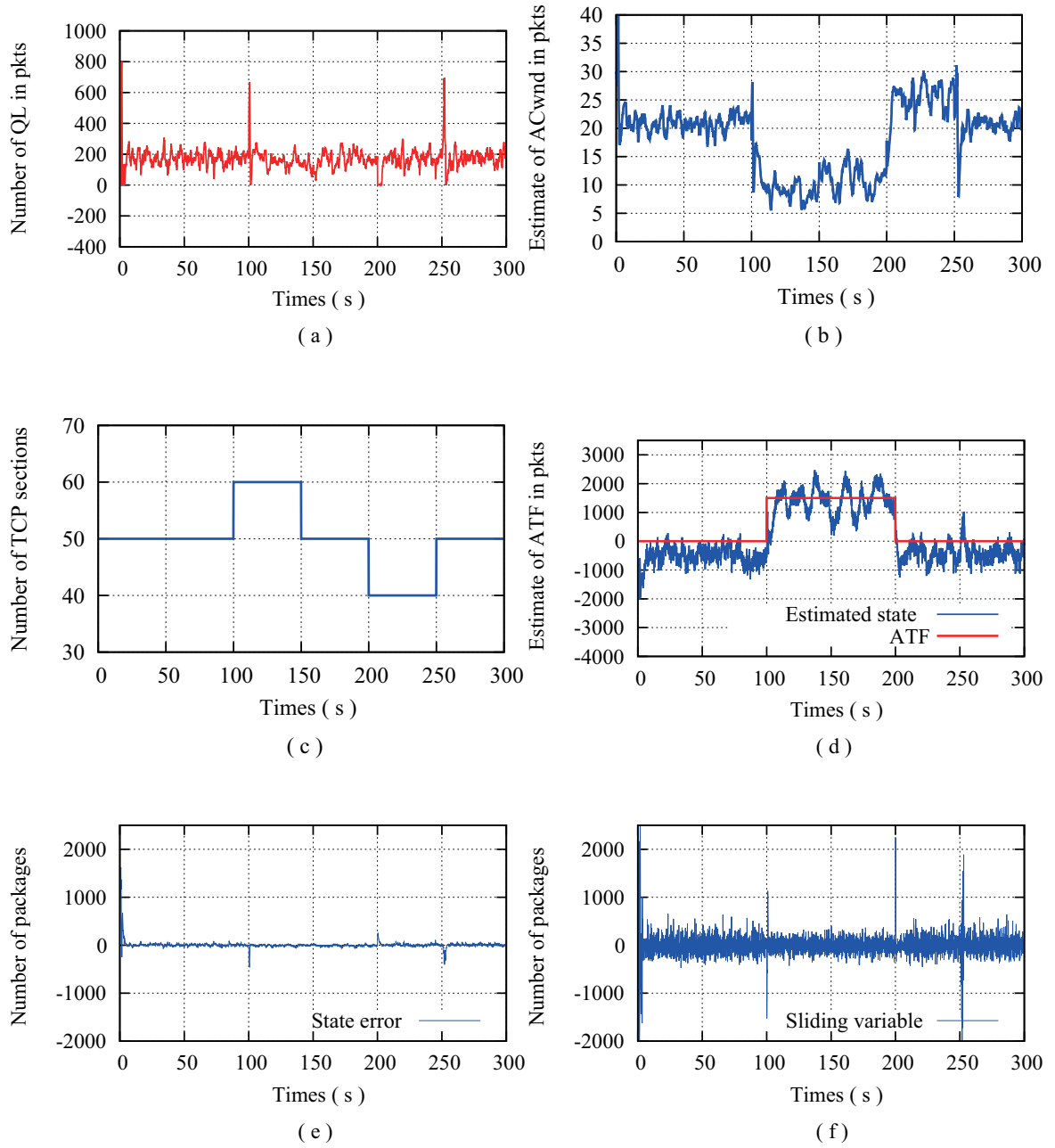


Fig. 6.2 State and control of the proposed FTSMO in Scenario 2.: (a) The number of QL  $q(t)$  in router buffer. (b) Estimated ACwnd  $w(t)$  in *packets* at the router. (b) The number of TCP sections. (d) Estimated dynamics of ATF  $d(t)$  and the true DDoS flooding rate. (e) Estimation error  $e_f^2(t)$  in *packets*. (f) The value of the sliding variable  $s_f(t)$  in *packets*.

40 – 60, while it is set as a fixed value in the previous case. By the proposed fuzzy TSMO by using fuzzy logic theory, the global observation performance is achieved that the unknown

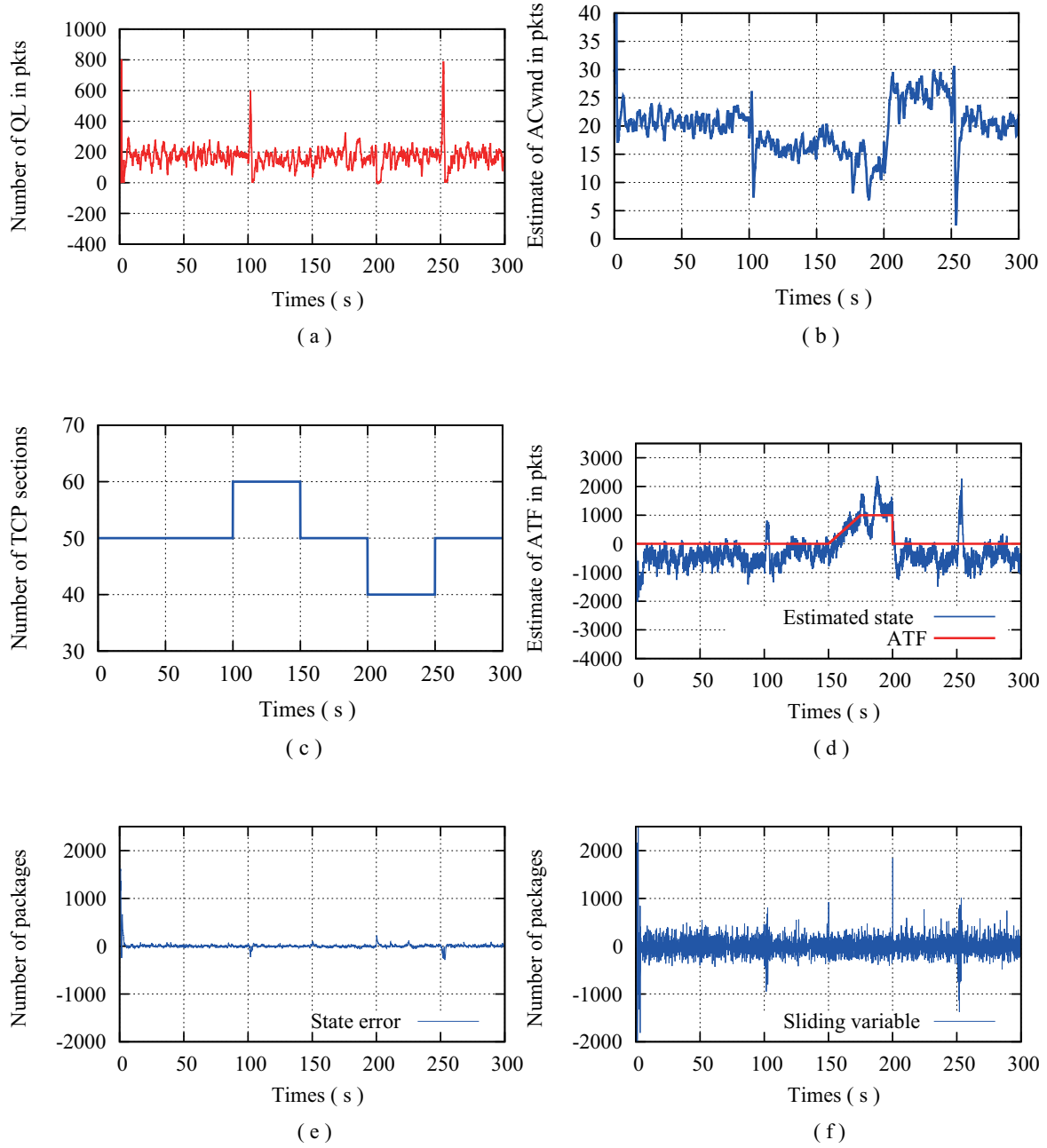


Fig. 6.3 State and control of the proposed FTSMO in Scenario 2.: (a) The number of QL  $q(t)$  in router buffer. (b) Estimated ACwnd  $w(t)$  in *packets* at the router. (b) The number of TCP sections. (d) Estimated dynamics of ATF  $d(t)$  and the true DDoS flooding rate. (e) Estimation error  $e_f^2(t)$  in *packets*. (f) The value of the sliding variable  $s_f(t)$  in *packets*.

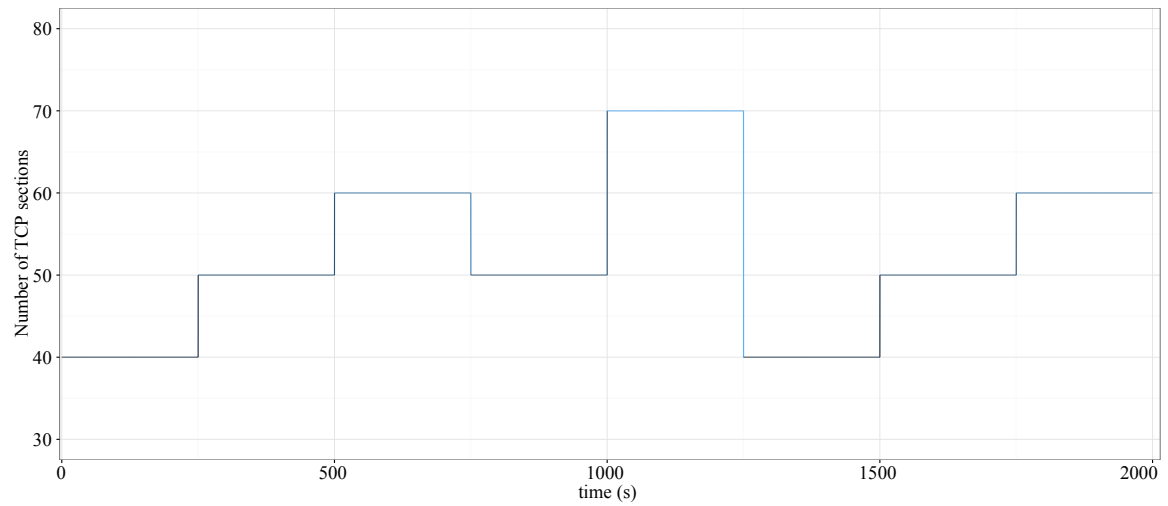


Fig. 6.4 The estimated ACwnd by the proposed Fuzzy TSMO algorithm in Scenario 3.

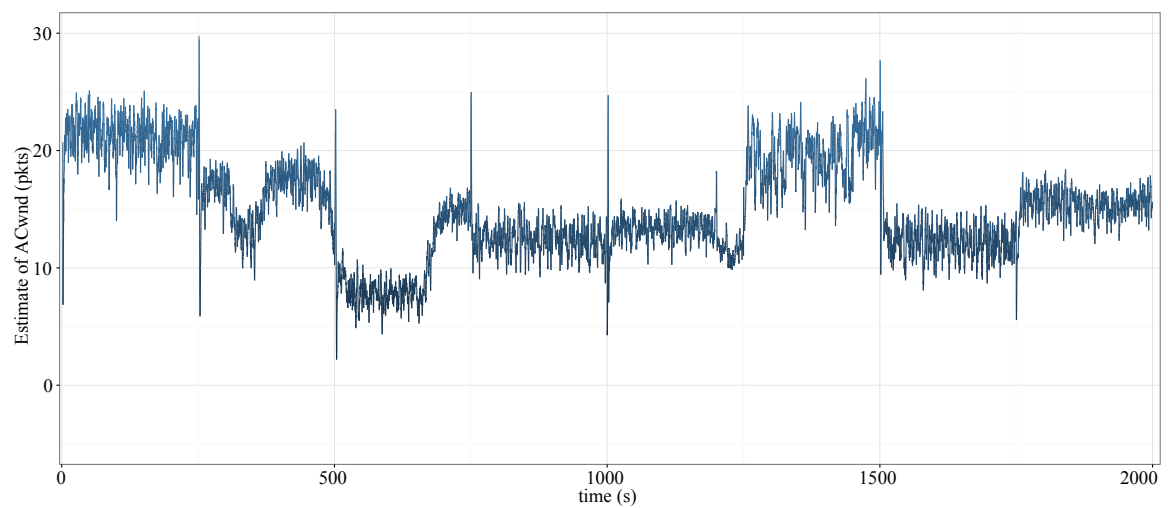


Fig. 6.5 The estimated ACwnd by the proposed Fuzzy TSMO algorithm in Scenario 3.

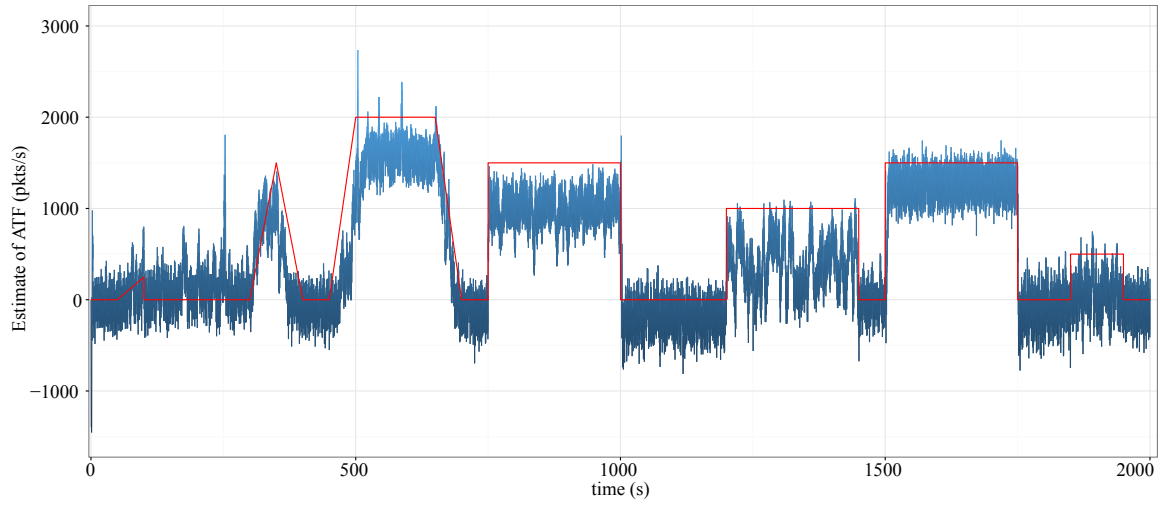


Fig. 6.6 The estimated ACwnd by the proposed Fuzzy TSMO algorithm in Scenario 3.

traffic behaviour i.e., the ACwnd and the dynamics of ATF are accurately estimated. As demonstrated in Figs. 6.2e and 6.3e, the estimation error  $e_f^2(t)$  is converged to zero in finite-time. Moreover, the sliding surface is illustrated in Figs. 6.2f and 6.3f to be reached and maintained thereafter. In addition, the ACwnd  $w(t)$  and ATF  $d(t)$  are quickly and accurately estimated as validated in Figs. 6.2b, 6.3b, 6.2d and 6.3d respectively. The global estimation of ACwnd illustrates that there exists a degradation of throughputs in hosts and link's availability in the networks.

The simulation results of the proposed fuzzy terminal sliding mode observer in scenario 3 are shown in Figs. 6.4, 6.5 and 6.6. The number of TCP sections are time-varying, as shown in Fig. 6.4. By the proposed fuzzy TSMO using fuzzy logic theory, the global performance is achieved to estimate ACwnd  $w(t)$ , as shown in Fig. 6.5. It is accurately reflect the serious degradations in sending rate, throughput and bandwidth utilization in the networks. As depicted in Fig. 6.6, the dynamics ATF  $d(t)$  generated by the mixed CBR and VBR types of traffics is quickly and accurately estimated.

### 6.4.3 Experimental Results

Performance evaluation is important for any attack defense system. Performance for detecting DDoS attacks is mainly dependent on the approach and whether it is possible to dynamically update attack traffic information [274]. When designing a DDoS attack defence mechanism, these issues should be taken into concentration to design a better defence mechanism.

This section presents the results from the study in applying the proposed RNTD algorithms to the CAIDA DDoS 2007 datasets to estimate the DDoS attacks [275]. This dataset contains approximately one hour of anonymized traffic traces from a DDoS attack on August 4, 2007 (20 : 50 : 08 UTC to 21 : 56 : 16 UTC). This type of DoS attack attempts to block access to the targeted server by consuming computing resources on the server and by consuming all of the bandwidth of the network connecting the server to the Internet. The one-hour trace is split up in 5-minute pcap files. The total size of the dataset is 5.3 *GB* (compressed; 21 *GB* uncompressed). Only attack traffic to the victim and responses to the attack from the victim are included in the traces. Non-attack traffic has as much as possible been removed. Traces in this dataset are anonymized using CryptoPAN prefix-preserving anonymization using a single key. The payload has been removed from all packets.

The network scenario in Fig. 3.2 is constructed via NS-II. There are 60 hosts and 60 clients connected via the network router. The output link capacity  $C$  of the router is set to be 15 *Mb*. The connections between each host/client and the router use full-duplex that construct bidirectional links at propagation delay  $T_p = 200$  *ms*. The maximum Cwnd  $\bar{w}$  is set to be 0.12 *Mb*. The packet size is set to be 500 *bytes*. The PI-AQM algorithm is used [125] to regulate the QL at desired level  $q_0 = 175$  packets. The buffer capacity  $\bar{q}$  is set to be 800 *packets*. Furthermore, the DDoS attack data traces of the CAIDA DDoS 2007 datasets are deployed to the traffic agent "Application/Traffic/Trace" in NS-II to generate the real DoS attacks.

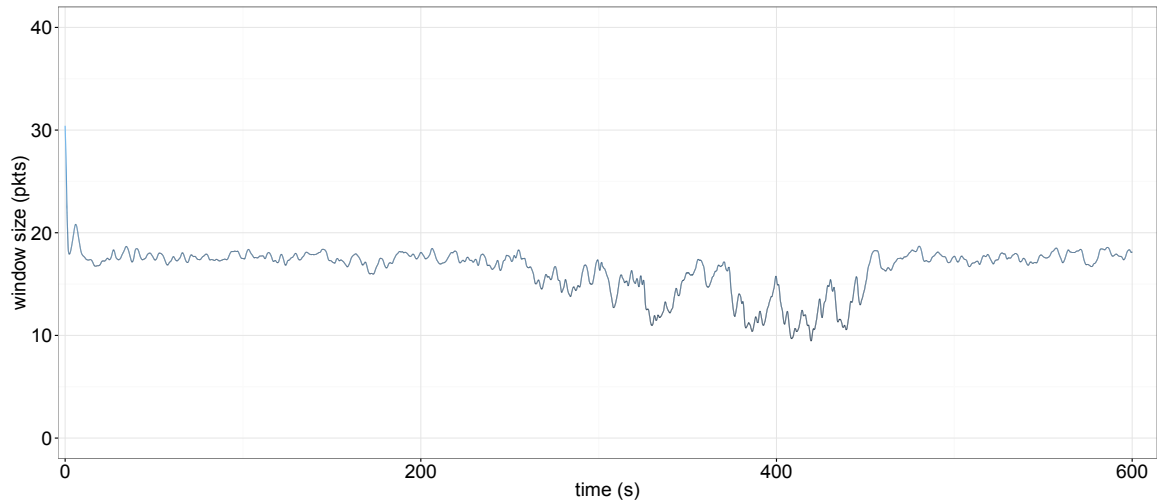


Fig. 6.7 The estimated ACwnd by the proposed Fuzzy TSMO algorithm in "CAIDA DDoS 2007 attack dataset".

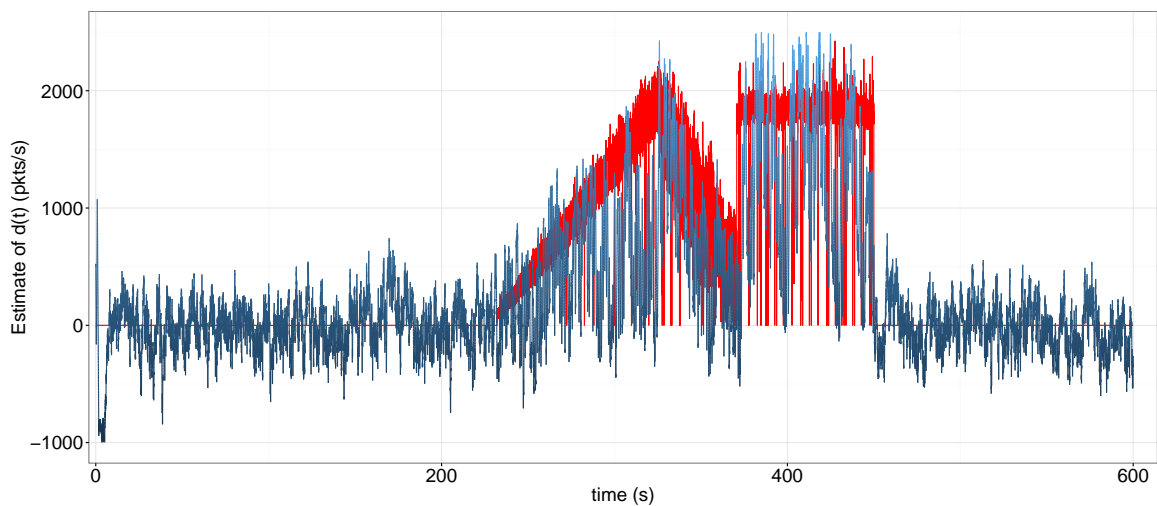


Fig. 6.8 The estimated ACwnd by the proposed Fuzzy TSMO algorithm in "CAIDA DDoS 2007 attack dataset".

The simulation results of the proposed RNT0 algorithms in "CAIDA DDoS 2007 attack dataset" are shown in Figs. 6.7 and 6.8. From Fig. 6.7, the average Cwnd is accurately estimated, which demonstrates the declines of sending rate in TCP source ends. As demonstrated in Fig. 6.8, the dynamics ATF  $d(t)$  from "CAIDA DDoS 2007 attack dataset" is quickly and accurately estimated.

## 6.5 Summary

In this chapter, a problem of the local stability in traffic estimation has been studied to develop the real-time global RNT0 schemes. The T-S fuzzy models representing the dynamics of the router-based network have been constructed by using fuzzy logic theory. Based on the models, a fuzzy terminal sliding mode observer with the fuzzy logic has been developed to achieve the real-time global performance in RNT0. Furthermore, the novel fuzzy control laws have been designed to be a smooth signal that is directly applied for estimating the dynamics of ATF without any low-pass filters. Meanwhile, the estimation error of the queue length has been guaranteed to converge to zero in a finite-time by the fuzzy control algorithms. This contribution fills a gap that is associated with the key issues of the local performance in RNT0 schemes in the present literature.





# Chapter 7

## Conclusions

This chapter presents the conclusions to the research and suggests some directions for future work. **Section 7.1** presents the overall conclusions to the research in this thesis. Moreover, **Section 7.2** concludes the thesis by pointing out possible research extensions and directions for further work.

### 7.1 Research Findings Summary

In this thesis, the real-time dynamic router-based network traffic observation methods have been proposed by using terminal sliding mode control theory. The novel methods, such as the real-time terminal sliding mode observer, full-order terminal sliding mode observer, event-triggered sliding mode observer and the fuzzy terminal sliding mode observer, have been proposed for different issues in RNTOs, where the corresponding theory and methodology have been established. The research in this thesis takes significant methodological step forward in making dynamic RNTO a possibility for network traffic observation and anomaly detection.

1. For the problem of router-based network traffic monitoring, the thesis has demonstrated that the sliding mode based observation algorithms can be adopted as real-time

dynamic RNT0 for traffic state estimation. The main contributions can be summarized as follows.

- (i) Sliding mode based observation methods are studied for traffic dynamic state estimation to address the issue of static analysis in the router-based network traffic monitoring, where the sliding mode methods are featuring the property of high robustness to network uncertainties and external disturbance.
- (ii) To solve the problem of asymptotic stability of RNT0, a novel terminal sliding mode observation framework is proposed, where the trajectory of error system is forced towards to the terminal sliding surface, once reached the surface, it will maintain there and converge to zero in a finite-time.
- (iii) For estimating the dynamics of ATF, the novel control strategy of TSMO is designed as a continuous signal that is directly used for estimation without any low-pass filter, which causes a phase lag, a long response time and inaccuracy in ATF estimation.
- (iv) To estimate the ACwnd that is unmeasurable and unknown at network routers, the estimation error of ACwnd is guaranteed asymptotically converging to zero, where the estimation accuracy is improved.

However, there are still existing some disadvantages in the sliding mode based RNT0 algorithms

- (i) Some system states are unmeasurable. Therefore, the estimation for ATF is not accurate.
- (ii) There is no control strategy for the estimation of Cwnd. The convergence speed for Cwnd estimation is too slow.
- (iii) The real-time criteria for the state estimation cannot be meet.

2. Concerning the problem of the internal dynamics in RNT0 system, a full-order terminal sliding mode based observation framework is proposed for the fast dynamic RNT0 strategy, where the goal of this framework is to accelerate the convergence rate of the internal dynamics for fast dynamic estimation. To achieve that, a novel control strategy is investigated by using the finite-time stability theory to speed up the convergence rate of the internal dynamics in the error system:

- (i) A class of systems where some system states are unmeasurable is studied to establish an observation framework, where the objective of this research is to develop the RNT0 scheme for the class of systems.
- (ii) A full-order terminal sliding mode control strategy is designed to drive the estimation error of queue length converging to zero in a finite-time to meet the time criteria in real-time estimation. Moreover, the stability of the proposed FTSMO is proved.
- (iii) The full-order control laws of the FTSMO is proposed to be a smooth control signal, which is used to estimate the dynamics of ATF for anomaly detection without any low-pass filter that can lead to phase lag.
- (iv) A novel control strategy is designed to speed up the convergence rate of the internal dynamics by using the finite-time stability theory, which accelerates the convergence in state estimation to meet the real-time requirement in RNT0.

However, some drawbacks are existed in the full order sliding mode based RNT0 algorithms

- (i) High computational load in network routers under the real time observation algorithms.
- (ii) The observation strategy is designed based on the optimal equivalent point, which may not deal with the time varying conditions in real environment.

(iii) The proposed algorithm is validated in star topology and need to consider a networked router-based network.

3. In order to improve the computational efficiency, memory saving and bandwidth utilization, the problem of algorithm-efficient RNT0 is considered. In this research, the event-triggered sliding mode based observation framework is developed to reduce the computational load and the communication burden for traffic monitoring:

(i) For the issue of high computational load in network routers, a sliding mode observer is proposed under the event triggered scheme.

(ii) The sliding mode control strategy is designed with the event-triggering criteria to reduce the computational load, while the conventional control strategy is triggered by time-driven scheme. Thereby, the periodical observation in the communication channel is replaced by the event-triggered environment to improve the efficiency of the communication resource.

(iii) To estimate the  $AC_{wnd}$  at the router, the estimation error of  $AC_{wnd}$  is guaranteed to converge to zero asymptotically under the event triggered environment.

(iv) The novel event-triggered control laws is proposed to be a continuous signal that is directly used to estimate the dynamics of ATF without any low-pass filter.

Nevertheless, some disadvantages are still existed in the event triggered sliding mode based RNT0 algorithms

(i) The sliding mode surface is designed as a linear surface, which features asymptotical convergence for state estimation.

(ii) The estimation errors cannot be driven to zero in a finite time. Moreover, the sliding variable is only stabilized into a bounded area.

- (iii) Due to its inherent features under event triggered schemes, the RNTTO may not meet the real time criteria in terms of time and accuracy in real environment.
4. In the research on fuzzy terminal sliding mode based observation strategy, the global stability of RNTTO is achieved. The T-S fuzzy models are constructed for the problem of the input-output linearisation. Moreover, the fuzzy terminal sliding mode observer is proposed based on the T-S models by using fuzzy logic theory for RNTTO applications.
- (i) Considering the problem of the input-output linearisation in RNTTO, the T-S fuzzy models for the network traffic dynamics of the interactions in a set of TCP flows are constructed by using fuzzy logic theory.
  - (ii) To achieve the global performance in estimating dynamic states in RNTTO, a real-time fuzzy terminal sliding mode observer is proposed. Moreover, the overall stability of the proposed observer is analysed and proved.
  - (iii) In the fuzzy TSMO, the estimation error of the queue length is converged to zero in a finite-time by the novel fuzzy control strategy, which accelerates the convergence rate to obtain the global performance.
  - (iv) For estimating the ATF, the fuzzy control laws are designed to be smooth to directly estimate the dynamics of ATF without any low-pass filter.
  - (v) To obtain the unmeasurable state  $ACwnd$ , the estimation error of its value is proved to converge to zero asymptotically in the fuzzy observer. Thus, global performance of QoS in the router-based network can be achieved.

However, there are still some drawbacks in the fuzzy terminal sliding mode based RNTTO schemes

- (i) The sliding-mode motion of one fuzzy set may be changed to the sliding surface of the other fuzzy set. The subsystem stability may not be guaranteed.
- (ii) There is no control strategy designed in fuzzy TSM RNT0 to accelerate the convergence speed of the estimation error for  $C_{wnd}$ .
- (iii) The global RNT0 strategy is designed in the star topology, i.e., one node in the network. It fails to deal with the global networked router based network.

## 7.2 Future Research Directions

In further research, there are many aspects to the distributed computation on router-based network traffic observation that could be studied further. A few possible directions of future research can be listed as follows.

### 7.2.1 Prototype Implementation and Analysis for RNT0

The focus of this thesis was on developing RNT0 algorithms and the analysis of the stability of the observer systems. Therefore, a real-time prototype has not yet been implemented. Building a prototype of RNT0 algorithm built-in router would pose interesting challenges, such as the efficient on-the-fly creation of time series. Even though our approach is based on a NS-2 type of information, we believe that a running prototype would benefit from using newer technologies. In addition, a prototype would bring us to investigate the usability of the system.

### 7.2.2 Global Analysis for Multi-router based RNT0

The research conducted in studying the RNT0 algorithms in a router-based network. However, we are aware that this promising result has left some global unanswered questions.

We believe that a compelling one concerns how to extend the current one-node RNTO architecture such that we can monitor and analyse the dynamics of the network traffic in the multi-router based networks. Of course, the local observation of one-node router-based RNTO are investigated in the thesis, which poses us the challenge of finding a new approach in the global view of multi-node router-based RNTO for anomaly detection.

### **7.2.3 RNTO in Software-defined Network**

Software-defined networking (SDN) is an umbrella term encompassing several kinds of network technology aimed at making the network as agile and flexible as the virtualized server and storage infrastructure of the modern data centre. The challenge is to construct the model that representing the dynamic behaviours of the network traffic in SDN. Thereafter, the another issue is to develop the real-time dynamic RNTO algorithms for anomaly detection in SDN. The key technologies for SDN implementation are functional separation, network virtualization and automation through programmability. Thus, a network administrator can monitor and management the network traffic from a centralized control console without having to touch individual RNTO routers, and can deliver observation services to wherever they are needed in the network, without regard to what specific devices a server is connected to.





# Bibliography

- [1] “International telecommunication union. ict statistics. <http://www.itu.int/itud/ict/>,” 2017.
- [2] Cisco, “Cisco visual networking index: Global mobile data traffic forecast update,” *2016–2021 White Paper*, 2017.
- [3] Internetworldstats, “<https://www.internetworldstats.com/sp/au.htm>.”
- [4] “<https://wearesocial.com/au/blog/2018/02/2018-digital-report-australia>,” *DIGITAL REPORT AUSTRALIA*, 2018.
- [5] S. Sridhar and M. Govindarasu, “Model-based attack detection and mitigation for automatic generation control,” *IEEE Transactions on Smart Grid*, vol. 5, no. 2, pp. 580–591, 2014.
- [6] A. Heydari, M. ali Tavakoli, N. Salim, and Z. Heydari, “Detection of review spam: A survey,” *Expert Systems with Applications*, vol. 42, no. 7, pp. 3634–3642, 2015.
- [7] J. Quittek, T. Zseby, B. Claise, and S. Zander, “Requirements for ip flow information export (ipfix),” *Request for Comments (RFC): 3917*, 2004.

- [8] B. Claise, B. Trammell, and P. Aitken, “Specification of the ip flow information export (ipfix) protocol for the exchange of flow information,” *Request for Comments (RFC): 7011*, 2013.
- [9] J. Rajahalme, A. Conta, B. Carpenter., and S. Deering, “Ipv6 flow label specification,” *Request for Comments (RFC): 3697*, 2004.
- [10] C. Kruegel, F. Valeur, G. Vigna, and R. Kemmerer, “Stateful intrusion detection for high-speed networks,” *Proceedings of the 2002 IEEE Symposium on Security and Privacy*, pp. 285–293, 2002.
- [11] B. Heintz, A. Chandra, R. K. Sitaraman, and J. Weissman, “End-to-end optimization for geo-distributed mapreduce,” *IEEE Transactions on Cloud Computing*, vol. 4, no. 3, pp. 293–306, 2016.
- [12] C. Kruegel, F. Valeur, and G. Vigna, *Intrusion Detection and Correlation: Challenges and Solutions*. Springer Science & Business Media, 2004.
- [13] R. Bace and P. Mell, *National Institute of Standards and Technology (NIST) Special Publication on Intrusion Detection Systems*. BOOZ-ALLEN AND HAMILTON INC MCLEAN VA, 2001.
- [14] H. J. Liao, C. H. R. Lin, Y. C. Lin, and K. Y. Tung, “Intrusion detection system: A comprehensive review,” *Journal of Network and Computer Applications*, vol. 36, no. 1, pp. 16–24, 2013.

- [15] H. Debar, M. Dacier, and A. Wespi, "Towards a taxonomy of intrusion-detection systems," *Computer Networks*, vol. 31, no. 8, pp. 805–822, 1999.
- [16] S. Axelsson, "Intrusion detection systems: A survey and taxonomy," *Technical Report*, vol. 99, 2000.
- [17] G. Creech and J. Hu, "A semantic approach to host-based intrusion detection systems using contiguous and discontiguous system call patterns," *IEEE Transactions on Computers*, vol. 63, no. 4, pp. 807–819, 2014.
- [18] C. Modi, D. Patel, B. Borisaniya, H. Patel, A. Patel, and M. Rajarajan, "A survey of intrusion detection techniques in cloud," *Journal of Network and Computer Applications*, vol. 36, no. 1, pp. 42–57, 2013.
- [19] P. Garcia-Teodoro, J. Diaz-Verdejo, G. Maciá-Fernández, and E. Vázquez, "Anomaly-based network intrusion detection: Techniques, systems and challenges," *Computers & Security*, vol. 28, no. 1–2, pp. 18–28, 2009.
- [20] V. Kumar, J. Srivastava, and A. Lazarevic, *Managing Cyber Threats: Issues, Approaches, and Challenges*. Springer Science & Business Media, 2006.
- [21] W. Li, "Using genetic algorithm for network intrusion detection," *Proceedings of the United States Department of Energy Cyber Security Group*, pp. 1–8, 2004.
- [22] R. Sekar, A. Gupta, J. Frullo, T. Shanbhag, A. Tiwari, H. Yang, and S. Zhou, "Specification-based anomaly detection: a new approach for detecting network intru-

- sions,” *Proceedings of the 9th ACM Conference on Computer and Communications Security*, pp. 265–274, 2002.
- [23] A. Sperotto, G. Schaffrath, R. Sadre, C. Morariu, A. Pras, and B. Stiller, “An overview of ip flow-based intrusion detection,” *IEEE Communications Surveys & Tutorials*, vol. 12, no. 3, pp. 343–356, 2010.
- [24] G. Vasiliadis, S. Antonatos, M. Polychronakis, E. Markatos, and S. Ioannidis, “Gnort: High performance network intrusion detection using graphics processors,” in *Recent Advances in Intrusion Detection*. Springer Berlin/Heidelberg, 2008, pp. 116–134.
- [25] Z. M. Fadlullah, T. Taleb, A. V. Vasilakos, M. Guizani, and N. Kato, “Dtrab: Combating against attacks on encrypted protocols through traffic-feature analysis,” *IEEE/ACM Transactions on Networking*, vol. 18, no. 4, pp. 1234–1247, 2010.
- [26] A. Finamore, M. Mellia, M. Meo, M. M. Munafo, P. D. Torino, and D. Rossi, “Experiences of internet traffic monitoring with tstat,” *IEEE Network*, vol. 25, no. 3, pp. 8–14, 2011.
- [27] P. Casas, A. D’Alconzo, P. Fiadino, A. Bär, A. Finamore, and T. Zseby, “When youtube does not work-analysis of qoe-relevant degradation in google cdn traffic,” *IEEE Transactions on Network & Service Management*, vol. 11, no. 4, pp. 441–457, 2014.
- [28] B. Heintz, A. Chandra, R. K. Sitaraman, and J. Weissman, “End-to-end optimiza-

- tion for geo-distributed mapreduce,” *IEEE Transactions on Cloud Computing*, vol. 4, no. 3, pp. 293–306, 2016.
- [29] S. T. Zargar, J. Joshi, and D. Tipper, “A survey of defense mechanisms against distributed denial of service (ddos) flooding attacks,” *IEEE Communications Surveys & Tutorials*, vol. 15, no. 4, pp. 2046–2069, 2013.
- [30] R. Hofstede, P. Čeleda, B. Trammell, I. Drago, R. Sadre, A. Sperotto, and A. Pras, “Flow monitoring explained: From packet capture to data analysis with netflow and ipfix,” *IEEE Communications Surveys & Tutorials*, vol. 16, no. 4, pp. 2037–2064, 2014.
- [31] N. Lasierra, Álvaro Alesanco, and J. García, “An snmp-based solution to enable remote iso/ieee 11073 technical management,” *IEEE Transactions on Information Technology in Biomedicine*, vol. 16, no. 4, pp. 709–719, 2012.
- [32] B. Claise and B. Trammell, “Information model for ip flow information export (ipfix),” *Request for Comments (RFC): 7012*, 2013.
- [33] R. Hofstede, L. Hendriks, A. Sperotto, and A. Pras, “Ssh compromise detection using netflow/ipfix,” *ACM SIGCOMM Computer Communication Review*, vol. 44, no. 5, pp. 20–26, 2014.
- [34] Q. Zheng and G. Cao, “Minimizing probing cost and achieving identifiability in probe-based network link monitoring,” *IEEE Transactions on Computers*, vol. 62, no. 3, pp. 510–523, 2013.

- [35] T. Kiravuo, M. Sarela, and J. Manner, "A survey of ethernet lan security," *IEEE Communications Surveys & Tutorials*, vol. 15, no. 3, pp. 1477–1491, 2013.
- [36] J. D. Case, M. Fedor, M. L. Schoffstall, and J. Davin, "Simple network management protocol (snmp)," *Request for Comments (RFC): 1157*, 1990.
- [37] W. Stallings, *SNMP, SNMPv2, SNMPv3, and RMON 1 and 2*. Addison-Wesley Longman Publishing Co., Inc, 1998.
- [38] S. Waldbusser, "Remote network monitoring management information base," *Request for Comments (RFC): 1757*, 1995.
- [39] D. T. Perkins, *RMON: Remote Monitoring of SNMP-Managed LANs*. Prentice Hall PTR, 1999.
- [40] B. Claise, "Cisco systems netflow services export version 9," *Request for Comments: 3954*, 2004.
- [41] M. Al-Fares, A. Loukissas, and A. Vahdat, "A scalable, commodity data center network architecture," *ACM SIGCOMM Computer Communication Review*, vol. 38, no. 4, pp. 63–74, 2008.
- [42] V. Misra, W. Gong, and D. Towsley, "Fluid-based analysis of a network of aqm routers supporting tcp flows with an application to red," *ACM SIGCOMM Computer Communication Review*, vol. 30, no. 4, pp. 151–160, 2000.
- [43] F. Zheng and J. Nelson, "An  $H^\infty$  approach to the controller design of aqm routers supporting tcp flows," *Automatica*, vol. 45, no. 3, pp. 757–763, 2009.

- [44] L. D. Cicco, Y. Gong, D. Rossi, and E. Leonardi, “A control-theoretic analysis of low-priority congestion control reprioritization under aqm,” *ACM Transactions on Modeling and Performance Evaluation of Computing Systems (TOMPECS)*, vol. 1, no. 4, pp. 17:1–33, 2016.
- [45] Y. Ariba, F. Gouaisbaut, S. Rahmé, and Y. Labit, “Traffic monitoring in transmission control protocol/active queue management networks through a time-delay observer,” *IET Control Theory & Applications*, vol. 6, no. 4, pp. 506–517, 2012.
- [46] K. Lefrouni and R. Ellaia, “Congestion control in tcp network with observer-based state-feedback and geometric considerations,” *Applied Mathematical Sciences*, vol. 9, no. 100, pp. 4987–4996, 2015.
- [47] Y. Cui, M. Fei, and D. Du, “Design of a robust observer-based memoryless  $H^\infty$  control for internet congestion,” *International Journal of Robust and Nonlinear Control*, vol. 26, no. 8, pp. 1732–1747, 2016.
- [48] X. Ma, S. M. Djouadi, and H. Li, “State estimation over a semi-markov model based cognitive radio system,” *IEEE Transactions on Wireless Communications*, vol. 11, no. 7, pp. 2391–2401, 2012.
- [49] Y. Ariba, Y. Labit, and F. Gouaisbaut, “Network anomaly estimation for tcp/aqm networks using an observer,” *Proceedings of the 3rd ACM International Workshop on Feedback Control Implementation and Design in Computing Systems and Networks*, pp. 3818–3823, 2008.

- [50] X. Cao, X. Zhou, L. Liu, and Y. Cheng, “Energy-efficient spectrum sensing for cognitive radio enabled remote state estimation over wireless channels,” *IEEE Transactions on Wireless Communications*, vol. 14, no. 4, pp. 2058–2071, 2015.
- [51] S. Rahmé, Y. Labit, and F. Gouaisbaut, “An unknown input sliding observer for anomaly detection in tcp/ip networks,” *Proceedings of International Conference on Ultra Modern Telecommunications & Workshops*, pp. 1–7, 2009.
- [52] —, “Sliding modes for anomaly observation in tcp networks: From theory to practice,” *IEEE Transactions on Control Systems Technology*, vol. 21, no. 3, pp. 1031–1038, 2013.
- [53] P. Tabuada, “Event-triggered real-time scheduling of stabilizing control tasks,” *IEEE Transactions on Automatic Control*, vol. 52, no. 9, pp. 1680–1685, 2007.
- [54] E. Kohler, J. Li, V. Paxson, and S. Shenker, “Observed structure of addresses in ip traffic,” *IEEE/ACM Transactions on Networking (TON)*, vol. 14, no. 6, pp. 1207–1218, 2006.
- [55] J. Nelson and D. P. Woodruff, “Fast manhattan sketches in data streams,” *Proceedings of the 29th ACM SIGMOD-SIGACT-SIGART Symposium on Principles of Database Systems*, pp. 99–110, 2010.
- [56] T. Kiravuo, M. Sarela, and J. Manner, “Statistical detection of congestion in routers,” *IEEE Transactions on Signal Processing*, vol. 58, no. 3, pp. 957–968, 2010.
- [57] B. Braden, D. Clark, J. Crowcroft, B. Davie, S. Deering, D. Estrin, and S. Floyd,



- “Recommendations on queue management and congestion avoidance in the internet,” *Request for Comments (RFC): 2309*, 1998.
- [58] C. Briat, E. A. Yavuz, H. Hjalmarsson, K. H. Johansson, U. T. Jönsson, G. Karlsson, and H. Sandberg, “The conservation of information, towards an axiomatized modular modeling approach to congestion control,” *IEEE/ACM Transactions on Networking*, vol. 23, no. 3, pp. 851–865, 2015.
- [59] R. R. Chen and K. Khorasani, “Markovian jump guaranteed cost congestion control strategies for large scale mobile networks with differentiated services traffic,” *Automatica*, vol. 50, no. 7, pp. 1875–1883, 2014.
- [60] J. Sijs and M. Lazar, “Event based state estimation with time synchronous updates,” *IEEE Transactions on Automatic Control*, vol. 57, no. 10, pp. 2650–2655, 2012.
- [61] S. Trimpe, “Event-based state estimation with switching static-gain observers,” *Proceedings of the 3rd IFAC Workshop on Distributed Estimation and Control in Networked Systems*, vol. 45, no. 26, pp. 91–96, 2012.
- [62] J. Weimer, J. Araújo, and K. H. Johansson, “Distributed event-triggered estimation in networked systems,” *IFAC Proceedings Volumes*, vol. 45, no. 9, pp. 178–185, 2012.
- [63] J. Wu, Q. Jia, K. H. Johansson, and L. Shi, “Event-based sensor data scheduling: Trade-off between communication rate and estimation quality,” *IEEE Transactions on Automatic Control*, vol. 58, no. 4, pp. 1041–1046, 2013.

- [64] D. Han, Y. Mo, J. Wu, S. Weerakkody, B. Sinopoli, and L. Shi, “Stochastic event-triggered sensor schedule for remote state estimation,” *IEEE Transactions on Automatic Control*, vol. 60, no. 10, pp. 2661–2675, 2015.
- [65] D. Shi, R. J. Elliott, and T. Chen, “Event-based state estimation of discrete-state hidden markov models,” *Automatica*, vol. 65, pp. 12–26, 2016.
- [66] L. Wang, Z. Wang, T. Huang, and G. Wei, “An event-triggered approach to state estimation for a class of complex networks with mixed time delays and nonlinearities,” *IEEE Transactions on Cybernetics*, vol. 46, no. 11, pp. 2497–2508, 2016.
- [67] L. Zou, Z. Wang, H. Gao, and X. Liu, “Event-triggered state estimation for complex networks with mixed time delays via sampled data information: The continuous-time case,” *IEEE Transactions on Cybernetics*, vol. 45, no. 12, pp. 2804–2815, 2015.
- [68] H. Wang, C. Yu, and Y. Jing, “Active queue management algorithm based on ts fuzzy control,” *Proceedings of 2010 Chinese Control and Decision Conference*, pp. 4095–4099, 2010.
- [69] Y. Jing, Z. Chen, and G. M. Dimirovski, “Robust fuzzy observer-based control for tcp/aqm network systems with state delay,” *Proceedings of American Control Conference (ACC)*, pp. 1350–1355, 2010.
- [70] B. A. Forouzan and S. C. Fegan, *TCP/IP Protocol Suite*. McGraw-Hill Higher Education, 2002.
- [71] M. K. Mehmet-Ali, J. F. Hayes, and A. K. Elhakeem, “Traffic analysis of a local area

- network with a star topology,” *IEEE Transactions on Communications*, vol. 36, no. 6, pp. 703–712, 1988.
- [72] M. F. Umer, M. Sher, and Y. Bi, “Flow-based intrusion detection: Techniques and challenges,” *Computers & Security*, vol. 70, pp. 238–254, 2017.
- [73] S. X. Wu and W. Banzhaf, “The use of computational intelligence in intrusion detection systems: A review,” *Applied Soft Computing*, vol. 10, no. 1, pp. 1–35, 2010.
- [74] M. Drašar, M. Vizváry, and J. Vykopal, “Similarity as a central approach to flow-based anomaly detection,” *International Journal of Network Management*, vol. 24, no. 4, pp. 318–336, 2014.
- [75] E. Vasilomanolakis, S. Karuppayah, M. Mühlhäuser, and M. Fischer, “Taxonomy and survey of collaborative intrusion detection,” *ACM Computing Surveys (CSUR)*, vol. 47, no. 4, pp. 55:1–33, 2015.
- [76] Y. Xiang, K. Li, and W. Zhou, “Low-rate ddos attacks detection and traceback by using new information metrics,” *IEEE Transactions on Information Forensics and Security*, vol. 6, no. 2, pp. 426–437, 2011.
- [77] S. S. Kim and A. N. Reddy, “A study of analyzing network traffic as images in real-time,” *Proceedings of the 24th Annual Joint Conference of the IEEE Computer and Communications Societies*, vol. 3, pp. 2056–2067, 2005.
- [78] A. J. Romiszowski, *Computer mediated communication: a selected bibliography*. Vol. 5. Educational Technology, 1992.

- 
- [79] S. Kent and K. Seo., “Security architecture for the internet protocol,” *Request for Comments (RFC): 4301*, 2005.
- [80] G. Xie, J. Su, X. Wang, T. He, G. Zhang, S. Uhlig, and K. Salamatian, “Index-trie: Efficient archival and retrieval of network traffic,” *Computer Networks*, vol. 124, pp. 140–156, 2017.
- [81] W. Aiello, C. Kalmanek, P. McDaniel, S. Sen, O. Spatscheck, and J. V. der Merwe, “Analysis of communities of interest in data networks,” *Proceedings of International Workshop on Passive and Active Network Measurement*, pp. 83–96, 2005.
- [82] P. Kalmbach, A. Blenk, M. Kluegel, and W. Kellerer, “Generating synthetic internet- and ip-topologies using the stochastic-block-model,” *Proceedings of IFIP/IEEE Symposium on Integrated Network and Service Management (IM)*, pp. 911–916, 2017.
- [83] W. Lu and A. A. Ghorbani, “Network anomaly detection based on wavelet analysis,” *EURASIP Journal on Advances in Signal Processing*, vol. 2009, no. 837601, pp. 1–16, 2009.
- [84] N. Ye, S. Vilbert, and Q. Chen, “Computer intrusion detection through ewma for autocorrelated and uncorrelated data,” *IEEE Transactions on Reliability*, vol. 52, no. 1, pp. 75–82, 2003.
- [85] A. Lakhina, M. Crovella, and C. Diot, “Mining anomalies using traffic feature distributions,” *ACM SIGCOMM Computer Communication Review*, vol. 35, no. 4, pp. 217–228, 2005.

- [86] M. Rao, Y. Chen, B. C. Vemuri, and F. Wang, “Cumulative residual entropy: a new measure of information,” *IEEE Transactions on Information Theory*, vol. 50, no. 6, pp. 1220–1228, 2004.
- [87] W. Lee and D. Xiang, “Information-theoretic measures for anomaly detection,” *Proceedings of IEEE Symposium on Security and Privacy*, pp. 130–143, 2001.
- [88] K. Xu, Z.-L. Zhang, and S. Bhattacharyya, “Profiling internet backbone traffic: behavior models and applications,” *ACM SIGCOMM Computer Communication Review*, vol. 35, no. 4, pp. 169–180, 2005.
- [89] J. Jung, V. Paxson, A. W. Berger, and H. Balakrishnan, “Fast portscan detection using sequential hypothesis testing,” *Proceedings of IEEE Symposium on Security and Privacy*, pp. 211–225, 2004.
- [90] C. C. Zou, W. Gong, D. Towsley, and L. Gao, “The monitoring and early detection of internet worms,” *IEEE/ACM Transactions on Networking (TON)*, vol. 13, no. 5, pp. 961–974, 2005.
- [91] N. Duffield, C. Lund, and M. Thorup, “Estimating flow distributions from sampled flow statistics,” *Proceedings of the Conference on Applications, Technologies, Architectures, and Protocols for Computer Communications*, pp. 325–336, 2003.
- [92] A. Sperotto, G. Schaffrath, R. Sadre, C. Morariu, A. Pras, and B. Stiller, “An overview of ip flow-based intrusion detection,” *IEEE Communications Surveys & Tutorials*, vol. 12, no. 3, pp. 343–356, 2010.

- 
- [93] N. Duffield, C. Lund, and M. Thorup, “Flow sampling under hard resource constraints,” *ACM SIGMETRICS Performance Evaluation Review*, vol. 32, no. 1, pp. 85–96, 2004.
- [94] J. Mai, A. Sridharan, C.-N. Chuah, H. Zang, and T. Ye, “Impact of packet sampling on portscan detection,” *IEEE Journal on Selected Areas in Communications*, vol. 24, no. 12, pp. 2285–2298, 2006.
- [95] W. Liu, W. Qu, J. Gong, and K. Li, “Detection of superpoints using a vector bloom filter,” *IEEE Transactions on Information Forensics and Security*, vol. 11, no. 3, pp. 514–527, 2016.
- [96] R. Schweller, Z. Li, Y. Chen, Y. Gao, A. Gupta, Y. Zhang, P. A. Dinda, M.-Y. Kao, and G. Memik, “Reversible sketches: enabling monitoring and analysis over high-speed data streams,” *IEEE/ACM Transactions on Networking (ToN)*, vol. 15, no. 5, pp. 1059–1072, 2007.
- [97] G. Cormode and S. Muthukrishnan, “An improved data stream summary: the count-min sketch and its applications,” *Journal of Algorithms*, vol. 55, no. 1, pp. 58–75, 2005.
- [98] P. Flajolet and G. N. Martin, “Probabilistic counting algorithms for data base applications,” *Journal of Computer and System Sciences*, vol. 31, no. 2, pp. 182–209, 1985.
- [99] B. Krishnamurthy, S. Sen, Y. Zhang, and Y. Chen, “Sketch-based change detection:

- methods, evaluation, and applications,” *Proceedings of the 3rd ACM SIGCOMM Conference on Internet Measurement*, pp. 234–247, 2003.
- [100] B. Landfeldt, P. Sookavatana, and A. Seneviratne, “The case for a hybrid passive/active network monitoring scheme in the wireless internet,” *Proceedings of the IEEE International Conference on Networks*, pp. 139–143, 2000.
- [101] A. W. Jackson, J. P. Sterbenz, M. N. Condell, and R. R. Hain, “Active network monitoring and control: The sencomm architecture and implementation,” *Proceedings of the DARPA Active Networks Conference and Exposition*, pp. 379–393, 2002.
- [102] S. Keshav, “Packet-pair flow control,” *IEEE/ACM Transactions on Networking*, pp. 1–45, 1995.
- [103] V. Jacobson, “Pathchar: A tool to infer characteristics of internet paths,” 1997.
- [104] N. Hu and P. Steenkiste, “Evaluation and characterization of available bandwidth probing techniques,” *IEEE Journal on Selected Areas in Communications*, vol. 21, no. 6, pp. 879–894, 2003.
- [105] R. Prasad, C. Dovrolis, M. Murray, and K. C. Claffy, “Bandwidth estimation: metrics, measurement techniques, and tools,” *IEEE Network*, vol. 17, no. 6, pp. 27–35, 2003.
- [106] V. Paxson, “Measurements and analysis of end-to-end internet dynamics,” 1997.
- [107] J. Kim, A. Chandra, and J. B. Weissman, “Passive network performance estimation for large-scale, data-intensive computing,” *IEEE Transactions on Parallel and Distributed Systems*, vol. 22, no. 8, pp. 1365–1373, 2011.

- [108] S. Seshan, M. Stemm, and R. H. Katz, "Spand: Shared passive network performance discovery," *USENIX Symposium on Internet Technologies and Systems*, pp. 1–13, 1997.
- [109] K. K. Ramakrishnan and H. Yang, "The ethernet capture effect: Analysis and solution," *Proceedings of the 19th IEEE Conference on Local Computer Networks*, pp. 228–240, 1994.
- [110] M. Zangrilli and B. B. Lowekamp, "Using passive traces of application traffic in a network monitoring system," *Proceedings of the 13th IEEE International Symposium on High Performance Distributed Computing*, pp. 77–86, 2004.
- [111] G. Jin, B. Karlo, L. Jason, and L. Craig, "Self-configuring network monitor, version 00," 5 2004. [Online]. Available: <https://www.osti.gov/servlets/purl/1230978>
- [112] M. R. Waldbusser, S., J. Case, and K. McCloghrie, "Introduction to community-based snmpv2," *Request for Comments (RFC): 1901*, 1996.
- [113] W. Stallings, "Snmpv3: A security enhancement for snmp," *IEEE Communications Surveys*, vol. 1, no. 1, pp. 2–17, 1998.
- [114] D. B. Levi, B. Stewart, and P. Meyer, "Simple network management protocol (snmp) applications," *Request for Comments (RFC): 3413*, 2002.
- [115] J. Schonwalder, A. Pras, M. Harvan, J. Schippers, and R. van de Meent, "Snmp traffic analysis: Approaches, tools, and first results," *Proceedings of the 10th IFIP/IEEE International Symposium on Integrated Network Management*, pp. 323–332, 2007.



- [116] H. Choi, N. Kim, and H. Cha, “6lowpan-snmp: Simple network management protocol for 6lowpan,” *Proceedings of the 11th IEEE International Conference on High Performance Computing and Communications*, pp. 305–313, 2009.
- [117] R. S. Moreira, R. S. Morla, L. P. Moreira, and C. Soares, “A behavioral reflective architecture for managing the integration of personal ubicomp systems: automatic snmp-based discovery and management of behavior context in smart-spaces,” *Personal and Ubiquitous Computing*, vol. 20, no. 2, pp. 229–243, 2016.
- [118] S. Waldbusser, “Remote network monitoring management information base,” *Request for Comments (RFC): 1757*, 1995.
- [119] ———, “Remote network monitoring management information base version 2,” *Request for Comments (RFC): 4502*, 2006.
- [120] C. Estan, K. Keys, D. Moore, and G. Varghese, “Building a better netflow,” *ACM SIGCOMM Computer Communication Review*, vol. 34, no. 4, pp. 245–256, 2004.
- [121] R. Hofstede, P. Čeleda, B. Trammell, I. Drago, R. Sadre, A. Sperotto, and A. Pras, “Flow monitoring explained: From packet capture to data analysis with netflow and ipfix,” *IEEE Communications Surveys & Tutorials*, vol. 16, no. 4, pp. 2037–2064, 2014.
- [122] D. van der Steeg, R. Hofstede, A. Sperotto, and A. Pras, “Real-time ddos attack detection for cisco ios using netflow,” *Proceedings of the IFIP/IEEE International Symposium on Integrated Network Management*, pp. 972–977, 2015.

- [123] M. M. Najafabadi, T. M. Khoshgoftaar, C. Calvert, and C. Kemp, "Detection of ssh brute force attacks using aggregated netflow data," *Proceedings of the 14th IEEE International Conference on Machine Learning and Applications*, pp. 283–288, 2015.
- [124] Y. Ariba, F. Gouaisbaut, and Y. Labit, "Feedback control for router management and tcp/ip network stability," *IEEE Transactions on Network and Service Management*, vol. 6, no. 4, pp. 255–266, 2009.
- [125] C. V. Hollot, V. Misra, D. Towsley, and W. Gong, "On designing improved controllers for aqm routers supporting tcp flows," *Proceedings of IEEE 20th Annual Joint Conference of the IEEE Computer and Communications Societies*, vol. 3, pp. 1726–1734, 2001.
- [126] V. Utkin, *Sliding Modes in Control and Optimization*. Springer Science & Business Media, 2013.
- [127] Y. Feng, J. Zheng, X. Yu, and N. V. Truong, "Hybrid terminal sliding-mode observer design method for a permanent-magnet synchronous motor control system," *IEEE Transactions on Industrial Electronics*, vol. 56, no. 9, pp. 3424–3431, 2009.
- [128] A. Levant, "Homogeneity approach to high-order sliding mode design," *Automatica*, vol. 41, no. 5, pp. 823–830, 2005.
- [129] Y. Shtessel, C. Edwards, L. Fridman, and A. Levant, *Sliding Mode Control and Observation*. New York, NY, USA: Birkhäuser, 2014.
- [130] Q. Xu, "Digital sliding-mode control of piezoelectric micropositioning system based

- on input–output model,” *IEEE Transactions on Industrial Electronics*, vol. 61, no. 10, pp. 5517–5526, 2014.
- [131] V. Jacobson and R. T. Braden, “Tcp extensions for long-delay paths,” *Request for Comments (RFC): 1072*, 1988.
- [132] C. Chen, T. Wu, W. Lee, H. Chao, and J. Chiang, “Qos-based active dropping mechanism for ngn video streaming optimization,” *The Knowledge Engineering Review*, vol. 29, no. 4, pp. 484–495, 2014.
- [133] R. Jain, “Congestion control in computer networks: Issues and trends,” *IEEE Network Magazine*, vol. 4, no. 3, pp. 24–30, 1990.
- [134] M. Arpaci and J. A. Copeland, “An adaptive queue management method for congestion avoidance in tcp/ip networks,” *Proceedings of the IEEE Global Telecommunications Conference*, vol. 1, pp. 309–315, 2000.
- [135] I. D. Barrera, S. Bohacek, and G. R. Arce, “Statistical detection of congestion in routers,” *IEEE Transactions on Signal Processing*, vol. 58, no. 3, pp. 957–968, 2010.
- [136] J. Wang, L. Rong, and Y. Liu, “A robust proportional controller for aqm based on optimized second-order system model,” *Computer Communications*, vol. 31, no. 10, pp. 2468–2477, 2008.
- [137] S. H. Low and D. E. Lapsley, “Optimization flow control. i. basic algorithm and convergence,” *IEEE/ACM Transactions on Networking*, vol. 7, no. 6, pp. 861–874, 1999.

- [138] S. Athuraliya, V. H. Li, S. H. Low, and Q. Yin, "Rem: Active queue management," *Teletraffic Science and Engineering*, vol. 4, pp. 817–828, 2001.
- [139] S. Floyd, R. Gummadi, and S. Shenker, "Adaptive red: An algorithm for increasing the robustness of red's active queue management," pp. 518–522, 2001.
- [140] J. Sun and M. Zukerman, "Raq: A robust active queue management scheme based on rate and queue length," *Computer Communications*, vol. 30, no. 8, pp. 1731–1741, 2007.
- [141] W. Wang, Q. Chen, W. Chen, and Y. Jiang, "The stability of tcp/rem congestion control mechanism," *Journal of Information & Computational Science*, vol. 8, no. 14, pp. 2925–2932, 2011.
- [142] S. S. Kunniyur and R. Srikant, "An adaptive virtual queue (avq) algorithm for active queue management," *IEEE/ACM Transactions on Networking*, vol. 12, no. 2, pp. 286–299, 2004.
- [143] C. Long, B. Zhao, and X. Guan, "Savq: stabilized adaptive virtual queue management algorithm," *IEEE Communications Letters*, vol. 9, no. 1, pp. 78–80, 2005.
- [144] L. Tan, Y. Yang, C. Lin, N. Xiong, and M. Zukerman, "Scalable parameter tuning for avq," *IEEE Communications Letters*, vol. 9, no. 1, pp. 90–92, 2005.
- [145] X. Deng, S. Yi, G. Kesidis, and C. R. Das, "Stabilized virtual buffer (svb)-an active queue management scheme for internet quality-of-service," *Proceedings of the IEEE Global Telecommunications Conference*, vol. 2, pp. 1628–1632, 2002.

- [146] ———, “Class-based stabilized virtual buffer-an aqm scheme with stability, fairness and qos assurance,” *Teletraffic Science and Engineering*, vol. 5, pp. 1281–1290, 2003.
- [147] J. Aweya, M. Ouellette, and D. Y. Montuno, “A control theoretic approach to active queue management,” *Computer Networks*, vol. 36, no. 2–3, pp. 203–235, 2001.
- [148] C. V. Hollot, V. Misra, D. Towsley, and W. Gong, “Analysis and design of controllers for aqm routers supporting tcp flows,” *IEEE Transactions on Automatic Control*, vol. 47, no. 6, pp. 945–959, 2002.
- [149] S. Ryu, C. Rump, and C. Qiao, “A predictive and robust active queue management for internet congestion control,” *Proceedings of the Eighth IEEE International Symposium on Computers and Communication*, pp. 991–998, 2003.
- [150] D. Agrawal and F. Granelli, “Redesigning an active queue management system,” *Proceedings of the IEEE Global Telecommunications Conference*, no. 2–3, pp. 702–706, 2004.
- [151] S. Ryu and C. Cho, “Pi-pd-controller for robust and adaptive queue management for supporting tcp congestion control,” *Proceedings of the 37th IEEE Annual Simulation Symposium*, pp. 132–139, 2004.
- [152] Y. Hong and O. W. Yang, “Adaptive aqm controllers for ip routers with a heuristic monitor on tcp flows,” *International Journal of Communication Systems*, vol. 19, no. 1, pp. 17–38, 2006.

- [153] X. Chang and J. K. Muppala, "A robust nonlinear pi controller for improving aqm performance," *Proceedings of the IEEE International Conference on Communications*, vol. 4, pp. 2272–2276, 2004.
- [154] Y. Hong, O. W. Yang, and C. Huang, "Self-tuning pi tcp flow controller for aqm routers with interval gain and phase margin assignment," *Proceedings of the IEEE Global Telecommunications Conference*, vol. 3, pp. 1324–1328, 2004.
- [155] D. Ustebay, "Switching resilient pi controllers for active queue management of tcp flows," *Proceedings of the IEEE International Conference on Networking, Sensing and Control*, pp. 574–578, 2007.
- [156] S. Mascolo, "Modeling the internet congestion control using a smith controller with input shaping," *Control Engineering Practice*, vol. 14, no. 4, pp. 425–435, 2006.
- [157] H. U. 'Unal, B. Ataslar, A. Iftar, and H. 'Ozbay, "H $\infty$ -based flow control in data-communication networks with multiple time-delays," *Teknik Rapor*, 2006.
- [158] A. Pietrabissa, F. D. Priscoli, A. Fiaschetti, and F. D. Paolo, "A robust adaptive congestion control for communication networks with time-varying delays," *Proceedings of the IEEE International Conference on Control Applications, IEEE International Symposium on Intelligent Control*, pp. 2093–2098, 2006.
- [159] P.-F. Quet, B. AtasLar, A. Iftar, H. 'OZbay, S. Kalyanaraman, and T. Kang, "Rate-based flow controllers for communication networks in the presence of uncertain time-varying multiple time-delays," *Automatica*, vol. 38, no. 6, pp. 917–928, 2002.

- [160] T. Ren, G. M. Dimirovski, and Y.-W. Jing, "Abr traffic control over atm network using fuzzy immune-pid controller," *Proceedings of the American Control Conference*, pp. 4876–4881, 2006.
- [161] L. He, Y. Zhou, Y. Jing, and H. Zhu, "A vrc algorithm based on fuzzy immune pid-smith," in *Intelligent Control and Automation*. Springer, Berlin, Heidelberg, 2006, pp. 463–468.
- [162] P. Baburaj, S. Kamal, and B. Bandyopadhyay, "Higher order sliding mode-based robust stabilisation of fluid-flow model of tcp/aqm scheme," *International Journal of Automation and Control*, vol. 8, no. 1, pp. 17–31, 2014.
- [163] K. Rahnamai, K. Gorman, and A. Gray, "Model predictive neural control of tcp flow in aqm network," *Proceedings of the Annual Meeting of the North American Fuzzy Information Processing Society*, pp. 493–498, 2006.
- [164] B. Hariri and N. Sadati, "Nn-red: an aqm mechanism based on neural networks," *Electronics Letters*, vol. 43, no. 19, pp. 1053–1055, 2007.
- [165] M. Sheikhan, R. Shahnazi, and E. Hemmati, "Adaptive active queue management controller for tcp communication networks using pso-rbf models," *Neural Computing and Applications*, vol. 22, no. 5, pp. 933–945, 2013.
- [166] Y. Qiao and H. Xiaojuan, "A new pid controller for aqm based on neural network," *Proceedings of the IEEE International Conference on Intelligent Computing and Intelligent Systems*, vol. 1, pp. 804–808, 2010.

- [167] X. Liu, J. Hu, S. Wang, H. Li, and H. Zhao, "Research of aqm strategy based on improved neuron adaptive pid," *Proceedings of the IEEE International Conference on Computer Science and Information Technology*, pp. 147–151, 2008.
- [168] J. Sun and M. Zukerman, "An adaptive neuron aqm for a stable internet," *Proceedings of the International Conference on Research in Networking*, pp. 844–854, 2007.
- [169] C. Zhou, D. Di, Q. Chen, and J. Guo, "An adaptive aqm algorithm based on neuron reinforcement learning," *Proceedings of the IEEE International Conference on Control and Automation*, pp. 1342–1346, 2009.
- [170] Q. Yan and Q. Lei, "A new active queue management algorithm based on self-adaptive fuzzy neural-network pid controller," *Proceedings of the IEEE International Conference on Internet Technology and Applications*, pp. 1–4, 2011.
- [171] H. H. Choi, "Robust stabilization of uncertain fuzzy systems using variable structure system approach," *IEEE Transactions on Fuzzy Systems*, vol. 16, no. 3, pp. 715–724, 2008.
- [172] J. Qiu, G. Feng, and J. Yang, "A new design of delay-dependent robust  $h_\infty$  filtering for discrete-time t-s fuzzy systems with time-varying delay," *IEEE Transactions on Fuzzy Systems*, vol. 17, no. 5, pp. 1044–1058, 2009.
- [173] X. Su, L. Wu, P. Shi, and C. P. Chen, "Model approximation for fuzzy switched systems with stochastic perturbation," *IEEE Transactions on Fuzzy Systems*, vol. 23, no. 5, pp. 1458–1473, 2015.



- [174] B. Niu and L. Li, “Adaptive backstepping-based neural tracking control for mimo nonlinear switched systems subject to input delays,” *IEEE Transactions on Neural Networks and Learning Systems*, DOI: 10.1109/TNNLS.2017.2690465, 2017.
- [175] D. J. Choi and P. Park, “Guaranteed cost controller design for discrete-time switching fuzzy systems,” *IEEE Transactions on Systems, Man, and Cybernetics, Part B (Cybernetics)*, vol. 34, no. 1, pp. 110–119, 2004.
- [176] W. Xiong, W. Yu, J. Lu, and X. Yu, “Fuzzy modelling and consensus of nonlinear multiagent systems with variable structure,” *IEEE Transactions on Circuits and Systems I: Regular Papers*, vol. 61, no. 4, pp. 1183–1191, 2014.
- [177] X. Zhu, H. Lin, and X. Xie, “Sampled-data fuzzy stabilization of nonlinear systems under nonuniform sampling,” *IEEE Transactions on Fuzzy Systems*, vol. 24, no. 6, pp. 1654–1667, 2016.
- [178] H. Li, J. Wang, L. Wu, H.-K. Lam, and Y. Gao, “Optimal guaranteed cost sliding mode control of interval type-2 fuzzy time-delay systems,” *IEEE Transactions on Fuzzy Systems*, vol. 26, no. 1, pp. 246–257, 2018.
- [179] Y. Wang, H. Shen, H. R. Karimi, and D. Duan, “Dissipativity-based fuzzy integral sliding mode control of continuous-time ts fuzzy systems,” *IEEE Transactions on Fuzzy Systems*, DOI: 10.1109/TFUZZ.2017.2710952, 2018.
- [180] P. K. Singh and S. K. Gupta, “Variable length virtual output queue based fuzzy con-

- gestion control at routers,” *Proceedings of the IEEE 3rd International Conference on Communication Software and Networks*, pp. 29–33, 2011.
- [181] C. Wang, B. Li, K. Sohraby, and Y. Peng, “Afred: An adaptive fuzzy-based control algorithm for active queue management,” *Proceedings of the 28th Annual IEEE International Conference on Local Computer Networks*, pp. 12–20, 2003.
- [182] S. Ghosh, Q. Razouqi, H. J. Schumacher, and A. Celmins, “A survey of recent advances in fuzzy logic in telecommunications networks and new challenges,” *IEEE Transactions on Fuzzy Systems*, vol. 6, no. 3, pp. 443–447, 1998.
- [183] J. Sun, M. Zukerman, and M. Palaniswami, “Stabilizing red using a fuzzy controller,” *Proceedings of the IEEE International Conference on Communications*, pp. 266–271, 2007.
- [184] M. Baklizi, H. Abdel-Jaber, A. A. Abu-Shareha, M. M. Abualhaj, and S. Ramadass, “Fuzzy logic controller of gentle random early detection based on average queue length and delay rate,” *International Journal of Fuzzy Systems*, vol. 16, no. 1, pp. 9–19, 2014.
- [185] G. Di Fatta, F. Hoffmann, G. L. Re, and A. Urso, “A genetic algorithm for the design of a fuzzy controller for active queue management,” *IEEE Transactions on Systems, Man, and Cybernetics, Part C (Applications and Reviews)*, vol. 33, no. 3, pp. 313–324, 2003.
- [186] C. Xu and F. Li, “A congestion control algorithm of fuzzy control in routers,” *Pro-*

- ceedings of the 4th International Conference on Wireless Communications, Networking and Mobile Computing*, pp. 1–4, 2008.
- [187] S. S. Masoumzadeh, G. Taghizadeh, K. Meshgi, and S. Shiry, “Deep blue: A fuzzy q-learning enhanced active queue management scheme,” *Proceedings of the International Conference on Adaptive and Intelligent Systems*, pp. 43–48, 2009.
- [188] C. N. Nyirenda and D. S. Dawoud, “Multi-objective particle swarm optimization for fuzzy logic based active queue management,” *Proceedings of the International Conference on Fuzzy Systems*, pp. 2231–2238, 2006.
- [189] S. Mohammadi, H. M. Pour, M. Jafari, and A. Javadi, “Fuzzy-based pid active queue manager for tcp/ip networks,” *Proceedings of the 10th IEEE International Conference on Information Sciences Signal Processing and their Applications*, pp. 434–439, 2010.
- [190] C. Zhou and X. Li, “A robust aqm algorithm based on fuzzy-inference,” *Proceedings of the IEEE 10th International Conference on Measuring Technology and Mechatronics Automation*, vol. 2, pp. 534–537, 2009.
- [191] P. K. Singh and S. K. Gupta, “Variable length virtual output queue based fuzzy congestion control at routers,” *Proceedings of the IEEE 3rd International Conference on Communication Software and Networks*, pp. 29–33, 2011.
- [192] Q. Yan and Q. Lei, “A new active queue management algorithm based on self-

- adaptive fuzzy neural-network pid controller,” *Proceedings of the International Conference on Internet Technology and Applications*, pp. 1–4, 2011.
- [193] Y. Qiao and H. Xiaojuan, “A new pid controller for aqm based on neural network,” *Proceedings of the IEEE International Conference on Intelligent Computing and Intelligent Systems*, vol. 1, pp. 804–808, 2010.
- [194] F. Yanfei, R. Fengyuan, and L. Chuang, “Design of an active queue management algorithm based fuzzy logic decision,” *Proceedings of the IEEE International Conference on Communication Technology Proceedings*, vol. 1, pp. 286–289, 2003.
- [195] Y. H. Aoul, A. Nafaa, D. Négru, and A. Mehaoua, “Fafc: fast adaptive fuzzy aqm controller for tcp/ip networks,” *Proceedings of the IEEE Global Telecommunications Conference*, vol. 3, pp. 1319–1323, 2004.
- [196] M. H. Yaghmaee and H. S. Farmad, “Improving the loss performance of random early detection gateway using fuzzy logic control,” *Proceedings of the IEEE 9th International Symposium on Computers and Communications*, vol. 2, pp. 927–932, 2004.
- [197] C. Luo and C. Ran, “An adaptive retransmission and active drop mechanism based on fuzzy logic,” *Proceedings of the IEEE Asia-Pacific Radio Science Conference*, pp. 162–165, 2004.
- [198] F. Ren, C. Lin, and B. Wei, “A robust active queue management algorithm in large delay networks,” *Computer Communications*, vol. 28, no. 5, pp. 485–493, 2005.
- [199] P. Yan, Y. Gao, and H. Ozbay, “A variable structure control approach to active queue

- management for tcp with ecn,” *IEEE Transactions on Control Systems Technology*, vol. 13, no. 2, pp. 203–215, 2005.
- [200] Y. Jing, N. Yu, Z. Kong, and G. M. Dimirovski, “Active queue management algorithm based on fuzzy sliding model controller,” *IFAC Proceedings Volumes*, vol. 41, no. 2, pp. 6148–6153, 2008.
- [201] N. Zhang, Y. Jing, M. Yang, and S. Zhang, “Robust aqm controller design for diffserv network using sliding mode control,” *IFAC Proceedings Volumes*, vol. 41, no. 2, pp. 5635–5639, 2008.
- [202] N. Zhang, M. Yang, Y. Jing, and S. Zhang, “Zheng, xiuping, nannan zhang, georigi m. dimirovski, and yuanwei jing,” *IFAC Proceedings Volumes*, vol. 41, no. 2, pp. 12 983–12 987, 2008.
- [203] —, “Congestion control for diffserv network using second-order sliding mode control,” *IEEE Transactions on Industrial Electronics*, vol. 56, no. 9, pp. 3330–3336, 2009.
- [204] F. Yin, G. M. Dimirovski, and Y. Jing, “Robust stabilization of uncertain input delay for internet congestion control,” *Proceedings of the American Control Conference*, pp. 5576–5580, 2006.
- [205] H. Wang, Y. Jing, Y. Zhou, Z. Chen, and X. Liu, “Active queue management algorithm based on fuzzy sliding model controller,” *IFAC Proceedings Volumes*, vol. 41, no. 2, pp. 12 013–12 018, 2008.

- [206] Y. Jing, L. He, G. M. Dimirovski, and H. Yu Zhu, "Robust stabilization of state and input delay for active queue management algorithm," *Proceedings of the IEEE American Control Conference*, pp. 3083–3087, 2007.
- [207] M. Yan, T. D. Kolemisevska-Gugulovska, Y. Jing, and G. Dimirovski, "Robust discrete-time sliding mode control algorithm for tcp networks congestion control," *Proceedings of the IEEE 8th International Conference on Telecommunications in Modern Satellite, Cable and Broadcasting Services*, pp. 393–396, 2007.
- [208] Y. Zhou, H. Wang, Y. Jing, and X. Liu, "Observer-based robust controller design for active queue management," *IFAC Proceedings Volumes*, vol. 41, no. 2, pp. 12 007–12 012, 2008.
- [209] A. K. Behera and B. Bandyopadhyay, "Self-triggering-based sliding-mode control for linear systems," *IET Control Theory & Applications*, vol. 9, no. 17, pp. 2541–2547, 2015.
- [210] —, "Robust sliding mode control: an event-triggering approach," *IEEE Transactions on Circuits and Systems II: Express Briefs*, vol. 64, no. 2, pp. 146–150, 2017.
- [211] S. Wen, T. Huang, X. Yu, M. Z. Chen, and Z. Zeng, "Sliding-mode control of memristive chua's systems via the event-based method," *IEEE Transactions on Circuits and Systems II: Express Briefs*, vol. 64, no. 1, pp. 81–85, 2017.
- [212] S. V. Emelyanov, "Control of first order delay systems by means of an astatic con-

- troller and nonlinear correction,” *Automation and Remote Control*, pp. 983–991, 1959.
- [213] ———, *Variable structure control systems*. Moscow, Nauka, 1967.
- [214] S. V. Emelyanov, V. I. Utkin, V. A. Taran, N. E. Kostyleva, A. M. Shubladze, and V. B. Ezerov, *Theory of variable structure systems*. Moscow, Nauka, 1970.
- [215] V. Utkin, “Variable structure systems with sliding modes,” *IEEE Transactions on Automatic Control*, vol. 22, no. 2, pp. 212–222, 1977.
- [216] C. Edwards and S. Spurgeon, *Sliding Mode Control: Theory and Applications*. Crc Press, 1998.
- [217] A. Levant, “Sliding order and sliding accuracy in sliding mode control,” *International Journal of Control*, vol. 58, no. 6, pp. 1247–1263, 1993.
- [218] G. Bartolini, A. Ferrara, and E. Usai, “Chattering avoidance by second-order sliding mode control,” *IEEE Transactions on Automatic Control*, vol. 43, no. 2, pp. 241–246, 1998.
- [219] A. Levant, “Universal siso sliding-mode controllers with finite-time convergence,” *IEEE Transactions on Automatic Control*, vol. 46, no. 9, pp. 1447–1451, 2001.
- [220] E. Kayacan, Y. Oniz, and O. Kaynak, “A grey system modeling approach for sliding-mode control of antilock braking system,” *IEEE Transactions on Industrial Electronics*, vol. 56, no. 8, pp. 3244–3252, 2009.

- [221] Y. Xia, Z. Zhu, M. Fu, and S. Wang, "Attitude tracking of rigid spacecraft with bounded disturbances," *IEEE Transactions on Industrial Electronics*, vol. 58, no. 2, pp. 647–659, 2011.
- [222] E. Kayacan, O. Cigdem, and O. Kaynak, "Sliding mode control approach for online learning as applied to type-2 fuzzy neural networks and its experimental evaluation," *IEEE Transactions on Industrial Electronics*, vol. 59, no. 9, pp. 3510–3520, 2012.
- [223] A. Levant, "Robust exact differentiation via sliding mode technique," *Automatica*, vol. 34, no. 3, pp. 379–384, 1998.
- [224] Y. B. Shtessel, I. A. Shkolnikov, and M. D. Brown, "An asymptotic second-order smooth sliding mode control," *Asian Journal of Control*, vol. 5, no. 4, pp. 498–504, 2003.
- [225] A. Levant, "Principles of 2-sliding mode design," *Automatica*, vol. 43, no. 4, pp. 576–586, 2007.
- [226] Y. Feng, J. Zheng, X. Yu, and N. V. Truong, "On nonsingular terminal sliding-mode control of nonlinear systems," *Automatica*, vol. 49, no. 6, pp. 1715–1722, 2013.
- [227] Y. Feng, F. Han, and X. Yu, "Chattering free full-order sliding-mode control," *Automatica*, vol. 50, no. 4, pp. 1310–1314, 2014.
- [228] H. Wang, Z. Man, H. Kong, Y. Zhao, M. Yu, Z. Cao, J. Zheng, and M. T. Do, "Design and implementation of adaptive terminal sliding-mode control on a steer-by-wire



- equipped road vehicle,” *IEEE Transactions on Industrial Electronics*, vol. 63, no. 9, pp. 5774–5785, 2016.
- [229] G. Chen, Y. Song, and Y. Guan, “Terminal sliding mode-based consensus tracking control for networked uncertain mechanical systems on digraphs,” *IEEE Transactions on Neural Networks and Learning Systems*, vol. 29, no. 3, pp. 749–756, 2018.
- [230] Q. Xu, “Piezoelectric nanopositioning control using second-order discrete-time terminal sliding-mode strategy,” *IEEE Transactions on Industrial Electronics*, vol. 62, no. 12, pp. 7738–7748, 2015.
- [231] T. Madani, B. Daachi, and K. Djouani, “Modular-controller-design-based fast terminal sliding mode for articulated exoskeleton systems,” *IEEE Transactions on Control Systems Technology*, vol. 25, no. 3, pp. 1133–1140, 2017.
- [232] C. U. Solis, J. B. Clempner, and A. S. Poznyak, “Fast terminal sliding-mode control with an integral filter applied to a van der pol oscillator,” *IEEE Transactions on Industrial Electronics*, vol. 64, no. 7, pp. 5622–5628, 2017.
- [233] J. Zheng, H. Wang, Z. Man, J. Jin, and M. Fu, “Robust motion control of a linear motor positioner using fast nonsingular terminal sliding mode,” *IEEE/ASME Transactions on Mechatronics*, vol. 20, no. 4, pp. 1743–1752, 2015.
- [234] Y. Feng, X. Yu, and Z. Man, “Non-singular terminal sliding mode control of rigid manipulators,” *Automatica*, vol. 38, no. 12, pp. 2159–2167, 2002.

- [235] M. Jin, J. Lee, and K. K. Ahn, “Continuous nonsingular terminal sliding-mode control of shape memory alloy actuators using time delay estimation,” *IEEE/ASME Transactions on Mechatronics*, vol. 20, no. 2, pp. 899–909, 2015.
- [236] S. S.-D. Xu, C.-C. Chen, and Z.-L. Wu, “Study of nonsingular fast terminal sliding-mode fault-tolerant control,” *IEEE Transactions on Industrial Electronics*, vol. 62, no. 6, pp. 3906–3913, 2015.
- [237] ———, “Study of nonsingular fast terminal sliding-mode fault-tolerant control,” *IEEE Transactions on Industrial Electronics*, vol. 62, no. 6, pp. 3906–3913, 2015.
- [238] M. Van, S. S. Ge, and H. Ren, “Finite time fault tolerant control for robot manipulators using time delay estimation and continuous nonsingular fast terminal sliding mode control,” *IEEE Transactions on Cybernetics*, vol. 47, no. 7, pp. 1681–1693, 2017.
- [239] J. Lee, P. H. Chang, and M. Jin, “Adaptive integral sliding mode control with time-delay estimation for robot manipulators,” *IEEE Transactions on Industrial Electronics*, vol. 64, no. 8, pp. 6796–6804, 2017.
- [240] R. Cui, L. Chen, C. Yang, and M. Chen, “Extended state observer-based integral sliding mode control for an underwater robot with unknown disturbances and uncertain nonlinearities,” *IEEE Transactions on Industrial Electronics*, vol. 64, no. 8, pp. 6785–6795, 2017.
- [241] V. Parra-Vega, S. Arimoto, Y.-H. Liu, G. Hirzinger, and P. Akella, “Dynamic slid-

- ing pid control for tracking of robot manipulators: Theory and experiments,” *IEEE Transactions on Robotics and Automation*, vol. 19, no. 6, pp. 967–976, 2003.
- [242] G. P. Incremona, A. Ferrara, and L. Magni, “Mpc for robot manipulators with integral sliding modes generation,” *IEEE/ASME Transactions on Mechatronics*, vol. 22, no. 3, pp. 1299–1307, 2017.
- [243] Q. Xu, “Continuous integral terminal third-order sliding mode motion control for piezoelectric nanopositioning system,” *IEEE/ASME Transactions on Mechatronics*, vol. 22, no. 4, pp. 1828–1838, 2017.
- [244] —, “Digital integral terminal sliding mode predictive control of piezoelectric-driven motion system,” *IEEE Transactions on Industrial Electronics*, vol. 63, no. 6, pp. 3976–3984, 2016.
- [245] S. Yin and B. Xiao, “Tracking control of surface ships with disturbance and uncertainties rejection capability,” *IEEE/ASME Transactions on Mechatronics*, vol. 22, no. 3, pp. 1154–1162, 2017.
- [246] G. P. Incremona, M. Rubagotti, and A. Ferrara, “Sliding mode control of constrained nonlinear systems,” *IEEE Transactions on Automatic Control*, vol. 62, no. 6, pp. 2965–2972, 2017.
- [247] J. Zhang, X. Liu, Y. Xia, Z. Zuo, and Y. Wang, “Disturbance observer-based integral sliding-mode control for systems with mismatched disturbances,” *IEEE Transactions on Industrial Electronics*, vol. 63, no. 11, pp. 7040–7048, 2016.

- [248] Y. Cao and X. B. Chen, "Disturbance-observer-based sliding-mode control for a 3-dof nanopositioning stage," *IEEE/ASME Transactions on Mechatronics*, vol. 19, no. 3, pp. 924–931, 2014.
- [249] N. M. Dehkordi, N. Sadati, and M. Hamzeh, "A robust backstepping high-order sliding mode control strategy for grid-connected dg units with harmonic/interharmonic current compensation capability," *IEEE Transactions on Sustainable Energy*, vol. 8, no. 2, pp. 561–572, 2017.
- [250] S. Saks, *Theory of the Integral*. Inc. New York, 1964.
- [251] L. Fridman and A. Levant, "Higher order sliding modes as a natural phenomenon in control theory," in *Robust Control via Variable Structure and Lyapunov Techniques*, F. Garofalo and G. Luigi, Eds. Springer, Berlin, Heidelberg, 1996, pp. 107–133.
- [252] A. Levant, "Higher-order sliding modes, differentiation and output-feedback control," *International Journal of Control*, vol. 76, no. 9–10, pp. 924–941, 2003.
- [253] S. T. Venkataraman and S. Gulati, "Control of nonlinear systems using terminal sliding modes," *Journal of Dynamic Systems, Measurement, and Control*, vol. 115, no. 3, pp. 554–560, 1993.
- [254] M. Zhihong, A. P. Paplinski, and H. Wu, "A robust mimo terminal sliding mode control scheme for rigid robotic manipulators," *IEEE Transactions on Automatic Control*, vol. 39, no. 12, pp. 2464–2469, 1994.

- [255] X. Yu and Z. Man, "Model reference adaptive control systems with terminal sliding modes," *International Journal of Control*, vol. 64, no. 6, pp. 1165–1176, 1996.
- [256] Y. Wu, X. Yu, and Z. Man, "Terminal sliding mode control design for uncertain dynamic systems," *Systems & Control Letters*, vol. 34, no. 5, pp. 281–287, 1998.
- [257] X. Yu and O. Kaynak, "Sliding-mode control with soft computing: A survey," *IEEE Transactions on Industrial Electronics*, vol. 56, no. 9, pp. 3275–3285, 2009.
- [258] M. Zak, "Terminal attractors in neural networks," *Neural Networks*, vol. 2, no. 4, pp. 259–274, 1989.
- [259] J. Postel, "Transmission control protocol," *Request for Comments (RFC): 793*, 1981.
- [260] M. Allman, V. Paxson, and E. Blanton, "Tcp congestion control," *Request for Comments (RFC): 5681*, 2009.
- [261] V. Jacobson, R. Braden, and D. Borman, "Tcp extensions for high performance," *Request for Comments (RFC): 1072, RFC: 1185*, 1992.
- [262] P. Borgnat, G. Dewaele, K. Fukuda, P. Abry, and K. Cho, "Seven years and one day: Sketching the evolution of internet traffic," *Proceedings of the IEEE Conference on Computer Communications (INFOCOM)*, pp. 711–719, 2009.
- [263] K. R. Fall and W. R. Stevens, *TCP/IP Illustrated, Volume 1: The Protocols*. Addison-Wesley, 2011.

- [264] C. Fraleigh, S. Moon, B. Lyles, C. Cotton, M. Khan, D. Moll, R. Rockell, T. Seely, and S. C. Diot, "Packet-level traffic measurements from the sprint ip backbone," *IEEE Network*, vol. 17, no. 6, pp. 6–16, 2003.
- [265] G. Appenzeller, I. Keslassy, and N. McKeown, "Sizing router buffers," *ACM SIGCOMM Computer Communication Review*, vol. 34, no. 4, pp. 281–292, 2004.
- [266] W. R. Stevens, "Tcp slow start, congestion avoidance, fast retransmit, and fast recovery algorithms," *Request for Comments (RFC): 2001*, 1997.
- [267] Y. He, Q. Wang, C. Lin, and M. Wu, "Delay-range-dependent stability for systems with time-varying delay," *Automatica*, vol. 34, no. 2, pp. 371–376, 2007.
- [268] T. Issariyakul and E. Hossain, *Introduction to Network Simulator NS2*. Springer Science & Business Media, 2011.
- [269] S. P. Bhat and D. S. Bernstein, "Finite-time stability of continuous autonomous systems," *SIAM Journal on Control and Optimization*, vol. 38, no. 3, pp. 751–766, 2000.
- [270] S. Wen, T. Huang, X. Yu, M. Z. Chen, and Z. Zeng, "Aperiodic sampled-data sliding-mode control of fuzzy systems with communication delays via the event-triggered method," *IEEE Transactions on Fuzzy Systems*, vol. 24, no. 5, pp. 1048–1057, 2016.
- [271] H. K. Khalil, *Nonlinear Systems*. Prentice-Hall, New Jersey, 1996.
- [272] T. Takagi and M. Sugeno, "Fuzzy identification of systems and its applications to modeling and control," *IEEE Transactions on System, Man and Cybernetics*, vol. 15, no. 1, pp. 116–132, 1985.

- 
- [273] Y.-Y. Cao and P. M. Frank, “Analysis and synthesis of nonlinear time-delay systems via fuzzy control approach,” *IEEE Transactions on Fuzzy Systems*, vol. 8, no. 2, pp. 200–211, 2000.
- [274] D. K. B. Bhuyan, Monowar H. and J. K. Kalita, “Information metrics for low-rate ddos attack detection: A comparative evaluation,” *Proceedings of the 2014 Seventh International Conference on Contemporary Computing*, pp. 80–84, 2014.
- [275] CAIDA, “The cooperative analysis for internet data analysis,” <http://www.caida.org>, 2011.

